FTD-MT-64-319

FOREIGN TECHNOLOGY DIVISION

JOURNAL OF APPLIED MECHANICS AND TECHNICAL PHYSICS

(COLLECTION OF ARTICLES)

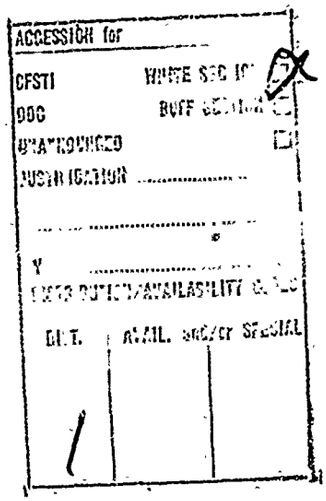

This document is a machine translation of Russian text which has been processed by the AN/GSQ-16(XW-2) Machine Translator, owned and operated by the United States Air Force. The machine output has been post-edited to correct for major ambiguities of meaning, words missing from the machine's dictionary, and words out of the context of meaning. The sentence word order has been partially rearranged for readability. The content of this translation does not indicate editorial accuracy, nor does it indicate USAF approval or disapproval of the material translated.

DISTRIBUTION STATEMENT

Distribution of this document is unlimited.

EDITED MACHINE TRANSLATION

JOURNAL OF APPLIED MECHANICS AND TECHNICAL PHYSICS
(COLLECTION OF ARTICLES)

English Pages: 331

S/0207/064/000/003

PREPARED BY:

TRANSLATION DIVISION
FOREIGN TECHNOLOGY DIVISION
WP-AFB, OHIO.

Akademiya Nauk SSSR — Sibirskoye Otdeleniye

PMTF

ZHURNAL PRIKLADNOY MEKHANIKI I TEKHNICHESKOY FIZIKI

No. 3

May - Iyun'

1964

Izdatel'stvo "Nauka"

Pages 1-184

TABLE OF CONTENTS

U. S. BOARD ON GEOGRAPHIC NAMES TRANSLITERATION SYSTEM

Block	Italic	Transliteration	Block	Italic	Transliteration
А а	*А а*	A, a	Р р	*Р р*	R, r
Б б	*Б б*	B, b	С с	*С с*	S, s
В в	*В в*	V, v	Т т	*Т т*	T, t
Г г	*Г г*	G, g	У у	*У у*	U, u
Д д	*Д д*	D, d	Ф ф	*Ф ф*	F, f
Е е	*Е е*	Ye, ye; E, e*	Х х	*Х х*	Kh, kh
Ж ж	*Ж ж*	Zh, zh	Ц ц	*Ц ц*	Ts, ts
З з	*З з*	Z, z	Ч ч	*Ч ч*	Ch, ch
И и	*И и*	I, i	Ш ш	*Ш ш*	Sh, sh
Й й	*Й й*	Y, y	Щ щ	*Щ щ*	Shch, shch
К к	*К к*	K, k	Ъ ъ	*Ъ ъ*	"
Л л	*Л л*	L, l	Ы ы	*Ы ы*	Y, y
М м	*М м*	M, m	Ь ь	*Ь ь*	'
Н н	*Н н*	N, n	Э э	*Э э*	E, e
О о	*О о*	O, o	Ю ю	*Ю ю*	Yu, yu
П п	*П п*	P, p	Я я	*Я я*	Ya, ya

* ye initially, after vowels, and after ъ, ь; e elsewhere. When written as ё in Russian, transliterate as yё or ё. The use of diacritical marks is preferred, but such marks may be omitted when expediency dictates.

FOLLOWING ARE THE CORRESPONDING RUSSIAN AND ENGLISH

DESIGNATIONS OF THE TRIGONOMETRIC FUNCTIONS

Russian	English
sin	sin
cos	cos
tg	tan
ctg	cot
sec	sec
cosec	csc
sh	sinh
ch	cosh
th	tanh
cth	coth
sch	sech
csch	csch
arc sin	$\sin^{-1}$
arc cos	$\cos^{-1}$
arc tg	$\tan^{-1}$
arc ctg	$\cot^{-1}$
arc sec	$\sec^{-1}$
arc cosec	$\csc^{-1}$
arc sh	$\sinh^{-1}$
arc ch	$\cosh^{-1}$
arc th	$\tanh^{-1}$
arc cth	$\coth^{-1}$
arc sch	sech^{-1}
arc csch	csch^{-1}
rot	curl
lg	log

MT-64-319
Journal of Applied Mechanics and
Technical Physics, Academy of
Sciences of USSR — Siberian
Branch, No. 3, 1964.
Pages: Cover-184

ON STATIONARY PROPAGATION OF A SYSTEM OF CRACKS IN AN ELASTIC-BRITTLE MATERIAL

V. M. Kuznetsov

(Novosibirsk)

Questions of the dynamics of cracks during brittle rupture have attracted significant attention recently [1]. In [2] there is considered stationary propagation of one semi-infinite crack, on the surface of which there are applied symmetrically distributed normal and tangent stresses. Below we investigate generalization of [2] to the case of an infinitely large number of cracks. For simplicity we assume that there are no tangent stresses on the surface of crack.

1. Mathematical formulation of the problem. Let us consider an infinite elastic body in a plane state of stress in plane xy. Let us assume that in the body is there is an infinitely large number of cracks, parallel to the axis of abscissas, located distance 2h from one another in region $x \leq Vt$, where V — constant, t — time. Let us assume, further, that on both sides of the surface of the crack normal and tangent stresses are equal and have form

$$\sigma_{yy} = -f(x - Vt), \qquad \sigma_{xy} = 0 \tag{1.1}$$

Behavior of components of the stress tensor at infinity we define as follows:

$$R\sigma_{xx},\ R\sigma_{xy},\ R\sigma_{yy} \to 0 \quad \text{as} \quad R \to \infty \tag{1.2}$$

We designate by u_x and u_y components of the displacement vector and introduce scalar and vector potentials φ and ψ:

$$u_x = \frac{\partial \varphi}{\partial x} + \frac{\partial \psi}{\partial y}, \qquad u_y = \frac{\partial \varphi}{\partial y} - \frac{\partial \psi}{\partial x} \tag{1.3}$$

As it is known, φ and ψ satisfy the following equations:

$$\frac{\partial^2 \varphi}{\partial t^2} = c_1^2 \left(\frac{\partial^2 \varphi}{\partial x^2} + \frac{\partial^2 \varphi}{\partial y^2} \right), \qquad \frac{\partial^2 \psi}{\partial t^2} = c_2^2 \left(\frac{\partial^2 \psi}{\partial x^2} + \frac{\partial^2 \psi}{\partial y^2} \right)$$
$$\left(c_1^2 = \frac{\lambda + 2\mu}{\rho}, \quad c_2^2 = \frac{\mu}{\rho} \right) \tag{1.4}$$

Here ρ – density of the medium, λ and μ – Lamé constants.

From physical considerations it is clear that with an infinitely large number of cracks there is symmetry both relative to any straight line which passes through the crack and its continuation, and also relative to any straight line which passes parallel to cracks at half the distance between them. Due to this it is possible to limit our consideration to the region (Fig. 1), constituting the strip $0 \leq y \leq h$.

On boundaries of the strip we should have

$$\sigma_{xy} = 0, \quad \frac{\partial u_y}{\partial t} = 0 \quad \text{when } y = h, \; y = 0, \; x > Vt \tag{1.5}$$

due to symmetry, and

$$\sigma_{yy} = -f(x - Vt), \quad \sigma_{xy} = 0 \quad \text{when } y = 0, \; x < Vt \tag{1.6}$$

due to (1.1).

Following [2], we seek a solution of equations (1.4) in the form

$$\varphi = \varphi(x - Vt, y), \qquad \psi = \psi(x - Vt, y) \tag{1.7}$$

We introduce designations

$$x - Vt = X, \quad \beta_1 y = Y_1, \quad \beta_2 y = Y_2$$
$$\beta_1 = \left(1 - \frac{V^2}{c_1^2}\right)^{1/2}, \qquad \beta_2 = \left(1 - \frac{V^2}{c_2^2}\right)^{1/2} \tag{1.8}$$

Putting (1.7) in (1.4) and using (1.8), we obtain

$$\frac{\partial^2 \varphi}{\partial X^2} + \frac{\partial^2 \varphi}{\partial Y_1^2} = 0, \qquad \frac{\partial^2 \psi}{\partial X^2} + \frac{\partial^2 \psi}{\partial Y_2^2} = 0 \tag{1.9}$$

It follows from this that it is possible to introduce into consideration two functions

$$w_1(z_1) = \varphi + i\chi, \quad w_2(z_2) = \psi + ik \quad (z_1 = X + iY_1,\ z_2 = X + iY_2) \tag{1.10}$$

Functions φ, χ and ψ, k are connected by D'Alembert-Euler conditions

$$\frac{\partial\varphi}{\partial X} = \frac{\partial\chi}{\partial Y_1}, \quad \frac{\partial\varphi}{\partial Y_1} = -\frac{\partial\chi}{\partial X}; \quad \frac{\partial\psi}{\partial X} = \frac{\partial k}{\partial Y_2}, \quad \frac{\partial\psi}{\partial Y_2} = -\frac{\partial k}{\partial X} \tag{1.11}$$

For components of the stress tensor we have

$$\sigma_{xx} = \lambda\nabla^2\varphi + 2\mu\left(\frac{\partial^2\varphi}{\partial x^2} + \frac{\partial^2\psi}{\partial x\,\partial y}\right), \quad \sigma_{xy} = \mu\left[2\frac{\partial^2\varphi}{\partial x\partial y} + \frac{\partial^2\psi}{\partial y^2} - \frac{\partial^2\psi}{\partial x^2}\right]$$
$$\sigma_{yy} = \lambda\nabla^2\varphi + 2\mu\left(\frac{\partial^2\varphi}{\partial x^2} - \frac{\partial^2\psi}{\partial x\,\partial y}\right) \qquad \left(\nabla^2 = \frac{\partial^2}{\partial x^2} + \frac{\partial^2}{\partial y^2}\right) \tag{1.12}$$

Using (1.7)-(1.11), we transform these relationships to form

$$\frac{\sigma_{xx}}{\mu} = (1 + 2\beta_1^2 - \beta_2^2)\frac{\partial^2\varphi}{\partial X^2} - 2\beta_2\frac{\partial^2 k}{\partial X^2}$$
$$\frac{\sigma_{yy}}{\mu} = -(1 + \beta_2^2)\frac{\partial^2\varphi}{\partial X^2} + 2\beta_2\frac{\partial^2 k}{\partial X^2}$$
$$\frac{\sigma_{xy}}{\mu} = -2\beta_1\frac{\partial^2\chi}{\partial X^2} - (1 + \beta_2^2)\frac{\partial^2\psi}{\partial X^2} \tag{1.13}$$

In the same designations

$$\frac{\partial u_y}{\partial t} = V\left(\beta_1\frac{\partial^2\chi}{\partial X^2} + \frac{\partial^2\psi}{\partial X^2}\right) \tag{1.14}$$

Now we formulate the problem. It is required to find function $w_1(z_1)$ and $w_2(z_2)$ in region

$$0 \leqslant Y_n \leqslant \beta_n h \qquad (n = 1, 2)$$

satisfying the following boundary conditions:

$$2\beta_1\frac{\partial^2\chi}{\partial X^2} + (1 + \beta_2^2)\frac{\partial^2\psi}{\partial X^2} = 0 \quad \text{when } Y_n = \beta_n h,\ Y_n = 0 \tag{1.15}$$

$$(1 + \beta_2^2)\frac{\partial^2\varphi}{\partial X^2} - 2\beta_2\frac{\partial^2 k}{\partial X^2} = \frac{f(X)}{\mu} \quad \text{when } Y_n = 0,\ X < 0 \tag{1.16}$$

$$\beta_1\frac{\partial^2\chi}{\partial X^2} + \frac{\partial^2\psi}{\partial X^2} = 0 \quad \text{when } Y_n = \beta_n h,\ Y_n = 0,\ X > 0 \tag{1.17}$$

and the condition at infinity

$$\frac{d^2 w_n}{dz_n^2}|z_n| \to 0 \quad \text{when } |z_n| \to \infty \tag{1.18}$$

2. Formal solution. We introduce instead of $w_1(z_1)$ and $w_2(z_2)$

$$W_1 = \frac{d^2 w_1}{dz_1^2}, \qquad W_2 = \frac{d^2 w_2}{dz_2} \tag{2.1}$$

We map the strip of (Fig. 1) in the upper half-plane of (Fig. 2)

$$\zeta_n = \xi_n + i\eta_n = \exp\frac{\pi z_n}{\beta_n h} \qquad (n = 1, 2) \tag{2.2}$$

So far, formally, we make no distinctions between variables ζ_1 and ζ_2 and set $W_1 = W_1(\zeta)$, $W_2 = W_2(\zeta)$. In plane ζ boundary conditions (1.15)-(1.17) for functions W_1 and W_2 have form

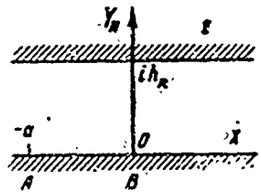

Fig. 1

$$2\beta_1 \operatorname{Im} W_1 + (1+\beta_2^2) \operatorname{Re} W_2 = 0 \qquad (\eta = 0) \tag{2.3}$$

$$(1+\beta_2^2)\operatorname{Re} W_1 - 2\beta_1 \operatorname{Im} W_2 = \frac{1}{\mu} f[X(\xi)] \equiv \frac{1}{\mu} F(\xi) \qquad (\eta = 0,\ 0 < \xi < 1) \tag{2.4}$$

$$\beta_1 \operatorname{Im} W_1 + \operatorname{Re} W_2 = 0 \qquad (\eta = 0,\ \xi > 1,\ \xi < 0) \tag{2.5}$$

We designate by W* a function, the conjugate of W, and we rewrite (2.3) in the form

$$2\beta_1 i (W_1 - W_1^*) - (1+\beta_2^2)(W_2 + W_2^*) = 0 \tag{2.6}$$

We integrate this equality over a contour, consisting of a segment of the real axis and a semicircle of radius R. Directing R to infinity we obtain, considering (1.18), by the Cauchy theorem [3]

$$\frac{1}{2\pi i}\int_{-\infty}^{\infty} \frac{W(t)\,dt}{t-\zeta} = W(\zeta), \quad \frac{1}{2\pi i}\int_{-\infty}^{\infty} \frac{W^*(t)\,dt}{t-\zeta} = 0$$

Fig. 2

and, consequently,

$$W_1(\zeta) = -i\frac{1+\beta_2^2}{2\beta_1} W_2(\zeta) \tag{2.7}$$

We replace in (2.2) and (2.3) function W_2 by W_1 with the help of (2.7):

$$\begin{aligned} &\operatorname{Re} W_1 = \alpha F(\xi) && (\eta = 0,\ 0 < \xi < 1) \\ &\operatorname{Im} W_1 = 0 && (\eta = 0,\ \xi > 1,\ \xi < 0) \end{aligned} \qquad \left(\alpha = \frac{1+\beta_2^2}{\mu[(1+\beta_2^2) - 4\beta_1\beta_2]}\right) \tag{2.8}$$

For function $W_1(\zeta)$, thus, we obtain a mixed boundary value problem. Its solution comes from the Keldysh-Sedov formula [3], which in this case has form

$$W_1(\zeta) = \frac{\alpha}{\pi i g(\zeta)}\int_0^1 \frac{F(t)\,g(t)\,dt}{t-\zeta} + \frac{W_1(\infty)}{g(\zeta)} \qquad \left(g(\zeta) = \left(\frac{\zeta-1}{\zeta}\right)^{1/2}\right) \tag{2.9}$$

Due to the condition at infinity (1.18) $W_1(\infty) = 0$.

3. Particular case. Let us assume that, just as in [2],

$$f(X) = \begin{cases} 0 & (-\infty < X < -a) \\ P & (-a < X < 0) \end{cases} \tag{3.1}$$

In plane ζ for function $F(\xi) \equiv f[X(\xi)]$ this condition has the form

$$F(\xi) = \begin{cases} 0 & (\exp(-\pi a/\beta h) > \xi > 0) \\ P & (1 > \xi > \exp(-\pi a/\beta h)) \end{cases} \tag{3.2}$$

Putting (3.2) in (2.9), we obtain after integration

$$W_1(\zeta) = -\frac{aP}{\pi g(\zeta)}\left[2 \operatorname{arc\,tg} b - \frac{\sqrt{1-\zeta}}{\sqrt{\zeta}} \ln \frac{\sqrt{1-\zeta} + b\sqrt{\zeta}}{\sqrt{1-\zeta} - b\sqrt{\zeta}}\right] \tag{3.3}$$

$$b = \sqrt{\exp(\pi a/\beta h - 1)} \tag{3.4}$$

Branches of the ambiguous functions in this expression are determined as follows: $g(\xi) > 0$ when $\xi > 1$; the imaginary part of the logarithm is equal to 2 arc tg b; when $\xi \to \infty$, arc tg $b \leq 1/2\pi$. Expression (3.3), together with (2.1), (2.2) and (2.7), gives the solution to the problem at hand. Components of the stress tensor are determined from this by formulas (1.13). Let us note that with replacement of ζ by ζ_1 and ζ_2 the magnitude of b should be replaced according to (3.4), where, correspondingly $\beta = \beta_1$ and $\beta = \beta_2$.

We pass now to determination of the rate of spread of cracks. From (3.3) it is simple to verify that components of the stress tensor and vector components of the rate of displacement are quantities $O(\exp(-\pi\beta/\beta h))$ when $R \to \infty$. Thus, the flux of energy at infinity is absent. On the other hand, in environment of singular point $z = -a$ stresses and the rate are quantities $O(\ln r)$, where $r^2 = [(x - Vt + a)^2 + y^2]$, so that work per unit time is $O[r(\ln r)^2]$ and seeks zero together with r. Consequently, one may assume that the whole flux of energy created in an elastic body by external forces P is connected with the peculiarity at point $z = 0$, i.e., at the beginning of the crack.

Hence we naturally assume that work of external forces is wholly expended on creation of the free surface of crack.

We designate by T the energy per unit area of the forming surface. Then the rate of growth of surface energy is TV. This quantity should be equal to the work of external forces per unit time:

$$TV = \int_{-a}^{a} P \left[\frac{\partial u_y}{\partial t}\right]_{y=0} dx \tag{3.5}$$

Due to (1.14) and (2.7) we have

$$\left[\frac{\partial u_y}{\partial t}\right]_{y=0} = V\left\{\beta_1 \operatorname{Im} W_1(\xi_1) - \frac{2\beta_2}{1+\beta_2^2} \operatorname{Im} W_1(\xi_2)\right\} \tag{3.6}$$

We place (3.6) in (3.5) and pass under the integral to variable $v = \sqrt{(1-\xi)/\xi}$; we obtain

$$T = \frac{2\alpha P^2 \beta_1 h}{\pi^2}\left\{\beta_1\left[2 \operatorname{arc tg} b_1 \int_0^{b_1} \frac{dv}{1+v^2} - \int_0^{b_1} \ln\frac{b_1+v}{b_1-v}\frac{vdv}{1+v^2}\right] - \right.$$
$$\left. - \frac{2\beta_2}{1+\beta_2^2}\left[2 \operatorname{arc tg} b_2 \int_0^{b_2} \frac{dv}{1+v^2} - \int_0^{b_2} \ln\frac{b_2+v}{b_2-v}\frac{vdv}{1+v^2}\right]\right\} \tag{3.7}$$

Noting that

$$\int_0^b \ln\frac{b+v}{b-v}\frac{vdv}{1+v^2} = \operatorname{arc tg}^2 b$$

we obtain from (3.7), taking into account (2.8),

$$\frac{P^2 a}{\pi\mu T} = \frac{\pi a}{2\beta_1 h}\frac{4\beta_1\beta_2 - (1+\beta_2^2)^2}{2\beta_2 \operatorname{arc tg}^2 b_2 - \beta_1(1+\beta_2^2)\operatorname{arc tg}^2 b_1} \tag{3.8}$$

4. Analysis of results. Let us consider first formula (3.8) in the limiting case $h \to \infty$. Considering $a/h \ll 1$, we have, with accuracy up to members of higher order of smallness,

$$b_n = \frac{\sqrt{\pi a}}{\sqrt{h\beta_n}}, \qquad \operatorname{arc tg} b_n = b_n \tag{3.9}$$

Substituting these quantities and expressions β_1 and β_2 from (1.8) in (3.8), we obtain

$$\frac{P^2 a}{\pi\mu T}\frac{V^2}{c_2^2}\left(1-\frac{V^2}{c_2^2}\right)^{1/2} =$$
$$= 4\left(1-\frac{V^2}{c_1^2}\right)^{1/2}\left(1-\frac{V^2}{c_2^2}\right)^{1/2} - \left(2-\frac{V^2}{c_2^2}\right)^2 \tag{4.1}$$

This expression coincides with the finding of [2] for a single crack. In particular, equality to zero of the right side of (4.1)

$$4\left(1-\frac{V^2}{c_1^2}\right)^{1/2}\left(1-\frac{V^2}{c_2^2}\right)^{1/2}-\left(2-\frac{V^2}{c_2^2}\right)=0$$

constitutes the equation, determining the rate of propagation of Rayleigh surface waves. Thus, in the case of the stationary propagation of of one crack in an unlimited elastic medium its rate has a limiting value, equal to elastic medium Rayleigh velocity.

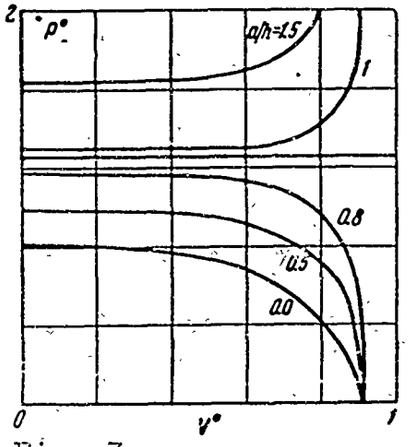

Fig. 3

The second limiting case, which is obtained from (3.8) when $V \to 0$, corresponds to the static problem

$$\frac{P^2a}{\pi\mu T}=\left\{\frac{\operatorname{arc\,tg}\left[\exp(\pi a/h)-1\right]^{1/2}}{(\exp(\pi a/h)-1)^{1/2}}+\frac{a}{\pi a}\frac{c_2^2}{c_1^2-c_1^2}\operatorname{arc\,tg}^2\left[\exp\frac{\pi a}{h}-1\right]^{1/2}\right\}^{-1} \qquad (4.2)$$

Hence when $h \to \infty$ we obtain

$$\frac{P^2a}{\pi\mu T}=1-\frac{c_2^2}{c_1^2}$$

This also coincides with the result obtained in [2].

We consider now formula (3.8) in general form. Results of calculation in case $\lambda = \mu$, $c_1^2/c_2^2 = 3$ for different values of parameter a/h are presented in Fig. 3, where

$$P^\circ = Pa^{1/2}(\pi\mu T)^{-1/2}, \qquad V^\circ = V/c_2$$

Meriting attention is the circumstance that formula (3.8) determines in plane $P^\circ V^\circ$ two families of curves, corresponding to two different conditions of spreading of cracks. In one of them (the lower one in Fig. 3) the velocity of cracks decreases with increase of pressure; in the other, it increases. Formally this depends on which turns into zero earlier with growth of velocity, the numerator or the denominator of formula (3.8). It is obvious that the critical curve, dividing these two families, is determined by simultaneous conversion into zero of the numerator and denominator. Since the

numerator turns into zero at a velocity, equal to Rayleigh's, the critical value of parameter $(a/h)_*$ is determined from equation

$$2\beta_2^\circ \operatorname{arc\,tg}^2 b_2^\circ - \beta_2^\circ [1 + (\beta_2^\circ)^2] \operatorname{arc\,tg}^2 b_1 = 0 \qquad (4.3)$$

Here

$$\beta_n^\circ = \sqrt{1 - c_0^2/c_n^2}, \qquad b_n^\circ = \sqrt{\exp(\pi a/h\beta_n) - 1} \qquad (n = 1,2)$$

c_0 signifies Rayleigh velocity. When $\lambda = \mu$ we find $(a/h)_* = 0.94$. Critical pressure is determined for the found value of $(a/h)_*$ from expression (4.2). In this case we obtain

$$\frac{P_* a^{1/2}}{(\pi\mu T)^{1/2}} = 1.27$$

The physical meaning of the two conditions of development of cracks consists of the following. The rate of stationary spreading of a single crack increases with decrease of pressure. Thus, if in material under the action of certain loads there appears and spreads a crack, it can continue to develop after the loads are removed. In the case of a larger number of cracks such conditions are not always possible. With greater distance between cracks, such that $a/h < (a/h)_*$, every crack develops approximately just as a single one. If, however, the distance between cracks is small, so that $a/h > (a/h)_*$, the spreading of every crack is substantially influenced by the other cracks. Development of a crack as it were is restrained by compressive forces acting from neighboring cracks.

From formula (3.8) there ensues one more important result. With sufficiently small distance between cracks, when $a/h > (a/h)_*$, there exists a limiting rate of spreading as $P \to \infty$, smaller in magnitude, or equal to Rayleigh's velocity. For a given value parameter a/h this rate is determined from equation

$$2\beta_2 \operatorname{arc\,tg}^2 b_2 - \beta_1 (1 + \beta_2^2) \operatorname{arc\,tg}^2 b_1 = 0 \qquad (4.4)$$

In particular, if $a/h \gg 1$, then it is approximately possible t

take arc tg $b_1 \approx 1/2\pi$, arc tg $b_2 \approx 1/2\pi$, and from (3.8) we obtain

$$\frac{V^2}{c_2^2} = \frac{1}{2}\left(4 + \frac{c_1^2}{c_2^2}\right)\left\{1 - \left[1 - \frac{16}{(4 + c_1^2/c_2^2)^2}\right]^{1/2}\right\} \qquad (4.5)$$

When $\lambda = \mu$ the limiting value of velocity, determined from this expression, is equal to $0.8\, c_2$.

Submitted
15 October 1963

Literature

1. G. I. Barenblatt. Mathematical Theory of Equilibrium Cracks, Formed During Brittle Rupture, PMTF, 1961, No. 4.

2. I. W. Craggs. On the Propagation of a Crack in an Elastic-Brittle Material. J. Mech. Phys. Solids, 1960, 8, 66-75.

3. M. A. Lavrent'yev and B. V. Shabat. Methods of the Theory of Functions of a Complex Variable. Fizmatgiz, 1958.

ON THE DYNAMIC COMPRESSIBILITY OF HARD ROCKS AND METALS

S. A. Khristianovich and Ye. I. Shemyakin

(Novosibirsk)

Methods of dynamic testing of solids by explosive and shock loading are the subject of many works. Works of Soviet and American physicists [1-15] contain numerous data on impact adiabats of solids and equations of the state of these bodies up to pressures of ~10 megabars calculated on this base. At the same time a comparatively small number of works pertain to the range of pressures below 100-150 kilobars, which is of great practical and scientific interest. To this range pertain practical blastings in rocks; in this range there occurs transition of solids from elastic to plastic and, possibly, to a hydrodynamic state; this same range corresponds to a change of ground pressure in the earth to a depth of 500 km, i.e., covers the region of depths of interest in geophysical applications.

In experiments in dynamic testing of solids by explosive loading there usually is realized a state of stress, corresponding to a plane wave. In recent years there have been measurements of parameters of spherical and cylindrical waves, appearing during explosion in hard rocks [11, 16].

In these experiments there were noted unexpectedly high attenuation of stress amplitudes: amplitude decreased with distance r according to the law r^{-n}, where n = 1.6 to 1.8.

As it is known, for an elastic medium in the case of a spherical wave n = 1. Calculations of attenuation stress waves, based on contemporary concepts of plastic flows of solids (theory of flow and the theory of small elasto-plastic flows) and about an elastic unloading wave, lead to values n = 1.1 to 1.2.

This poses the problem of more precise definition of concepts of plastic flows of solids under rapid loading and loads significantly exceeding the elastic limit. Consideration of data of experiments in dynamic compression of metals in the region of large stresses leads to the same problem.

Below there is discussed a physical model of a solid medium, in which during rapid loading there is revealed significant internal friction. On the basis of this model there are considered phenomena of damping of spherical waves in solids and results of experiments in dynamic compression of iron and quartz in the wave plane shock.

Till now concepts about the mechanism of damping of amplitude stress waves with distance from the explosion were based on an analogy with the corresponding phenoma in liquid and gas.

Damping of a plane shock wave in a gas or fluid is connected with irreversible processes of compression in the shock wave; behind the front of the shock wave the process of expansion can be considered adiabatic. In solids the irreversibility of the process of deformation in the load zone is mainly connected with plastic shearing strains and, to a significantly lesser extent, with irreversibility of volumetric strains; process of unloading in a continuous wave is considered reversible and straing are considered elastic. Irreversible processes cause decrease in the propagation velocity of perturbations in the load zone as compared to the velocity of sound in an elastic medium. The difference between these velocities directly determines the rate of decrease of maximum amplitude of the wave. On this effect is based the term "hydrodynamic damping." During research of propagation of spherical and cylindrical waves in the frames of these concepts in principle nothing is changed: the effect of hydrodynamic damping is imposed on weakening of amplitudes at the expense of geometric divergence.

§ 1.1. Estimation of the effect of "hydrodynamic damping" is most simple for a weak wave (L. D. Landau [18]). A wave is considered weak if pressure jump p or amplitude of stresses σ_r is much less than the bulk modulus of the medium K or modulus of compression K_1 in the direction of propagation of wave allowing for strength of the medium

$$\frac{p}{K} \ll 1, \qquad \frac{\sigma_r}{K_1} \ll 1 \tag{1.1}$$

In a weak wave, as follows from (1.1), volumetric strains are small; it is possible to show that in a weak wave the propagation

velocities differ from the velocity of sound in a medium at rest by a magnitude of the same order as the strain.

In hard rocks and most metal waves with amplitude ~50-150 kilobars are weak, since the bulk modulus has an order of 10^3 kilobars.

Attenuation of the amplitude of a weak spherical shock wave with distance in liquid and gas [18, 19] is proportional to $(r\sqrt{\ln r})^{-1}$, which gives comparatively small correction to geometric law r^{-1} (instead of n = 1, usually n = 1.1 to 1.2). Calculations of parameters of spherical waves in solids show that the effect of "hydrodynamic damping" leads to corrections of the same order (n = 1.1 to 1.2).

Experimental data [16, 17] about attenuation of stress waves in hard rocks during explosions of spherical charges indicate a faster decrease of amplitudes; therefore we naturally think about the presence of new phenomena, which can appear in solids and influence damping of stresses.

1.2. Let us consider a model of a solid, composed of "balls," close-packed and strongly cemented together. During compression of such a body there can occur both volumetric strain of the "balls" and also slipping of them over each other with disturbing of bonds and with friction. As "balls" in rocks we can take separate crystals or blocks of the rock, and in metals — crystals or groups of neighboring crystals with specially strong bonds between them.

Let us consider uniaxial compression of such a medium in a cylinder with rigid walls, stress along the axis of the cylinder σ_r, and stress on the radius σ_θ: we have

$$\varepsilon_r = \varepsilon.$$

Under compression, depending upon the force applied, there can be realized the following cases.

1. Friction between particles is great (cohesion is not disturbed): in this case strain is elastic (or nonlinearly elastic) because of compression of grains — "balls." In this case the ratio of stresses σ_r and σ_θ is determined by Hooke's law

$$\sigma_\theta / \sigma_r = \alpha, \qquad \alpha = \nu / (1 - \nu) \quad (\nu - \text{Poisson's ratio}) \tag{1.2}$$

2. Cohesion is disturbed; friction between particles is negligible. Then

$$(\sigma_\theta / \sigma_r) = \alpha^* \approx 1 \tag{1.3}$$

which corresponds to a hydrodynamic state or a state of ideal fluidity close to it:

$$\sigma_r - \sigma_\theta = 2\tau_s \qquad (\sigma_r \gg \tau_s,\ \tau_s = \text{const}) \tag{1.4}$$

3. Cohesion is disturbed, but friction of particles cannot be disregarded:

$$\sigma_\theta / \sigma_r = \alpha^* < 1 \tag{1.5}$$

This state of stress we call a state with internal friction.

When $\alpha^* = \nu/(1 - \nu)$ there is a transition from the elastic state to the state with internal friction; as $\alpha^* \to 1$ the coefficient of friction decreases; $\alpha^* = 1$ corresponds to the hydrodynamic state.

The mechanism of internal friction can be described if we introduce the condition of plasticity in the form of the relationship of tangent stress $\tau = 1/2\ (\sigma_r - \sigma_\theta)$ (second invariant of the stress tensor) with $\sigma = 1/3(\sigma_r + 2\sigma_\theta)$ — the first invariant; this relationship may be nonlinear, so that $\alpha^* = \alpha^*(\sigma)$.

Let us consider dynamic loading. The velocity of sound in a state of stress with internal friction for $\alpha^* = \alpha_0^* = \text{const}$ and $\rho = \text{const}$ will be

$$a = \left(\frac{3K}{\rho_0 (1 + 2\alpha_0^*)}\right)^{1/2} \qquad K = \lambda + \tfrac{2}{3}\mu \quad (\lambda,\ \mu - \text{Lamé parameters}). \tag{1.6}$$

When $\alpha^* = \nu/(1 - \nu)$ we have

$$a = a_0 = (\lambda + 2\mu / \rho_0)^{1/2} \tag{1.7}$$

Here a_0 — propagation velocity of the elastic wave

When $\alpha^* = 1$, we have

$$a = c_0 = (K / \rho_0)^{1/2} \tag{1.8}$$

Here c_0 - hydrodynamic velocity of sound.

If α^* depends on σ, and the relationship of σ and ε has a weakl linear character, then, instead of (1.6), we have

$$a^2 = \frac{3K}{\rho_0(1 + 2\alpha_0^*)}(1 + l\varepsilon) \qquad |l\varepsilon| \ll 1 \tag{1.9}$$

Let us consider a solid, for which $\sigma = K\varepsilon$ (K = const) and for which according to experiment with plane waves there is established dependence $\sigma_r(\varepsilon)$ in a certain ran of stresses, which corresponds to constant velocity of sound during loading and unloading.

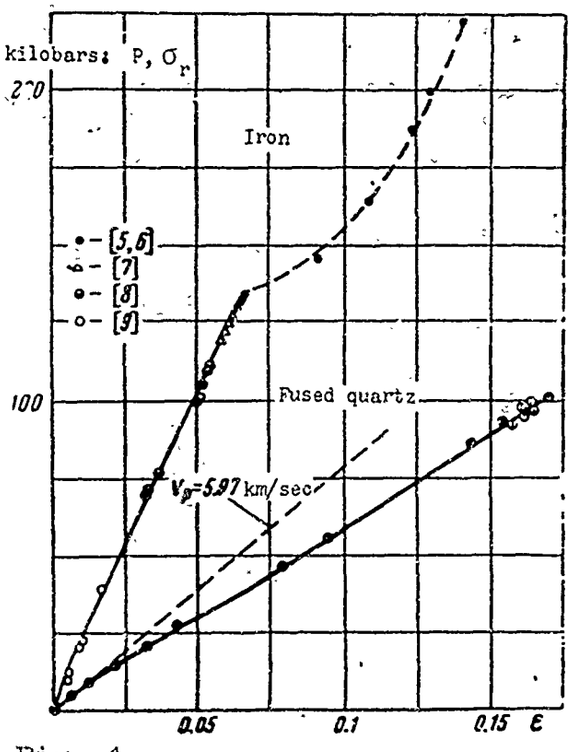

Fig. 1.

On the basis of these data w can make two equally justified hypotheses: the medium is in an elastic state $\alpha = \nu/(1 - \nu)$, or i state with internal friction $\alpha^* = \nu/(1 - \nu)$.

Consider now a spherical wave propagating in this medium.

If, during propagation of the wave cohesion between the "balls" is not disturbed, then strains in the wave will be elastic and damping of amplitudes will follow the law r^{-1}. If the bonds are broken, there is a state of stress with

internal friction, and damping occurs [21] according to the law $r^{-(2-\alpha)}$. This damping is connected with the work of forces of friction during relative displacement of particles in the divergent wave. This effect occurs not only during build-up of stresses in the wave, but also in the unloading zone. Considering damping of maximum amplitudes in a spherical wave, it is possible to establish the elastic limit.

This effect is clearly seen in Figs. 1 and 2, where there are given data of experiments with plane and spherical waves for iron, fused quartz, granite and rock salt [17]. The authors of [17] note that this dependence remains practically linear in that range of deformations which corresponds to data in Fig. 2.

§ 2.1. Let us consider in more detail results of certain experiments pertaining to plane waves. In experiments of dynamic (explosive loading of a test piece in a certain environment of the axis of a cylindrical piece there is realized a plane stress wave. The stress wave can have a shock nature, have continuous build-up or to disintegrate into a group (two to three) of continuous or shock waves, moving at different velocities (Fig. 3a and 3b).

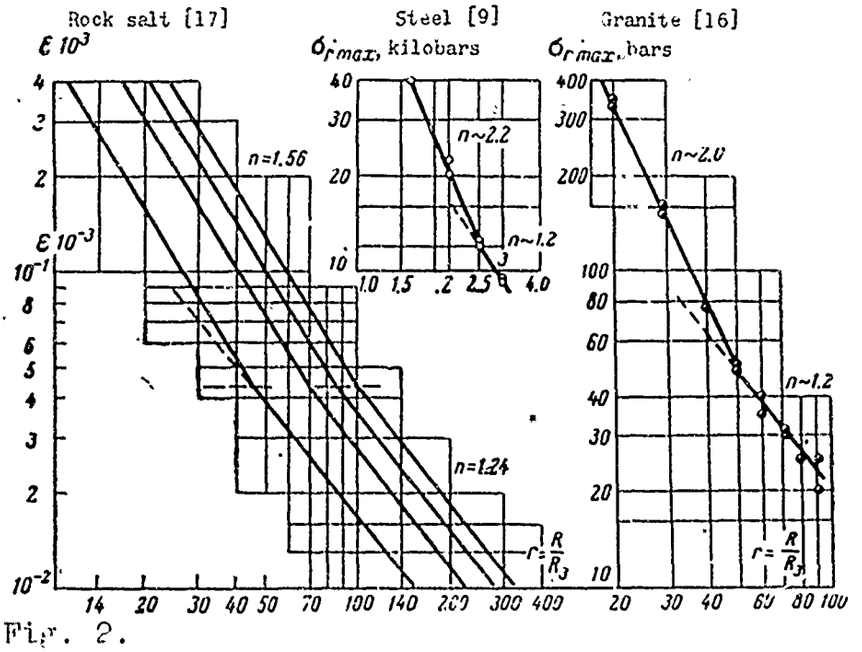

Fig. 2.

In Fig. 3a is a "stress – time" diagram in steel [5], where 4 – time of arrival of an elastic wave with velocity 5.85 km/sec and amplitude 15.7 kilobars; 3 – time of arrival of a shock wave with velocity 5.1 km/sec and amplitude of 225 kilobars. In Fig. 3b is the "velocity of surface movement – time" diagram for a piece of fused quartz [13]: beginning of recording corresponds to wave velocity of 5.97 km/sec; first shock wave has velocity of 5.15 km/sec and amplitude of 100 kilobars.

The state of stress is determined by the principal normal stresses σ_r and σ_θ and volumetric strain ε. In experiments we usually measure the propagation velocity D of the shock wave and the rate of particle displacement u, after which stress σ_r and strain ε are determined by Hugoniot equations:

$$\sigma_r - \sigma_{r0} = \rho_0 (D - u_0)(u - u_0) \tag{2.1}$$

$$\varepsilon = \frac{u - u_0}{D - u_0} \quad \left(\varepsilon = 1 - \frac{\rho_0}{\rho}\right) \tag{2.2}$$

Here index 0 designates quantities in front of the wave. For propagation velocity D of the shock wave and velocity of sound a we have

$$D = \left(\frac{\sigma_r}{\rho_0 \varepsilon}\right)^{1/2}, \quad a = \left(\frac{1}{\rho_0}\frac{d\sigma_r^*}{d\varepsilon}\right)^{1/2} \tag{2.3}$$

Here $\sigma_r^* = \sigma_r^*(\varepsilon)$ – adiabatic dependence.

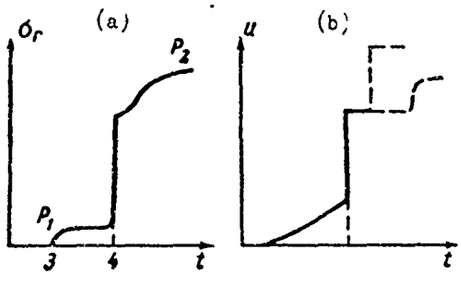

Fig. 3.

As noted, for weak waves difference of velocities a, D and a_0 has the same order as ε. Relationships (2.1) and (2.2) are exact for a shock wave and are approximately satisfied (with accuracy up to ε^2) for a continuous weak shock wave [19, 21].

By (2.1) and (2.2) we can present experimental data [5, 13]

compression of iron and fused quartz in the following form (Fig. 1). As follows from these data, the velocity of shock waves in this range of stresses changes slightly, by magnitude of no more than 10-15%. To estimate deviation of the velocity of perturbations from the velocity of sound in the elastic state the diagram of (Fig. 1) can be presented in the form of two straight segments. Then in iron and steels slopes of these lines correspond to velocities of perturbations: with minute (elastic) amplitudes of waves they are 5.86-6.0 km/sec, and with large stresses [20] right up to 130 kilobars they are 5.1 to 5.15 km/sec; in fused quartz they are 6.0 and 5.15 km/sec, respectively.

The presence of irreversible strains can be judged, if the dependence $\sigma_r(\varepsilon)$ differs during loading and unloading. Without delving into the mechanism of irreversible strains, we can set dependence $\sigma_r(\varepsilon)$ at the base of the theory of plane waves, but as one may see from the preceding, without additional data, we must not base our consideration of a more complex state of stress on this dependence. If to supplement dependence $\sigma_r(\varepsilon)$ we have data on relationships $\sigma(\varepsilon)$, it is possible to establish the magnitude of strain ε, at which a solid passes into a hydrodynamic state. This is possible to do by comparison of slopes of tangents on curves $\sigma_r(\varepsilon)$ and $\sigma(\varepsilon)$ for the same value of ε.

2.3. If we turn to a model of a medium with internal friction, then experimental data on dependence $\sigma_r(\varepsilon)$ can be interpreted as follows.

Change of the propagation velocity can occur both because of nonlinearity of dependence

$$\alpha^*(\sigma) = \alpha_0^*(1 + \chi\sigma), \qquad |\chi\sigma| \ll 1$$

and due to nonlinearity of volumetric compression

$$\sigma = K\varepsilon(1 + l_1\varepsilon), \qquad |l_1\varepsilon| \ll 1$$

Dependence $\sigma_r(\varepsilon)$ allows to determine α_0^*. Thus, in case of the diagram $\sigma_r(\varepsilon)$ for iron, having a break we have

$$\alpha_0^* = \alpha - \frac{1+\nu}{1-\nu}\Delta \qquad \left(\Delta = \frac{a - a_0}{a_0}\right)$$

Here Δ – relative jump of the velocity of sound. If, however, change of the velocity of sound occurs continuously, which is observed in many cases during tests of metals [10] and rocks [16],

$$\alpha_0^* = \frac{\nu}{1-\nu} \tag{2.4}$$

Wave attenuation due to friction is determined first of all by α_0^*. If nonlinearity of dependence $\sigma_r(\varepsilon)$ is connected with irreversible processes of volumetric strain, the influence of these processes on wave attenuation is determined by the relative difference of the velocity of sound under load, i.e., it appears in additional "hydrodynamic damping" of the wave.

2.4. As noted, experimental data on $\sigma_r(\varepsilon)$ is insufficient for a simple conclusion about the mechanism of irreversible deformations.

Such information can be obtained either from experiments with divergent waves, or from other experiments, supplementing data on $\sigma_r(\varepsilon)$ with data about compression $\sigma(\varepsilon)$ and friction $\tau(\sigma)$.

As illustration we consider experimental data of Bridgman on $\tau(\sigma)$ (Fig. 4. line 1) [23] and data of Buchanan (Fig. 4, line 2) [24]. Dependence $\tau(\sigma)$ has a form, characteristic for a medium with internal tension: τ increases with growth of σ. Slope of line $\tau(\sigma)$ can depend on the rate of loading $\dot{\sigma}$.

It is possible to assume that with high rates of loading friction no longer depends on the rate of loading and coefficient α_0^* can be determined from observations of weakening of amplitudes of pressure in a spherical wave, considering here the additional effect of

hydrodynamic damping.

Experiments in spatial attenuation of stress waves in metals in spherical and cylindrical cases practically have not been discussed in the literature. Here it is possible to give only certain data of J. Rinehart [9] on damping of stress waves with axisymmetric loading of metals (imposed concentrated charge in blocks of iron or steel of different thickness d) (Fig. 2). From these data it follows that upon achievement of the elastic limit the law of damping of maximum stress sharply changes: the exponent in the exponential law, somewhat larger than 2, becomes somewhat larger than one, although the velocity of perturbations according to Rinehart remains 5.53 km/sec

The experiments of Rinehart were conducted in more complex conditions than a spherical explosion in a solid medium; this does not allow us to directly compare data of experiments [9] with conclusions of theory; accuracy of determination of σ_r and a is also insufficient; apparently, a = 5.53 km/sec is the average value of a when $\sigma_r \approx 40$ kilobars and $\sigma_r \approx 10$ kilobars.

More complete data were obtained during explosions of spherical charges in hard rock (marble, granite, diabase, hard limestones [16]; rock salt [17]). In Fig. 2 are given data from [17], indicating various laws of damping of stress waves in a state with internal friction and in the presence only of hydrodynamic damping, although, as the authors of [17] note, the dependence $\sigma_r(\varepsilon)$ remains practically linear in the whole range of deformations for which these data are given.

These data were obtained in the same conditions for which there is obtained the theoretical law of damping of maximum stresses $\sigma_r \sim r^{-(\lambda-\lambda')}$, which allows us to calculate value $\gamma^* \approx 0.14$. By formula

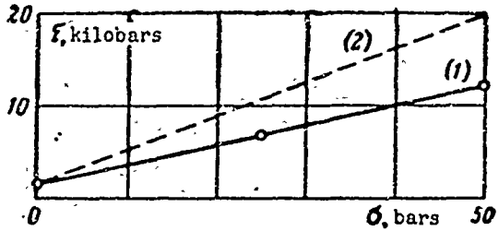

Fig. 4.

(2.4) we find $\nu = 0.305$, which is very close to the value of ν for rock salt: $\nu = 0.30$ to 0.33.

Thus, experiments in dynamic testing of solids (if results are to be used for calculation of parameters of the divergent wave) should be supplemented by study of the laws of damping of spherical stress waves or data on dependence $\tau(\sigma)$, obtained in experiments at different rates of loading.

3.1. Let us consider propagation of a spherical shock wave; behind the shock wave front unloading occurs, but unloading must not be considered elastic: one should take into account internal friction.

For the unloading wave in the stress wave in a medium with internal friction we have

$$\sigma - \sigma_0 = K(e - e_0), \qquad \sigma_\theta^* - \sigma_{\theta 0} = \alpha^*(\sigma_r - \sigma_{r_0}) \qquad (3.1)$$

where the magnitudes with index 0 pertain to the state at the beginning of unloading.

At present there are no direct data on dependence $\tau(\sigma)$ during rapid change of σ. From certain data of Bridgman on the behavior of $\tau(\sigma)$ during slow loading and unloading [23] it follows that dependence $\tau(\sigma)$ during loading is similar to the same during unloading.

We determine the law of damping of spherical shock waves of stresses in the range of pressures at which internal friction appears.

For a continuous short wave we have [12]

$$r^{3-\alpha}\sigma_r^\circ = G(\xi), \qquad \sigma_r^\circ = \frac{\sigma_r}{K_1}, \quad \sigma_r = K_1 e(1 + le)$$
$$\xi = r\left[1 - \frac{\varkappa \sigma_r^\circ}{1-\alpha}\right] - a_0 t \qquad (\varkappa \sim 1) \qquad (3.2)$$

Here r — coordinate; K_1 — modulus of compression; $G(\xi)$ — arbitrary function.

Let us consider the simple case of a linear profile behind the front of the shock wave:

$$G(\xi) = C_1(\xi - \xi_0) \qquad C_1 = \text{const}$$

For a weak shock wave the propagation velocity in a medium at rest is equal to

$$D = \frac{dr}{dt} = a_0\left(1 - \frac{l}{2}\sigma_r^0\right)^{-1} \tag{3.3}$$

Determining dr/dt from (3.2) and equating it to (3.3), we find

$$\frac{dX}{X} = \frac{l}{2}\frac{C_1}{r^{2-\alpha}}\left[1 + \frac{l}{(1-\alpha)}\frac{C_1}{r^{1-\alpha}}\right]^{-1}dr \qquad (X = \sigma_r^0 r^{2-\alpha})$$

From this we obtain the law of damping of a stress shock in a medium with internal friction:

$$\frac{\sigma_r}{K_1} = \frac{C_2}{r^{2-\alpha}}\left[1 + \frac{l}{1-\alpha}\frac{C_1}{r^{1-\alpha}}\right]^{1/2} \qquad (C_2 = \text{const}) \tag{3.4}$$

As follows from (3.4), the shock wave of stresses attenuates faster than the continuous wave.

Submitted
25 February 1964

Literature

1. L. V. Al'tshuler, A. A. Bakanova, and R. F. Trunin. Shock adiabats and zero isotherms of seven metals at high pressures. Journal of experimental and theoretical physics, 1962, Vol. 42, Issue 1.

2. L. V. Al'tshuler, et al. Dynamic compressibility and the equation of state of iron at high pressures. Journal exper. and theor. physics, 1958, Vol. 34, Issue 4.

3. J. M. Walsh and M. H. Rice. Shock-Wave Compressions of Twenty-Seven Metals. Equation of state of Metals. Phys. Rev., 1957, 108, 2.

4. R. C. McQueen and S. P. Marsh. Equation of State for Nineteen Metallic Elements from Shock-Wave Measurements to Two Megabars. J. Appl. Phys., 1960, 31, 7.

5. R. W. Goranson, et al. Dynamic Determination of the Compressibility of Metals. J. Appl. Phys., 1955, 26, 12.

6. D. Bancroft, E. Peterson, and St. Minshall. Polymorphism of Iron at High Pressure. J. Appl. Phys., 1956, Vol. 27, 3.

7. S. Katz, D. G. Doran, and D. R. Curran. Hugoniot Equations of State of Aluminum and Steel. J. Appl. Phys., 1959, Vol. 30, 4.

8. St. Minshall. Properties of Elastic and Plastic Waves Determined by Pin Contactors and Crystals. J. Appl. Phys., 1955, Vol. 26, 4.

9. J. Rinehart. Some Quatitative Data Bearing on the Scabbing of Metals Under Explosive Attack. J. Appl. Phys., 1951, Vol. 22, 5.

10. A. G. Ivanov, S. A. Novikov, and V. A. Sinitsyn. Research of elasto-plastic waves in iron and steel under an explosive load Solid state physics, 1963, Vol. 5, Issue 1.

11. V. M. Gogolev, V. G. Myrkin, and G. I. Yablokova. Approximate equation of state of solids. PMTF, 1963, Issue 5.

12. A. G. Ivanov and S. A. Novikov. On shock waves of rarefaction in iron and steel, Journal exper. and theor. physics, 1961, Vol. 40, No. 6.

13. J. Wackerle. Shock Wave Compression of Quartz. J. Appl. Phys., 1962, 33, 2.

14. G. A. Adadurov, et al. Shock compression of quartz. PMTF, 1962, No. 4.

15. G. E. Duvall. Shock waves in the study of solids. Appl. Mech. Rev., 1962, 33, 2.

16. A. N. Khanukayev, I. F. Vanyagin, V. M. Gogolev, and V. G. Myrkin. On propagation of stress waves during explosion in hard rocks. Notes of Leningrad. Mining. Inst. in the name of G. V. Plekhanov, 1961, Vol. XIV, Issue 1.

17. H. R. Nichols and W. Duvall. Effect of characteristic impedance on explosion-generated strain pulses in rock. Rock. Mech. Pergamon Press, 1963.

18. L. D. Landau. On shock waves at great distances from the place of their appearance. PMM, 1945, Vol. 9, No. 4.

19. S. A. Khristianovich. Shock wave at great distances from the explosion site, PMM, 1956, Vol. XX, Issue 6.

20. J. Taylor and N. Rice. Elastic-plastic properties of iron. J. Appl. Phys., 1963, Vol. 34, 2.

21. Ye. I. Shemyakin. Stress waves during underground explosion in hard rocks. PMTF, 1963, Issue 5.

22. N. S. Medvedeva and Ye. I. Shemyakin. Waves of loading during underground explosion in rocks. PMTF, 1961, No. 6.

23. P. Bridgman. Research of large plastic flows and breaking. IL, 1955.

24. J. S. Buchanan and H. J. James. Measurement of high intensity stress pulses. Brit. J. Appl. Phys., 1959, Vol. 10, 6.

TOWARD A THEORY OF ANISOTROPIC CREEP

N. I. Malinin

(Novosibirsk)

Certain anisotropic materials have the property of anisotropic creep. Anisotropic creep will appear during the action of mechanical stresses in single crystals at high temperatures, in reinforced plastics [1], reinforced concrete, etc. During designing of certain constructions from anisotropic creeping materials there arises the necessity of estimating the magnitude of creep in a body for detecting, for instance, the distribution of stresses in it. Unfortunately, solution of such problems is hampered by the fact that the theory of anisotropic creep is extremely under-developed at present. Absent also are experimental data on research of anisotropic creep of real materials.

Below we consider certain possible variants of recording of equations of anisotropic creep. The latter, on the one hand, constitute a generalization of equations of anisotropic plasticity, and on the other, a generalization of dependences of isotropic creep. In experiments lasting 50 days we studied anisotropic creep during compression of glass-fiber-reinforced plastic AG-4S (uniform strength) at at temperature of 30°C.

1. Works, devoted to research of anisotropic creep, are not numerous. In the work of Takizawa [2] there are offered fairly general dependences of the theory of linear hereditary anisotropic bodies, consisting of a generalization of known equations of hereditary [illegible] Volterra. In monograph [3] there is [illegible] the possibility [illegible] structure for an initially and [illegible]

of potential type, whereas the potential of flow S it is proposed to take the homogeneous quadratic form

$$S = C_{ijkl}\sigma_{ij}\sigma_{kl} \qquad (1.1)$$

where C_{ijkl} – parameters of material ($C_{ijkl} = C_{jikl}$, $C_{ijlk} = C_{ijkl}$, since stress tensor σ_{ij} is symmetric; $C_{ijkl} = C_{klij}$ due to symmetry of form (1.1) with respect to σ_{ij} and σ_{kl}).

Unfortunately, the cited works on the theory of anisotropic creep cannot satisy the researcher for the following reasons. In [2] it is not indicated, even approximately, the number of parameters describing anisotropic creep, and also nothing is said about methods of determination of parameters of material from experimental data. The theory of flow, for which in [3] there is offered a potential in the form of (1.1), badly describes creep during changing stresses.

Contemporary theories of creep of an isotropic body constitute a generalization of theories of plasticity. Thus, for instance, equations of the theory of small elastoplastic flows for an isotropic body are recorded in the form

$$\varepsilon_{ij}^{p} = \Psi(T)\,\sigma_{ij}^{*} \qquad (1.2)$$

where ε_{ij}^{p} – plastic flow; σ_{ij}^{*} – component of the deviator of stresses; Ψ – function of intensity of tangent stresses T.

If we consider function Ψ (T) dependent not only on T, but also on time t, then instead of (1.2) we will have equation of one of the theories of creep – the theory of aging – where in these equations instead of ε_{ij}^{p} one should write ε_{ij}^{c} (ε_{ij}^{c} – creep).

Analogously we make generalizations of the flow theory of plasticity, equations of which for an isotropic body are recorded in the form

$$(\varepsilon_{ij}^{p})^{\cdot} = \Lambda(T)\,\sigma_{ij}^{*} \qquad (()^{\cdot} = d/dt) \qquad (1.3)$$

If we consider Λ a function not only of T, but also of time t, we obtain the theory of flow for creep; instead of $(\varepsilon_{ij}^{p})^{\cdot}$ one should as above, write $(\varepsilon_{ij}^{c})^{\cdot}$. If it is considered that Λ does not depend on t, but depends on ε_{ij} or ε_{ij}^{c}, or on the work of stresses, then we have one of the theories of hardening.

Among theories of creep the theory of heredity occupies a special place. The theory of linear heredity uses the principle of superposition, according to which deformations caused by the sum of separate stages of stresses $\Delta\sigma_{ij}$ are equal to the sum of deformations from each of $\Delta\sigma_{ij}$. Here, the laws of creep have the form of linear integral Volterra equations with a variable upper limit. For the nonlinear theory of heredity the principle of superposition no longer is observed. Equations of the nonlinear theory of heredity constitute a generalization of linear equations, where in the corresponding integral Volterra equations instead of functions $\sigma_{ij}(t)$ or $\varepsilon_{ij}^{c}(t)$ there are substituted nonlinear functions $f(\sigma_{ij})$ [4] or $f_1(\varepsilon_{ij}^{c})$ [5

Summing up what has been said above, it is possible to state that the theory of creep is a generalization of the theory of plasticity. The theory of creep, in distinction from the theory of plasticity, considers time effects. Equations of creep differ from equations of the theory of plasticity in that in the corresponding terms, determining ε^{c} (or $\cdot(\varepsilon^{c})\cdot$), along with stress (or some invarian of stress) there enters time. Thus, every theory of plasticity can, in principle, be generalized for creep, if we consider functions W or Λ or their equivalents dependent not only on stresses, but also on time.

Usually the theory of plasticity uses criteria of yielding in the form of the St. Venant criterion or the Von Mises criterion.

The St. Venant criterion of yielding was generalized for an anisotropic plastic body by A. Sawczuk [6] and D. D. Ivlev [7]. The concepts developed by A. Sawczuk and D. D. Ivlev were generalized for anisotropic creep by O. V. Sosin [8].

Unfortunately, the theory developed by A. Sawczuk and D. D. Ivlev has the following deficiency. With rotation of the principal axes the shape of the surface, depicting the condition of plasticity (or creep), will change. Consequently, changed also will be numerical values of parameters, in the equations of plasticity (or creep). Dependences of these parameters on angles of rotation are not fixed; in principle they can be discontinuous functions [7]. Thus, for complete characterization of the properties of anisotropic plasticity (creep) of a material it is necessary to carry out a very large number of experiments. In connection with this we subsequently will use the criterion of plasticity (or creep) of Von Mises for the anisotropic body, offered in [9].

The equation of the plastic potential is recorded in the Cartesian system of coordinates Oxyz, axes of which are connected with the principal axes of anisotropy. In general this equation for an anisotropic body has the form

$$S = C_{ijkl}\sigma_{ij}\sigma_{kl} = \text{const} \qquad (1.4)$$

Coefficients C_{ijkl} constitute parameters of the material. In general, criterion (1.4) contains 21 coefficients C_{ijkl}. If plastic flows are not accompanied by changes in volume, then the number of parameters C_{ijkl} decreases to 15. For an orthotropic body, incompressible during plastic flows, properties of the material are described by 9 parameters C_{ijkl} and on the principal axes of anisotropy the equation of the plastic potential is recorded in the form [10]

$$S = C_x(\sigma_y - \sigma_z)^2 + C_y(\sigma_z - \sigma_x)^2 + C_z(\sigma_x - \sigma_y)^2 + \\ + 2C_{yz}\tau_{yz}^2 + 2C_{zx}\tau_{zx}^2 + 2C_{xy}\tau_{xy}^2 = \text{const} \quad (1.5)$$

where $C_x, \ldots, C_{xy}$ – parameters of the material. Here the rate of plastic flow $(\varepsilon_{ij}^p)^\cdot$ is determined by formula

$$(\varepsilon_{ij}^p)^\cdot = \partial S / \partial \sigma_{ij} \quad (1.6)$$

In the case of imperfect plasticity S may also not be constant, and by analogy with the theory of plastic flow of potential type we can write

$$(\varepsilon_{ij}^p)^\cdot = f(\sigma_{ij})\, \partial S / \partial \sigma_{ij} \quad (1.7)$$

It is not difficult to show that the criterion of yielding $f(\sigma_{ij})$ for an anisotropic body should satisfy requirements imposed by the condition of compressibility or incompressibility of the material, and also properties of deformation symmetry. These conditions will be satisfied if as the argument of function f we take quadratic form $S^* = C^*_{ijkl}\sigma_{ij}\sigma_{kl}$, as for the elastic potential (coefficients C_{ijkl} and C^*_{ijkl} in general may not coincide). Expression (1.7) will be significantly simplified if we set $f(\sigma_{ij}) = \Phi'(S)$. Here we will have

$$(\varepsilon_{ij}^p)^\cdot = \Phi'(S)\frac{\partial S}{\partial \sigma_{ij}} = \frac{\partial \Phi}{\partial \sigma_{ij}} \quad (1.8)$$

Subsequently the theory described by equation (1.8) is generalized for the case of creep. For creep this equation has the form

$$(\varepsilon_{ij}^p)^\cdot = \frac{\partial \Phi(S, t)}{\partial S}\frac{\partial S}{\partial \sigma_{ij}} = \frac{\partial \Phi(S, t)}{\partial \sigma_{ij}} \quad (1.9)$$

2. For creep of a body Φ (see formula (1.8)) will depend not only on S, but also on time. If S is considered a parameter (such consideration is possible only when stress, and consequently also magnitude S preserve a constant value during the period of the experiment), then for a creeping body it is possible to consider

potential Φ a function of time t, i.e., $\Phi = \Phi(S,t)$. If curves of creep, obtained for different stresses, are similar, then function Φ can be presented in the form of the product of two co-factors, one of which depends only on stresses and the other, only on time, i.e.,

$$\Phi(S, t) = F(S)\theta^*(t) \qquad (2.1)$$

Subsequently it will be shown that curves of creep for identical samples of glass-fiber-reinforced plastic AG-4S, taken with different stresses, can with a sufficient degree of accuracy be considered similar. In connection with this we subsequently will use the hypothesis described by formula (2.1).

As $\theta^*(t)$ in theories of creep they frequently use an exponential function [4], i.e.,

$$\theta^*(t) = t^n \quad (n - \text{parameter of the material}). \qquad (2.2)$$

Function $\Phi(S)$ is the dependence of the rate of creep on stress. For linear creep it is possible to set

$$F(S) = S \qquad (2.3)$$

For nonlinear creep two cases are possible:

$$\partial\varepsilon^c / \partial\sigma = G \quad \text{when } t = \text{const}, \qquad \partial\varepsilon^c / \partial\sigma = \text{const} \neq 0 \quad \text{when } t = \text{const} \qquad (2.4)$$

where in the first case they usually use an exponential function of the dependence of creep on stresses [3], and in second one in the form of a hyperbolic sine wave [11-12] (or cosine wave), so that, for an anisotropic body it is possible to write

$$F(S) = S^m, \qquad F(S) = A \operatorname{ch} \sqrt{S} \qquad (2.5)$$

In these dependences the quantities m characterize the material.

3. If it is considered that dependence (1.8) is also satisfied

for alternating stresses, we arrive at one possible variant of the theory of flow during creep. If stresses do not change, equation (1.8) for creep can be written with allowance for (2.1) and (2.2) in the form

$$(\varepsilon_{ij}^{\theta})^{\cdot} = \theta^{*}(t)\,\partial F / \partial \sigma_{ij}$$

From this we easily find the equation of the creep cur. , having form

$$\varepsilon_{ij}^{c} = \frac{\partial F}{\partial \sigma_{ij}}\theta(t) \qquad \left(\theta(t) = \int_{0}^{t} \theta^{*}(t)\,dt\right) \tag{3.1}$$

If it is considered that equation (3.1) is also useful for stresses changing in time, we obtain one of the variants of the theory of aging.

As it was shown by Yu. N. Rabotnov [5], the theories of aging and flow have a deficiency, consisting of the fact that their equations are not invariant relative to the beginning of the reading of time. Therefore, these theories cannot give satisfactory solutions to problems when the loads change rapidly in time. More promising in this respect are theories of hardening and heredity.

According to the theory of hardening, in distinction from the theory of flow, function Φ (see equation (1.9)) depends on the set of parameters characterizing the state of the material [13]. In particular cases the determining parameter (along with stress) can be considered creep [14], work stresses in creeps [15], and others.

Thus we consider possible variants of construction of the theory of hardening for an anisotropic body. Let us assume that magnitude Φ in equation (1.9) depends on certain functions of stresses and strains, i.e.,

$$\Phi = \Phi[\xi(\sigma_{ij}), \zeta(\varepsilon_{ij}^{c})] \tag{3.2}$$

Functions $\xi(\sigma_{ij})$ and $\zeta(\varepsilon_{ij}^{c})$ play the role of stresses and strains, respectively, for the one-dimensional case; therefore we call them generalized stress and strain. For calculations in the case of a complex state of stress it is essential that equations (1.9) and (3.2) lead to a dependence between ξ and ζ having the same structure as formula (1.9) for uniaxial extension or compression. For an isotropic body as ξ it is convenient to take the intensity of tangent stresses, as ζ — the intensity of shearing strains during creep.

For an anisotropic body functions ξ and ζ should satisfy the requirements imposed by conditions of symmetry of deformation properties of the material. For material incompressible under creep to them we join the condition of incompressibility. As generalized stress it is possible to take, for instance, $\sqrt{S}$, which, as already noted above, satisfies the set requirements. It is possible to show that requirements concerning forms of the relationship of ζ and ξ will be satisfied if as generalized strain we take function

$$\zeta = \int_0^t (b_{ijkl}\, \dot{e}_{ij}\, \dot{e}_{kl}^{c})^{1/2}\, dt \qquad (3.3)$$

Here coefficients b_{ijkl} one can determine from equations

$$b_{ijk}\, C_{im}C_{klvr} = C_{mnpr} \qquad (3.4)$$

Between coefficients b_{ijkl} there exist the obvious relationships

$$b_{ijkl} = b_{jikl}, \quad b_{ijkl} = b_{ijlk}, \quad b_{ijkl} = b_{klij}$$

In general, system (3.4) consists of 21 linear equation with 21 unknowns b_{ijkl}. For an orthotropic body we have a system of 9 equations with 9 unknowns, disintegrating into 2 system of 6 and 3 unknowns.

Let us assume, following [15], that creep depends on the work

of stresses in creeps a. Here the equation of creep can be written in the form *

$$(\varepsilon_{ij}^c)^{\cdot} = U(a)\,\partial V(S)/\partial\sigma_{ij} = U(a)\,V'(S)\,\partial S/\partial\sigma_{ij} \qquad (3.5)$$

For a hereditary medium it is possible to generalize the nonlinear equation of M. I. Rozovskiy [4]. This equation for an anisotropic body will have the form

$$\varepsilon_{ij}^c = \int_{-\infty}^{t} \theta_1(t-\omega)\frac{\partial F(S)}{\partial\sigma_{ij}}\,d\omega = \int_{-\infty}^{t} \theta_1(t-\omega)\,F'(S)\frac{\partial S}{\partial\sigma_{ij}}\,d\omega \qquad (3.6)$$

For a linear body $F'(S) = 1$, and equation (3.6) is a particular case of the more general equation of Takizawa [2].

4. A thorough check of the theory presented in the preceding sections can be made in experiments during a complex state of stress. However, certain conclusions can also be made on the basis of experiments during simple extension (compression).

A limited check of the developed theory was undertaken on uniform-strength glass-fiber-reinforced plastic AG-4S, for which in conditions of uniaxial compression we took curves of creep.

Uniform-strength glass-fiber-reinforced plastic AG-4S is a nonhomogeneous material, glued together from alternating layers of glass fiber, where the direction of fibers in adjacent layers are mutually perpendicular. Anisotropy of deformation properties of glass-fiber plastics is a particular case of structural anisotropy. To describe elastic properties of a structurally anisotropic body, as shown in [16], it is possible to use the framework of the theory of continuous physical anisotropy. This was confirmed in a number of works (for instance, in [17]), in which it was shown that the nonhomogeneity and

*Equation (3.5) was offered by Yu. N. Rabotnov.

layered nature of a material do not play an essential role, and elastic properties of glass-fiber plastics are described by the same equations as for solid anisotropic media.

As for plastic properties and also creep of structurally anisotropic bodies, for them the framework of the theory of physical anisotropy frequently is unsuitable, and it is necessary in every concrete case to consider peculiarities of construction of the body [16]. Therefore, the theories recounted above can be considered applicable to glass-fiber-reinforced plastics only as a first approximation.

As has been noted, e.g., in [18], during experiments on compression it is necessary to pay special attention to centering of the test piece relative to the applied force. Centering is more easily ensured for short test pieces. But for short pieces essential influence on the results of tests can be rendered by non-uniformity of the state of stress near faces of the test piece, for which the problem of selection of optimum flexibility of the sample in compression experiments is of essential importance. Therefore, preliminarily we conducted a experimental check of the uniformity of the state of stress by section and length of the sample. The test piece had the shape of a rectangular parallelpiped with a cross section 14 × 14 mm and length 80 mm. For loading we used a reverser, created by the author of [18] and modified by us.

In the first series of experiments on each of the lateral faces near the center of a piece of uniform-strength AG-4S there was fastened a strain gauge with a base of 20 mm. Readings of the strain gauges were fixed by an eight-channel strain gauge installation 8ANCh-7M. It was established that readings of the strain gauges differ by not more than 5% and calculated eccentricity turned out

to be minute.

In the second series of experiments we estimated error caused by friction on faces. On one of the faces of the piece there were fastened four strain gauges with a base of 5 mm. At the edge of transducer 4 the paper sublayer was cut away as much as possible and the transducer was fastened to the actual edge of the piece. Strain gauges 3, 2 and 1 were glued approximately at distances of 1/8, 1/4, and 1/2 the length of the sample from its end. Readings of transducers 1-3 during tests practically coincided; readings of transducer 4 differed from those of the first three by not more than 6-7%. If this deviation is caused by the influence of friction on the faces, possible error caused by non-uniformity of the state of stress in the sample will not exceed 0.8-1.0%. These results are in qualitative conformity with the data of Binder and Müller [19], establishing identity of diagrams of compression and extension in very short samples for a large number of glass-fiber plastics (change of the cross sectional area of the sample during its deformation was considered in [19]).

Tests for creep were conducted on machines described in [20] at a temperature of 30 ± 0.3°C. Control of temperature was through a contact thermometer. Samples were cut from one block of uniform-strength AG-4S. Axes of the samples had different directions in space, i.e., angles φ and ψ (Fig. 1) were different. Axes x and y of the coordinate system are parallel to directions of the glass fibers in adjacent layers, axis z is perpendicular to the layers (direction upwards).

Elastic moduli for different angles φ and ψ could be determined by the magnitude of elastic deformation, developed practically

instantaneously at the moment of loading, or during unloading.

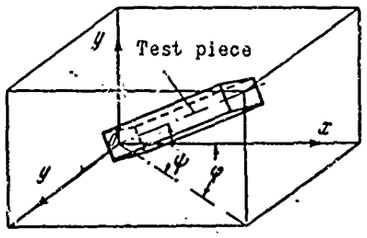

Fig. 1.

Furthermore, it was possible to calculate elastic moduli from the diagrams of compression in Fig. 2 (where there are given curves of deformation of glass-fiber plastic AG-4S: a) $\varphi = 0$, $\psi = 0$; b) $\varphi = 0$, $\psi = 90^\circ$; c) $\varphi = 45^\circ$, $\psi = 0$; d) $\varphi = 45^\circ$; $\psi = 45^\circ$; e) $\varphi = 45^\circ$, $\psi = 30^\circ$). Experiments, results of which are presented in Fig. 2, were conducted as follows. Load was applied in small equal portions and at equal intervals of time from zero to a maximum value. Strain was recorded after the addition of each new step. After the last step of load was applied, we recorded creep for 1-2 days.

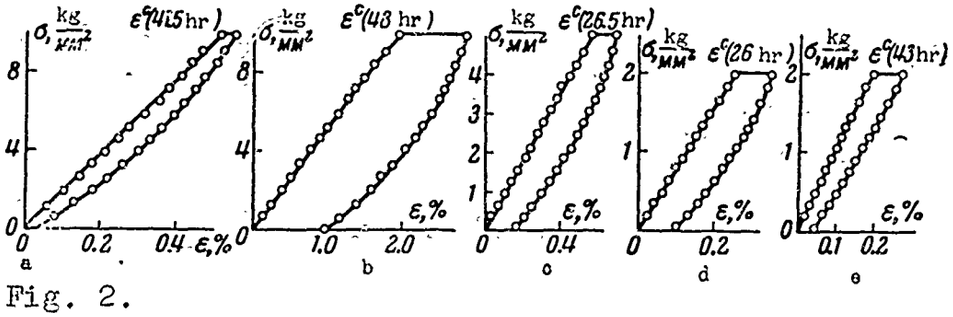

Fig. 2.

Horizontal area in the diagram of Fig. 2 thus corresponds to creep, built-up from the moment of termination of loading to the beginning of the load. After expiration of 1-2 days we produced unloading, the diagram of which is also given in Fig. 2. From the diagram of loading it was possible to determine the modulus of compression. For samples cut in direction $\varphi = \psi = 0$ the modulus of compression turned out to be equal to the elastic modulus, determined during rapid application of load.

For angles φ and $\psi = 0$ the modulus, calculated from diagrams of the type presented in Fig. 2, turned out to be 10-25% lower than

during rapid loading. These divergences are caused, apparently, by the influence of creeps, built-up in the period of loading (≈3 min).

Curves of creep of uniform-strength AG-4S for samples, cut at different angles, during loads changing in steps, are presented in Fig. 3 (where (a) $\varphi = 0$, $\psi = 0$; (b) $\varphi = 0$, $\psi = 90^\circ$; (c) $\varphi = 45^\circ$, $\psi = 0$; (d) $\varphi = 0$, $\psi = 45^\circ$; (e) $\varphi = 45^\circ$, $\psi = 45^\circ$; (f) $\varphi = 45^\circ$, $\psi = 30^\circ$). On the basis of analysis of data presented in Fig. 3 we established that the dependence of creeps on time during constant stresses may be expressed by formula

$$\varepsilon^c = Ct^{0.3} \tag{4.1}$$

where C — parameter, dependent on stresses σ and angles φ and ψ. Comparing formula (4.1) with (1.9), we see that function Φ is presented in the form of the product of two co-factors as (2.1), of which one depends only on stresses, and the other depends on time.

With respect to the dependence of creeps of glass-fiber plastic on stresses it is possible to say the following. The best way of satisfying (with stress σ constant during the period of experiment, the latter can be considered a parameter) the dependence of ε^c on σ is in the form of a hyperbolic sine wave [12]. With small loads, in connection with the fact that for small α sh $\alpha \approx \alpha$ creeps ε^c are approximately proportional to stresses, which is confirmed by [21]. During our check of the theories developed above we shall limit ourselves to the area of linear creep, i.e., we set $F(S) = S$. From the graphs presented in Fig. 3 it is clear that ε^c is approximately proportional to σ everywhere except the curves in Fig. 3a and c for stresses of 10 and 5 kg/mm^2, respectively.

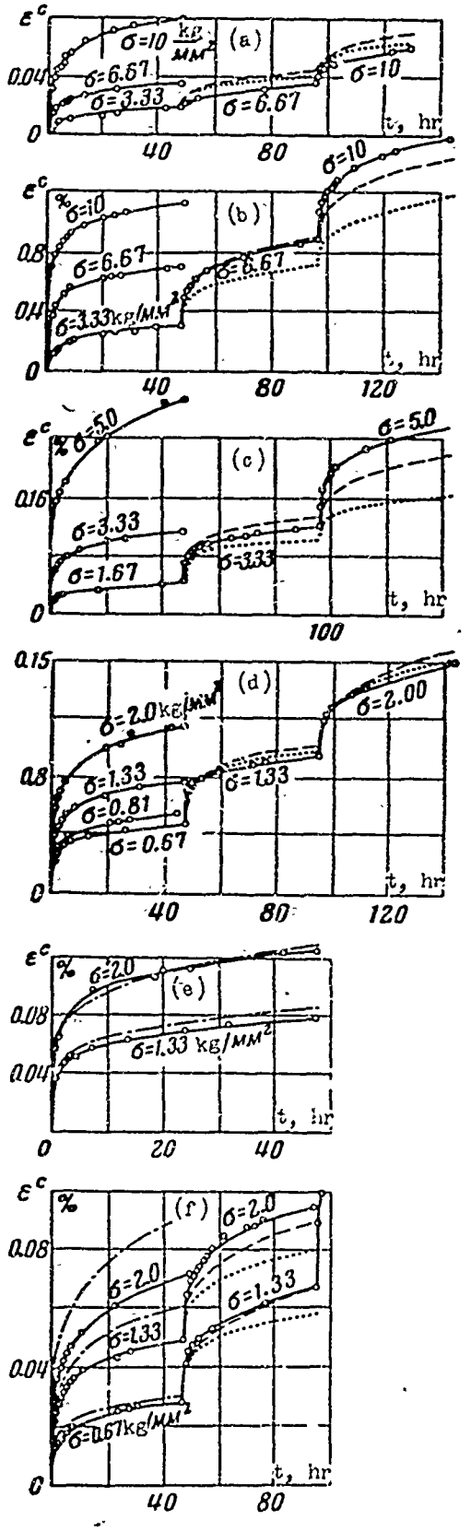

Fig. 3.

From the graphs in Fig. 3a, b, c, and d it is possible to calculate parameters $C_x = C_y$ (since densities of reinforcement by glass fibers in directions x and y are identical), C_z, $C_{yz} = C_{zx}$ and C_{xy}. As a result of analysis of data for glass-fiber-reinforced plastic AG-4S (uniform-strength) at a temperature of 30°C we obtain values $C_x = C_y = 10.7 \cdot 10^{-5}$; $C_z = -9.35 \cdot 10^{-5}$; $C_{xy} = 2.0 \cdot 10^{-5}$, $C_{yz} = C_{zx} = 14.2 \cdot 10^{-5}$ $kg^{-1}mm^2hours^{-0.2}$. With the help of equations (1.9) taking into account (1.5), (2.1), and (4.1), there are constructed curves of creep (theoretical) for angles $\varphi = \psi = 45^\circ$ and $\varphi = 45^\circ$, $\psi = 30^\circ$ for stresses of 0.67, 1.33, and 2 kg/mm^2, depicted in Fig. 3e and f by dot-dash lines. Here, for the same stresses there are given experimental curves. For direction $\varphi = \psi = 45^\circ$, as one can see from Fig. 3e, experimental curves correspond well to theoretical ones. For $\varphi = 45^\circ$, $\psi = 30^\circ$ errors are somewhat higher and reach 25%. However, these errors are still small as compared with errors which could be obtained by ignoring the anisotropy of creep.

For checking above-described theory for variable stresses, on one of samples from each series we formulated experiments in which

load upon the expiration of a definite period increased in stages. Curves of creep for loads varying intermittently are presented also in Fig. 3. Here the dash lines plot "theoretical" curves of creep; here we used the hypothesis of hardening of Yu. N. Rabotnov, descril by equation (3.5) taking into account (1.5), (2.1), and (4.1). Dependences U(a) and V(S) were selected in the form of exponential functions, i.e., $U = ka^{-\alpha}$ and $V = S^{\beta}$; for AG-4S we obtained values $\alpha = 4$ and $\beta = 5$. Dotted lines plot "theoretical" curves of creep according to the theory of heredity described by equation (3.6) taking into account (1.5), (2.1), (2.3), and (4.1). From Fig. 3 it is clear that experimental curves are close to theoretical ones everywhere, with the exception of the region where stresses are too high.

(All experiments, results of which are shown in Fig. 3, were repeated. Creeps differed in parallel experiments by not more than 15%. The relatively small magnitude of scattering was, apparently, caused by the fact that samples are cut from the same plate.)

Analogous calculations were carried out for the theories of aging and flow. Here we obtained the already known fact that these theories satisfactorily describe the process of creep only during smoothly-varying loads. During sharp changes of stresses the theori of aging and flow give results significantly deviating from experime

Subsequently it is necessary to create a more universal theory of creep for reinforced plastics, which should consider features of structural anisotropy of these materials, different nonlinear effect and which would, furthermore, be useful for description of the behavior of material during non-monotonically changing loads, as for

instance, in [22].

Submitted
25 December 1963

Literature

1. N. I. Malinin. Creep of a reinforced layer during biaxial extension. PMTF, 1962, No. 6.

2. E. I. Takizawa. Rheological theory of anisotropic media. Memoirs of the Faculty of Engineering Nagoya Univ., 1956, Vol. 8, No. 1, 118.

3. L. M. Kachanov. Theory of creep. Fizmatgiz, 1960.

4. M. I. Rozovskiy. Creep and prolonged deterioration of materials. Journal of tech. physics, 1951, Vol. 21, No. 11.

5. Yu. N. Rabotnov. Certain questions of the theory of creep. Herald of Moscow State University, 1948, No. 10.

6. A. Sawczuk. Linear theory of plasticity of anisotropic bodies and its applications to problems of limit analysis. Arch. Mechaniki Stosowanej, 1959, 5, No. 5.

7. D. D. Ivlev. To a theory of ideal plastic anisotropy. PMM, 1959, 23, No. 6.

8. O. V. Sosnin. Steady anisotropic creep of disks. PMTF, 1963, No. 4.

9. R. Von Mises. Mechanik der plastishen Formänderung von Kristallen. ZAMM, 1928, 8, No. 3.

10. R. Hill. A theory of the yielding and plastic flow of anisotropic metals. Proc. Roy. Soc., Ser. A., 1948, A193, 1033, 281.

11. A. Nadai. Influence of time on creep. In coll. Theory of plasticity, Edited by Yu. N. Rabotnov, IL. 1948.

12. W. Findley. Creep and relaxation of plastics. Machine Design, 1960, Vol. 32, No. 10.

13. Yu. N. Rabotnov. On creep rupture. PMTF, 1963, No. 2.

14. Yu. N. Rabotnov. On certain possibilities of describing unsteady creep with application of research of creep of rotors. News of AS of USSR, Dept. of Tech. Sci., 1957, No. 5.

15. N. Rabotnov. On the equations of state for creep. In coll. Progress in applied mechanics. The Prager anniversary volume. Macmillan Co., N.Y., 1963, p. 307.

16. Yu. V. Nemirovskiy. Supporting power of round reinforced plates. News of AS of USSR, Dept. of Tech. Sci., Mechanics and machine building, 1963, No. 2.

17. A. L. Rabinovich, M. G. Shtarkov, and Ye. I. Dmitriyeva. Methods of determination and magnitude of elastic constants of fiber-glass laminate at high temperature. Trans MFTI, Oborongiz, 1958. Issue 1, p. 115.

18. N. G. Torshenov. Creep of aluminum alloy D16T during compression. PMTF. 1961, No. 6.

19. G. Binder and F. H. Müller. Nicht-lineare Deformation. I. Stauchung zilindrischen Proben. Kolloid Z., 1961, 177, No. 2.

20. L. V. Bayev, N. I. Malinin, Yu. N. Rabotnov, and I. A. Shubin. Plant for tests of plastics for creep and relaxation. Factory laboratory, 1962, 28, No. 4.

21. G. I. Bryzgalin. Description of anisotropic creep of glass-fiber-reinforced plastics. PMTF, 1963, No. 6.

22. G. I. Bryzgalin. On creep under variable stresses. PMTF, 1962, No. 3.

ON SINGLE-COMPONENT BEAMS OF LIKE-CHARGED PARTICLES

V. A. Syrovoy

(Moscow)

By single-component is understood flow in the direction of one of the coordinate axes (for instance, in the x^1-direction) of an arbitrary orthogonal system of coordinates x^i ($i = 1, 2, 3$). Below, the question about coordinate systems allowing such flows is investigated. It is shown that in the two-dimensional case (§ 2) single-component flows are possible only in three orthogonal coordinate systems: Cartesian x, y, polar R, ψ, and helical q_1, q_2. In three-dimensional space (§ 3) there are considered coordinate systems for which

$$g_{11} = h_1(x^1)\,h_2(x^2)\,h_3(x^3), \qquad g_{22} = k(x^2)\,K(x^1, x^3), \qquad g_{33} = l(x^3)\,L(x^1, x^2)$$

Here, to the three cylindrical coordinate systems, corresponding to the shown two-dimensional systems, there are added spherical coordinates r, θ, ψ.

§ 1. Formulation of the problem and fundamental equations. A monoenergetic non-relativistic beam of like-charged particles in the stationary case in the absence of an external magnetic field is described, as we know [1, 2], by one nonlinear fourth order differential equation for W — action per particle mass. In the arbitrary curved system of coordinates x^i ($i = 1, 2, 3$) the metric, in which there is given by relationship

$$dS^{(2)} = g_{ik}\,dx^i\,dx^k \qquad (1.1)$$

this equation, has the form

$$\frac{\partial}{\partial x^m}\left\{ g^{mn}\frac{\partial W}{\partial x^n}\frac{\partial}{\partial x^j}\left[\sqrt{g}\,g^{jl}\frac{\partial}{\partial x^l}\left(g^{ik}\frac{\partial W}{\partial x^i}\frac{\partial W}{\partial x^k}\right)\right]\right\}=0 \qquad (1.2)$$

Clarification of the question of those orthogonal systems of coordinates which allow single-component flows is the subject of a series of works [3-8]. However, their goal was to obtain necessary and sufficient conditions for the possibility of a single-component flow in the x^1-direction (abbreviated as x^1-flow). The question of the existence in the given system of coordinates of x^1-flow was solved by means of application of developed criteria to the metric tensor of this system. It is clear that the number of coordinate systems satisfying these criteria could not be established because with such an approach it was necessary to act by trial-and-error. Thus in [6] they studied eleven curvilinear coordinate systems, encountered in the theory of electromagnetic fields.

In [2, 3] it is shown that in the case of flow in x^1-direction equation (1.2) takes form

$$f(x)w^{1/2}\frac{d^2w}{(dx^1)^2}+\frac{\partial f(x)}{\partial x^1}w^{1/2}\frac{dw}{dx^1}+h(x)w^{3/2}=F(x^2,x^3)$$
$$f(x)=[(g^{11})^5 g_{22}g_{33}]^{1/4},\quad h(x)=\frac{(g_{11})^2}{\sqrt{g}}\frac{\partial}{\partial x^i}\left(\sqrt{g}\,g^{ik}\frac{\partial g^{11}}{\partial x^k}\right),\quad w=\left(\frac{dW}{dx^1}\right)^2 \qquad (1.3)$$

Here $F(x^2, x^3)$ is a certain function, appearing as a result of integration with respect to x^1, and $f(x) = f(x^1, x^2, x^3)$. Since components of the metric tensor, having in orthogonal coordinates a diagonal form, depend, in general, on all three coordinates, and $w = w(x^1)$, on g_{hh} (h – fixing index) there shold be placed certain limitations. Sufficient conditions of the possibility of x^1-flow were obtained in [7] proceeding from the requirement that equation (1.3) be an ordinary differential equation for w, and consist of the

following:

$$f(x) = \Phi(x^1) F(x^2, x^3) + G(x)$$
$$f(x) h(x) = \Psi(x^1) F(x^2, x^3) + H(x) \qquad (1.4)$$

For w we have equation

$$\Phi(x^1) w'' + \Phi'(x^1) w' + \Psi(x^1) w = w^{-1/3} \qquad (1.5)$$

Here Φ, Ψ – certain functions of x^1, and G, H, and w are connected thus:

$$G(x) \frac{d^2w}{(dx^1)^2} + \frac{\partial G(x)}{\partial x^1} \frac{dw}{\partial x^1} + H(x) w = 0 \qquad (1.6)$$

When G = H = 0 formulas (1.4) determine conditions, fixed earlier in [3]:

$$f(x) = \Phi(x^1) F(x^2, x^3), \qquad h(x) = \Psi(x^1) \qquad (1.7)$$

Conditions (1.4) and (1.7) pertain to two qualitatively different classes of flows. For satisfaction of boundary conditions on the emitter the solution should contain two arbitrary constants. If, however, on the metric there are imposed limitations (1.4), then it will have not more than one arbitrary constant. In this sense, solutions for which (1.4) is satisfied are degenerate. Solutions of this type were validly contrasted in [3, 4] to solutions, describing single-component flows from a surface on which there are realized conditions of thermal emission. Actually, expressing w" from (1.6) and substituting it in (1.5), we have

$$\left[\Phi'(x^1) - \frac{\partial \ln G(x)}{\partial x^1} \Phi(x^1)\right] \frac{dw}{dx^1} + \left[\Psi(x^1) - \frac{H(x)}{G(x)} \Phi(x^1)\right] w = \frac{1}{\sqrt{w}} \qquad (1.8)$$

Requiring, as above, that (1.8) be an ordinary differential equation for w, we obtain

$$\Phi'(x^1) - \frac{\partial \ln G(x)}{\partial x^1}\Phi(x^1) = \alpha(x^1) + U(x)$$
$$\Psi(x^1) - \frac{H(x)}{G(x)}\Phi(x^1) = \beta(x^1) + V(x) \qquad (1.9)$$

$$\alpha(x^1)\frac{dw}{dx^1} + \beta(x^1)w = \frac{1}{\sqrt{w}}, \qquad U(x)\frac{dw}{dx^1} + V(x)w = 0 \qquad (1.10)$$

It is easy to prove that solutions of [9, 10] given in [4, 5]

$$W = x^1, \qquad (1)\quad x^1 = {}^1/_2(x^2 - y^2),$$
$$(2)\quad x^1 = \mathrm{Re}\,(2i \ln \mathrm{sc}\, z) \qquad (z = x + iy) \qquad (1.11)$$

simultaneously satisfy equations (1.6) and (1.10). They correspond to the case when U = V = 0 and

$$f = 1/g = \Phi(x^1)F(x^2) + K(x^1)L(x^2) \qquad (g = |g_{ik}|)$$

For the first of them Φ = L = 1; for the second Φ = 1. In each of cases (1) and (2) solutions (1.11) will, apparently, be the only possible ones.

Subsequently we will be interested in systems of coordinates, for which we have conditions (1.7), and, consequently, nondegenerate solutions.

Besides fulfillment of conditions (1.7) it is necessary that the metric be Euclidean. This requirement is expressed by equality to zero of the Riemann-Christoffel tensor [11]

$$R^{p}_{.rst} = 0 \qquad (1.12)$$

or of the symmetric tensor of second order S^{ij}

$$S^{ij} = (4g)^{-1}e^{ikl}e^{jmn}R_{klmn} = 0 \qquad (R_{prst} = g_{pm}R^{m}_{.rst}) \qquad (1.13)$$

Conditions (1.13) are called Lamé identities and in detailed notation have form [12]

$$2\frac{\partial^2 \ln g_{\alpha\alpha}}{\partial x^\beta \partial x^\gamma} + \frac{\partial \ln g_{\alpha\alpha}}{\partial x^\beta}\frac{\partial \ln g_{\alpha\alpha}}{\partial x^\gamma} - \frac{\partial \ln g_{\alpha\alpha}}{\partial x^\beta}\frac{\partial \ln g_{\beta\beta}}{\partial x^\gamma} - \frac{\partial \ln g_{\alpha\alpha}}{\partial x^\gamma}\frac{\partial \ln g_{\gamma\gamma}}{\partial x^\beta} = 0 \qquad (1.14)$$

$$g_{\alpha\alpha}\left[2\frac{\partial^2 \ln g_{\alpha\alpha}}{(\partial x^\beta)^2}+\frac{\partial \ln g_{\alpha\alpha}}{\partial x^\beta}\frac{\partial}{\partial x^\beta}\ln\frac{g_{\alpha\alpha}}{g_{\beta\beta}}\right]+g_{\beta\beta}\left[2\frac{\partial^2 \ln g_{\beta\beta}}{(\partial x^\alpha)^2}+\frac{\partial \ln g_{\beta\beta}}{\partial x^\alpha}\frac{\partial}{\partial x^\alpha}\ln\frac{g_{\beta\beta}}{g_{\alpha\alpha}}\right]+$$
$$+g^{\gamma\gamma}\frac{\partial g_{\alpha\alpha}}{\partial x^\gamma}\frac{\partial g_{\beta\beta}}{\partial x^\gamma}=0 \qquad (1.15)$$

Three conditions (1.14) unite identities $R_{\beta\alpha\alpha\gamma} = 0$, and three conditions (1.15) unite identities $R_{\beta\alpha\alpha\beta} = 0$; here α, β, γ – fixing indices and $\alpha \neq \beta \neq \gamma$.

In §§ 2, 3 there is an attempt to obtain a solution of equations (1.14) and (1.15) during fulfillment of conditions (1.7) in a plane and in three-dimensional space. Analogous research for the Schroedinge equation was conducted by Eisenhart [13-15]. Linearity of the equation under analysis facilitated complete solution of the problem: in [13-15] there are shown eleven curvilinear orthogonal systems in which the wave function of a particle can be presented in the form $\Psi = \prod_i \Psi_i(x^i)$. Below there is considered a more specific problem: there are found systems of coordinates in which $W = W(x^1)$.

§ 2. Plane flows. Without loss of generality one may assume that an arbitrary orthogonal system of coordinates in a plane is given by expressions of form [16]

$$x^1 = \mathrm{Re}\, f(z), \quad x^2 = \mathrm{Im}\, f(z) \qquad (z = x + iy) \qquad (2.1)$$

Here f(z) – certain analytic function of complex variable z. In this case

$$g_{11} = g_{22} = \sqrt{g} \qquad (g = |g_{ik}|) \qquad (2.2)$$

Using (2.2), we obtain conditions (1.7) in the form

$$\frac{1}{g} = \Phi(x^1)F(x^2), \quad \sqrt{g}\,\Delta\frac{1}{\sqrt{g}} = \Psi(x^1) \qquad \left(\Delta = \frac{\partial^2}{(\partial x^1)^2}+\frac{\partial^2}{(\partial x^2)^2}\right) \qquad (2.3)$$

All equations of (1.14) and (1.15) are satisfied identically, with the exception of one: $S^{33} = 0$ or $R_{1212} = 0$

$$\Delta(\sqrt{g}) = \frac{1}{\sqrt{g}}\left[\left(\frac{\partial\sqrt{g}}{\partial x^1}\right)^2 + \left(\frac{\partial\sqrt{g}}{\partial x^2}\right)^2\right] \qquad (2.4)$$

This equation and the second condition of (2.3) can be presented in the form

$$\frac{1}{4g^2}\left[\left(\frac{\partial g}{\partial x^1}\right)^2 + \left(\frac{\partial g}{\partial x^2}\right)^2\right] = \Psi(x^1), \qquad \Delta g = \frac{1}{g}\left[\left(\frac{\partial g}{\partial x^1}\right)^2 + \left(\frac{\partial g}{\partial x^2}\right)^2\right] \qquad (2.5)$$

Using the expression for the determinant of the metric tensor from (2.3), we obtain equations for determination of $\varphi = \Phi^{-1}$, $f = F^{-1}$ and

$$\frac{\varphi'^2}{\varphi^2} - \Psi = \frac{f'^2}{f^2} = b^2, \quad \frac{\varphi''}{\varphi} - \frac{\varphi'^2}{\varphi^2} = -\frac{f''}{f} + \frac{f'^2}{f^2} = \delta. \quad (b, \delta = \text{const}) \qquad (2.6)$$

The first of these equations shows that $f \sim \exp(bx^2)$. Substituting this expression in the second equation of (2.6) we find that $\delta = 0$. Consequently, $\varphi \sim \exp(ax^1)$, and $\Psi = a^2 - b^2$. Thus, the general solution of equations (2.5) has the form

$$g = \gamma \exp(\alpha x^1 + \beta x^2), \qquad \Psi = a^2 - b^2 \qquad (\alpha = -a, \ \beta = -b) \qquad (2.7)$$

When $\gamma = 1$, $\alpha = \beta = 0$ we obtain Cartesian coordinates x, y; when $\gamma = 1$ and $\alpha \neq 0$, $\beta = 0$ or $\alpha = 0$, $\beta \neq 0$ expression (2.7) corresponds to coordinates ln R, ψ. Spiral coordinates q_1, q_2 are determined by formulas (2.1) when

$$f(z) = (b_1 + ib_2) / (b_1^2 + b_2^2) \ln z \qquad (b_1, b_2 = \text{const})$$

In spiral coordinates

$$g = (b_1^2 + b_2^2)^2 \exp[4(b_1 q_1 + b_2 q_2)] \qquad (2.8)$$

It is clear that when $\gamma = (b_1^2 + b_2^2)^2$, $\alpha = 4b_1$, $\beta = 4b_2$, formula (2.7) passes into (2.8). In each of the enumerated coordinate systems single-component flows are possible in the direction of any coordinate axis. Emitting surfaces can be plane x, y = const, cylinders R = = const, half-plane ψ = const, spiral cylinders q_1, q_2 = const. Here,

particles move in straight lines, circles or spirals.

§ 3. Three-dimensional flows. Conditions of a space being Euclidean (1.14), (1.15) in detailed notations have form

$$2p_{23}^{1} + p_2^1 p_3^1 - p_2^1 p_3^2 - p_3^1 p_2^3 = 0 \tag{3.1}$$

$$2p_{13}^{2} + p_1^2 p_3^2 - p_3^1 p_1^2 - p_3^2 p_1^3 = 0 \tag{3.2}$$

$$2p_{12}^{3} + p_1^3 p_2^3 - p_1^2 p_2^3 - p_2^1 p_1^3 = 0 \tag{3.3}$$

$$p_k^h = \frac{\partial \ln g_{hh}}{\partial x^k}, \qquad p_{kl}^h = \frac{\partial^2 \ln g_{hh}}{\partial x^k \partial x^l}$$

$$2\left[\frac{\partial^2 g_{22}}{(\partial x^3)^2} + \frac{\partial^2 g_{33}}{(\partial x^2)^2}\right] = -g^{11}\frac{\partial g_{22}}{\partial x^1}\frac{\partial g_{33}}{\partial x^1} + g^{22}\left[\left(\frac{\partial g_{22}}{\partial x^3}\right)^2 + \frac{\partial g_{22}}{\partial x^3}\frac{\partial g_{33}}{\partial x^2}\right] + g^{33}\left[\left(\frac{\partial g_{33}}{\partial x^2}\right)^2 + \frac{\partial g_{22}}{\partial x^3}\frac{\partial g_{33}}{\partial x^3}\right] \tag{3.4}$$

$$2\left[\frac{\partial^2 g_{33}}{(\partial x^1)^2} + \frac{\partial^2 g_{11}}{(\partial x^3)^2}\right] = g^{11}\left[\left(\frac{\partial g_{11}}{\partial x^3}\right)^2 + \frac{\partial g_{11}}{\partial x^1}\frac{\partial g_{33}}{\partial x^1}\right] - g^{22}\frac{\partial g_{11}}{\partial x^2}\frac{\partial g_{33}}{\partial x^2} + g^{33}\left[\left(\frac{\partial g_{33}}{\partial x^1}\right)^2 + \frac{\partial g_{11}}{\partial x^3}\frac{\partial g_{33}}{\partial x^3}\right] \tag{3.5}$$

$$2\left[\frac{\partial^2 g_{11}}{(\partial x^2)^2} + \frac{\partial^2 g_{22}}{(\partial x^1)^2}\right] = g^{11}\left[\left(\frac{\partial g_{11}}{\partial x^2}\right)^2 + \frac{\partial g_{11}}{\partial x^1}\frac{\partial g_{22}}{\partial x^1}\right] - g^{33}\frac{\partial g_{11}}{\partial x^3}\frac{\partial g_{22}}{\partial x^3} + g^{22}\left[\left(\frac{\partial g_{22}}{\partial x^1}\right)^2 + \frac{\partial g_{11}}{\partial x^2}\frac{\partial g_{22}}{\partial x^3}\right] \tag{3.6}$$

Here there can be presented the following cases:

1°. $p_3^2 \neq 0,\ p_2^1 = p_3^1 = 0;$ 2°. $p_3^1 \neq 0,\ p_1^2 = p_3^2 = 0$

3°. $p_3^1 = 0,\ p_3^2 = 0;$ 4°. $p_3^1 \neq 0,\ p_3^2 \neq 0$

Final results in the three-dimensional case can be obtained if we assume that

$$g_{11} = h_1(x^1)\, h_2(x^2)\, h_3(x^3), \quad g_{22} = k(x^2)\, K(x^1, x^3), \quad g_{33} = l(x^3)\, L(x^1, x^2)$$

The first conditicn of (1.7) is satisfied only when K and L are presented in the form of the product of functions which depend on x^1 and x^3, x^1 and x^2, respectively. Introduction of new variables is possible in order to get

$$g_{hh} = \prod_{i \neq h} f_i(x^i) \tag{3.7}$$

1°. In this case, on the basis of what has been said, one should consider that $g_{11} = 1$. The second condition of (1.7) is here

satisfied identically. Using the first condition of (1.7) we obtain a solution of equation (3.2):

$$g_{22} = \sqrt{\Phi(x^1)}\, S(x^2, x^3) + T(x^1, x^2) \tag{3.8}$$

Then the following noncontradictory combinations are possible

$$\left.\begin{array}{ll} \alpha) & p_1^2 \neq 0, \quad p_3^1 \neq 0 \\ \beta) & p_1^2 = 0, \quad p_1^3 = 0 \end{array}\right\} \; p_2^3 \neq 0, \qquad \left.\begin{array}{ll} \gamma) & p_1^2 \neq 0, \quad p_1^3 \neq 0 \\ \delta) & p_1^2 = 0, \quad p_1^3 \neq 0 \end{array}\right\} \; p_2^3 \neq 0$$

α) When $p_2^3 \neq 0$ equation (3.3) gives for g_{33}

$$g_{33} = \sqrt{\Phi(x^1)}\, U(x^2, x^3) + V(x^1, x^3) \tag{3.9}$$

Solving equations (3.5), (3.6), we have

$$g_{22} = [\alpha(x^2, x^3)\, x^1 + \beta(x^2, x^3)]^2, \quad g_{33} = [\gamma(x^2, x^3)\, x^1 + \delta(x^2, x^3)]^2 \tag{3.10}$$

Analyzing different situations, conceived of as possible for simultaneous satisfaction of (3.8)-(3.10), we find that only one of them has meaning, T = V = 0 (or $\beta = \delta = 0$). Thus

$$g_{11} = 1, \qquad g_{22} = (x^1)^2 S(x^2, x^3), \qquad g_{33} = (x^1)^2 U(x^2, x^3)$$

Functions S and U are connected by equation (3.4)

$$2\left[\frac{\partial^2 S}{(\partial x^3)^2} + \frac{\partial^2 U}{(\partial x^3)^2}\right] + 4US = \frac{\partial \ln US}{\partial x^2}\frac{\partial U}{\partial x^3} + \frac{\partial \ln US}{\partial x^3}\frac{\partial S}{\partial x^3} \tag{3.11}$$

Assuming that (3.7) is valid, i.e., $S = S(x^3)$, $U = U(x^2)$, we obtain instead of (3.11)

$$[2S'' - S'(\ln S)'] + [2U'' - U'(\ln U)'] + 4US = 0$$

Considering that $p_2^3 \neq 0$ and, consequently, $U \neq \text{const}$, we have the sole possibility for which this equation exists

$$S = 1, \qquad 2UU'' - U'^2 + 4U^2 = 0 \tag{3.12}$$

Solving equation (3.12), we obtain

$$g_{11} = 1, \qquad g_{22} = (x^1)^2, \qquad g_{33} = (x^1 \sin x^2)^2 \tag{3.13}$$

Formulas (3.13) determine the metric in spherical coordinates r, θ, ψ. The considered case shows the possibility of r-flow.

β) All conditions of the space being Euclidean, except equation (3.4), are satisfied identically. From (3.8), (3.9) and $p_1^2 = p_1^3 = 0$ it follows that $\Phi = 1$, $T = V = 0$, $g_{22} = S(x^2, x^3)$, $g_{33} = U(x^2, x^3)$.

Conditions (1.7) here are satisfied. With the same assumptions as in the preceding point, we obtain formula (1.1) in the form

$$dS^{(2)} = (dx^1)^2 + S(x^3)(dx^2)^2 + U(x^2)(dx^3)^2$$

Introducing new variables ξ, η, ζ by formulas

$$\xi = x^1, \qquad dx^2 = \sqrt{U(x^2)}\,d\eta, \qquad dx^3 = \sqrt{S(x^3)}\,d\zeta$$

we change the expression for $dS^{(2)}$ as follows

$$dS^{(2)} = d\xi^2 + U(\eta)\,S(\zeta)(d\eta^2 + d\zeta^2) \tag{3.14}$$

Formula (3.14) determines the metric in a certain cylindrical coordinate system, where flow is carried out in z-direction ($\xi = z$). Since in Cartesian coordinates x, y, z flow is possible in the direction of any axis, the form of functions U and S may not be of interest. Case γ) leads to the same result as α).

δ) Considering (3.7), we obtain $g_{hh} = 1$. These are Cartesian coordinates.

2°. In this case $g_{22} = 1$, and possible are the following noncontradictory combinations

$$\left.\begin{array}{ll} \alpha) & p_2^1 \neq 0, \quad p_2^3 \neq 0 \\ \beta) & p_2^1 = 0, \quad p_2^3 = 0 \end{array}\right\} \; p_1^3 \neq 0, \qquad \left.\begin{array}{ll} \gamma) & p_2^1 \neq 0, \quad p_2^3 \neq 0 \\ \delta) & p_2^1 \neq 0, \quad p_2^3 = 0 \\ \varkappa) & p_2^1 = 0, \quad p_2^3 = 0 \end{array}\right\} \; p_1^3 = 0$$

α) Equations (3.4), (3.6) give for g_{11} and g_{33} expressions of form

$$g_{11} = [\alpha(x^1, x^3)\,x^2 + \beta(x^1, x^3)]^2, \quad g_{33} = [\gamma(x^1, x^3)\,x^2 + \delta(x^1, x^3)]^2 \tag{3.15}$$

The first condition of (1.7) is satisfied in two cases:

$$\text{(1)}\quad \delta = \beta = 0, \qquad g_{11} = (x^2)^2 S(x^1, x^3), \qquad g_{22} = (x^2)^2 U(x^1, x^3)$$
$$\text{(2)}\quad g_{11} = g_{33} = f(x^3)\,[\alpha(x^3)\,x^2 + \beta(x^3)]^2$$

In the first case equations (3.1)-(3.3) are satisfied identically; the second is valid when $p_{23}^{1} = 0$, i.e., when $\alpha \sim \beta$, and thus coincides with case (1). Functions U and S are connected by a relationship obtained from (3.5),

$$2\left[\frac{\partial^2 S}{(\partial x^3)^2} + \frac{\partial^2 U}{(\partial x^1)^2}\right] + 4US = \frac{\partial \ln US}{\partial x^1}\frac{\partial U}{\partial x^1} + \frac{\partial \ln US}{\partial x^3}\frac{\partial S}{\partial x^3}$$

which, with fulfillment of (3.7), gives a solution in the form

$$g_{11} = (x^2)^2, \qquad g_{22} = 1, \qquad g_{33} = (x^2 \sin x^1)^2 \tag{3.16}$$

Formulas (3.16) determine the metric in spherical coordinates r, θ, ψ with flow in the θ-direction.

β) In this case $g_{11} = S(x^1, x^3)$, $g_{22} = 1$, $g_{33} = U(x^1, x^3)$, where for U and S there remain equation (3.5) and conditions (1.7)

$$2\left[\frac{\partial^2 S}{(\partial x^3)^2} + \frac{\partial^2 U}{(\partial x^1)^2}\right] = \frac{\partial \ln US}{\partial x^1}\frac{\partial U}{\partial x^1} + \frac{\partial \ln US}{\partial x^3}\frac{\partial S}{\partial x^3} \tag{3.17}$$

With fulfillment of (3.7) the first condition of (1.7) is satisfied identically, and (3.17) and the second condition of (1.7) take the form

$$2U'' - U'(\ln U)' = -2S'' + S'(\ln S)' = a, \quad 2S'' - 3S'(\ln S)' = b \quad (a, b = \text{const})$$

Joint solution of the two equations for S shows that $S = (x^3)^2$. Consequently, a = 0 and $U = (x^1)^2$. Thus

$$dS^{(2)} = (x^3 dx^1)^2 + (dx^2)^2 + (x^1 dx^3)^2$$

Introducing new variables from formulas

$$x^1 = b_1^{-1}\sqrt{b_1^2 + b_2^2}\, e^{b_1 q_1}, \qquad x^2 = z, \qquad x^3 = b_2^{-1}\sqrt{b_1^2 + b_2^2}\, e^{b_1 q_3}$$

we obtain for $dS^{(2)}$ an expression, determining the metric in a spiral cylindrical coordinate system. Here flows in the q_1- and q_2-directions are possible.

γ) Solving equations (3.4), (3.6), we have

$$g_{11} = [\alpha(x^1, x^3)\, x^2 + \beta(x^1, x^3)]^2, \qquad g_{33} = [\gamma(x^3)\, x^2 + \delta(x^3)]^2 \qquad (\alpha, \gamma \neq 0)$$

The first condition of (1.7) is satisfied if $\beta = \delta = 0$, and $\alpha(x^1, x^3) = \alpha_1(x^1)\alpha_3(x^3)$. Thus, the solution can be sought in the form

$$g_{11} = (x^2)^2 S(x^3), \quad g_{22} = 1, \quad g_{33} = (x^2)^2$$

Just as and in α), there exists the possibility of fulfillment of the first condition of (1.7) for $g_{11} = g_{33}$; from consideration of (3.1) it follows that this case is included in the preceding one. Equation (3.5) takes form (3.12) for S. Thus

$$dS^{(2)} = (x^2 \sin x^3 dx^1)^2 + (dx^2)^2 + (x^2 dx^3)^2$$

This corresponds to flow in the ψ-direction in coordinates r, θ, ψ.

δ) In this case $g_{22} = 1$, $g_{33} = 1$. Solving (3.5), we obtain

$$g_{11} = [\alpha(x^1, x^2)\, x^3 + \beta(x^1, x^2)]^2$$

The first condition of (1.7) exists in two cases:

$$(1) \quad \beta = 0, \; g_{11} = (x^3)^2 S(x^1, x^3), \qquad (2) \quad g_{11} = [\alpha(x^2)\, x^3 + \beta(x^2)]^2$$

The first of them contradicts the initial assumptions, since from consideration of (3.1) it follows that $p_2^1 \cdot p_3^1 = 0$. In the second case solution of (3.1) and (3.6) gives for g_{11}

$$g_{11} = (\alpha x^2 + x^3)^2 \qquad (\alpha = \text{const})$$

We now introduce instead of x^2 and x^3 new orthogonal coordinates

$$\xi = x^1, \qquad \eta = \alpha x^2 + x^3, \qquad \zeta = -x^2 + \alpha x^3$$

In the new coordinates

$$dS^{(3)} = \eta^2 d\xi^2 + d\eta^2 + d\zeta^2 \qquad (3.18)$$

Formula (3.18) determines the metric in coordinates R, ψ, z with flow in ψ-direction. Consideration of n leads to the same result.

3°. We immediately consider that we have limitation (3.7). Then, requiring fulfillment of the first condition of (1.7), we have

$$g_{11} = S(x^2), \qquad g_{22} = T(x^1), \qquad g_{33} = U(x^1)V(x^2)$$

Considering (3.3), we find that there can exist the following cases:

(α) $(\ln S)'/(\ln V)' = a$, $(\ln T)'/(\ln U)' = 1 - a$ $(U', V' \neq 0, a = \text{const})$.
(β) $U = T = 1$, $g_{11} = S(x^2)$, $g_{22} = 1$, $g_{33} = V(x^2)$ $(V' \neq 0)$
(γ) $V = S = 1$, $g_{11} = 1$, $g_{22} = T(x^1)$, $g_{33} = U(x^1)$ $(U' \neq 0)$
(δ) $U = V = 1$, $g_{11} = S(x^2)$, $g_{22} = T(x^1)$, $g_{33} = 1$

Equations (3.4)-(3.6) lead to expressions

$$(2V'' - V'^2/V) = bV, \qquad (\ln T)'(\ln U)' = -b$$
$$T(2U'' - U'^2/U) = cU, \qquad S'(\ln V)' = -c \qquad (b, c, d = \text{const})$$
$$2S'' - S'^2/S = d, \qquad 2T'' - T'^2/T = -d$$

All cases, with the exception of γ) for T = 1, repeat already known results.

β) When T = 1 we have $U = (x^1)^2$ and

$$dS^{(3)} = (dx^1)^2 + (dx^2)^2 + (x^1 dx^3)^2$$

which corresponds to flow in the R-direction in coordinates R, ψ, z.

It is possible to show that upon fulfillment of (3.7) case 4° does not lead to any new results.

Thus, to the three cylindrical coordinate systems, corresponding to the two-dimensional systems shown in § 2, we added spherical coordinates r, θ, ψ. Particles can be emitted from spheres r = const

and cones θ = const, moving on radial lines or circles.

Let us note that the four enumerated coordinate systems arose naturally during research of group properties of the equations of a beam [17, 18].

Note: In the work of V. T. Ovcharov [19] it is shown that upon fulfillment of conditions (1.7) particles in the two-dimensional case can move in spirals, straight lines or circles; in three-dimensional space there were considered coordinate systems with rotary symmetry.

Submitted
17 January 1964

Literature

1. K. Spangenberg. Use of the Action Function to Obtain the General Differential Equations of Space Charge Flow in More Than One Dimension. J. Franklin Institute 1941, Vol. 232, No. 4.

2. B. Meltzer. Single-Component Stationary Electron Flow Under Space-Charge Conditions. J. Electronics, 1956, Vol. 2, No. 2.

3. A. R. Lucas, B. Meltzer, and G. A. Stuart. A General Theorem for Dense Electron Beams. J. Electronics and Control, 1958, Vol. 4, No. 2.

4. B. Meltzer and A. R. Lucas. Sufficient and Necessary Trajectory Conditions for Dense Electron Beams. J. Electronics and Control, 1958, Vol. 4, No 5.

5. P. T. Kirstein. Comments on "A General Theorem for Dense Electron Beams" by A. R. Lucas, B. Meltzer, and G. A. Stuart. J. Electronics and Control, 1958, Vol. 4, No 5.

6. W. M. Mueller. Necessary and Sufficient Trajectory Conditions for Dense Electron Beams. J. Electronics and Control, 1959, Vol. 5, No. 6.

7. W. M. Mueller. Comments on Necessary and Sufficient Trajectory Conditions for Dense Electron Beams. J. Electronics and Control, 1960, Vol. 8, No. 2.

8. J. Rosenblatt. Three-Dimensional Space-Charge Flow. J. Appl. Phys., 1960, Vol. 31, No. 8.

9. B. Meltzer. Electron Flow in Curved Paths Under Space-Charge Conditions. Proc. Phys. Soc. B, 1949, Vol. 62, No. 355.

10. P. T. Kirstein. The Complex Formulation of the Equations of Two-Dimensional Space-Charge Flow. J. Electronics and Control, 1958, Vol. 4, No. 5.

11. A. J. McConnel. Introduction to tensor analysis. Fizmatgiz, 1963.

12. L. P. Eisenhart. Riemann Geometry. Princeton, Princeton University Press, 1926.

13. L. P. Eisenhart. Separable Systems in Euclidean 3-space. Phys. Rev., 1934, Vol. 45, No. 6.

14. L. P. Eisenhart. Enumeration of Potentials for Which One-Particle Schroedinger Equations Are Separable. Phys. Rev., 1948, Vol. 74, No. 1.

15. L. P. Eisenhart. Separation of the Variables in One-Particle Schroedinger Equation in 3-space. Proc. National Acad. Sci. USA, 1949, Vol. 35, No. 7.

16. F. M. Morse and G. Fishbach. Methods of theoretical physics. IL, Vol. 1, p. 474, 1958; Vol 2, p. 166, 1960.

17. V. A. Syrovoy. Invariant-group solutions of equations of a two-dimensional stationary charged-particle beam. PMTF, 1962, No. 4.

18. V. A. Syrovoy. Invariant-group solutions of equations of three-dimensional stationary charged-particle beam, PMTF, 1963, No. 3.

19. V. T. Ovcharov. On potential motion of charged particles. Radio engineering and electronics, 1959, Vol. 6, Issue 10.

TENSOR OF VISCOUS STRESSES AND THERMAL FLUX IN A TWO-TEMPERATURE PARTIALLY IONIZED GAS

M. Ya. Aliyevskiy, V. M. Zhdanov, and V. A. Polyanskiy

(Sverdlovsk, Moscow)

In [1] on the basis of the kinetic equation using an approximation of 13 moments to the distribution function there is found a closed system of transport equations for a multicomponent ionized gas in a magnetic field. Temperatures of components were assumed different. In the present work there are considered relationships for the tensor of viscous stresses ensuing from [1], and the vector of the thermal flux in such a gas (§ 1). The starting point is linear algebraic equations for separate components, following from the general system of transport equations on the assumption that macroscopic parameters of the gas change little at distances of the order of the effective path length and in the course of times of the order of the time between collisions of particles.

Coefficients of the obtained expressions in general are extremely complex, but they can be noticeably simplified for the particular case of a three-component partially ionized gas with temperature of electrons, differing from the temperature of ions and atoms ($T_e \geq T_i = T_a$). In §§ 3 and 4 there are given detailed expressions for coefficients of viscosity and thermal conductivity of such a two-temperature gas in a magnetic field. There is calculated the contribution of each of the components to the total tensor of viscous stresses and the thermal flux (including heat transfer by diffusion) depending upon the degree of ionization, strength of the magnetic field and the degree of non-isothermalness of the plasma.

1. Initial system of equations for determination of tensor of viscous stresses of the α-component π_α^{ik} and of the relative flux of heat $\mathbf{h}_\alpha$ is written in form [1]

$$\sum_\beta a_{\alpha\beta}\pi_\beta^{ik} = -\eta_\alpha W^{ik} + \frac{1}{2}\left(\pi_\alpha^{li}\sigma^{klm} + \pi_\alpha^{lk}\sigma^{ilm}\right)\omega_\alpha{}^m\tau_\alpha \qquad (1.1)$$

$$\sum_\beta b_{\alpha\beta}h_\beta{}^i = -\lambda_\alpha R_\alpha{}^i + h_\alpha{}^k\sigma^{ikl}\omega_\alpha{}^l\tau_\alpha^* \qquad \left(\omega_\alpha = \frac{e_\alpha}{m_\alpha}|\mathfrak{B}|\right) \qquad (1.2)$$

Here

$$\mathbf{h}_\alpha = \mathbf{q}_\alpha - \frac{5}{2}p_\alpha\mathbf{w}_\alpha \qquad (\mathbf{w}_\alpha = \mathbf{u}_\alpha - \mathbf{u}) \qquad (1.3)$$

$$W^{ik} = \frac{\partial u^i}{\partial x_k} + \frac{\partial u^k}{\partial x_i} - \frac{2}{3}\delta^{ik}\frac{\partial u^l}{\partial x_l} \qquad (1.4)$$

$$\mathbf{R}_\alpha = \nabla T_\alpha + \frac{2}{5}\frac{T_\alpha}{p_\alpha}\operatorname{div}\pi_\alpha + \frac{m_\alpha}{k}\sum_\beta \tau_{\alpha\beta}^{-1}\left[c_{\alpha\beta}\left(\mathbf{w}_\alpha - \mathbf{w}_\beta\right) + d_{\alpha\beta}\mathbf{w}_\alpha\right] \qquad (1.5)$$

Here W_α, p_α, T_α and q_α – correspondingly, relative velocity, partial pressure, temperature and thermal flux of the α-component; u – mean mass velocity of the gas, m_α – mass of particle of α-type; k -- Boltzmann's constant. The influence of the magnetic field on transport properties is described by the second terms in the right sides of (1.1)-(1.2); here ω_α – cyclotron frequency of a particle with charge e_α, and σ^{ikl} – permutable tensor. In expressions (1.4)-(1.5) there are omitted terms which depend on the electrical field and which are essential only in very strong fields [1].

Coefficients η_α and λ_α are connected with effective times of collisions τ_α and τ_α^* by relationships of form

$$\eta_\alpha = \frac{1}{2}p_\alpha\tau_\alpha, \qquad \lambda_\alpha = \frac{5k}{2m_\alpha}p_\alpha\tau_\alpha^* \qquad (1.6)$$

Let us note that for the single-component case η_α and λ_α coincide with usual coefficients of viscosity and thermal conductivity of a simple gas (first approximation of Chapman-Cowling [2]). Magnitudes, the inverse of effective collision times, τ_α^{-1} and $(\tau_\alpha^*)^{-1}$ are recorded as linear combinations of magnitudes $\tau_{\alpha\beta}^{-1}$ – effective frequencies of collisions of particles of the α and β-type. Expressions for τ_α, τ_α^* and $\tau_{\alpha\beta}$, and also for coefficients $a_{\alpha\beta}$, $b_{\alpha\beta}$, $c_{\alpha\beta}$, $d_{\alpha\beta}$ are given in work [1]*; in the particular case of a three-component plasma with $T_e \geq T_i = T_a$ and $m_i = m_a$ these expressions are given below (§ 2).

In general, coefficients $a_{\alpha\beta}$, $b_{\alpha\beta}$, $c_{\alpha\beta}$ in a complex manner depend on ratios of temperatures and concentrations of components, and also on mass ratios and effective collision diameters for particles of different types. Here, by definition we have $a_{\alpha\alpha} = 1$, $b_{\alpha\alpha} = 1$; furthermore $d_{\alpha\beta} = 0$ when $T_\alpha = T_\beta$.

In the absence of magnetic field ($|B| = 0$) general solutions of equations (1.1)-(1.2) are written in an obvious manner

$$\pi_\alpha^{ik} = -\sum_\beta \frac{|a|_{\beta\alpha}}{|a|}\eta_\beta W^{ik}, \qquad \mathbf{h}_\alpha = -\sum_\beta \frac{|b|_{\beta\alpha}}{|b|}\lambda_\beta \mathbf{R}_\beta \tag{1.7}$$

Here $|a|$ and $|b|$ are determinants of corresponding systems of equations; $|a|_{\beta\alpha}$ and $|b|_{\beta\alpha}$ are cofactors of element $\beta\alpha$ of the determinants.

For solution of systems (1.1)-(1.2) with an arbitrarily oriented magnetic field we form, with the help of (1.1), an equation for convolutions of tensor π_α^{ik}, with tensor $\sigma^{ris}n^k$, with vector n^k, with tensors $\sigma^{ris}n^s n^k$ and $n^s n^k$, and with the help (1.2) we form equations

---

*In [1] there are not written the explicit expressions for $c_{\alpha\beta}$ and $d_{\alpha\beta}$, however, their form is easily established by comparison of (1.5) with expression (2.10) in [1]. Furthermore, the value of $\tau^{\alpha-1}$ differs from that given in [1] by a factor of 3/4.

for $h_\alpha^i \sigma^{ris} n^k$ and $h_\alpha^i n^i$, where $n = B/|B|$ is the unit vector in the direction of the magnetic field. Using then properties of antisymmetric unit tensor σ^{ikl}, after a series of cumbersome, but simple calculations, we arrive at an expression for π_α^{kr}, recorded with the help of five coefficients of viscosity:

$$\pi_\alpha^{kr} = -\eta_\alpha^{(0)} W_0^{kr} - \eta_\alpha^{(1)} W_1^{kr} - \eta_\alpha^{(2)} W_2^{kr} + \eta_\alpha^{(3)} W_3^{kr} + \eta_\alpha^{(4)} W_4^{kr} \tag{1.8}$$

where

$$\eta_\alpha^{(0)} = \sum_\beta \frac{|a|_{\beta\alpha}}{|a|} \eta_\beta, \qquad \eta_\alpha^{(1)} = \sum_\beta \frac{|a^*|_{\beta\alpha}}{|a^*|} \eta_\beta, \qquad \eta_\alpha^{(2)} = \sum_\beta \frac{|a^{**}|_{\beta\alpha}}{|a^{**}|} \eta_\beta$$
$$\eta_\alpha^{(3)} = \sum_\beta \omega_\beta \tau_\beta \frac{|a^*|_{\beta\alpha}}{|a^*|} \eta_\beta^{(0)}, \qquad \eta_\alpha^{(4)} = \frac{1}{2} \sum_\beta \omega_\beta \tau_\beta \frac{|a^{**}|_{\beta\alpha}}{|a^{**}|} \eta_\beta^{(0)} \tag{1.9}$$

Analogously we find the expression for h_α^i, which is conveniently presented in vector form, introducing components of $\mathbf{R}_\alpha$, correspondingly parallel and perpendicular to the magnetic field

$$\mathbf{h}_\alpha = -\sum_\beta \frac{|b|_{\beta\alpha}}{|b|} \lambda_\beta \mathbf{R}_\beta'' - \sum_\beta \frac{|b^*|_{\beta\alpha}}{|b^*|} \left\{ \lambda_\beta \mathbf{R}_\beta^\perp + \omega_\beta \tau_\beta \sum_\gamma \frac{|b|_{\gamma\beta}}{|b|} \lambda_\gamma (\mathbf{R}_\gamma' \times \mathbf{n}) \right\} \tag{1.10}$$

where

$$\mathbf{R}_\alpha'' = \mathbf{n}(\mathbf{n}\mathbf{R}_\alpha), \qquad \mathbf{R}_\alpha^\perp = \mathbf{n} \times (\mathbf{R}_\alpha \times \mathbf{n})$$

Elements of determinants, marked by one and two asterisks, are connected with coefficients $a_{\alpha\beta}$ and $b_{\alpha\beta}$ by the relationships

$$a_{\alpha\beta}^* = a_{\alpha\beta} + \frac{|a|_{\beta\alpha}}{|a|} \omega_\alpha \tau_\alpha \omega_\beta \tau_\beta$$
$$a_{\alpha\beta}^{**} = a_{\alpha\beta} + \frac{1}{4} \frac{|a|_{\beta\alpha}}{|a|} \omega_\alpha \tau_\alpha \omega_\beta \tau_\beta \tag{1.11}$$
$$b_{\alpha\beta}^* = b_{\alpha\beta} + \frac{|b|_{\beta\alpha}}{|b|} \omega_\alpha \tau_\alpha^* \omega_\beta \tau_\beta^*$$

Let us note that the above form of notation of expressions (1.8) and (1.10) is analogous to that used in the survey article of Braginskiy [3] for the case of a two-temperature stripped plasma. In

the same place (p. 233) are general expressions for tensors W_p^{kr}, constituting different convolutions of tensor W^{il} with tensor quantities of type $n^k n^r n^i n^l$, $\delta^{kr} n^i n^l$, $\sigma^{kmi} n^r n^m n^l$, and $\sigma^{kmi} \delta^{rl} n^m$.

The form of tensors W_p^{kr} is noticeably simplified in a specially selected system of coordinates, where axis x is directed along the magnetic field. For components of tensor of viscous stresses π_α^{ik} in this system of coordinates we have

$$\begin{aligned}
\pi_\alpha^{xx} &= -\eta_\alpha^{(0)} W^{xx} \\
\pi_\alpha^{yy} &= -\eta_\alpha^{(0)} \tfrac{1}{2}(W^{yy} + W^{zz}) - \eta_\alpha^{(1)} \tfrac{1}{2}(W^{yy} - W^{zz}) - \eta_\alpha^{(3)} W^{yz} \\
\pi_\alpha^{zz} &= -\eta_\alpha^{(0)} \tfrac{1}{2}(W^{zz} + W^{yy}) - \eta_\alpha^{(1)} \tfrac{1}{2}(W^{zz} - W^{yy}) + \eta_\alpha^{(3)} W^{yz} \\
\pi_\alpha^{yz} &= \pi_\alpha^{zy} = -\eta_\alpha^{(1)} W^{yz} + \eta_\alpha^{(3)} \tfrac{1}{2}(W^{yy} - W^{zz}) \\
\pi_\alpha^{xy} &= \pi_\alpha^{yx} = -\eta_\alpha^{(2)} W^{xy} - \eta_\alpha^{(4)} W^{xz} \\
\pi_\alpha^{xz} &= \pi_\alpha^{zx} = -\eta_\alpha^{(2)} W^{xz} + \eta_\alpha^{(4)} W^{xy}
\end{aligned} \tag{1.12}$$

Relationships (1.8) (or (1.12)) and (1.10) obtained about allow us to calculate the tensor of viscous stresses and the relative thermal flux for any of the components of a nonisothermal multicomponent plasma in a magnetic field. The total tensor of viscous stresses π^{ik} and the thermal flux q in the plasma are found by simple summation of the corresponding quantities for the components:

$$\pi^{ik} = \sum_\alpha \pi_\alpha^{ik}, \qquad \mathbf{q} = \sum_\alpha \mathbf{h}_\alpha + 2.5 \sum_\alpha p_\alpha \mathbf{w}_\alpha \tag{1.13}$$

Analysis of expressions for the tensor of viscous stresses and the thermal flux in general constitutes a fairly difficult problem due to the complexity of the expressions themselves and also the coefficients in them. Therefore, in the subsequent account we consider the particular case of a three-component plasma with $T_e \geq T_i = T_a$ and $m_i = m_a$. Besides its practical interest, consideration of this case allows us to write coefficients of viscosity and thermal conductivity

in a form accessible for detailed analysis of their dependence on the ratio of temperatures of components (degree of "nonisothermalness") the ratio of particle densities (degree of ionization) and the magnitude of the magnetic field (degree of "magnetization" of the plasma).

Let us note that in [1] there were already expressed a series of general considerations about the form of the coefficients of viscosity and thermal conductivity of a two-temperature partially ionized gas. Here they used a simplified initial system of equations, obtained as a result of disregarding cross-terms in the equations for electrons and terms containing electron magnitudes in the equations for ions and atoms (analogously to how this was done earlier in [4, 5]). The following analysis of exact solutions shows, in particular, under what conditions we take such an approach to solution of the initial systems of equations.

2. Below is a summary of coefficients of the initial system of equations (1.1)-(1.2) for the case of a two-temperature partially ionized gas. Masses of ions and atoms, and also temperatures of heavy components are assumed identical ($T_i = T_a = T$, $m_i = m_a = m$). In simplification of general expressions for coefficients [1] we essentially use conditions

$$\varepsilon = m_e/m \ll 1, \qquad \varepsilon\theta \ll 1 \qquad (\theta = T/T_e) \tag{2.1}$$

Coefficients $a_{\alpha\beta}$, $b_{\alpha\beta}$, $c_{\alpha\beta}$, $d_{\alpha\beta}$ are

$$a_{ee} = a_{ii} = a_{aa} = 1 \tag{2.2}$$

$$a_{ei} = -0.4\,\varepsilon\tau_e\tau_{ie}^{-1}, \qquad a_{ie} = -0.2\,\varepsilon(30-1)\,\tau_i\tau_{ei}^{-1}$$

$$a_{ea} = -4\varepsilon f_{ea}\tau_e\tau_{ae}^{-1}, \qquad a_{ae} = -4\varepsilon\left[f_{ea} + {}^1/_4\zeta_{ea}(1-\theta)\right]\tau_a\tau_{ea}^{-1}$$

$$a_{ia} = -f_{ia}\tau_i\tau_{ai}^{-1}, \qquad a_{ai} = -f_{ia}\tau_a\tau_{ia}^{-1}$$

$$b_{ee} = b_{ii} = b_{aa} = 1 \tag{2.3}$$

$$b_{ei} = -2.7\varepsilon\tau_e^*\tau_{ie}^{-1}, \qquad b_{ie} = -4.5\varepsilon^2[\theta^2 - 0.4\theta - {}^4/_{45}(\ln\Lambda)^{-1}]\,\tau_i^*\tau_{ei}^{-1}$$

$$b_{ea} = -8\varepsilon g_{ea}\tau_e^*\tau_{ae}^{-1}, \qquad b_{ae} = -8\varepsilon^2[g_{ea}\theta^2 - s_{ea}\theta(1-\theta) + t_{ea}(1-\theta)^2]\,\tau_a^*\tau_{ea}^{-1}$$

$$b_{ia} = -g_{ia}\tau_i^*\tau_{ai}^{-1}, \qquad b_{ai} = -g_{ia}\tau_a^*\tau_{ia}^{-1}$$

$$c_{ei} = -{}^3/_5, \qquad c_{ie} = {}^6/_5\varepsilon^2(1-1.5\theta), \qquad c_{ai} = c_{ia} = {}^1/_4\zeta_{ia} \tag{2.4}$$

$$c_{ea} = \zeta_{ea} - {}^4/_3\varepsilon(1-\theta)(1+6f_{ea}+1.5\zeta_{ea})$$

$$c_{ae} = \varepsilon^2[\zeta_{ea}\theta - 2\zeta_{ea}(1-\theta) + {}^4/_3(1+6f_{ea}+3\zeta_{ea})(\theta^{-1}-1)]$$

$$d_{ee} = d_{ii} = d_{aa} = d_{ia} = d_{ai} = 0 \tag{2.5}$$

$$d_{ei} = d_{ea} = 2\varepsilon(1-\theta), \qquad d_{ie} = d_{ae} = 2\varepsilon(1-\theta^{-1})$$

Quantities τ_α, τ_α^*

$$\tau_e^{-1} = 0.3\tau_{ee}^{-1} + 0.6\tau_{ei}^{-1} + 0.6A_{ea}^*\tau_{ea}^{-1} \tag{2.6}$$

$$\tau_i^{-1} = 0.3\tau_{ii}^{-1} + f_{ia}'\tau_{ia}^{-1} + \varepsilon\tau_{ie}^{-1}, \qquad \tau_a^{-1} = 0.3A_{aa}^*\tau_{aa}^{-1} + f_{ia}'\tau_{ai}^{-1} + \varepsilon\tau_{ae}^{-1}$$

$$(\tau_e^*)^{-1} = 0.4\tau_{ee}^{-1} + 1.3\tau_{ei}^{-1} + (2.5 - 1.2B_{ea}^*)\,\tau_{ea}^{-1} \tag{2.7}$$

$$(\tau_i^*)^{-1} = 0.4\tau_{ii}^{-1} + g_{ia}'\tau_{ia}^{-1} + 3\varepsilon\tau_{ie}^{-1}$$

$$(\tau_a^*)^{-1} = 0.4A_{aa}^*\tau_{aa}^{-1} + g_{ia}'\tau_{ai}^{-1} + 3\varepsilon\tau_{ae}^{-1}$$

Here

$$f_{\alpha\beta} = {}^1/_4(1 - 0.6A_{\alpha\beta}^*), \qquad g_{\alpha\beta} = {}^{11}/_{16} - 0.2A_{\alpha\beta}^* - 0.15B_{\alpha\beta}^* \tag{2.8}$$

$$f'_{\alpha\beta} = {}^1/_4(1 + 0.6A_{\alpha\beta}^*), \qquad g'_{\alpha\beta} = {}^{11}/_{16} + 0.2A_{\alpha\beta}^* - 0.15B_{\alpha\beta}^*$$

$$\zeta_{\alpha\beta} = 1.2C_{\alpha\beta}^* - 1 \tag{2.9}$$

$$s_{\alpha\beta} = 0.625 + 0.2A_{\alpha\beta}^* + 0.3B_{\alpha\beta}^* + 0.3D_{\alpha\beta}^* - 2.4C_{\alpha\beta}^* \tag{2.10}$$

$$t_{\alpha\beta} = 1.5C_{\alpha\beta}^* - 0.6B_{\alpha\beta}^* - 0.3D_{\alpha\beta}^*$$

Collision times $\tau_{\alpha\beta}$ and coefficients $A_{\alpha\beta}^*$, $B_{\alpha\beta}^*$, $C_{\alpha\beta}^*$, $D_{\alpha\beta}^*$ are expressed through known integrals [2] of Chapman-Cowling $\Omega_{\alpha\beta}^{lr}$

$$\tau_{\alpha\beta}^{-1} = \frac{16}{3}n_\beta\Omega_{\alpha\beta}^{11} \tag{2.11}$$

$$A_{\alpha\beta}^* = \frac{\Omega_{\alpha\beta}^{22}}{2\Omega_{\alpha\beta}^{11}}, \qquad B_{\alpha\beta}^* = \frac{5\Omega_{\alpha\beta}^{12} - \Omega_{\alpha\beta}^{13}}{3\Omega_{\alpha\beta}^{11}} \tag{2.12}$$

$$C_{\alpha\beta}^* = \frac{\Omega_{\alpha\beta}^{12}}{3\Omega_{\alpha\beta}^{11}}, \qquad D_{\alpha\beta}^* = \frac{2\Omega_{\alpha\beta}^{23} - 5\Omega_{\alpha\beta}^{22}}{6\Omega_{\alpha\beta}^{11}},$$

Here n_β – density of particles of β-type

$$\Omega_{\alpha\beta}^{lr} = \sqrt{\pi}\int_0^\infty\int_0^\infty \zeta^{2r+2}e^{-\zeta^2}g_{\alpha\beta}(1-\cos^l\chi_{\alpha\beta})\,b\,db\,d\zeta \tag{2.13}$$

Here

$$g_{\alpha\beta} = \left(\frac{2}{\tau_{\alpha\beta}}\right)^{1/2}\zeta, \qquad \tau_{\alpha\beta}^{-1} = \frac{kT_\alpha}{m_\alpha} + \frac{kT_\beta}{m_\beta} \tag{2.14}$$

and the scattering angle $\chi_{\alpha\beta}$ is a function of $g_{\alpha\beta}$ and b, determined by the form of the law of interaction of particles of α- and β-type.

For particles, interacting as solid elastic balls

$$\frac{1}{\tau_{\alpha\beta}} = \frac{16}{3} n_\beta \left(\frac{1}{2\pi\tau_{\alpha\beta}}\right)^{1/2} Q_{\alpha\beta}, \quad A_{\alpha\beta}^* = B_{\alpha\beta}^* = C_{\alpha\beta}^* = D_{\alpha\beta}^* = 1 \tag{2.15}$$

Here $Q_{\alpha\beta}$ – geometric collision cross section of particles of type α and β.

Expression (2.15) is conveniently used in the case of other laws of interaction, where $Q_{\alpha\beta}$ can be considered a certain effective collision cross section appearing in the general function of temperatures of the components. Here A*, B*, C*, D* also turn out to be weakly varying functions of temperatures.

In the case considered by us ($m_i = m_a$, $T_i = T_a$, $m_e T/mT_e \ll 1$) collision times of charged particles with neutral ones and of neutral ones among themselves are written in the form

$$\begin{aligned} &\frac{1}{\tau_{ea}} = \frac{16}{3} n_a \left(\frac{kT_e}{2\pi m_e}\right)^{1/2} Q_{ea}(T_e), \qquad \frac{1}{\tau_{ae}} = \frac{n_e}{n_a}\frac{1}{\tau_{ea}} \\ &\frac{1}{\tau_{ia}} = \frac{16}{3} n_a \left(\frac{kT}{\pi m}\right)^{1/2} Q_{ia}(T), \qquad \frac{1}{\tau_{ai}} = \frac{n_i}{n_a}\frac{1}{\tau_{ia}} \\ &\frac{1}{\tau_{aa}} = \frac{16}{3} n_a \left(\frac{kT}{\pi m}\right)^{1/2} Q_{aa}(T) \end{aligned} \tag{2.16}$$

For interactions of charged particles we have

$$\begin{aligned} &\frac{1}{\tau_{ei}} = \frac{16}{3} n_i \left(\frac{kT_e}{2\pi m_e}\right)^{1/2} Q_{ei}, \qquad \frac{1}{\tau_{ie}} = \frac{n_e}{n_i}\frac{1}{\tau_{ei}} \\ &\frac{1}{\tau_{ee}} = \frac{16}{3} n_e \left(\frac{kT_e}{\pi m_e}\right)^{1/2} Q_{ee}, \qquad \frac{1}{\tau_{ii}} = \frac{16}{3} n_i \left(\frac{kT}{\pi m}\right)^{1/2} Q_{ii} \end{aligned} \tag{2.17}$$

Here

$$Q_{ee} = \frac{\pi}{2}\frac{e^4}{(kT_e)^2}\ln\Lambda_{ee}, \; Q_{ei} = \frac{\pi}{2}\frac{z^2e^4}{(kT_e)^2}\ln\Lambda_{ei}, \qquad Q_{ii} = \frac{\pi}{2}\frac{z^4e^4}{(kT)^2}\ln\Lambda_{ii} \tag{2.18}$$

Here $e = |e_e|$ – charge of electron; ze – charge of an ion; $\ln \Lambda_{\alpha\beta}$ – Coulomb logarithm, values of which are tabulated, for instance, in [6].

Subsequently we will need estimates of ratios $\tau_{\alpha\beta}^{-1}/\tau_{\delta\gamma}^{-1}$, or, since these magnitudes are proportional to Q, estimates of ratios $Q_{\alpha\beta}/Q_{\delta\gamma}$.

For electrons and ions, assuming without great error [4] that $\ln \Lambda_{ee} \approx \ln \Lambda_{ie} \approx \ln \Lambda_{ii}$, directly from (2.18) we have

$$Q_{ee}/Q_{ii} \sim \theta^2/z^4, \quad Q_{ei}/Q_{ii} \sim \theta^2/z^2, \quad Q_{ee}/Q_{ei} \sim 1/z^2$$

To estimate ratios Q_{ea}/Q_{aa} it is possible to use theoretical and experimental data of [7-8], in which there are given total effective elastic collision cross sections of electrons with atoms and with molecules of different gases. The diffusion scattering cross sections interesting us, through which Q_{ea} are expressed, differ from total cross sections by not more than 10% for most gases [7]. In [10] there is discussed a great amount of data on cross sections Q_{ea} for inert gases. Sections Q_{aa} for different potentials of interaction can be calculated, using values of Ω_{aa}^{11*} given in [9]. Comparing these results, it is possible to consider approximately that in ranges of temperatures $5 \cdot 10^2\ ^\circ K \leq T \leq 10^4\ ^\circ K$, $5 \cdot 10^3\ ^\circ K \leq T_e \leq 5 \cdot 10^5\ ^\circ K$ we have estimate

$$Q_{ea}/Q_{aa} \sim 1 \div 10$$

On interaction cross section of ions with atoms there is comparatively little data, but judging by certain results (see, for instance, [11, 12]), it is possible to limit ourselves to approximation

$$Q_{ia}/Q_{aa}^{\pi} \sim 1$$

In estimating Q_{ii} one should consider that for the considered temperature range and in the range of densities of charged particles

$10^9 \leq n_i \leq 10^{15}$ cm^{-3} the Coulomb logarith ln Λ is included in limits from 5 to 13. Then, using results of [9] for sections Q_{aa}, we arrive at

$$Q_{ea} / Q_{ii} \sim (10^{-2} \div 10^{-3})$$

3. Using values of coefficients $a_{\alpha\beta}$, given in § 2 it is possible to noticeably simplify the general expression for coefficients of viscosity (1.9). With accuracy up to magnitudes of the order of $(\varepsilon\theta)^{3/2}$ with respect to the remaining ones determinants $|a|$, $|a^*|$ and $|a^{**}|$ are equal to

$$|a| \approx 1 - a_{ia}a_{ai} = \Delta, \quad |a^*| \approx \Delta(1+\omega_e^2\tau_e^2)(1+\Delta^{-2}\omega_i^2\tau_i^2)$$
$$|a^{**}| \approx \Delta(1+{}^1/_4\omega_e^2\tau_e^2)(1+{}^1/_4\Delta^{-2}\omega_i^2\tau_i^2) \qquad (3.1)$$
$$\Delta = 1 - f_{ia}^2\tau_i\tau_a\tau_{ai}^{-1}\tau_{ia}^{-1} \qquad (3.2)$$

Coefficients $\eta_e^{(p)}$ for the electron component when $\omega_i\tau_i \ll 1$ take form

$$\eta_e^{(0)} = \frac{1}{2}p_e\tau_e, \quad \eta_e^{(1)} = \frac{\eta_e^{(0)}}{1+\omega_e^2\tau_e^2}, \quad \eta_e^{(2)} = \frac{\eta_e^{(0)}}{1+{}^1/_4\omega_e^2\tau_e^2}$$
$$\eta_e^{(3)} = \frac{\omega_e\tau_e}{1+\omega_e^2\tau_e^2}\eta_e^{(0)}, \quad \eta_e^{(4)} = \frac{{}^1/_2\omega_e\tau_e}{1+{}^1/_4\omega_e^2\tau_e^2}\eta_e^{(0)} \qquad (3.3)$$

In (3.3) there are omitted terms which have the order $\varepsilon^{1/2}\theta^{5/2}$ with respect to the remaining ones. Let us note that coefficients $\eta_e^{(p)}$ in form (3.3) can also be obtained directly from (1.1), if we use the equation for the electron component, disregarding in it the ion and atom cross terms. A similar method was used earlier in [4,5]. Analysis of exact solutions shows, however, that when $\omega_i\tau_i \gtrsim 1$ calculation of cross-terms can lead to marked corrections in coefficients $\eta_e^{(1)}$ and $\eta_e^{(2)}$. In the case of a fully ionized gas, for instance, along with terms of order $\varepsilon^{1/2}\theta^{5/2}$, in coefficients with $\omega_i^2\tau_i^2$ there appear terms, having order $\varepsilon^{1/2}\theta^{5/2}|\omega_e\tau_e|/\omega_i\tau_i \sim \theta$ as

compared to one. Then, for $\omega_i\tau_i \gg 1$ coefficients $\eta_e^{(1)}$ and $\eta_e^{(2)}$ for that case take form

$$\eta_e^{(1)} = \frac{1}{2}\frac{p_e}{\omega_e^2\tau_e}(1+0.4\theta), \qquad \eta_e^{(2)} = 2\frac{p_e}{\omega_e^2\tau_e}(1+0.4\theta) \tag{3.4}$$

This result differs from the expressions given in [3, 4] by factor $(1 + 0.4\theta)$. Divergence with [3] is connected, apparently, with the fact that transport factors for each of components were determined in this work by solution of a system of "loose" kinetic equations for electrons and ions, obtained as a result of a series of simplifications in cross-colliding members.* In [4] cross terms are rejected already in the transport equations themselves.

Coefficients $\eta_i^{(p)}$ and $\eta_a^{(p)}$ for ions and atoms can be presented in the form

$$\eta_i^{(0)} = {}^1/_2 p_i\tau_i\xi_i\Delta^{-1}, \qquad \eta_i^{(1)} = \frac{\eta_i^{(0)}}{1+\Delta^{-2}\omega_i^2\tau_i^2}, \qquad \eta_i^{(2)} = \frac{\eta_i^{(0)}}{1+{}^1/_4\Delta^{-2}\omega_i^2\tau_i^2}$$

$$\eta_i^{(3)} = \frac{\omega_i\tau_i\Delta^{-1}}{1+\Delta^{-2}\omega_i^2\tau_i^2}\eta_i^{(0)}, \qquad \eta_i^{(4)} = \frac{{}^1/_2\omega_i\tau_i\Delta^{-1}}{1+{}^1/_4\Delta^{-2}\omega_i^2\tau_i^2}\eta_i^{(0)} \tag{3.5}$$

$$\eta_a^{(0)} = {}^1/_2 p_a\tau_a\xi_a\Delta^{-1}, \qquad \eta_a^{(1)} = {}^1/_2 p_a\tau_a\Delta^{-1}\frac{\xi_a+\Delta^{-1}\omega_i^2\tau_i^2}{1+\Delta^{-2}\omega_i^2\tau_i^2}$$

$$\eta_a^{(2)} = \frac{1}{2}p_a\tau_a\Delta^{-1}\frac{\xi_a+{}^1/_4\Delta^{-1}\omega_i^2\tau_i^2}{1+{}^1/_4\Delta^{-2}\omega_i^2\tau_i^2} \tag{3.6}$$

$$\eta_a^{(3)} = \frac{1}{2}p_a\tau_a\Delta^{-2}\frac{(\xi_a-\Delta)\omega_i\tau_i}{1+\Delta^{-2}\omega_i^2\tau_i^2}, \qquad \eta_a^{(4)} = \frac{1}{4}p_a\tau_a\Delta^{-2}\frac{(\xi_a-\Delta)\omega_i\tau_i}{1+{}^1/_4\Delta^{-2}\omega_i^2\tau_i^2}$$

$$\xi_a = 1 + f_{ia}\tau_i\tau_{ai}^{-1}, \qquad \xi_i = 1 + f_{ia}\tau_a\tau_{ia}^{-1} \tag{3.7}$$

In (3.5) and (3.6) there are omitted the term whose maximum order is $\varepsilon\theta^{-1}$ with respect to the remaining ones. Obtained expressions are valid, thus, for conditions, where

$$T_e/T \ll m/m_e \tag{3.8}$$

*In comparing (3.4) with expressions of [3] one should consider that τ_e in [3] corresponds in our designations to τ_{ei} and that, although coefficients $\eta^{(p)}_e$ in [3] are calculated taking into account a large number of terms of the expansion of the distribution function for large values of $\omega_i\tau_i$ any order of approximation gives coinciding results.

It is necessary to note that coefficients of viscosity, determined by expressions (3.3) and (3.5)-(3.6), actually have the same form as in [5], where there was considered the case of a partially ionized gas with identical temperatures of components. The difference is that τ_{ee}^{-1}, τ_{ei}^{-1} and τ_{ea}^{-1}, in the effective collision times τ_e, τ_a, τ_i, should now be written at the temperature of electrons T_e instead of T. Furthermore, obviously, $p_e = n_e kT_e$, $p_i = n_i kT$, $p_a = n_a kT$.

In conclusion of this paragraph we analyze briefly the contribution of each of the components to the total coefficient of viscosity $\eta^{(p)} = \eta_e^{(p)} + \eta_i^{(p)} + \eta_a^{(p)}$ depending upon the degree of ionization $\alpha = n_i/(n_i + n_a)$, the degree of "nonisothermalness" and magnitudes of $\omega_e\tau_e$, $\omega_i\tau_i$.

For this purpose instead of $\eta_\alpha^{(p)}$ it is convenient to introduce values of reduced coefficients of viscosity, defined as

$$\eta_\alpha^{(p)*} = \eta_\alpha^{(p)} \frac{Q_{aa}}{(mkT)^{1/2}} \tag{3.9}$$

Considering that ξ_i, ξ_a and Δ are close to one, using expressions for τ_e, τ_a, τ_i and estimates for ratio $Q_{\alpha\beta}/Q_{\delta\gamma}$, given in § 2 we have

$$\eta_e^{(0)*} \sim \varepsilon^{1/5}\theta^{-3/2}\frac{\alpha\beta}{\alpha + (1-\alpha)\beta\theta^{-2}}, \qquad \eta_i^{(0)*} \sim \frac{\alpha\beta}{\alpha + (1-\alpha)\beta}, \qquad \eta_a^{(0)*} \sim \frac{1-\alpha}{1+\alpha} \tag{3.10}$$

where

$$\beta = Q_{aa}/Q_{ii} \sim (10^{-2} \div 10^{-5})$$

As can be seen, relative contribution of $\eta_e^{(0)}$ to the total coefficient of viscosity is negligible when $\theta = 1$, but can be comparable to the contribution of $\eta_i^{(0)}$ already when $\theta \sim \varepsilon^{1/5}$, i.e., when $T_e/T \sim$ $\sim$ (5 to 10). We note here that the role of $\eta_i^{(0)}$ becomes essential only for high degrees of ionization $\alpha \gtrsim 1 - \beta$. For $\alpha \ll 1 - \beta$ the main contribution is introduced by the coefficient of viscosity of $\eta_a^{(0)}$.

For analysis of the relative contribution of coefficients $\eta_\alpha^{(1)}$ and $\eta_\alpha^{(3)}$ besides (3.10) we need additional estimates

$$\frac{\omega_i\tau_i}{|\omega_e\tau_e|}\sim\varepsilon^{1/2}\theta^{-1/2}\frac{\alpha\theta^2+(1-\alpha)\beta}{\alpha+(1-\alpha)\beta},\qquad \xi_a-\Delta\sim\frac{\alpha\beta}{\alpha+(1-\alpha)\beta} \tag{3.11}$$

Comparing expression for reduced coefficients of viscosity, we find that the contribution of separate components to $\eta^{(1)}$ is analogous to the preceding case with this difference only, that in a strong magnetic field ($\omega_i\tau_i \gg 1$) the influence of $\eta_i^{(1)}$ shows at still higher degrees of ionization $\alpha \sim 1 - \beta/\omega_i^2\tau_i^2$.

The contribution of $\eta_e^{(3)}$, $\eta_i^{(3)}$ and $\eta_a^{(3)}$ to $\eta^{(3)}$ is approximately identical in weak magnetic field ($|\omega_e|\tau_e \lesssim 1$) when $\alpha \ll 1$. With growth of the degree of ionization the contribution of $\eta_a^{(3)}$ decreases, and with growth of the magnetic field the role of $\eta_e^{(3)}$ decreases, so that when $\omega_i\tau_i \gg 1$, $\eta_e^{(3)} \ll \eta_i^{(3)}, \eta_a^{(3)}$. Nonisothermalness only increases the relative contribution of $\eta_e^{(3)}$. For coefficients $\eta^{(2)}$ and $\eta^{(4)}$ the conclusions drawn during analysis of $\eta^{(1)}$ and $\eta^{(3)}$ are valid.

4. Relative thermal flux of each of the components h_α, in accordance with the structure R_α, is composed of several independent parts. Let us consider first that part of it which is determined by temperatures gradients of components.

Calculating determinants $|b|$ and $|b^*|$ with accuracy up to magnitudes of an order of $\varepsilon^{5/2}\theta^{3/2}$, we find

$$|b|\approx 1-b_{ia}b_{ai}=\delta,\qquad |b^*|=\delta(1+\omega_e^2\tau_e^{*2})(1+\delta^{-2}\omega_i^2\tau_i^{*2}) \tag{4.1}$$

$$\delta=1-\varepsilon^2\tau_i^*\tau_e^*\tau_{ia}^{-1}\tau_{ai}^{-1} \tag{4.2}$$

From (1.10) it follows that the expression for $h_\alpha^{(t)}$ in general contains terms proportional to temperature gradients of all components. Analysis of corresponding coefficients shows, however, that the basic contribution to the electron thermal flux $h_e^{(t)}$ is from

terms which depend only on ∇T_e. Then the expression for $h_e^{(t)}$ can be presented in form

$$h_e^{(t)} = -\lambda_e^{\parallel}\nabla_{\parallel}T_e - \lambda_e^{\perp}\nabla_{\perp}T_e - \lambda_e^{\wedge}(\nabla T_e \times \varkappa) \tag{4.3}$$

Coefficients of thermal conductivity λ_e are defined here as

$$\lambda_e^{\parallel} = \frac{5}{2}\frac{k}{m_e}p_e\tau_e^*, \quad \lambda_e^{\perp} = \frac{\lambda_e^{\parallel}}{1+(\omega_e\tau_e^*)^2}, \quad \lambda_e^{\wedge} = \frac{\omega_e\tau_e^*\lambda_e^{\parallel}}{1+(\omega_e\tau_e^*)^2} \tag{4.4}$$

In the notation of (4.3)-(4.4) there are omitted members, whose order are $\varepsilon^{1/2}\theta^{1/2}|\nabla_{\parallel}T|/|\nabla_{\parallel}T_e|$ and $\varepsilon\theta|\nabla_{\perp}T|/|\nabla_{\perp}T_e|$ with respect to the others.

Analogous calculations in expressions for $h_i^{(t)}$ and $h_a^{(t)}$ allow us, under certain conditions, to omit in them terms proportional to gradients ∇T_e. Then

$$h_{i,a}^{(t)} = -\lambda_{i,a}^{\parallel}\nabla_{\parallel}T - \lambda_{i,a}^{\perp}\nabla_{\perp}T - \lambda_{i,a}^{\wedge}(\nabla T \times \varkappa) \tag{4.5}$$

where

$$\lambda_i^{\parallel} = \frac{5}{2}\frac{k}{m}p_i\tau_i^*\xi_i^*\delta^{-1}, \quad \lambda_i^{\perp} = \frac{\lambda_i^{\parallel}}{1+\delta^{-2}(\omega_i\tau_i^*)^2}, \quad \lambda_i^{\wedge} = \frac{\omega_i\tau_i^*\delta^{-1}\lambda_i^{\parallel}}{1+\delta^{-2}(\omega_i\tau_i^*)^2}$$

$$\lambda_a^{\parallel} = \frac{5}{2}\frac{k}{m}p_a\tau_a^*\xi_a^*\delta^{-1}, \quad \lambda_a^{\perp} = \frac{5}{2}\frac{k}{m}p_a\tau_a^*\delta^{-1}\frac{\xi_a^*+\delta^{-1}(\omega_i\tau_i^*)^2}{1+\delta^{-2}(\omega_i\tau_i^*)^2} \tag{4.6}$$

$$\lambda_a^{\wedge} = \frac{5}{2}\frac{k}{m}p_a\tau_a^*\delta^{-2}\frac{(\xi_a^*-\delta)\omega_i\tau_i^*}{1+\delta^{-2}(\omega_i\tau_i^*)^2} \tag{4.7}$$

Here

$$\xi_i^* = 1 + g_{ia}\tau_e^*\tau_{ia}^{-1}, \qquad \xi_a^* = 1 + g_{ia}\tau_i^*\tau_{ai}^{-1} \tag{4.8}$$

In (4.5)-(4.7) there are omitted terms the maximum order of which is $\varepsilon|\nabla T_e|/|\nabla T|$ and $\varepsilon\theta^{-1}(5\ \text{in}\ \Lambda)^{-1}|\nabla T_e|/|\nabla T|$ with respect to the others. When $|\nabla T_e| \sim |\nabla T|$ this leads to condition $T_e/T \ll 5\ \ln \Lambda m/m_e$. Since $\ln \Lambda \sim 10$, this condition turns out to be less strict than (3.8). If $|\nabla T_e|/|\nabla T| \sim T_e/T$, the limitation on quantity T_e/T turns out to be somewhat more strict than (3.8), namely

$$(T_e / T)^2 \ll 5 \ln \Lambda m / m_e$$

Let us note that with the shown limitations coefficients of thermal conductivity (4.4), (4.6)-(4.7) are described by the same expressions as in the case of identical temperatures of components [5]. Here, times τ_{ee}^{-1}, τ_{ei}^{-1} and τ_{ea}^{-1}, in τ_e^*, τ_i^*, τ_a^*, and pressure $p_e = n_e k T_e$ are recorded at electron temperature of T_e.

For analysis of the contribution of each of the components to the thermal flux $h^{(t)} = h_e^{(t)} + h_i^{(t)} + h_a^{(t)}$ we use the circumstance, that for τ_α^*, ξ_α^* and δ there are the same estimates for τ_α, ξ_α, and Δ. We introduce instead of λ_α reduced coefficients of thermal conductivity

$$\lambda_\alpha^* = \lambda_\alpha \left(\frac{m}{kT}\right)^{1/2} \frac{Q_{aa}}{k} \qquad (4.9)$$

Then

$$\lambda_e^{\parallel *} \sim \varepsilon^{-1/2}\theta^{-5/2} \frac{\alpha\beta}{\alpha + (1-\alpha)\beta\theta^{-2}}$$

$$\lambda_i^{\parallel *} \sim \frac{\alpha\beta}{\alpha + (1-\alpha)\beta}, \qquad \lambda_a^{\parallel *} \sim \frac{1-\alpha}{1+\alpha} \qquad (4.10)$$

From comparison of expressions for λ_α^* it follows that the total flux of heat along the magnetic field is determined basically by values of h_e and h_a, the contribution of ions is negligible, and nonisothermalness only strengthens this circumstance. With increase of the degree of ionization the electron thermal flux rapidly increases, and at $\alpha \sim (\varepsilon\theta)^{1/2} |\nabla_\parallel T| / |\nabla_\parallel T_e|$ thermal fluxes of atoms and of electrons become comparable.

Increase of the magnetic field noticeably limits the electron thermal flux across the field; therefore at $|\omega_e \tau_e^*| \gg 1$ the basic contribution to transverse heat flow is introduced by h_a and h_i. Here, the contribution of ions becomes essential only at high degrees of ionization $\alpha \sim 1 - \beta$, and for $\omega_i \tau_i^* \gtrsim 1$ when $\alpha \sim 1 - \beta/(\omega_i \tau_i^*)^2$.

The total thermal flux perpendicular both to the magnetic field and to the temperature gradient at $|\omega_e \tau_e^*| \lesssim 1$ is determined basically by h_e. With growth of the magnetic field the contribution of h_i and h_a increases and becomes of the order of h_e at $\omega_i \tau_i^* \gtrsim 1$. Nonisothermalness leads to noticeable growth of the relative contribution of h_e.

We now consider that part of the thermal flux $\mathbf{h}_\alpha$ which is proportional to relative velocities of the components.* In the case interesting us, of a three-component plasma, the corresponding part of vector R_α is conveniently expressed through the density of electrical current $\mathbf{j} = -n_e e(w_e - w_i)$ and "slip" velocity of ions $S = w_i - w_a$. Then in the relative thermal flux of α-component $\mathbf{h}_\alpha$, besides the above-considered "temperature" part $\mathbf{h}_\alpha^{(t)}$, there are isolated terms

$$\begin{aligned} \mathbf{h}_\alpha^{(j)} &= -\chi_\alpha^{\parallel} \mathbf{j}_\parallel - \chi_\alpha^{\perp} \mathbf{j}_\perp - \chi_\alpha^{\wedge} (\mathbf{j} \times \varkappa) \\ \mathbf{h}_\alpha^{(s)} &= -\mu_\alpha^{\parallel} \mathbf{S}_\parallel - \mu_\alpha^{\perp} \mathbf{S}_\perp - \mu_\alpha^{\wedge} (\mathbf{S} \times \varkappa) \end{aligned} \tag{4.11}$$

so that

$$\mathbf{h}_\alpha = \mathbf{h}_\alpha^{(t)} + \mathbf{h}_\alpha^{(j)} + \mathbf{h}_\alpha^{(s)} \tag{4.12}$$

Coefficients χ_e, with accuracy up to terms $\sim \varepsilon^{5/2} \theta^{-1/2}$, are determined by expressions

$$\begin{aligned} \chi_e^{\parallel} &= -\alpha_T \frac{kT_e}{e}, \qquad \chi_e^{\perp} = -\frac{\alpha_T}{1 + (\omega_e \tau_e^*)^2} \frac{kT_e}{e} \\ \chi_e^{\wedge} &= -\frac{\alpha_T \omega_e \tau_e^*}{1 + (\omega_e \tau_e^*)^2} \frac{kT_e}{e} \end{aligned} \tag{4.13}$$

where

$$\alpha_{T_i} = {}^5/_2 \tau_e^* (\zeta_{ea} \tau_{ea}^{-1} - 0.6 \tau_{ei}^{-1}) \tag{4.14}$$

During calculation of coefficients χ_i and χ_a, in them there appear

*The term with div π_α in thermal flux h_α turns out to be in most problems of little importance and, therefore, is not considered subsequently.

noticeable additions, connected with allowance for electron cross terms. However, these very coefficients have an order of $\varepsilon^{3/2}\theta^{5/2}$ and $\varepsilon^{3/2}\theta^{-1/2}$ as compared to χ_e; therefore, their relative contribution to total coefficients in projections of j in the expression for $h^{(j)} = h_e^{(j)} + h_i^{(j)} + h_a^{(j)}$ can be ignored.

As for coefficients μ_α, their contribution to total coefficients in projections of vector S in the expression for $h^{(s)}$ turns out to be of the same order for all components. Not writing concrete expressions for each of these coefficients, we immediately give the expression for the total thermal flux q, in which, besides contributions from $h^{(j)}$ and $h^{(s)}$, it is necessary to consider the additional contribution to coefficients for $j_\parallel$, $j_\perp$, $S_\parallel$, $S_\perp$, arising due to term $5/2\ \Sigma p_\alpha w_\alpha$ in (1.13):

$$\mathbf{q} = \mathbf{q}^{(l)} + \mathbf{q}^{(j)} + \mathbf{q}^{(s)} \tag{4.15}$$

where

$$\mathbf{q}^{(l)} = \mathbf{h}_e^{(l)} + \mathbf{h}_i^{(l)} + \mathbf{h}_a^{(l)} \tag{4.16}$$

$$\mathbf{q}^{(j)} = -\chi^{\parallel}\mathbf{j}_\parallel - \chi^{\perp}\mathbf{j}_\perp - \chi^{\wedge}(\mathbf{j}\times\varkappa), \quad \mathbf{q}^{(s)} = -\mu^{\parallel}\mathbf{S}_\parallel - \mu^{\perp}\mathbf{S}_\perp - \mu^{\wedge}(\mathbf{S}\times\hat{\varkappa})$$

and

$$\chi^{\parallel} = \left(\frac{5}{2} - \alpha_T\right)\frac{kT_e}{e}, \qquad \chi^{\perp} = \left(\frac{5}{2} - \frac{\alpha_T}{1+(\omega_e\tau_e^*)^2}\right)\frac{kT_e}{e} \tag{4.17}$$

$$\chi^{\wedge} = -\frac{\omega_e\tau_e^*\alpha_T}{1+(\omega_e\tau_e^*)^2}\frac{kT_e}{e}$$

$$\mu^{\parallel} = \left[d_e^s - \frac{5}{2}(1-\alpha)\right]p_e + \frac{d_i^s p_i \xi_i^* + d_a^s p_a \xi_a^*}{\delta}$$

$$\mu^{\perp} = \left[\frac{d_e^s}{1+(\omega_e\tau_e^*)^2} - \frac{5}{2}(1-\alpha)\right]p_e + \frac{d_i^s p_i \xi_i^* + d_a^s p_a (\xi_a^* + \delta^{-1}\omega_i^2\tau_i^{*2})}{(1+\delta^{-2}\omega_i^2\tau_i^{*2})\delta} \tag{4.18}$$

$$\mu^{\wedge} = \frac{\omega_e\tau_e^*}{1+(\omega_e\tau_e^*)^2} d_e^s p_e + \frac{d_i^s p_i \xi_i^* + d_a^s p_a (\xi_a^* - \delta)}{(1+\delta^{-2}\omega_i^2\tau_i^{*2})\delta}\omega_i\tau_i^*$$

Here

$$\begin{aligned} d_e^s &= {}^5/_2\tau_e^* \quad [\zeta_{ea}\tau_{ea}^{-1} + 2\varepsilon(1-\theta)(1-\alpha)\tau_{ei}^{-1}] \\ d_i^s &= {}^5/_2\tau_i^* \ [{}^1/_4\zeta_{ia}\tau_{ia}^{-1} + 2\varepsilon\theta^{-1}(1-\theta)(1-\alpha)\tau_{ie}^{-1}] \\ d_a^s &= -{}^5/_2\tau_a^* \ [{}^1/_4\zeta_{ia}\tau_{ai}^{-1} + 2\varepsilon\theta^{-1}(1-\theta)\alpha\tau_{ae}^{-1}] \end{aligned} \tag{4.19}$$

and δ, ξ_i^*, and ξ_a^* are determined by expressions (4.2), (4.8).

In conclusion let us note that with fulfillment of condition

$$(T_e / T)^{1/2} \ll (m / m_e)^{1/2}$$

for j and S it is possible to use relationships, given in [5], if one were to determine τ_{ee}^{-1}, τ_{ei}^{-1}, τ_{ea}^{-1}, and $p_e = n_e k T_e$ at temperature T_e, and also to replace ∇T by ∇T_e.

Submitted
10 March 1964

Literature

1. M. Ya. Aliyevskiy and V. M. Zhdanov. Transport equations for a nonisothermal multitype plasma. PMTF, 1963, No. 5.

2. S. Chapman and T. Cowling. Mathematical theory of nonuniform gases. IL, 1960.

3. S. I. Braginskiy. Transport phenomena in plasma. In coll. Problems of plasma theory. State Atomic Pub. House, 1963, Issue 1, Journal of experimental and theoretical phys., 1957, Vol. 33, Issue 2.

4. R. Herdan and B. Liley. Dynamical equations and transport relationships for a thermal plasma. Rev. Mod. Phys., 1960, Vol. 32, p. 731.

5. V. M. Zhdanov. Transport phenomena in partially ionized gas. PMM, 1962, Vol. 26, Issue 2.

6. L. Spitzer. Physics of a fully ionized gas. IL, 1957.

7. S. Braun. Elementary processes in gas discharge plasma. State Atomic Publishing House, 1961.

8. G. Massey and E. Barhop. Electron and ion collisions. IL, 1958.

9. G. Hirshfelder, C. Curtiss and R. Bird. Molecular theory of gases and fluids, IL, 1961.

10. T. O'Malley. Extrapolation of electro-rare gas atom cross sections to zero energy. Phys. Rev., 1963, Vol. 130, p. 1020.

11. E. Mason and H. Shamp. Mobility of gaseous ions in weak electric fields. Ann. Phys., 1958, Vol. 4, No. 3.

12. A. Dalgagno. Charged particles in the upper atmosphere. Ann. geophys., 1961, Vol.17, p. 16. (Progress of Physical Sciences, 1963, Vol. 79, No. 1).

HEAT TRANSFER AND DIFFUSION IN A PARTIALLY IONIZED TWO-TEMPERATURE PLASMA

G. S. Bïsnovatyy-Kogan

(Moscow)

There is given a solution of the Boltzmann system of equations for plasma in a magnetic field by the Chapman-Enskog method. The plasma is considered partially ionized, and the temperature of electrons can differ from the temperature of heavy particles. Tensors are obtained, connecting the thermal fluxes and the diffusion velocities with temperature gradients and diffusion vectors.

1. The Boltzmann equation, describing change in time of the distribution function of particles of type α in coordinates and velocities $f_\alpha(t, x_i, c_i)$, has the form [1]

$$\frac{\partial f_\alpha}{\partial t} + c_{\alpha i}\frac{\partial f_\alpha}{\partial x_i} + \frac{e_\alpha}{m_\alpha}\left(E_i + \frac{1}{c}\varepsilon_{ikl}c_{\alpha k}B_l\right)\frac{\partial f_\alpha}{\partial c_{\alpha i}} + J_\alpha = 0 \qquad (1.1)$$

Here e_α, m_α — charge and mass of particles of type $\alpha = 1, 2, 3$ correspondingly, for singly charged ions, electrons and neutrals; E_i, B_i — electric field strength and magnetic induction; ε_{ikl} — permutable tensor; c — velocity of light

$$J_\alpha = \sum_{\beta=1}^{3} J_{\alpha\beta}(f_\alpha f_\beta) = \sum_{\beta=1}^{3}\int (f_\alpha f_\beta - f_\alpha' f_\beta')\, g_{\alpha\beta} b\,db\,d\varepsilon\,dc_{\beta i} \qquad \begin{pmatrix} dc_{\beta i} = dc_{\beta 1}dc_{\beta 2}dc_{\beta 3} \\ g_{\alpha\beta} = |c_{\alpha i} - c_{\beta i}| \end{pmatrix} \qquad (1.2)$$

Strokes designate functions of velocities after collisions; $g_{\alpha\beta}$ — relative velocity during collision; b, ε — geometric parameters of collision. We consider only elastic collisions. Let us turn in equation (1.1) to relative velocity $v_{\alpha i}$, equal to

$$v_{\alpha i} = c_{\alpha i} - c_{0i}, \qquad c_{0i} = \frac{1}{\rho}\sum_{\alpha=1}^{3}\rho_\alpha \langle c_{\alpha i}\rangle, \qquad \langle c_{\alpha i}\rangle = \frac{1}{n_\alpha}\int f_\alpha c_{\alpha i}\,dc_{\alpha i}$$

$$n_\alpha = \int f_\alpha\,dc_{\alpha i}, \qquad \rho = \sum_{\alpha=1}^{3}\rho_\alpha = \sum_{\alpha=1}^{3} m_\alpha n_\alpha \tag{1.3}$$

We obtain

$$\frac{df_\alpha}{dt} = v_{\alpha i}\frac{\partial f_\alpha}{\partial x_i} + \left[\frac{e_\alpha}{m_\alpha}\left(E_i + \frac{1}{c}\varepsilon_{ikl}c_{0k}B_l\right) - \frac{dc_{0i}}{dt}\right]\frac{\partial f_\alpha}{\partial v_{\alpha i}} + \\ + \left\{\frac{e_\alpha}{m_\alpha}\frac{1}{c}\varepsilon_{ikl}v_{\alpha k}B_l\frac{\partial f_\alpha}{\partial v_{\alpha i}}\right\} - \frac{\partial f_\alpha}{\partial v_{\alpha i}}v_{\alpha k}\frac{\partial c_{0i}}{\partial x_k} + J_\alpha = 0 \tag{1.4}$$

$$\left(\frac{d}{dt} = \frac{\partial}{\partial t} + c_{0i}\frac{\partial}{\partial x_i}\right)$$

Just as in [1], we obtain equations of transport of particles of each component, of transport of the momentum of the whole mixture and of transport of energy for electrons and heavy particles

$$\frac{dn_\alpha}{dt} + n_\alpha\frac{\partial c_{0i}}{\partial x_i} + \frac{\partial}{\partial x_i}(n_\alpha\langle v_{\alpha i}\rangle) = 0 \tag{1.5}$$

$$\rho\frac{dc_{0i}}{dt} = \frac{1}{c}\varepsilon_{ikl}j_k B_l - \frac{\partial}{\partial x_k}\Pi_{ik} + \rho_e\left(E_i + \frac{1}{c}\varepsilon_{ikl}c_{0k}B_l\right) \tag{1.6}$$

$$\frac{3}{2}kn_2\frac{dT_2}{dt} + \frac{\partial q_{2i}}{\partial x_i} + \Pi_{2ik}\frac{\partial c_{0i}}{\partial x_k} = j_{2i}\left(E_i + \frac{1}{e}\varepsilon_{ikl}c_{0k}B_l\right) + \\ + \frac{3}{2}kT_2\frac{\partial}{\partial x_i}(n_2\langle v_{2i}\rangle) - \rho_2\langle v_{2i}\rangle\frac{dc_{0i}}{dt} - Q_2 \tag{1.7}$$

$$\frac{3}{2}k(n_1+n_3)\frac{dT}{dt} + \frac{\partial}{\partial x_i}(q_{1i}+q_{3i}) + (\Pi_{1ik}+\Pi_{3ik})\frac{\partial c_{0i}}{\partial x_k} = \\ = j_{1i}\left(E_i + \frac{1}{c}\varepsilon_{ikl}c_{0k}B_l\right) + \frac{3}{2}kT\frac{\partial}{\partial x_i}(n_1\langle v_{1i}\rangle + n_3\langle v_{3i}\rangle) - \\ - (\rho_1\langle v_{1i}\rangle + \rho_3\langle v_{3i}\rangle)\frac{dc_{0i}}{dt} - Q \tag{1.8}$$

where k — Boltzmann's constant

$$\Pi_{\alpha ik} = n_\alpha m_\alpha\langle v_{\alpha i}v_{\alpha k}\rangle, \quad q_{\alpha i} = \frac{1}{2}n_\alpha m_\alpha\langle v_\alpha^2 v_{\alpha i}\rangle, \quad j_{\alpha i} = n_\alpha e_\alpha\langle v_{\alpha i}\rangle \tag{1.9}$$

$$\Pi_{ik} = \sum_{\alpha=1}^{3}\Pi_{\alpha ik}, \quad q_i = \sum_{\alpha=1}^{3}q_{\alpha i}, \quad j_i = j_{1i} + j_{2i}, \quad Q_2 = \int\frac{1}{2}m_2 v_2^2 J_2\,dc_{2i}$$

$$Q = \int\frac{1}{2}m_1 v_1^2 J_1\,dc_{1i} + \int\frac{1}{2}m_3 v_3^2 J_3\,dc_{3i} = -Q_2, \qquad \rho_e = e(n_1 - n_2)$$

$$\frac{3kT_2}{2} = \frac{m_2}{2}\langle v_2^2\rangle, \qquad \frac{3kT}{2} = \frac{m_1}{2}\langle v_1^2\rangle = \frac{m_3}{2}\langle v_3^2\rangle, \quad \langle\varphi_\alpha\rangle = \frac{1}{n_\alpha}\int\varphi_\alpha f_\alpha\,dc_{\alpha i}$$

Here e — absolute magnitude of the charge of an electron.

Temperature of electrons T_2 differs from temperature of heavy particles T. Relationships (1.5)-(1.8) are a system of hydrodynamic equations. To find dependences of $\Pi_{\alpha ik}$, $q_{\alpha i}$, $\langle v_{\alpha i}\rangle$, Q, $j_{\alpha i}$ on the electrical and magnetic fields, parameters n_α, T, T_2, c_{0i} and their gradients, it is necessary to solve system (1.4). Solution of this system is conducted by the method of successive approximations of Chapman-Enskog [1].

2. Let us consider the zero approximation. In kinetic equation (1.4) as basic terms there are considered collision and magnetic ones. If the plasma is "strongly ionized" in the sense of [2], the main parts of collision terms will have the form

$$J_1^0 = J_{11}(f_1^0 f_1^0) + J_{13}(f_1^0 f_3^0), \qquad J_2^0 = J_{22}(f_2^0 f_2^0),$$
$$J_3^0 = J_{31}(f_3^0 f_1^0) + J_{33}(f_3^0 f_3^0) \tag{2.1}$$

In equation (1.4) the magnetic term (in braces) is turned into zero by any spherically symmetric function of velocities. Collision terms in form (2.1) are turned into zero by Maxwellian distribution functions, and the temperature of electrons can differ from the temperature of heavy particles. Thus

$$f_\alpha^0 = n_\alpha \left(\frac{m_\alpha}{2\pi k T_\alpha}\right)^{3/2} \exp\left(-\frac{m_\alpha v_\alpha^2}{2kT_\alpha}\right), \qquad T_1 = T_3 = T \neq T_2 \tag{2.2}$$

3. Let us consider the first approximation. We substitute $f_\alpha = f_\alpha^0 + f_\alpha^1$ in (1.4). In small terms it is sufficient to leave f_α^0. Time derivatives of n_α, T, T_2, c_{0i} are excluded by transport equations (1.5)-(1.8), where magnitudes of (1.9) are calculated by Maxwellian function (2.2); only j_i in (1.6) is calculated by $f_\alpha = f_\alpha^0 + f_\alpha^1$. We obtain

$$\Pi_{\alpha ik}^0 = p_\alpha \delta_{ik}, \quad p_\alpha = n_\alpha k T_\alpha, \quad q_{\alpha i}^0 = 0, \quad j_{\alpha i}^0 = 0, \quad j_i^1 = j_i \neq 0 \tag{3.1}$$

If we use (2.2) and (1.2), then, according to (1.9), the magnitude of $Q \neq 0$; however, in the zero approximation we disregarded exchange of energy between electrons and heavy particles, i.e., J_α^0 was selected in form (2.1); therefore $Q^0 = Q_2^0 = 0$. In collision and magnetic terms we leave parts, linear in f_α^1. Collision term J_α^1 has the form

$$J_\alpha^1 = \sum_{\beta=1}^{3} [J_{\alpha\beta}(f_\alpha^0 f_\beta^1) + J_{\alpha\beta}(f_\alpha^1 f_\beta^0) + J_{\alpha\beta}(f_\alpha^0 f_\beta^0)] \tag{3.2}$$

Designating $f_\alpha^1 = f_\alpha^0 \Phi_\alpha$, we obtain a system for Φ_α

$$f_\alpha^0\left[\frac{m_\alpha}{kT_\alpha}\left(v_{\alpha i}v_{\alpha k} - \frac{1}{3}\delta_{ik}v_\alpha^2\right)\frac{\partial c_{0i}}{\partial x_k} + \left(\frac{m_\alpha v_\alpha^2}{2kT_\alpha} - \frac{5}{2}\right)\frac{1}{T_\alpha}\frac{\partial T_\alpha}{\partial x_i}v_{\alpha i} + v_{\alpha i}d_{\alpha i}\right] =$$
$$= -f_\alpha^0\left(\frac{m_\alpha}{\rho kT_\alpha}v_{\alpha i}\frac{1}{c}\varepsilon_{ikl}j_k B_l + \frac{e_\alpha}{m_\alpha c}\varepsilon_{ikl}v_{\alpha k}B_l\frac{\partial \Phi_\alpha}{\partial c_{\alpha i}}\right) - \sum_{\beta=1}^{3} J_{\alpha\beta}(f_\alpha^0 f_\beta^0) - I_\alpha(\Phi_\alpha) \tag{3.3}$$

where

$$I_\alpha = \sum_{\beta=1}^{3}\int [(\Phi_\alpha + \Phi_\beta)f_\alpha^0 f_\beta^0 - (\Phi_\alpha' + \Phi_\beta')f_\alpha^{0\prime} f_\beta^{0\prime}]g_{\alpha\beta}bdbdedc_{\beta i} \tag{3.4}$$

$$d_{\alpha i} = \frac{1}{p_\alpha}\frac{\partial p_\alpha}{\partial x_i} - \frac{\rho_\alpha}{p_\alpha \rho}\frac{\partial p}{\partial x_i} + \left(\frac{m_\alpha \rho_e}{\rho kT_\alpha} - \frac{e_\alpha}{kT_\alpha}\right)\left(E_i + \frac{1}{c}\varepsilon_{ikl}c_{0k}B_l\right)$$

$$\sum_{\alpha=1}^{3} p_\alpha d_{\alpha i} = 0 \qquad (p = p_1 + p_2 + p_3) \tag{3.5}$$

As independent diffusion vectors $d_{\alpha i}$ we select vectors d_{1i} and d_{3i}. Because of linearity, we seek solution of system (3.3) in the form

$$\Phi_\alpha = -A_{\alpha 1 i}\frac{1}{T}\frac{\partial T}{\partial x_i} - A_{\alpha 2 i}\frac{1}{T_2}\frac{\partial T_2}{\partial x_i} - G_{\alpha i k}\frac{\partial c_{0i}}{\partial x_k} - nD_{\alpha 1 i}d_{1i} - nD_{\alpha 3 i}d_{3i} - F_\alpha \qquad (n = n_1 + n_2) \tag{3.6}$$

Here $A_{\alpha\beta i}$, $D_{\alpha\beta i}$, $G_{\alpha i k}$, F_α – functions of $v_{\alpha i}$, B_i. Contribution to the thermal flux $q_{\alpha i}$ and to diffusion velocity $\langle v_{\alpha i}\rangle$ will come [1] only from terms in $A_{\alpha\beta i}$ and $D_{\alpha\beta i}$. We use henceforth designation

$$K_{\alpha i} = A_{\alpha 1 i},\ A_{\alpha 2 i},\ D_{\alpha 1 i},\ D_{\alpha 2 i} \tag{3.7}$$

We seek $K_{\alpha i}$ in the form

$$K_{\alpha i} = K_\alpha^1 v_{\alpha i} + K_\alpha^2 e_{ijk}v_{\alpha j}B_k + K_\alpha^3 B_i(v_{\alpha j}B_j), \qquad K_\alpha^\beta = K_\alpha^\beta(v_\alpha, B) \qquad (\alpha, \beta = 1, 2, 3) \tag{3.8}$$

Equations for K_α^β are obtained with substitution of expansions (3.6)-(3.8) in equations (3.3) and equating of coefficients in independent parameters to zero. We introduce $\zeta_\alpha = K_\alpha^1 + iBK_\alpha^2$ and shift to dimensionless velocity $u_{\alpha i} = [(1/2)(m_\alpha/kT_\alpha)]^{1/2} v_{\alpha i}$. Systems obtained for ζ_α with different $K_{\alpha i}$ from (3.7), linear, nonhomogeneous, differ from one another only by nonhomogeneous terms. They have form

$$M_\alpha = -\frac{i}{3} B f_\alpha^0 \frac{e}{c} \frac{m_\alpha}{\rho k T_\alpha} (L_1 - L_2) u_{\alpha i} + iB f_\alpha^0 \frac{e_\alpha}{m_\alpha c} \zeta_{0\alpha} u_{\alpha i} + I_\alpha (\zeta_{\alpha} u_{\alpha i}) \qquad (3.9)$$

Here

$$L_\alpha = \int \zeta_\alpha f_\alpha^0 v_\alpha^2 dc_{\alpha i} \qquad (\alpha = 1, 2, 3;\ e_1 = -e_2 = e,\ e_3 = 0). \qquad (3.10)$$

Left parts of system (3.9) for different $K_{\alpha i}$ from (3.7) have form

$$\begin{aligned}
&M_1 = f_1^0 \left(u_1^2 - \frac{5}{2}\right) u_{1i}, \quad M_2 = 0, \quad M_3 = f_3^0 \left(u_3^2 - \frac{5}{2}\right) u_{3i} && \text{when } K_{\alpha i} = A_{\alpha 1 i} \\
&M_1 = 0, \quad M_2 = f_2^0 \left(u_2^2 - \frac{5}{2}\right) u_{2i}, \quad M_3 = 0 && \text{when } K_{\alpha i} = A_{\alpha 2 i} \\
&M_1 = \frac{1}{n} f_1^0 u_{1i}, \quad M_2 = -\frac{n_1}{n n_2} f_2^0 \frac{T}{T_2} u_{2i}, \quad M_3 = 0 && \text{when } K_{\alpha i} = D_{\alpha 1 i} \\
&M_1 = 0, \quad M_2 = -\frac{n_3}{n n_2} f_2^0 \frac{T}{T_2} u_{2i}, \quad M_3 = \frac{1}{n} f_3^0 u_{3i} && \text{when } K_{\alpha i} = D_{\alpha 3 i}
\end{aligned} \qquad (3.11)$$

Solution of system (3.9) with right parts of (3.11) is sought in the form of expansion in a series of Sonin polynomials $S_{3/2}^{(p)}(x)$, which are determined as follows [1]

$$(1-s)^{-3/2} \exp \frac{-xs}{1-s} = \sum_{p=0}^{\infty} s^p S_{3/2}^{(p)}(x); \quad S_{3/2}^{(0)}(x) = 1, \quad S_{3/2}^{(1)}(x) = \frac{5}{2} - x \qquad (3.12)$$

$$\int_0^\infty e^{-x} S_{3/2}^{(p)}(x) S_{3/2}^{(q)}(x) \cdot x^{3/2} dx = \frac{\Gamma(p + 5/2)}{p!} \delta_{pq} \qquad (3.13)$$

In order we have

$$\zeta_{0\alpha} = \sum_{p=0}^{\infty} \gamma_{\alpha p} S_{3/2}^{(p)}(u_\alpha^2), \qquad L_\alpha = \frac{3kT_\alpha}{m_\alpha} n_\alpha \gamma_{\alpha 0} \qquad (3.14)$$

From the condition that correction to the Maxwellian function does not contribute to mean mass velocity, we obtain condition

$$n_1 T \gamma_{10} + n_2 T_2 \gamma_{20} + n_3 T \gamma_{30} = 0 \tag{3.15}$$

Substituting (3.14) in (3.9), multiplying by $S_{3/2}^{(p)}(u_\alpha^2) u_{\alpha i}$ and integrating with respect to $dc_{\alpha i}$, we obtain instead of system (3.9) an infinite system of linear nonhomogeneous algebraic equations

$$\begin{aligned}
N_{\alpha 0} &= -i\frac{3}{2}\frac{eB}{pc}\frac{m_\alpha}{T_\alpha}\left(\gamma_{10}\frac{n_1 T}{m_1} - \gamma_{20}\frac{n_2 T_2}{m_2}\right) n_\alpha + i\frac{3}{2}\frac{e_\alpha B}{m_\alpha c} n_\alpha \gamma_{\alpha 0} + \\
&+ \left(\frac{m_\alpha T}{m_1 T_\alpha}\right)^{1/2} \sum_{r=0}^{\infty} \gamma_{1r} a_{0r}^{\alpha 1} + \left(\frac{m_\alpha T_2}{m_2 T_\alpha}\right)^{1/2} \sum_{r=0}^{\infty} \gamma_{2r} a_{0r}^{\alpha 2} + \left(\frac{m_\alpha T}{m_3 T_\alpha}\right)^{1/2} \sum_{r=0}^{\infty} \gamma_{3r} a_{0r}^{\alpha 3} \\
N_{\alpha k} &= i\frac{2\Gamma(k+3/2)}{\sqrt{\pi}\, k!}\frac{e_\alpha B}{m_\alpha c} n_\alpha \gamma_{\alpha k} + \left(\frac{m_\alpha}{m_1}\frac{T}{T_\alpha}\right)^{1/2} \sum_{r=0}^{\infty} \gamma_{1r} a_{kr}^{\alpha 1} + \\
&+ \left(\frac{m_\alpha T_2}{m_2 T_\alpha}\right)^{1/2} \sum_{r=0}^{\infty} \gamma_{2r} a_{kr}^{\alpha 2} + \left(\frac{m_\alpha T}{m_3 T_\alpha}\right)^{1/2} \sum_{r=0}^{\infty} \gamma_{3r} a_{kr}^{\alpha 3} \qquad \begin{pmatrix} k \geqslant 1 \\ \alpha = 1, 2, 3 \end{pmatrix}
\end{aligned} \tag{3.16}$$

For different $K_{\alpha i}$ from (3.7) the left parts of system (3.16) have the form

$$\begin{aligned}
N_{11} &= -\frac{15}{4} n_1, \quad N_{31} = -\frac{15}{4} n_3 && \text{when } K_{\alpha i} = A_{\alpha 1 i} \\
N_{21} &= -\frac{15}{4} n_2 && \text{when } K_{\alpha i} = A_{\alpha 2 i} \\
N_{10} &= \frac{3}{2}\frac{n_1}{n}, \quad N_{20} = -\frac{3}{2}\frac{n_1 T}{n T_2} && \text{when } K_{\alpha i} = D_{\alpha 1 i} \\
N_{20} &= -\frac{3}{2}\frac{n_3}{n}\frac{T}{T_2}, \quad N_{30} = \frac{3}{2}\frac{n_3}{n} && \text{when } K_{\alpha i} = D_{\alpha 3 i}
\end{aligned} \tag{3.17}$$

In all these cases remaining values of $N_{\alpha j} = 0$. Quantities $a_{pq}^{\alpha\beta}$ are determined as follows:

$$\begin{aligned}
a_{pq}^{\alpha\alpha} &= \int f_\alpha^0 f^0 S_{3/2}^{(p)}(u_\alpha^2)\, u_{\alpha i} \left[S_{3/2}^{(q)}(u_\alpha^2)\, u_{\alpha i} + S_{3/2}^{(q)}(u^2)\, u_i - S_{3/2}^{(q)}(u_\alpha'^2)\, u_{\alpha i}' - \right. \\
&\left. - S_{3/2}^{(q)}(u'^2)\, u_i'\right] g_{\alpha\alpha} b\, db\, d\varepsilon\, dc_i\, dc_{\alpha i} + \\
&+ \sum_{\beta \neq \alpha} \int S_{3/2}^{(p)}(u_\alpha^2)\, u_{\alpha i} \left[f_\alpha^0 f_\beta^0 S_{3/2}^{(q)}(u_\alpha^2)\, u_{\alpha i} - f_\alpha^{0'} f_\beta^{0'} S_{3/2}^{(q)}(u_\alpha'^2)\, u_{\alpha i}'\right] g_{\alpha\beta} b\, db\, d\varepsilon\, dc_{\beta i}\, dc_{\alpha i} \\
&\qquad (\alpha, \beta = 1, 2, 3) \\
a_{pq}^{\alpha\beta} &= \int S_{3/2}^{(p)}(u_\alpha^2)\, u_{\alpha i} \left[f_\alpha^0 f_\beta^0 S_{3/2}^{(q)}(u_\beta^2)\, u_{\beta i} - f_\alpha^{0'} f_\beta^{0'} S_{3/2}^{(q)}(u_\beta'^2)\, u_{\beta i}'\right] g_{\alpha\beta} b\, db\, d\varepsilon\, dc_{\beta i}\, dc_{\alpha i} \\
&\qquad (\alpha_1, \beta = 1,2,3;\ \alpha \neq \beta)
\end{aligned} \tag{3.18}$$

The first three equations of system (3.16) will be linearly

dependent. This is a mathematical result of the same fact from which we obtained condition (3.15). Eliminating from system (3.16) with left parts (3.17) variable γ_{30} with the help of (3.15) and dropping the third of equations (3.16), we obtain a system which can be solved by Krammer's rule. Finding ζ_α, we can immediately write the solution for K_α^3 from the following considerations: without a magnetic field transport properties are determined only by the magnitude of K_α^1, in which it is assumed that B = 0. In a magnetic field transport properties do not change; therefore for B_i, parallel to any of vectors $\partial T_\alpha/\partial x_i$, $d_{\alpha i}$, transport properties connected with this vector will be the same as for B = 0. Therefore,

$$K_\alpha^1 + B^2 K_\alpha^3 = (K_\alpha^1)_{B=0} \tag{3.19}$$

This relationship determines K_α^3. If $\gamma_{\alpha r} = x_{\alpha r} + iBy_{\alpha r}$, and K_α^3 is expanded in a series of Sonin polynomials with coefficients $z_{\alpha r}$,

$$x_{\alpha r} + B^2 z_{\alpha r} = (x_{\alpha r})_{B=0} \tag{3.20}$$

4. Coefficients of the expansion of K_α^β in Sonin polynomials for different values of $K_{\alpha i}$ from (3.7) we designate as follows

$$\begin{array}{lccc} & K_\alpha^1 & K_\alpha^2 & K_\alpha^3 \\ A_{\alpha 1 i} & a_r^{\alpha 1} & b_r^{\alpha 1} & c_r^{\alpha 1} \\ A_{\alpha 2 i} & a_r^{\alpha 2} & b_r^{\alpha 2} & c_r^{\alpha 2} \\ D_{\alpha 1 i} & x_r^{\alpha 1} & y_r^{\alpha 1} & z_r^{\alpha 1} \\ D_{\alpha 3 i} & x_r^{\alpha 3} & y_r^{\alpha 3} & z_r^{\alpha 3} \end{array} \quad \begin{pmatrix} \alpha = 1, 2, 3 \\ r \geqslant 0 \end{pmatrix} \tag{4,1}$$

Then, using definition (1.9) for $q_{\alpha i}$, $\langle v_{\alpha i} \rangle$, j_i, considering $f_\alpha = f_\alpha^0(1 + \Phi_\alpha)$ and equalities (3.6), (3.8), (3.14), and (4.1), and also orthogonality of Sonin polynomials (3.13), we obtain

$$q_{\alpha i} = -\lambda_{ik}^{\alpha 1} \frac{\partial T}{\partial x_k} - \lambda_{ik}^{\alpha 2} \frac{\partial T_2}{\partial x_k} - \nu_{ik}^{\alpha 1} d_{1i} - \nu_{ik}^{\alpha 3} d_{3i} \tag{4.2}$$

$$\langle v_{\alpha i} \rangle = -\eta_{ik}^{\alpha 1} d_{1k} - \eta_{ik}^{\alpha 3} d_{3k} - \mu_{ik}^{\alpha 1} \frac{\partial T}{\partial x_k} - \mu_{ik}^{\alpha 2} \frac{\partial T_2}{\partial x_k} \tag{4.3}$$

where

$$\lambda_{ik}^{\alpha\beta} = \frac{5}{2}\frac{k^2 T_\alpha^2}{m_\alpha T_\beta} n_\alpha \left[(a_0^{\alpha\beta} - a_1^{\alpha\beta})\delta_{ik} - \varepsilon_{ikn}B_n(b_0^{\alpha\beta} - b_1^{\alpha\beta}) + B_iB_k(c_0^{\alpha\beta} - c_1^{\alpha\beta})\right]$$

$$(\alpha = 1, 2, 3; \quad \beta = 1, 2) \tag{4.4}$$

$$\nu_{ik}^{\alpha\beta} = \frac{5}{2}\frac{k^2 T_\alpha^2}{m_\alpha} n n_\alpha \left[(x_0^{\alpha\beta} - x_1^{\alpha\beta})\delta_{ik} - \varepsilon_{ikn}B_n(y_0^{\alpha\beta} - y_1^{\alpha\beta}) + B_iB_k(z_0^{\alpha\beta} - z_1^{\alpha\beta})\right]$$

$$(\alpha = 1, 2, 3; \quad \beta = 1, 3) \tag{4.5}$$

$$\eta_{ik}^{\alpha\beta} = \frac{kT_\alpha n}{m_\alpha}\left[x_0^{\alpha\beta}\delta_{ik} - \varepsilon_{ikn}B_n y_0^{\alpha\beta} + B_iB_k z_0^{\alpha\beta}\right] \qquad \begin{pmatrix}\alpha = 1, 2, 3\\ \beta = 1, 3\end{pmatrix} \tag{4.6}$$

$$\mu_{ik}^{\alpha\beta} = \frac{kT_\alpha}{m_\alpha T_\beta}\left[a_0^{\alpha\beta}\delta_{ik} - \varepsilon_{ikn}B_n b_0^{\alpha\beta} + B_iB_k c_0^{\alpha\beta}\right] \qquad \begin{pmatrix}\alpha = 1, 2, 3\\ \beta = 1, 2\end{pmatrix} \tag{4.7}$$

$$j_i = e(n_1\langle v_{1i}\rangle - n_2\langle v_{2i}\rangle) \tag{4.8}$$

Thus, to find the thermal fluxes and diffusion velocities it is sufficient to know the first two coefficients of the expansion.

5. We leave in expansion (3.14) the first two members. Elements $a_{ik}^{\alpha\beta}(i, k = 0, 1)$, in equations of the first approximation by Sonin polynomials defined in (3.18), will have form

$$a_{00}^{11} = \frac{x_1}{\tau_{12}} n\alpha(1-\alpha) + \frac{3}{2}\frac{n\alpha}{\tau_2}\frac{m_2}{m}, \qquad a_{01}^{11} = 0; \qquad a_{10}^{11} = \frac{15}{2}\frac{m_2}{m}\frac{T_2 - T}{T}\frac{n\alpha}{\tau_2}$$

$$a_{11}^{11} = \frac{3n\alpha}{\tau_1} + \frac{x_1}{\tau_{12}} n\alpha(1-\alpha), \qquad a_{00}^{12} = -\frac{3}{2}\left(\frac{m_2 T_2}{mT}\right)^{1/2}\frac{n\alpha}{\tau_2}$$

$$a_{01}^{12} = -\frac{9}{4}\left(\frac{m_2 T_2}{mT}\right)^{1/2}\frac{n\alpha}{\tau_2}, \qquad a_{10}^{12} = a_{11}^{12} = 0, \qquad a_{00}^{13} = -\frac{x_1}{\tau_{12}} n i(1-\alpha)$$

$$a_{10}^{13} = a_{01}^{13} = 0, \qquad a_{11}^{13} = -\frac{x_5}{\tau_{12}} n\alpha(1-\alpha), \qquad a_{00}^{21} = -\frac{3}{2}\left(\frac{m_2 T}{mT_2}\right)^{1/2}\frac{n\alpha}{\tau_2}$$

$$a_{01}^{21} = a_{11}^{21} = 0, \qquad a_{10}^{21} = -\frac{9}{4}\left(\frac{m_2 T}{mT_2}\right)^{1/2}\frac{n\alpha}{\tau_2} \tag{5.1}$$

$$a_{00}^{22} = \frac{3}{2}\frac{n\alpha}{\tau_2} + \frac{x_2}{\tau_{23}} n\alpha(1-\alpha), \qquad a_{10}^{22} = a_{01}^{22} = \frac{9}{4}\frac{n\alpha}{\tau_2}$$

$$a_{11}^{22} = \left(\frac{13}{4} + \sqrt{2}\right)\frac{3}{2}\frac{n\alpha}{\tau_2} + \frac{x_2}{\tau_{23}} n\alpha(1-\alpha), \qquad a_{00}^{23} = -\frac{x_2}{\tau_{23}} n\alpha(1-\alpha)\left(\frac{m_2 T}{mT_2}\right)^{1/2}$$

$$a_{10}^{23} = a_{01}^{23} = a_{11}^{23} = 0, \qquad a_{00}^{31} = -\frac{x_1}{\tau_{13}} n\alpha(1-\alpha), \qquad a_{10}^{31} = a_{01}^{31} = 0$$

$$a_{11}^{31} = -\frac{x_5}{\tau_{13}} n\alpha(1-\alpha), \qquad a_{00}^{32} = -\frac{x_2}{\tau_{23}} n\alpha(1-\alpha)\left(\frac{m_2 T_2}{mT}\right)^{1/2}, \quad a_{10}^{32} = a_{01}^{32} = a_{11}^{32} = 0$$

$$a_{00}^{33} = \frac{x_1}{\tau_{13}} n\alpha(1-\alpha), \quad a_{01}^{33} = 0, \quad a_{10}^{33} = \frac{x_6}{\tau_{23}} n\alpha(1-\alpha)\frac{m_2}{m}\frac{T_2 - T}{T}$$

$$a_{11}^{33} = \frac{n(1-\alpha)}{\tau_{23}} + \frac{x_4}{\tau_{13}} n\alpha(1-\alpha)$$

where

$$\tau_1 = \frac{3\sqrt{m}(kT)^{3/2}}{4\sqrt{\pi}\lambda_1 e^4 n x}, \qquad \tau_3 = \frac{1}{8\sqrt{\pi}\Omega^{(2,2)*}\sigma^2}\left(\frac{m}{kT}\right)^{1/2}\frac{1}{n(1-x)}$$
$$\tau_2 = \frac{3\sqrt{m_2}(kT_2)^{3/2}}{4\sqrt{2\pi}\lambda_2 e^4 n x}, \qquad \tau_{13} = \frac{\sqrt{m}}{\sqrt{\varphi_1 n}}, \qquad \tau_{23} = \frac{\sqrt{m_2}}{\sqrt{\varphi_2 n}} \tag{5.2}$$

Here λ_α — Coulomb logarithm [3] for ions and electrons

$$\lambda_\alpha = \frac{1}{2}\ln\frac{k^3 T_\alpha^2 T T_2}{\pi n x e^6 (T+T_2)} \qquad (\alpha = 1, 2) \tag{5.3}$$

Interaction of neutrals among themselves was calculated by the Lenard-Jones potential. Values of σ and $\Omega^{(2.2)*}$ for that potential are given in [4]. For the interaction of neutrals with charged particles we took Maxwellian interaction

$$F_{3\alpha} = \frac{\varphi_\alpha}{x^5} \qquad (\alpha = 1, 2) \tag{5.4}$$

The constant of interaction φ_2 for electrons can be estimated from the magnitude of polarizability of the molecule [5], which can be expressed through the dielectric constant of the gas [6]. Considering the picture of interaction from classical mechanics, we have

$$\varphi_2 = \frac{3}{2\pi}\frac{\varepsilon-1}{\varepsilon+2}\frac{e^2}{N} = 4.12\cdot 10^{-29}\frac{\varepsilon-1}{\varepsilon+2}\left[\frac{cm^6}{ce\kappa^2}\right] \tag{5.5}$$

Here ε — dielectric constant of the gas; N — number of particles per cm^3 under normal conditions. The value of φ_1 is larger than φ_2 by approximately one order due to the larger recharge cross section.

For Maxwellian interactions nondiagonal elements $a_{ik}^{3\alpha}$ and $a_{ik}^{\alpha 3}$ $(i \neq k)$ turn into zero. For real interactions of neutrals with ions and electrons these elements are much less than diagonal ones in the first approximation it is possible to disregard them. For Maxwellian interaction

$$x_1 = 2.81, \quad x_2 = 3.98, \quad x_3 = 9.95, \quad x_4 = 10.7, \quad x_5 = 3.4, \quad x_6 = 19.9 \tag{5.6}$$

During calculation of (5.1) we disregarded quantities $\sim(m_2 T_2/mT)^{1/2}$ as compared to one and assumed

$$m_1 = m_3 = m; \qquad n_1 = n_2 = n\alpha, \qquad \alpha = n_1/(n_1 + n_3) \tag{5.7}$$

Integrals of collisions (5.1) of neutrals with ions and electrons for real interactions it is necessary to calculate by formulas [1], which in the given approximation have form

$$\frac{x_1}{n\tau_{13}} = 4\Omega_{13}^{(1)}(1), \qquad \frac{x_2}{n\tau_{23}} = 8\Omega_{23}^{(1)}(1), \qquad \frac{x_5}{n\tau_{23}} = 49\Omega_{23}^{(1)}(1)$$
$$\frac{x_3}{n\tau_{23}} = 8\left[\frac{25}{4}\Omega_{23}^{(1)}(1) - 5\Omega_{23}^{(1)}(2) + \Omega_{23}^{(1)}(3)\right]$$
$$\frac{x_4}{n\tau_{13}} = 4\left[\frac{55}{16}\Omega_{13}^{(1)}(1) - \frac{5}{4}\Omega_{13}^{(1)}(2) + \frac{1}{4}\Omega_{13}^{(1)}(3) + \frac{1}{2}\Omega_{13}^{(2)}(2)\right]$$
$$\frac{x_6}{n\tau_{13}} = \frac{55}{4}\Omega_{13}^{(1)}(1) - 5\Omega_{13}^{(1)}(2) + \Omega_{13}^{(1)}(3) - 2\Omega_{13}^{(2)}(2) \tag{5.8}$$
$$\Omega_{\beta 3}^{(i)}(r) = \sqrt{\pi}\int_0^\infty e^{-z^2} z^{2r+3}\int_0^\infty (1 - \cos^i\chi_{3\beta})\, g_{3\beta} b\, db\, dz$$

In formulas (5.8) we use designations

$$z = \left[\frac{mm_\beta}{2k(mT_\beta + m_\beta T)}\right]^{1/2} g_{3\beta} \qquad (\beta = 1, 2) \tag{5.9}$$

Here $\chi_{3\beta}$ – scattering angle. Using (3.16), (5.1), disregarding $\sim(m_2T_2/mT)^{1/2}$ as compared with one and considering $\alpha\tau_2 \ll \tau_{23}$ for coefficients in (4.4)-(4.7), we obtain

$$a_0^{\beta 1} = b_0^{\beta 1} = c_0^{\beta 1} = a_1^{21} = b_1^{21} = c_1^{21} = 0 \qquad (\beta = 1, 2, 3) \tag{5.10}$$

For $\gamma_1^{\mu} = a_1^{\mu 1} + iBb_1^{\mu 1}$ ($\mu = 1, 3$) we obtain system

$$-\frac{15}{4}n\alpha = \left[\frac{3n\alpha}{\tau_1} + \frac{x_4 n\alpha(1-\alpha)}{\tau_{13}} + i\frac{15}{4}\omega_1 n\alpha\right]\gamma_1^1 - \frac{x_5}{\tau_{13}} n\alpha(1-\alpha)\gamma_1^3$$
$$-\frac{15}{4}n(1-\alpha) = -\frac{x_5}{\tau_{13}} n\alpha(1-\alpha)\gamma_1^1 + \left[\frac{n(1-\alpha)}{\tau_2} + \frac{x_4}{\tau_{13}} n\alpha(1-\alpha)\right]\gamma_1^3$$
$$\left(\omega_1 = \frac{eB}{mc}\right) \tag{5.11}$$

From (5.11), (5.2), (4.4) for $\alpha = 0$ we obtain the formula of the first approximation for the coefficient of thermal conductivity of a simple gas [1]

$$\lambda = \frac{75}{64}\frac{1}{\sigma^2\Omega^{(2,2)^*}}\left(\frac{k^3T}{\pi m}\right)^{1/2} \tag{5.12}$$

For a model of elastic spheres $\Omega^{(2.2)*} = 1$,

$$a_1^{\beta 2} = b_1^{\beta 2} = c_1^{\beta 2} = x_1^{\beta\mu} = y_1^{\beta\mu} = z_1^{\beta\mu} = 0 \qquad (\beta = 1, 3;\ \mu = 1, 3) \tag{5.13}$$

For coefficients

$$\begin{aligned} \rho_{11} &= a_0^{12} + iBb_0^{12}, \quad \rho_{12} = a_0^{22} + iBb_0^{22}, \quad \rho_{13} = a_1^{22} + iBb_1^{22} \\ \rho_{21} &= x_0^{11} + iBy_0^{11}, \quad \rho_{22} = x_0^{21} + iBy_0^{21}, \quad \rho_{23} = x_1^{21} + iBy_1^{21} \\ \rho_{31} &= x_0^{13} + iBy_0^{13}, \quad \rho_{32} = x_0^{23} + iBy_0^{23}, \quad \rho_{33} = x_1^{23} + iBy_1^{23} \end{aligned} \tag{5.14}$$

we obtain system

$$\begin{aligned} P_{\beta 1} &= n\alpha\left[i\frac{3}{2}\omega_1(1-\alpha) + \frac{x_1}{\tau_{12}} + \frac{3}{2\tau_2}\frac{m_2}{m}\right]\rho_{\beta 1} + \\ &\qquad \frac{T_2}{T} n\alpha\left[i\frac{3}{2}\omega_2\alpha - \frac{3}{2\tau_2}\right]\rho_{\beta 2} - \frac{T_2}{T}\alpha\alpha\frac{9}{4\tau_2}\rho_{\beta 3} \\ P_{\beta 2} &= -n\alpha\frac{3}{2\tau_2}\frac{m_2 T}{m T_2}\rho_{\beta 1} + n\alpha\left[\frac{3}{2\tau_2} + \frac{x_2(1-\alpha)}{\tau_{22}} - i\frac{3}{2}\omega_2\right]\rho_{\beta 2} + \frac{9}{4\tau_2}n\alpha\rho_{\beta 3} \\ P_{\beta 3} &= -\frac{9}{4\tau_2}n\alpha\frac{m_2}{m}\frac{T}{T_2}\rho_{\beta 1} + \frac{9}{4\tau_2}n\alpha\rho_{\beta 2} + n\alpha\left[\frac{7}{\tau_2} + \frac{x_2(1-\alpha)}{\tau_{22}} - i\frac{15}{4}\omega_2\right]\rho_{\beta 3} \\ &\left(\omega_2 = \frac{eB}{m_2 c},\ \beta = 1, 2, 3\right) \end{aligned} \tag{5.15}$$

where

$$P_{12} = -\frac{15}{4}n\alpha, \quad P_{21} = \frac{5}{2}\alpha, \quad P_{22} = -\frac{3}{2}\alpha\frac{T}{T_2}, \quad P_{32} = -\frac{3}{2}(1-\alpha)\frac{T}{T_2} \tag{5.16}$$

The other values of $P_{\beta\mu} = 0$. From system (5.15) for $\alpha = 1$ we obtained results of the first approximation of Landshoff [7] for transport factors along and cross a magnetic field and results of [8]. In [7] there is investigated the convergence of transport factors for stripped plasma in the case $B = 0$ with expansion in Sonin polynomials. For coefficients of diffusion and the diffusion thermoeffect the first approximation gives an error of ~1.5%; for coefficients of thermal conductivity and thermal diffusion error is ~15%. When $B = 0$ and $T_2 = T$, from (5.15) we obtain the results of the first approximation of [9]. Remaining coefficients in (4.4)-(4.7) are obtained from relationships

$$B^2 c_k^{\alpha\mu} = (a_k^{\alpha\mu})_{B=0} - a_k^{\alpha\mu}, \qquad B^2 z_k^{\alpha\beta} = (x_k^{\alpha\beta})_{B=0} - x_k^{\alpha\beta} \tag{5.17}$$

$$(\alpha = 1, 2, 3; \quad \mu = 1, 2; \quad \beta = 1, 3; \ k = 0, 1)$$

$$F_0^{3\beta} = -\frac{\alpha}{1-\alpha}F_0^{1\beta} \tag{5.18}$$

where

$$F = a, b, c \quad (\beta = 1, 2), \qquad F = x, y, z \quad (\beta = 1, 3)$$

Limits of applicability of the solution of the Boltzmann equations by the Chapman-Enskog method for a stripped plasma are given in [7, 9]. These also are necessary conditions for applicability of the present work. Furthermore, it is necessary that the plasma be "strongly ionized" in the sense of [2].

During proofreading the author was apprised of the recently appearing work [11], in which by the Chapman-Enskog method, analogously to S. I. Braginskiy [10], there is a calculation of transport factors for electrons and ions in partially ionized two-temperature plasma. Distribution of neutrals was assumed Maxwellian.

It is noted that analogous calculation of the influence of neutral particles on transport properties in partially ionized singe-temperature plasma is made in [12].

Submitted
20 February 1964

Literature

1. S. Chapman and T. Cowling. Mathematical theory of nonuniform gases, IL, 1960.

2. V. L. Ginzburg and A. V. Gurevich. Nonlinear Phenomena in plasma, in variable electromagnetic field. Progress of physical sciences, 1960, Vol. 70, Issue 2.

3. L. D. Landau. Kinetic equation in the case of Coulomb interaction. Journal of experimental and theoretical physics, 1937, Vol. 7, Issue 2.

4. G. Hirschfelder, C. Curtiss, and R. Bird. Molecular theory of gases and fluids. IL, 1961.

5. Baihet, Delcroix, and Denisse. Kinetic theory of uniform weakly ionized plasma. Coll. of trans. Problems of contemporary physics, IL, 1957, No. 5.

6. I. Ye. Tamm. Principles of the theory of electricity. Gostekhteoretizdat, 1957.

7. R. Landshoff. Transport phenomena in a completely ionized gas in presence of magnetic field. Phys. Rev., 1949, Vol. 76, p. 904; 1951, Vol. 82, p. 442 (Russian, trans. in Problems of contemporary physics, IL, 1956, No. 2).

8. W. Marshall. The kinetic theory of an ionized gas. p. III. At. Energy Res Estab. 1960, N T/R, 2419.

9. H. Schirmer, and I. Friedrich. Die electrische Leitfähigkeit eines Plasmas. Z. Physik, 1958, B. 151, H. 2, S. 174; 1958, B. 151, H 3, S. 375; Die Wärmesfähigkeit eines Plasmas. Z. Physik, 1959, B. 153, H. 5, S. 563. (Russ. trans. in coll. Moving plasma, IL, 1961).

10. S. I. Braginskiy. Transport phenomena in stripped two-temperature plasma. Journ. exp. and theor. physics, 1957, Vol. 33, Issue 2(8).

11. I. P. Stakhanov and A. S. Stepanov. Transport equations for 3-component plasma in a magnetic field. Journal tech. physics, 1964, Vol. 34, Issue 3.

12. J. Wright. Effect of neutral particles on the transport properties of a plasma in a uniform magnetic field. Phys. of fluids, 1961, Vol. 4, No. 11, p. 1341.

ON REGIONS OF APPLICABILITY OF VARIOUS EQUATIONS FOR STUDY OF COMPLETELY IONIZED GAS*

V. B. Baranov

(Moscow)

Transport factors for a completely ionized gas have been calculated by different authors from kinetic theory (see, for instance, [1, 2]), relying on the Boltzmann equation. Applicability of this equation for study of the behavior of systems of charged particles frequently evokes objections by virtue of the fact that it is usually derived on the assumption of the binaryness of collisions of particles, whereas Coulomb interactions spread to distances, significantly exceeding the average distance between particles, and collisions are not binary. In [3] there was derived an expression for the term with collisions of charged particles, which subsequently acquired the name of the integral of collisions in Landau form, and was used in [2] for calculation of transport factors for plasma. However, the derivation in [3] was also based on the assumption on binaryness of collisions.

In [4] it is shown that the kinetic Boltzmann equation can be obtained by breaking up the open chain of kinetic equations, obtained from the equation of Liouville for distribution function $f_N(\mathbf{q}_1, \mathbf{q}_2, \ldots, \mathbf{q}_N, \mathbf{p}_1, \mathbf{p}_2, \ldots, \mathbf{p}_N, t)$, which depends on coordinates $\mathbf{q}_i$ and pulses $\mathbf{p}_i$ of all N particles in the system, and on time t, where the kinetic equation with the integral of collisions in Landau form was obtained on the assumption of uniformity in space and in the case of the absence of a magnetic field.

*From report at Second All-Union Conference on theoretical and applied mechanics. Moscow, January 1964.

In this work, using the method offered by Yu. L. Klimontovich,* there are extracted those limitations which it is necessary to put on parameters of the plasma so that from Liouville's equation for the random function of the number of particles $N_a(q, p, t)$ we pass by means of averaging to the kinetic Boltzmann equation with the integral of collisions in the Landau form. The latter was used in [2] for calculation of transport factors for plasma in a strong magnetic field. On the basis of the obtained system of inequalities in the density-temperature plane there is constructed a diagram of regions, which gives a graphic presentation of the possibility of use of one or another equation for description of processes in plasma, if we know parameters of the investigated system (ionization potential of the gas, density, temperature, magnetic field, etc.). In the work of Yu. L. Klimontovich, mentioned above, it is shown that for Coulomb plasma the chain of equations, obtained as a result of averaging Liouville equations for a random function of the number of particles N_a, is equivalent to the chain of equations of N. N. Bogolyubov [4].

For a random function of the number of particles

$$N_a(\mathbf{q}, \mathbf{p}, t) = \sum_i \delta(\mathbf{q} - \mathbf{q}_{ai}(t))\,\delta(\mathbf{p} - \mathbf{p}_{ai}(t))$$

where under the sign of summation of all particles of type a there stands the product of Dirac δ-functions, $N_a d_q d_p$ – number of particles of a given type in an element of a six-dimensional space of coordinates q and pulses p; in the case of absence of inelastic processes the Liouville equation is valid.

For a system of charged particles it is written in the form [5-7]

$$\frac{\partial N_a}{\partial t} + \mathbf{v}\frac{\partial N_a}{\partial \mathbf{q}} + e_a\left(\mathbf{E}^m + \frac{1}{c}\mathbf{v}\times\mathbf{H}^m\right)\frac{\partial N_a}{\partial \mathbf{p}} = 0 \qquad (1)$$

Here e_a – charge of a particle of type a; $\mathbf{E}^m$ and $\mathbf{H}^m$ – microscopic intensity of electrical and magnetic fields, correspondingly, for which it is necessary to write Maxwell's equations

$$\begin{aligned} \operatorname{rot}\mathbf{H}^m &= \frac{1}{c}\frac{\partial \mathbf{E}^m}{\partial t} + \frac{4\pi}{c}\sum_a e_a \int \mathbf{v} N_a(\mathbf{q}, \mathbf{p}, t)\, d\mathbf{p} \\ \operatorname{rot}\mathbf{E}^m &= -\frac{1}{c}\frac{\partial \mathbf{H}^m}{\partial t}, \qquad \operatorname{div}\mathbf{H}^m = 0 \qquad (2) \\ \operatorname{div}\mathbf{E}^m &= 4\pi\sum_a e_a \int N_a(\mathbf{q}, \mathbf{p}, t)\, d\mathbf{p} \end{aligned}$$

*Yu. L. Klimontovich, Statistical theory of nonequilibrium processes in plasma. Doctor's dissertation, Moscow, 1962.

System of equations (1), (2) for random functions is a closed system for description of the behavior of plasma. We set

$$\mathbf{E}^m = \mathbf{E} + \delta\mathbf{E}^m, \qquad \mathbf{H}^m = \mathbf{H} + \delta\mathbf{H}^m, \qquad N_a = \langle N_a \rangle + \delta N_a \tag{3}$$

where E and H — average electrical and magnetic fields, both external, and internal, satisfying averaged Maxwell's equations; $\langle N_a \rangle$ — mean statistical value of the number of particles per unit phase volume, coinciding with the distribution function appearing in Boltzmann's equation (here and henceforth brackets $\langle\ \rangle$ will indicate averaging of the respective quantities by the distribution function depending on coordinates and pulses of all particles in the system, and also on the electrical and magnetic fields [8]); δE^m, δH^m and δN_a — deviations of random variables from their mean statistical value.

By virtue of the linearity of Maxwell's equations it is possible to set

$$\delta\mathbf{E}^m = \delta\mathbf{E}_1^m + \delta\mathbf{E}_2^m \tag{4}$$

Here quantity

$$\delta\mathbf{E}_1^m = -\frac{\partial}{\partial \mathbf{q}} \sum_b \int \frac{e_b}{|\mathbf{q}-\mathbf{q}'|} \delta N_b(\mathbf{q}', \mathbf{p}', t)\, d\mathbf{q}' d\mathbf{p}' \tag{5}$$

is the solution of equations

$$\operatorname{rot} \delta\mathbf{E}_1^m = 0, \qquad \operatorname{div} \delta\mathbf{E}_1^m = 4\pi \sum_b e_b \int \delta N_b(\mathbf{q}', \mathbf{p}', t)\, d\mathbf{p}'$$

Quantity δE_2^m in (4) is the solution of equations

$$\operatorname{rot} \delta\mathbf{E}_2^m = -\frac{1}{c}\frac{\partial \delta\mathbf{H}^m}{\partial t}, \qquad \operatorname{div} \delta\mathbf{E}_2^m = 0$$

Substituting (3), (4), and (5) in (1) and averaging the obtained equation, we have

$$\frac{\partial \langle N_a \rangle}{\partial t} + \mathbf{v}\frac{\partial \langle N_a \rangle}{\partial \mathbf{q}} + e_a\left(\mathbf{E} + \frac{1}{c}\mathbf{v}\times\mathbf{H}\right)\frac{\partial \langle N_a \rangle}{\partial p} - \\ - \sum_b \int \frac{\partial}{\partial \mathbf{q}}\left(\frac{e_a e_b}{|\mathbf{q}-\mathbf{q}'|}\right)\frac{\partial}{\partial \mathbf{p}} \langle \delta N_a \delta N_b \rangle\, d\mathbf{q}'\, d\mathbf{p}' + \\ + e_a\left\langle\left(\delta\mathbf{E}_2^m + \frac{1}{c}\mathbf{v}\times\delta\mathbf{H}^m\right)\frac{\partial \delta N_a}{\partial \mathbf{p}}\right\rangle = 0 \tag{6}$$

From this it is clear that in order to close the system of equations it is necessary to write equation for moments $\langle \delta N_a \delta N_b \rangle$, $\langle \delta E_2^m \delta N_a \rangle$, etc., since equations for average magnitudes of E and H are easily obtained from averaging system of equations (2). In order to obtain the equation for $\langle \delta N_a \delta N_b \rangle$, we substract from (1) equation (5). Then, taking into account (3), (4), and (5), we obtain

$$\frac{\partial \delta N_a}{\partial t} + \mathbf{v}\frac{\partial \delta N_a}{\partial \mathbf{q}} + e_a\left(\mathbf{E} + \frac{1}{c}\mathbf{v}\times\mathbf{H}\right)\frac{\partial \delta N_a}{\partial \mathbf{p}} -$$
$$- \sum_b \int \frac{\partial}{\partial \mathbf{q}}\left(\frac{e_a e_b}{|\mathbf{q}-\mathbf{q}'|}\right)\frac{\partial}{\partial \mathbf{p}}\left[\langle N_a\rangle \delta N_b + \delta N_a \delta N_b - \langle \delta N_a \delta N_b\rangle\right] d\mathbf{q}'d\mathbf{p}' +$$
$$+ e_a\left(\delta \mathbf{E}_2^m + \frac{1}{c}\mathbf{v}\times\delta\mathbf{H}^m\right)\frac{\partial \langle N_a\rangle}{\partial \mathbf{p}} + e_a\left(\delta \mathbf{E}_2^m + \frac{1}{c}\mathbf{v}\times\delta\mathbf{H}^m\right)\frac{\partial \delta N_a}{\partial \mathbf{p}} -$$
$$- e_a\left\langle\left(\delta \mathbf{E}_2^m + \frac{1}{c}\mathbf{v}\times\delta\mathbf{H}^m\right)\frac{\partial \delta N_a}{\partial \mathbf{p}}\right\rangle = 0 ;$$

Multiplying this equation by δN_b, adding it to the analogous equation for δN_b, multiplied by δN_a, and averaging, we obtain

$$\frac{\partial \langle \delta N_a \delta N_b\rangle}{\partial t} + \left(\mathbf{v}\frac{\partial}{\partial \mathbf{q}} + \mathbf{v}'\frac{\partial}{\partial \mathbf{q}'}\right)\langle \delta N_a \delta N_b\rangle + e_a\left(\mathbf{E} + \frac{1}{c}\mathbf{v}\times\mathbf{H}\right)\frac{\partial \langle \delta N_a \delta N_b\rangle}{\partial \mathbf{p}} +$$
$$+ e_b\left(\mathbf{E} + \frac{1}{c}\mathbf{v}'\times\mathbf{H}\right)\frac{\partial \langle \delta N_a \delta N_b\rangle}{\partial \mathbf{p}'} - \frac{\partial}{\partial \mathbf{q}}\sum_c \int \frac{e_a e_c}{|\mathbf{q}-\mathbf{q}''|}\frac{\partial}{\partial \mathbf{p}}\left(\langle N_a\rangle\langle \delta N_a \delta N_b\rangle +\right.$$
$$\left. + \langle \delta N_a \delta N_b \delta N_c\rangle\right) d\mathbf{q}''d\mathbf{p}'' - \frac{\partial}{\partial \mathbf{q}'}\sum_c \int \frac{e_b e_c}{|\mathbf{q}'-\mathbf{q}''|}\frac{\partial}{\partial \mathbf{p}'}\left(\langle N_b\rangle\langle \delta N_a \delta N_b\rangle +\right.$$
$$\left. + \langle \delta N_a \delta N_b \delta N_c\rangle\right) d\mathbf{q}''d\mathbf{p}'' + e_a\left(\langle \delta \mathbf{E}_2^m \delta N_b\rangle + \frac{1}{c}\mathbf{v}\times\langle \delta \mathbf{H}^m \delta N_b\rangle\right)\frac{\partial \langle N_a\rangle}{\partial \mathbf{p}} +$$
$$+ e_b\left(\langle \delta \mathbf{E}_2^m \delta N_a\rangle + \frac{1}{c}\mathbf{v}'\times\langle \delta \mathbf{H}^m \delta N_a\rangle\right)\frac{\partial \langle N_b\rangle}{\partial \mathbf{p}'} +$$
$$+ e_a\left\langle\left(\delta \mathbf{E}_2^m + \frac{1}{c}\mathbf{v}\times\delta\mathbf{H}^m\right)\frac{\partial \delta N_a \delta N_b}{\partial \mathbf{p}}\right\rangle +$$
$$+ e_b\left\langle\left(\delta \mathbf{E}_2^m + \frac{1}{c}\mathbf{v}'\times\delta\mathbf{H}^m\right)\frac{\partial \delta N_a \delta N_b}{\partial \mathbf{p}'}\right\rangle = 0 \qquad (7)$$

Thus, in the equation for second moments there entered moments of the third order. In the equation for moments of the third order there enter moments of the fourth order, etc. There is obtained an open chain of equations. In order to close this chain, it is necessary to place certain limitations on parameters of the plasma. For simplicity, which does not sacrifice generality, we consider that plasma consists of two types of ions, where

$$T_a \approx T_b = T, \qquad |e_a| = |e_b| = e, \qquad n_a \approx n_b = n$$

Here T_a, T_b, n_a, n_b – temperature and average number of particles per unit volume for the corresponding type of particle. Let us assume that

$$\mu = \frac{e^2}{r_d kT} \ll 1, \qquad r_d = \left(\frac{kT}{4\pi e^2 n}\right)^{1/2} \tag{8}$$

Here r_d – Debye shielding radius; k – Boltzmann's constant. Multiplying the numerator and denominator of (8) by $4\pi n$, we find that condition (8) is equivalent to condition

$$\frac{1}{4\pi n r_d^3} \ll 1 \tag{9}$$

i.e., inside the Debye sphere, on the assumption (8), there should always be many particles.

This condition gives the possibility of disregarding moments of the third order in equation (7) as compared to moments of the second order (see also, [4, 9]), and thereby the chain of equations is closed. If one were to use certain properties of a δ-function, there can be obtained formulas

$$\begin{aligned} \langle N_a \rangle &= n_a^* f_a (\mathbf{q}, \mathbf{p}, t) \\ \langle N_a N_b \rangle &= n_a^* n_b^* f_{ab} (\mathbf{q}, \mathbf{p}, \mathbf{q}', \mathbf{p}', t) + \delta_{ab} \delta (\mathbf{q} - \mathbf{q}') \delta (\mathbf{p} - \mathbf{p}') n_a^* f_a \end{aligned} \tag{10}$$

Here $\delta_{ab} = 1$ when $a = b$ and $\delta_{ab} = 0$ when $a \neq b$, n_a^* is equal to the total number of particles of type a in a system, divided by volume V, which is occupied by the whole system, and is considered subsequently a constant number (it is only a certain normalizing factor). Since, furthermore,

$$\begin{aligned} \langle N_a N_b \rangle &= \langle N_a \rangle \langle N_b \rangle + \langle \delta N_a \delta N_b \rangle \\ f_{ab} &= f_a f_b + g_{ab} (\mathbf{q}, \mathbf{q}', \mathbf{p}, \mathbf{p}', t) \end{aligned} \tag{11}$$

(here g_{ab} – correlation function; $g_{ab} \to 0$ as $|q - q'| \to \infty$),

$$\langle \delta N_a \delta N_b \rangle = \delta_{ab} \delta (\mathbf{q} - \mathbf{q}') \delta (\mathbf{p} - \mathbf{p}') n_a^* f_a + n_a^* n_b^* g_{ab} (\mathbf{q}, \mathbf{q}', \mathbf{p}, \mathbf{p}', t) \tag{12}$$

Using assumption (8), and also relationships (10)-(12) and properties of a δ-function, instead of equation (7) we obtain the following equation for correlation function g_{ab};

$$\frac{\partial g_{ab}}{\partial t}+\left(\mathbf{v}\frac{\partial}{\partial \mathbf{q}}+\mathbf{v}'\frac{\partial}{\partial \mathbf{q}'}\right)g_{ab}-\frac{\partial}{\partial \mathbf{q}}\sum_c n_c^*\int\frac{e_a e_c}{|\mathbf{q}-\mathbf{q}''|}g_{bc}(\mathbf{q}',\mathbf{p}',\mathbf{q}'',\mathbf{p}'',t)\,d\mathbf{q}''\,d\mathbf{p}''\frac{\partial f_a}{\partial \mathbf{p}}-$$
$$-\frac{\partial}{\partial \mathbf{q}'}\sum_c n_c^*\int\frac{e_b e_c}{|\mathbf{q}'-\mathbf{q}''|}g_{ac}(\mathbf{q},\mathbf{p},\mathbf{q}'',\mathbf{p}'',t)\,d\mathbf{q}''\,d\mathbf{p}''\frac{\partial f_b}{\partial \mathbf{p}'}+$$
$$+e_a\left(\mathbf{E}+\frac{1}{c}\mathbf{v}\times\mathbf{H}\right)\frac{\partial g_{ab}}{\partial \mathbf{p}}+e_b\left(\mathbf{E}+\frac{1}{c}\mathbf{v}'\times\mathbf{H}\right)\frac{\partial g_{ab}}{\partial \mathbf{p}'}+$$
$$+\frac{e_a}{n_b^*}\left(\langle\delta\mathbf{E}_2^m\delta N_b\rangle+\frac{1}{c}\mathbf{v}\times\langle\delta\mathbf{H}^m\delta N_b\rangle\right)\frac{\partial f_a}{\partial \mathbf{p}}+ \qquad (13)$$
$$+\frac{e_b}{n_a^*}\left(\langle\delta\mathbf{E}_2^m\delta N_a\rangle+\frac{1}{c}\mathbf{v}'\times\langle\delta\mathbf{H}^m\delta N_a\rangle\right)\frac{\partial f_b}{\partial \mathbf{p}'}=\frac{\partial}{\partial \mathbf{q}}\left(\frac{e_a e_b}{|\mathbf{q}-\mathbf{q}'|}\right)\left\{\frac{\partial f_a}{\partial \mathbf{p}}f_b-\frac{\partial f_b}{\partial \mathbf{p}'}f_a\right\}$$

The first four terms on the left and the term on the right entered in the equation for the correlation function in the dissertation of Yu. L. Klimontovich. Remaining terms were obtained by considering the total electromagnetic field. From comparison in equation (13) of term $v\partial g_{ab}/\partial q$ with term $e_a E\partial g_{ab}/\partial p$ it is clear that the latter can be ignored, if

$$e_a|\mathbf{E}|r_d\ll m_a v^{\circ 2} \qquad (14)$$

inasmuch as $|\partial g_{ab}/\partial q|\sim g_{ab}/r_d$ (as a result of shielding of charges in plasma g_{ab} seeks zero as $r\to r_d$, where r – distance between two particles). Here v° – thermal velocity of a particle (we consider that the order of magnitude of total velocity of a particle is determined by its thermal velocity). From comparison of term $v\partial g_{ab}/\partial q$ with term $(e_a/c)\mathbf{v}\times H\partial g_{ab}/\partial p$ it is clear that it is possible to ignore the last term when

$$r_d\ll r_l \qquad \left(r_l=\frac{m_a c v^\circ}{eH}\right) \qquad (15)$$

where r_l – radius of the Larmor orbit of a charged particle. Calculations for particles of type b are analogous. We calculate now certain terms in equation (13). We compare term

$$-\left[\frac{\partial}{\partial \mathbf{q}}\sum_c n_c^* \int \frac{e_a e_c}{|\mathbf{q}-\mathbf{q}''|} g_{bc}(\mathbf{q}', \mathbf{p}', \mathbf{q}'', \mathbf{p}'', t)\, d\mathbf{q}''\, d\mathbf{p}'' - \right.$$
$$\left. - \frac{\partial}{\partial \mathbf{q}}\left(\frac{e_a e_b}{|\mathbf{q}-\mathbf{q}'|}\right) f_b\right]\frac{\partial f_a}{\partial \mathbf{p}} = \frac{e_a}{n_b^*}\langle \delta \mathbf{E}_1^m \delta N_b\rangle \frac{\partial f_a}{\partial \mathbf{p}} \tag{16}$$

with term

$$\frac{e_a}{n_b^*}\langle \delta \mathbf{E}_2^m \delta N_b\rangle \frac{\partial f_a}{\partial \mathbf{p}} \tag{17}$$

Preliminarily we write Maxwell's equations for deviations of random variables from their mean statistical value

$$\begin{aligned} &\mathrm{rot}\, \delta \mathbf{H}^m = \frac{1}{c}\frac{\partial \delta \mathbf{E}_1^m}{\partial t} + \frac{1}{c}\frac{\partial \delta \mathbf{E}_2^m}{\partial t} + \frac{4\pi}{c}\sum_a e_a \int \mathbf{v}\delta N_a\, d\mathbf{p} \\ &\mathrm{rot}\, \delta \mathbf{E}_2^m = -\frac{1}{c}\frac{\partial \delta \mathbf{H}^m}{\partial t}, \qquad \mathrm{div}\, \delta \mathbf{H}^m = 0 \\ &\mathrm{div}\, \delta \mathbf{E}_1^m = 4\pi \sum_a e_a \int \delta N_a\, d\mathbf{p}, \qquad \mathrm{div}\, \delta \mathbf{E}_2^m = 0 \end{aligned} \tag{18}$$

Multiplying equations (18) by δN_b and averaging, it is possible from the equations obtained as a result to determine the order of all quantities interesting us, if functions change sufficiently smoothly. From the fourth equation of (18)

$$\langle \delta \mathbf{E}_1^m \delta N_b\rangle \sim 4\pi e r_d \int \langle \delta N_a \delta N_b\rangle\, d\mathbf{p}$$

From the second equation of (18)

$$\langle \delta \mathbf{E}_2^m \delta N_b\rangle \sim \frac{v^2}{c}\langle \delta \mathbf{H}''' \delta N_b\rangle$$

From the first equation of (18)

$$\langle \delta \mathbf{H}^m \delta N_b\rangle \sim \frac{4\pi}{c} r_d e v^\circ \int \langle \delta N_a \delta N_b\rangle\, d\mathbf{p}, \quad \text{or}$$
$$\langle \delta \mathbf{E}_2^m \delta N_b\rangle \sim \frac{4\pi v^{\circ 2}}{c^2} r_d^2 e \int \langle \delta N_a \delta N_b\rangle\, d\mathbf{p}$$

Using these estimates and taking the ratio of (16) to (17), we find that this ratio is great, and term (17) can be ignored as compared to (16), if

$$v^{\circ 2} \ll c^2 \tag{19}$$

i.e., we should consider the gas nonrelativistic. Instead of equation (13), with fulfillment of inequalities (14), (15) and (19), we have equation

$$\frac{\partial g_{ab}}{\partial t} + \left(\mathbf{v}\frac{\partial}{\partial \mathbf{q}} + \mathbf{v}'\frac{\partial}{\partial \mathbf{q}'}\right) g_{ab} - \frac{\partial}{\partial \mathbf{q}} \sum_c n_c^* \int \frac{e_a e_c}{|\mathbf{q}-\mathbf{q}''|} g_{bc}\, d\mathbf{q}''\, d\mathbf{p}'' \frac{\partial f_a}{\partial \mathbf{p}} -$$

$$- \frac{\partial}{\partial \mathbf{q}'} \sum_c n_c^* \int \frac{e_b e_c}{|\mathbf{q}'-\mathbf{q}''|} g_{ac}\, d\mathbf{q}''\, d\mathbf{p}'' \frac{\partial f_b}{\partial \mathbf{p}'} = \frac{\partial}{\partial \mathbf{q}} \left(\frac{e_a e_b}{|\mathbf{q}-\mathbf{q}'|}\right) \left\{\frac{\partial f_a}{\partial \mathbf{p}} f_b - \frac{\partial f_b}{\partial \mathbf{p}'} f_a\right\} \qquad (20)$$

coinciding with the equation obtained by Yu. L. Klimontovich.

For the case of a three-dimensional uniform plasma this equation was extracted earlier in [4].

Making analogous calculations in equation (6) and using the first formula of (10) and formula (12), instead of (6) we obtain

$$\frac{\partial f_a}{\partial t} + \mathbf{v}\frac{\partial f_a}{\partial \mathbf{q}} + e_a\left(\mathbf{E} + \frac{1}{c}\mathbf{v}\times\mathbf{H}\right)\frac{\partial f_a}{\partial \mathbf{p}} = \sum_b n_b^* \int \frac{\partial}{\partial \mathbf{q}} \left(\frac{e_a e_b}{|\mathbf{q}-\mathbf{q}'|}\right) \frac{\partial g_{ab}}{\partial \mathbf{p}}\, d\mathbf{q}'\, d\mathbf{p}' \qquad (21)$$

To obtain the kinetic equation for the first distribution function it is necessary to solve equation (20) for the correlation function and to substitute this solution in the right side of equation (21). In order to find from (20) a solution which brings the right side of equation (21) to the form of the integral of collisions in Landau form, it is necessary, as shown in the work of Yu. L. Klimontovich (see footnote on p. 86), to make certain other assumptions.

Let us assume that distribution function f_a varies little during the time of correlation (correspondingly, the length of correlation), i.e., we consider characteristic times t (length l), much larger than the correlation time τ_k (lengths of correlation r_k) during which two particles, near one another and moving with thermal velocity will reparate distance r_k, at which these two particles become statistically independent (do not interact).

From the solution of equation (20) for the case of equilibrium distribution of particles by velocities it follows that for that case

$$r_k \sim r_d, \quad \tau_k \sim r_d / v^\circ = 1/\omega_0$$

(here ω_0 – frequency of Langmuir oscillations), since, when

$$r \to r_d \quad (r = |\mathbf{q} - \mathbf{q}'|), \qquad f_{ab} \to f_a f_b \qquad (g_{ab} \to 0)$$

This also follows from the Debye-Hückel theory for electrolytes. During solution of kinetic equations we usually always linearize around the equilibrium distribution, i.e., we consider small deviation from equilibrium. Due to this one may assume that τ_k differs little from $r_d/v^0 = 1/\omega_0$, and r_k differs little from r_d. Thus, introducing the characteristic frequency of the problem $\Omega = 1/t$, we assume

$$\frac{\Omega}{\omega_0} \ll 1 \tag{22}$$

upon which in (20) it is possible to omit term $\partial g_{ab}/\partial t$, since by virtue of (22) initial correlations attenuate after the considered characteristic time. Applying to equation (20) the Fourier transform and assuming

$$k^2 r_d^2 \gg 1 \tag{23}$$

(k – reciprocal of the length of the wave vector), which means that dielectric constant $\varepsilon = 1$ (see for instance, [10]), as a result we obtain the equation for the correlation function, the solution of which, substituted in the right part of equation (21), leads to the integral of collisions in Landau form. If we pass to equations of a solid medium, using Boltzmann's equation, it is necessary to consider characteristic times, much greater than τ^0 – the time of establishment of an equilibrium state – the order of magnitude of which is determined by the order of magnitude of the free path of particles and is equal to $r_d/\mu v^0$, where μ – plasma parameter, determined by formula (8). Considering $l^0 \sim v^0 \tau^0$ (l^0 – so-called length of establishment), for transition to a solid medium we should assume that $l^0 \ll L$ (L – characteristic dimension), i.e.,

$$\frac{r_d}{\mu L} \ll 1 \qquad (24)$$

System of inequalities (8), (14), (15), (19), (22), and (23) means that for description of processes in plasma with parameters which satisfy these inequalities it is possible to use a closed system of equations, consisting of the kinetic Boltzmann equation with integral of collisions in Landau form and Maxwell equations for the electromagnetic field, where function $\langle N_a \rangle = n_a^* f_a$ corresponds to the first distribution function, usually appearing in the Boltzmann equation.

For transition to magnetohydrodynamic equations [2] it is necessary to make assumption (24).

In the diagram, in the same coordinates as the known diagram of Kantrovits and Petchek [11], there are depicted regions in which various inequalities are satisfied. Along the axis of abscissas is the decimal logarithm of temperature, expressed in electronvolts, and on the axis of ordinates, of electron density. For characteristic length we take magnitude L = 10 cm; for order of magnitude of electrical field E we take magnitude $E \sim v^{\circ}H/c$, i.e., maximum possible magnitude of separation of charges during motion of the medium with respect to the magnetic field. Below line 1 inequality (8) is satisfied; above line 2 inequality (14) and above line 3 inequality (15) are satisfied (for the latter two lines $H = 10^5_{oe}$; if, however the field is less, these inequalities in the marked regions are long since satisfied).

Above 4 is the condition of solidness of the medium (24); to the left of 5 — condition (19); the dotted line corresponds to thermal ionization of hydrogen (to the right, more than 50% ionization), where

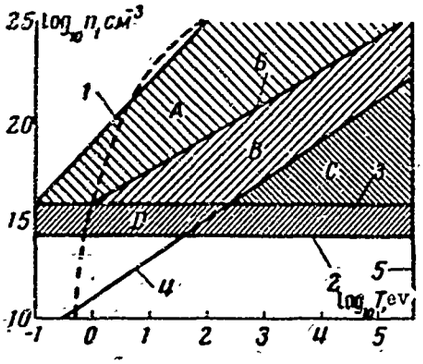

Fig. 1.

for gases with an ionization potential, smaller than for hydrogen, this line is shifted to the left.

Line 6 corresponds to $\omega_e \tau_e = 1$ (ω_e — cyclotron frequency of rotation of electrons, τ_e — "time of free path" of electrons, $\tau_e \sim \tau^0$ for completely ionized gas, $H = 10^4_{oe}$ for this line).

Region A corresponds to classical magnetohydrodynamics ($\omega_e \tau_e \ll 1$). Region B corresponds to magnetohydrodynamics with anisotropic transport properties of [12, 13]. If we are in region C, for description of processes in plasma it is necessary to use the kinetic Boltzmann equation with integral of collisions in Landau form. Region D corresponds to a kinetic equation with an integral of collisions which depends on the magnetic field [14, 15]. Inequality (22) is not marked on the diagram, since we consider it always satisfied.

With decrease of the magnetic field lines 2 and 3 shift downwards and correspondingly regions A, B and C increase in size. In region C far from line 4 it is possible to disregard the integral of collisions, since we have $l^0 \gg L$, and for description of processes in plasma it is possible to use the equations of a self-consistent field of A. A. Vlasov [16]. Near line 4 the integral of collisions should be accounted for. A generalization for relativistic plasma is contained in [8].

In conclusion the author thanks Yu. L. Klimontovich, A. G. Kulikovskiy, and N. N. Shirokov for valuable advice and discussion.

Submitted
20 February 1964

Note during proofreading. It is necessary to note that assumption (23) leads to divergence of integral of collisions at infinity. In [3] this divergence was removed by means of cutting off the integral of collisions at distances $\sim r_d$.

Thus, assumption (23) leads to ignoring the interaction of electrons with plasma oscillations, and also their influence on transport factors [2].

Recently there appeared a work [17], in which there is revealed the influence of these interactions on transport factors for a completely ionized gas. It is shown that, when temperatures of electrons and ions are comparable, calculation of interaction of electrons with plasma oscillations leads only to small corrections in transport factors, which, in general, can be ignored. With sufficiently strong nonisothermalness of plasma these interactions play a determining role.

Literature

1. S. Chapman and T. Cowling. Mathematical theory of nonuniform gases, IL, 1960.

2. S. I. Braginskiy. Transport phenomena in plasma. Collection: Problems of plasma theory, 1963, Issue 1.

3. L. D. Landau. Kinetic equation for Coulomb interaction. Journal of experimental and theoretical physics, 1937, Vol. 7, p. 203.

4. N. N. Bogolyubov. Problems of dynamic theory in statistical physics. State Technical Press, 1946.

5. Yu. L. Klimontovich. Secondary quantization in phase space. Reports of Academy of Sciences of the USSR, 1954, Vol. 96, 43.

6. Yu. L. Klimontovich. On a method of secondary quantization in phase space. Journal of experimental and theoretical physics, 1957, Vol. 33, No. 4.

7. Yu. L. Klimontovich and V. P. Silin. To a theory of fluctuation of the distribution of particles in plasma. Journal of experimental and theoretical physics, 1962, Vol. 43, No. 1.

8. Yu. L. Klimontovich. Relativistic kinetic equations for plasma. Journal of experimental and theoretical physics, 1959, Vol. 37, No. 3.

9. S. V. Iordanskiy and A. G. Kulikovskiy. On stability of higher correlation functions in plasma. Reports of Academy of Sciences of USSR, 1963, Vol. 152, No. 4.

10. V. P. Silin and A. A. Rukhadze. Electromagnetic properties of plasma and plasma-conducting media. State Atomic Publishing House, 1961.

11. Magnetohydrodynamics. IL, 1958 (Coll. of trans, ed. by D. A. Frank-Kamenetskiy).

12. A. I. Gubanov and Yu. P. Lun'kin. Equations of magnetoplasma-dynamics. Journal of tech. physics, 1960, Vol. 30, No. 9.

13. V. B. Baranov. Deriving equations of anisotropic magneto-hydrodynamics, PMM, 1962, Vol. XXVI, Issue 6.

14. S. T. Belyayev. Kinetics of ionized gas in a strong magnetic field. Plasma physics and problems of controlled thermonuclear reactions. Publishing House of the Academy of Sciences of USSR, 1958, Vol. III.

15. V. M. Yeleonskiy, P. S. Zyryanov, and V. P. Silin. Integral of collisions of charged particles in a magnetic field. Journal of experimental and theoretical physics, 1962, Vol. 42, No. 3.

16. A. A. Vlasov. Theory of large numbers. State Technical Press, 1950.

17. L. M. Gorbunov and V. I. Silin. Theory of transport phenomena in a nonisothermal stripped plasma. Journal of tech. physics, 1964, Vol. XXXIV, Issue 3.

THE ELECTRICAL FIELD IN A MAGNETOHYDRODYNAMIC CHANNEL OF RECTANGULAR SECTION WITH NONCONDUCTING WALLS

S. A. Regirer

(Moscow)

The two-dimensional problem of finding the electrical field in a channel with parallel nonconducting walls with constant and changing conductivity of the liquid was considered earlier [1-3]. The obtained distributions of electrical potential and current could be interpreted as the result of averaging of the corresponding distributions in a channel of rectangular section [4]. For certain other quantities, e.g., Joule dissipation, such a connection with average characteristics of a rectangular channel, in general, does not exist, if the velocity of the fluid changes in the direction of the magnetic field. At the same time, calculation of these changes is of interest, in particular, during calculation of the influence of the "transverse edge effect," i.e., of closed currents, circulating in the plane of the channel cross section. Below there is set forth a complete solution of the three-dimensional problem of distribution of currents in a channel of rectangular section with nonconducting walls, valid for any given dependence of vectors of velocity and the magnetic field on coordinates. There is also investigated a solution, corresponding to the particular case of rectilinear flow in a nonuniform transverse field. In conclusion there are discussed conditions which should be satisfied, in general, by the magnetic field assigned in the solution.

1. Let us consider rectangular channel $|x| < \infty$, $|y| < b$, $|z| < a$ with nonconducting walls, in which there occurs stationary motion of an isotropically conducting fluid (Fig. 1). If the external magnetic

field B(x, y, z) and distribution of velocities V(x, y, z) are known, and the induced field can be ignored, the distribution of electrical potential φ and of current density j can be found from system [4]

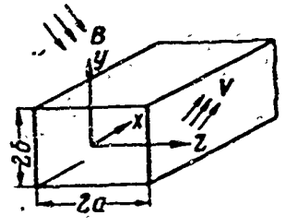

Fig. 1.

$$\Delta\varphi = \frac{1}{c}\,\mathbf{B}\,\mathrm{rot}\,\mathbf{V} \tag{1.1}$$

$$\mathbf{j} = \sigma\left(-\nabla\varphi + \frac{1}{c}\mathbf{V}\times\mathbf{B}\right) \qquad (\sigma = \mathrm{const}) \tag{1.2}$$

with boundary conditions

$$j_y = \sigma\left(-\frac{\partial\varphi}{\partial y} + f_\pm\right) = 0 \quad \text{when } y = \pm\delta$$
$$j_z = \sigma\left(-\frac{\partial\varphi}{\partial z} + g_\pm\right) = 0 \quad \text{when } z = \pm a \tag{1.3}$$

Here

$$f_\pm(x, z) = \frac{1}{c}(\mathbf{V}\times\mathbf{B})_y \quad \text{when } y = \pm\delta$$
$$g_\pm(x, y) = \frac{1}{c}(\mathbf{V}\times\mathbf{B})_z \quad \text{when } z = \pm a$$

We assume, further, that V and B — bounded functions of coordinates, where

$$\mathbf{B} \to 0, \quad \frac{\partial\mathbf{V}}{\partial x} \to 0 \quad \text{as } x \to -\infty$$
$$\mathbf{B} \to \mathbf{B}_\infty(y, z), \quad \frac{\partial\mathbf{V}}{\partial x} \to 0 \quad \text{as } x \to +\infty \tag{1.4}$$

and we seek the solution of system (1.1)-(1.3), satisfying asymptotic conditions

$$\varphi \to 0 \quad \text{as } x \to -\infty$$
$$j_x = \sigma\left[-\frac{\partial\varphi}{\partial x} + \frac{1}{c}(\mathbf{V}\times\mathbf{B})_x\right] \to 0 \quad \text{as } x \to \infty \tag{1.5}$$

It is easy to prove that function

$$\varphi^\circ = \frac{(z^2-a^2)^2[(y+\delta)^2 f_+ - (\delta-y)^2 f_-]}{4\delta[(z^2-a^2)^2 + (y^2-\delta^2)^2]} + \frac{(y^2-\delta^2)^2[(z+a)^2 g_+ - (a-z)^2 g_-]}{4a[(z^2-a^2)^2 + (y^2-\delta^2)^2]} \tag{1.6}$$

satisfies boundary conditions (1.3). Introducing auxiliary potential $\Phi = \varphi - \varphi^\circ$ and considering

$$A(x, y, z) = \frac{1}{c}\mathbf{B}\,\mathrm{rot}\,\mathbf{V} - \Delta\varphi^\circ \tag{1.7}$$

we obtain for Φ a boundary value problem

$$\Delta\Phi = A(x, y, z)$$
$$\frac{\partial\Phi}{\partial y} = 0 \quad \text{when } y = \pm\delta, \qquad \frac{\partial\Phi}{\partial z} = 0 \quad \text{when } z = \pm a \tag{1.8}$$

with asymptotic conditions

$$\Phi \to 0 \quad \text{as } x \to -\infty, \quad \frac{\partial \Phi}{\partial x} \to \frac{1}{c}(\mathbf{V} \times \mathbf{B})_x \quad \text{as } z \to \infty \tag{1.9}$$

It is known that the problem at hand has a solution, if the right sides in (1.8), (1.9) satisfy certain integral conditions. These conditions and limitations imposed by them on V and B, together with limitations ensuing from other considerations, are considered at the end of the article. Here it is assumed that a solution exists and can be presented as a series

$$\begin{aligned}\Phi = \frac{N_{00}}{4} + \frac{1}{2}\Big[\sum_{n=1}^{\infty}\Big(M_{n0}\sin\frac{r_n y}{\delta} + N_{n0}\cos\frac{\pi n y}{\delta}\Big) + \\ + \sum_{m=1}^{\infty}\Big(N_{0m}\cos\frac{\pi m z}{a} + T_{0m}\sin\frac{r_m z}{a}\Big)\Big] + \\ + \sum_{n=1}^{\infty}\sum_{m=1}^{\infty}\Big(M_{nm}\sin\frac{r_n y}{\delta}\cos\frac{\pi m z}{a} + N_{nm}\cos\frac{\pi n y}{\delta}\cos\frac{\pi m z}{a} + \\ + S_{nm}\sin\frac{r_n y}{\delta}\sin\frac{r_m z}{a} + T_{nm}\cos\frac{\pi n y}{\delta}\sin\frac{r_m z}{a}\Big)\end{aligned} \tag{1.10}$$

Then $M_{nm}(x)$, $N_{nm}(x)$, $S_{nm}(x)$, $T_{nm}(x)$ – solutions of ordinary equations, bounded as $|x| \to \infty$:

$$\begin{aligned} M_{nm}'' - \mu_{nm}^2 M_{nm} &= m_{nm}, & N_{nm}'' - \nu_{nm}^2 N_{nm} &= n_{nm} \\ S_{nm}'' - \sigma_{nm}^2 S_{nm} &= s_{nm}, & T_{nm}'' - \tau_{nm}^2 T_{nm} &= t_{nm} \end{aligned} \tag{1.11}$$

Here $r_n = \pi(n - 1/2)$ and

$$\begin{aligned} \mu_{nm}^2 &= \frac{r_n^2}{\delta^2} + \frac{\pi^2 m^2}{a^2}, & m_{nm} &= \frac{1}{a\delta}\int_{-a}^{a}\int_{-\delta}^{\delta} A\sin\frac{r_n y}{\delta}\cos\frac{\pi m z}{a}\,dy\,dz \\ \nu_{nm}^2 &= \frac{\pi^2 n^2}{\delta^2} + \frac{\pi^2 m^2}{a^2}, & n_{nm} &= \frac{1}{a\delta}\int_{-a}^{a}\int_{-\delta}^{\delta} A\cos\frac{\pi n y}{\delta}\cos\frac{\pi m z}{a}\,dy\,dz \\ \sigma_{nm}^2 &= \frac{r_n^2}{\delta^2} + \frac{r_m^2}{a^2}, & s_{nm} &= \frac{1}{a\delta}\int_{-a}^{a}\int_{-\delta}^{\delta} A\sin\frac{r_n y}{\delta}\sin\frac{r_m z}{a}\,dy\,dz \\ \tau_{nm}^2 &= \frac{\pi^2 n^2}{\delta^2} + \frac{r_m^2}{a^2}, & t_{nm} &= \frac{1}{a\delta}\int_{-a}^{a}\int_{-\delta}^{\delta} A\cos\frac{\pi n y}{\delta}\sin\frac{r_m z}{a}\,dy\,dz \end{aligned}$$

When n and m are not simultaneously equal to zero

$$M_{nm} = -\frac{1}{2\mu_{nm}}\int_{-\infty}^{\infty} m_{nm}(\xi)\exp(-\mu_{nm}|x-\xi|)\,d\xi \tag{1.12}$$

Analogously N_{nm} is expressed through ν_{nm} and $n_{nm}(x)$, S_{nm} is expressed through σ_{nm} and $s_{nm}(x)$, T_{nm} – through τ_{nm} and $t_{nm}(x)$. When $n = m = 0$

$$N_{00} = \int_{-\infty}^{x} n_{00}(\xi)(x - \xi)\, d\xi \tag{1.13}$$

After the distribution of potential is found, from Ohm's law (1.2) we determine current density

$$\mathbf{j} = \sigma\left(-\nabla\Phi - \nabla\varphi^{\circ} + \frac{1}{c}\mathbf{V}\times\mathbf{B}\right) \tag{1.14}$$

Joule dissipation Q is calculated after this, by formulas

$$Q = \frac{1}{\sigma}\int_{-\infty}^{\infty}\int_{-a}^{a}\int_{-\delta}^{\delta} j^2\, dy\, dz\, dx = \frac{1}{c}\int_{-\infty}^{\infty}\int_{-a}^{a}\int_{-\delta}^{\delta} \mathbf{jVB}\, dy\, dz\, dx \tag{1.15}$$

The second equality of (1.15) is valid only for channels with nonconducting walls.

2. Of interest is consideration of rectilinear flow with a symmetric velocity profile in the presence of a flat magnetic field, constant along one of the transverse coordinate axes. Let us assume, for instance that

$$\mathbf{V} = \mathbf{e}_x v(y, z), \qquad \mathbf{B} = \mathbf{e}_x B_x(x, z) + \mathbf{e}_z B_z(x, z) \tag{2.1}$$

where

$$v(y, z) = v(y, -z) = v(-y, z), \qquad B_z(x, z) = B_z(x, -z)$$
$$\lim_{x\to-\infty}\mathbf{B} = 0, \qquad \lim_{x\to\infty}\mathbf{B} = \mathbf{e}_z B_\infty, \qquad B_\infty = \text{const}$$

In this case

$$g_{\pm} = 0, \qquad f_+ = f_- = f(x, z)$$
$$\varphi^{\circ} = \frac{y(z^2 - a^2)f}{(z^2 - a^2)^2 + (y^2 - \delta^2)^2}, \qquad A = -\frac{1}{c}B_z\frac{\partial v}{\partial y} - \Delta\varphi^{\circ} \tag{2.2}$$

Function A(x, y, z) turns out to be even with respect to z and with respect to y, and in its trigonometric expansion differing from zero there are only coefficients m_{nm}. Therefore, solution of boundary

value problem (1.8) is presented by series

$$\Phi = \frac{1}{2}\sum_{n=1}^{\infty} M_{n0}\sin\frac{r_n y}{\delta} + \sum_{n=1}^{\infty}\sum_{m=1}^{\infty} M_{nm}\sin\frac{r_n y}{\delta}\cos\frac{\pi m z}{a}$$

coefficients of which M_{nm} are expressed according to (1.12) through m_{nm}, where in this case

$$m_{nm} = \frac{r_n}{ca\delta}\int_{-a}^{a} v_n B_z \cos\frac{\pi m z}{a}\,dz + \mu_{nm}^2\varphi_{nm}^{\circ}$$

$$v_n = \frac{1}{\delta}\int_{-\delta}^{\delta} v\cos\frac{r_n y}{\delta}\,dy, \qquad \varphi_{nm}^{\circ} = \frac{1}{a\delta}\int_{-a}^{a}\int_{-\delta}^{\delta}\varphi^{\circ}\sin\frac{r_n y}{\delta}\cos\frac{\pi m z}{a}\,dy\,dz \tag{2.3}$$

Setting $\varphi_{nm} = M_{nm} + \varphi_{nm}^{\circ}$, we obtain formal expansions of the potential and components of current density

$$\varphi = \frac{1}{2}\sum_{n=1}^{\infty}\varphi_{n0}\sin\frac{r_n y}{\delta} + \sum_{n=1}^{\infty}\sum_{m=1}^{\infty}\varphi_{nm}\sin\frac{r_n y}{\delta}\cos\frac{\pi m z}{a} \tag{2.4}$$

$$j_x = -\sigma\frac{\partial\varphi}{\partial x} = -\frac{\sigma}{2}\sum_{n=1}^{\infty}\varphi_{n0}'\sin\frac{r_n y}{\delta} - \sigma\sum_{n=1}^{\infty}\sum_{m=1}^{\infty}\varphi_{nm}'\sin\frac{r_n y}{\delta}\cos\frac{\pi m z}{a}$$

$$j_y = -\sigma\left(\frac{\partial\varphi}{\partial y} + \frac{vB_z}{c}\right) = -\frac{\sigma}{2}\sum_{n=1}^{\infty}\frac{\delta}{r_n}\left(\frac{r_n^2}{\delta^2}\varphi_{n0} + m_{n0} - \mu_{n0}^2\varphi_{n0}^{\circ}\right)\cos\frac{r_n y}{\delta} -$$

$$-\sigma\sum_{n=1}^{\infty}\sum_{m=1}^{\infty}\frac{\delta}{r_n}\left(\frac{r_n^2}{\delta^2}\varphi_{nm} + m_{nm} - \mu_{nm}^2\varphi_{nm}^{\circ}\right)\cos\frac{r_n y}{\delta}\cos\frac{\pi m z}{a} \tag{2.5}$$

$$j_z = -\sigma\frac{\partial\varphi}{\partial z} = \sigma\sum\sum\varphi_{nm}\frac{\pi m}{a}\sin\frac{r_n y}{\delta}\sin\frac{\pi m z}{a}$$

Let us note that functions A(x, y, z) and φ°(x, y, z) do not depend on the longitudinal component B_x of the magnetic field. Therefore, the solution of (2.4), (2.5) also does not depend on it.

Joule dissipation in the channel is calculated by one of the formulas

$$Q = \sigma a\delta\int_{-\infty}^{\infty}\left\{\frac{1}{2}\sum_{n=1}^{\infty}\left[\varphi_{n0}'^2 + \frac{\delta^2}{r_n^2}\left(\frac{r_n^2}{\delta^2}\varphi_{n0} + m_{n0} - \mu_{n0}^2\varphi_{n0}^{\circ}\right)^2\right] +\right.$$

$$\left. + \sum_{n=1}^{\infty}\sum_{m=1}^{\infty}\left[\varphi_{nm}'^2 + \frac{\delta^2}{r_n^2}\left(\frac{r_n^2}{\delta^2}\varphi_{nm} + m_{nm} - \mu_{nm}^2\varphi_{nm}^{\circ}\right)^2 + \varphi_{nm}^2\frac{\pi^2 m^2}{a^2}\right]\right\}dx \tag{2.6}$$

$$Q = \sigma a\delta\int_{-\infty}^{\infty}\left\{\frac{1}{2}\sum_{n=1}^{\infty}\left[\frac{\delta^2}{r_n^2}\left(\frac{r_n^2}{\delta^2}\varphi_{n0} + m_{n0} - \mu_{n0}^2\varphi_{n0}^{\circ}\right)\left(m_{n0} - \mu_{n0}^2\varphi_{n0}^{\circ}\right)\right] +\right.$$

$$\left. + \sum_{n=1}^{\infty}\sum_{m=1}^{\infty}\left[\frac{\delta^2}{r_n^2}\left(\frac{r_n^2}{\delta^2}\varphi_{nm} + m_{nm} - \mu_{nm}^2\varphi_{nm}^{\circ}\right)\left(m_{nm} - \mu_{nm}^2\varphi_{nm}^{\circ}\right)\right]\right\}dx \tag{2.7}$$

These expressions have meaning when $B_\infty = 0$, where the field attenuates along x as $|x| \to \infty$ so fast that its energy is bounded, i.e., when B_z is a function, square-integrable along the whole x-axis. If this condition is not observed, then integrals in (2.6) and (2.7) diverge, and it is possible to investigate only the "linear density" of dissipation, determined by the integrand in (2.6). The integrand in (2.7) for this purpose is unfit, since it is not equal to the integral from $j^2/a\delta\sigma^2$ with respect to the channel section.

The obtained solution is intimately connected with certain previously known ones. Thus, when $x \to \infty$, $B_z \to B_\infty \neq 0$, it asymptotically approaches the Longuet-Higgins solution [5]. In another case, when V and B do not depend on z, the double sums in (2.4)-(2.7) disappear and there is obtained a solution of the corresponding two-dimensional problem of distribution of potential, which for special forms of dependence of V and B on coordinates x and y is considered in [1-3].

3. Let us assume that the velocity distribution satisfies conditions of adhesion on walls and is expressed by series

$$v = U_0 \sum_{n=1}^{\infty} \chi_n(z) \cos \frac{r_n y}{\delta} \qquad \left(\chi_n = \frac{r_n}{U_0},\ \chi_n(\pm a) = 0 \right) \tag{3.1}$$

Let us assume also that change of the transverse magnetic field along axis z, at least in section $|z| < a$, can be ignored and we can set $B_z = B_0 b(x)$. Function $b(x)$ we consider even and attenuating rather rapidly as $|x| \to \infty$. Constants U_0 and B_0 have the meaning of characteristic values of velocity and field, respectively. With the indicated assumptions

$$\varphi^\circ \equiv 0, \qquad m_{nm} = \frac{r_n \chi_{nm}}{c\delta} U_0 B_0 b(x), \qquad \chi_{nm} = \frac{1}{a} \int_{-a}^{a} \chi_n(z) \cos \frac{\pi m z}{a}\, dz$$

$$M_{nm} = \frac{r_n}{c\delta} B_0 U_0 \psi_{nm}(x)\, \chi_{nm} \tag{3.2}$$

$$\psi_{nm}(x) = -\frac{1}{2\mu_{nm}} \int_{-\infty}^{\infty} b(\xi) \exp(-\mu_{nm} |x - \xi|)\, d\xi$$

From formula (2.6) for Q we obtain

$$Q = \frac{3aU_0^2B_0^2}{c^2\delta}\left(\frac{1}{2}\sum_{n=1}^{\infty}\chi_{n0}^2 q_{n0} + \sum_{n=1}^{\infty}\sum_{m=1}^{\infty}\chi_{nm}^2 q_{nm}\right) \tag{3.3}$$

$$Q = Q^*\left[1 + 2\sum_{m=1}^{\infty}\left(\sum_{n=1}^{\infty}\chi_{nm}^2 q_{nm} \Big/ \sum_{n=1}^{\infty}\chi_{n0}^2 q_{n0}\right)\right] \tag{3.4}$$

Here

$$Q^* = \frac{3aU_0^2B_0^2}{2c^2\delta}\sum_{n=1}^{\infty}\chi_{n0}^2 q_{n0}, \qquad q_{nm} = \int_{-\infty}^{\infty}(\delta^2 b^2 + r_n^2 b\psi_{nm})\,dx \geqslant 0$$

If velocity changes along axis z practically only in narrow boundary layers on walls z = ±a, then, in general, coefficients χ_{nm} are small (for m ≥ 1). In the limiting case, when v = v(y) when |y| ≤ δ, |z| < a, from (3.3) we obtain the formula of two-dimensional theory $Q = Q^*$. It is obvious that two-dimensional theory gives a satisfactory approximation to the more exact result (3.4), if

$$\omega = 2\sum_{m=1}^{\infty}\left(\sum_{n=1}^{\infty}\chi_{nm}^2 q_{nm} \Big/ \sum_{n=1}^{\infty}\chi_{n0}^2 q_{n0}\right) \ll 1 \tag{3.5}$$

Functionals $q_{n0}\{b(x)\}$ in this formula are bounded from above by a certain number, not depending on n and the form of function b(x), if only b(x) is bounded (b ≤ 1). Functionals $q_{nm}\{b(x)\}$ when m ≥ 1 do not possess this property. Therefore, if the extent of the region where the field is substantial, i.e., b ~ 1, is great in comparison with δ, q_{nm} can become so large that inequality (3.5) obviously will not be satisfied even for small values of χ_{nm}. Investigating quantity ω for the given v(y, z) and b(x), it is possible for each problem to indicate the maximum extent of the zone of the magnetic field at which the contribution to dissipation from closed transverse currents still remains negligible.

Quantity ω in general can be calculated as follows. Let us assume that

$$q_{nm} < \beta_1, \quad q_{1m} > \beta_2, \quad q_{n0} < \beta_3 \quad \text{when } n \geqslant 1,\ m \geqslant 1 \tag{3.6}$$

Then

$$2\left(\frac{3_2}{3_3}\right)\left(\sum_{m=1}^{\infty}\chi_{1m}^2 \Big/ \sum_{n=1}^{\infty}\chi_{n0}^2\right) < \omega < \frac{23_1}{\chi_{10}^2 q_{10}} \sum_{n=1}^{\infty}\sum_{m=1}^{\infty}\chi_{nm}^2 \qquad (3.7)$$

Sums in these inequalities are calculated in final form by the Parseval formula. It is obvious that (3.7) can be modified and improved, for instance, by more precise definition of inequalities (3.6).

4. As an example, consider flow in an exponentially attenuating magnetic field [1]:

$$b(x) = \begin{cases} e^{p(x+\lambda)/\delta} & \text{when } x < -\lambda \\ 1 & \text{when } |x| < \lambda \\ e^{-p(x-\lambda)/\delta} & \text{when } x > \lambda \end{cases} \qquad (4.1)$$

when functions $\psi_{nm}(x)$ and constants q_{nm} are expressed by formulas

$$\psi_{nm} = -\frac{1}{2\mu_{nm}^2} \begin{cases} Me^{p(x-\lambda)/\delta} - M_- e^{\mu_{nm}(x+\lambda)} - M_+ e^{\mu_{nm}(x-\lambda)} & (x < -\lambda) \\ 2(1 - M_+ e^{-\mu_{nm}\lambda} \operatorname{ch} \mu_{nm} x) & (|x| < \lambda) \\ Me^{-p(x-\lambda)/\delta} - M_- e^{-\mu_{nm}(x-\lambda)} - M_+ e^{-\mu_{nm}(x+\lambda)} & (x > \lambda) \end{cases} \qquad (4.2)$$

$$q_{nm}(p, \lambda) = \frac{r_n^2}{\mu_{nm}^2} M_+ (1 - M e^{-2\mu_{nm}\lambda}) + \left(\delta^2 - \frac{r_n^2}{\mu_{nm}^2}\right)\left(2\lambda + \frac{\delta}{p}\right) \qquad (4.3)$$

$$M = \frac{2\mu_{nm}^2}{\mu_{nm}^2 - p^2/\delta^2}, \quad M_\mp = \frac{p/\delta}{\mu_{nm} \mp p/\delta}$$

The velocity distribution, following [2, 5], we take in the form of the product

$$v = U_0 \chi^{(1)}(N_1, y)\, \chi^{(2)}(N_2, z)$$

$$\chi^{(1)} = \frac{N_1}{f(N_1)}(\operatorname{ch} N_1 - \operatorname{ch} N_1 y/\delta), \quad \chi^{(2)} = \frac{N_2}{f(N_2)}(\operatorname{ch} N_2 - \operatorname{ch} N_2 z/a) \qquad (4.4)$$

$$f(N_k) = N_k \operatorname{ch} N_k - \operatorname{sh} N_k \qquad (k = 1, 2)$$

Here U_0 -- mean velocity, N_k – geometric parameters, characterizing fullness of the profile. With a real N_k, varying from 0 to ∞, the velocity profile in plane z = const (for k = 1) or y = const (for k = = 2) is deformed, passing from parabolic to uniform. When $N_k = \pi i/2$ in the corresponding planes there is obtained a cosinusoidal profile

[1], and series (3.1) then is broken on the first term. For larger N_k the relative thickness of boundary layer on walls $y = \pm\delta$ and $z = \pm a$ in order of magnitude is equal to N_1^{-1} and N_2^{-1}, respectively.

Coefficients of trigonometric expansion of $\chi(y, z)$ have form

$$\chi_n(z) = \frac{2N_1^3N_2(-1)^{n+1}}{r_n f(N_1) f(N_2)} \frac{\operatorname{ch} N_1}{r_n^2 + N_1^2} (\operatorname{ch} N_2 - \operatorname{ch} N_2 z/a)$$

$$\chi_{n0} = \frac{4N_1^2}{r_n f(N_1)} \frac{(-1)^{n+1} \operatorname{ch} N_1}{r_n^2 + N_1^2}, \quad \chi_{nm} = \frac{(-1)^{n+m} N_2^3 \operatorname{sh} N_2}{(\pi^2 m^2 + N_2^2) f(N_2)} \chi_{n0} \tag{4.5}$$

Joule dissipation in this case depends on parameters N_k, p, λ/δ, b/a. In order to investigate their influence, we consider ω, for which, taking into account (4.5), we obtain

$$\omega = 2 \sum_{m=1}^{\infty} \varepsilon_m^2 \omega_m$$

$$\varepsilon_m = \frac{\chi_{nm}}{\chi_{n0}}, \quad \omega_m = \left(\sum_{n=1}^{\infty} \frac{q_{nm}}{r_n^2 (r_n^2 + N_1^2)^2} \right) \left(\sum_{n=1}^{\infty} \frac{q_{n0}}{r_n^2 (r_n^2 + N_1^2)^2} \right)^{-1} \tag{4.6}$$

For q_{nm} here we can establish more exact estimates than (3.6)

$$\delta^3 \left(\frac{\alpha_1}{r_n^4} + \frac{\alpha_2}{r_n^2} \right) < q_{n0} < \delta^3 \alpha_3, \qquad \delta^3 \frac{\alpha_4}{r_n^2} < q_{nm} < \delta^3 \alpha_5 \tag{4.7}$$

$$\alpha_1 = \frac{\pi^3 p^2 (1 - e^{-\pi\lambda/\delta})}{8 (p + \pi/2)^2}, \qquad \alpha_2 = \frac{\pi^2 p}{4 (p + \pi/2)^2}$$

$$\alpha_3 = \frac{16\alpha_1}{\pi^4} + \frac{4\alpha_2}{\pi^2}, \qquad \alpha_4 = \frac{\delta^2 \pi^2 / a^2}{1 + 4\delta^2/a^2} \left(2 \frac{\lambda}{\delta} + \frac{1}{p} \right) \tag{4.8}$$

$$\alpha_5 = \frac{p^2 (1 - e^{-2\mu_{11}\lambda}) + p\delta\mu_{11}}{\delta\mu_{11} (p + \delta\mu_{11})^2} + 2 \frac{\lambda}{\delta} + \frac{1}{p}$$

Taking into account identities

$$\psi_1(N) = \sum_{n=1}^{\infty} \frac{1}{r_n^2 (r_n^2 + N^2)^2} = \frac{2N \operatorname{ch} 2N - 3 \operatorname{sh} 2N + 4N}{8N^3 \operatorname{ch}^2 N}$$

$$\psi_2(N) = \sum_{n=1}^{\infty} \frac{1}{r_n^4 (r_n^2 + N^2)^2} = \frac{2N(N^2 - 6) \operatorname{ch} 2N + 15 \operatorname{sh} 2N + 2N(N^2 - 9)}{24 N^3 \operatorname{ch}^2 N}$$

$$\psi_3(N) = \sum_{n=1}^{\infty} \frac{1}{r_n^6 (r_n^2 + N^2)^2} = \frac{(4N^5 - 20N^3 + 90N) \operatorname{ch} 2N - 105 \operatorname{sh} 2N + 4N^5 - 20N^3 + 120N}{120 N^5 \operatorname{ch}^2 N}$$

proved by the Parseval formula, we find for ω_m

$$\frac{\alpha_1 \psi_2(N_1)}{\alpha_3 \psi_1(N_1)} < \omega_m < \frac{\alpha_5 \psi_1(N_1)}{\alpha_1 \psi_3(N_1) + \alpha_2 \psi_2(N_1)} \tag{4.9}$$

From this, turning to (4.6), we find as estimate for ω

$$\frac{\alpha_1}{\alpha_2}\Psi_1(N_1)\Psi_2(N_2) < \omega < \frac{\alpha_1\Psi_2(N_2)}{\alpha_1\Psi_2(N_1)+\alpha_2\Psi_1(N_1)} \qquad (4.10)$$

Here

$$\Psi_1 = \frac{\Psi_2}{\Psi_1}, \qquad \Psi_2 = \frac{\Psi_3}{\Psi_1}, \qquad \Psi_3(N) = \frac{N^2 + N\,\mathrm{sh}\,N\,\mathrm{ch}\,N - 2\,\mathrm{sh}^2 N}{2f^2(N)}$$

Curves of functions $\Psi_1(N)$, $\Psi_2(N)$ and $\Psi_3(N)$ are presented in Fig. 2. For large values of N

$$\Psi_1 \approx \frac{1}{3}, \qquad \Psi_2 \approx \frac{2}{15}, \qquad \Psi_3 \approx \frac{1}{2N}$$

Dependence of α_4/α_3 on λ/δ for different values of p and $\delta/a = 1$ is depicted in Fig. 3 for $\lambda/\delta \leq 2$ and $p \geq 1$. Let us note that with further increase of λ/δ ratio α_4/α_3 increases almost linearly. Decrease of p leads to more rapid growth of α_4/α_3, since from (4.8) it follows that $\alpha_4/\alpha_3 \sim p^{-2}$ when $p \leq 1$. With growth of δ/a values of α_4/α_3 also increase, but they preserve the same order of magnitude as when $\delta/a = 1$.

From consideration of these results it follows that when $\delta/a \geq 1$ parameter ω has an order of magnitude at least as large as N_2^{-1}, and for $\lambda/\delta \geq 4$ or $p < 1$ it exceeds N_2^{-1} by an order. Therefore, even with small relative thickness of the boundary layer on walls, perpendicular to the magnetic field the contribution of transverse currents to dissipation can be marked. For instance, for $N_2^{-1} = 0.05$, $\lambda/\delta \geq 4$, $p = 3$, $\delta/a = 2$ we have $\omega > 0.2$, i.e., real dissipation by more than 20% exceeds that calculated by two-dimensional theory. With greater relative thickness of the boundary layer on walls $z = \pm a$ (for smaller N_2) the influence of cross currents becomes essential correspondingly for smaller λ/δ and larger values of p.

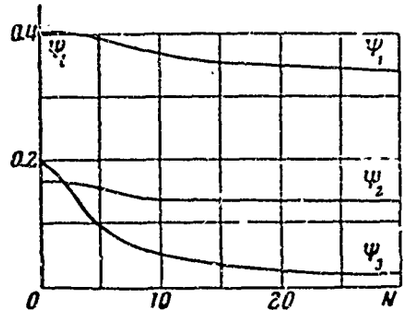

Fig. 2.

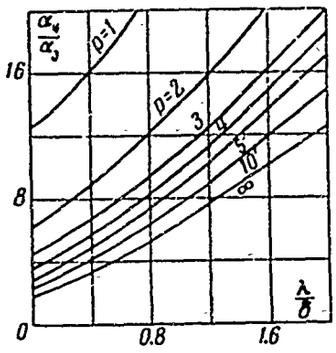

Fig. 3.

Thickness of boundary layers on walls $y = \pm\delta$, parallel to the magnetic field, is characterized by parameter N_1. As can be seen from the given calculations, its influence on ω is small, and conclusions, made above, are valid for any N_1. At the same time, in the expression for total Joule dissipation (3.4) this paramter enters not only in ω, but in Q^*, where Q^* strongly depends on N_1. Thus, with change of N_1 from 0 to ∞, Q^* and, consequently, Q decreases by a factor of one and a half [2].

5. The solution investigated above was obtained on the assumption that $V(x, y, z)$, $B(x, y, z)$ are given functions. It is obvious that solvability of system (1.1)-(1.3) requires only fulfillment of equality

$$\lim_{l\to\infty} \iiint_D \mathbf{B}\,\mathrm{rot}\,\mathbf{V}\,dD = \lim_{l\to\infty} \iint_\Sigma (\mathbf{V}\times\mathbf{B})_n\,d\Sigma \qquad (5.1)$$

under D, Σ — volume and surface of parallelpiped $|x| \leq l$, $|y| < \delta$, $|z| < a$. This condition is fulfilled exactly if B — arbitrary potential vector. It also takes place for different cases of joint assignment of V and B in special form, for instance in such a form as in Sections 2-4, when V rot B = 0.

During solution of problems there frequently arises the necessity of introducing in system (1.1)-(1.3) a simple approximate expression for the external magnetic field B instead of the exact expression, which satisfies equations div B = 0 and rot B = 0 and having, as a rule, very complex form. Here it may be (as in Sections 3-4) that the introduced vector does not satisfy equation rot B = 0. If the flow of liquid is nonrectilinear, then condition (5.1) may also be disturbed. Therefore, in such cases the classes of approximating

functions of V and B are bounded by condition (5.1) or the equivalent requirement

$$\lim_{t\to\infty}\iiint_D \mathbf{V}\,\mathrm{rot}\,\mathbf{B}\,dD = 0 \qquad (5.2)$$

The latter can be considered the condition of conversion into zero of the V-weighted average value of rot B. Let us note that current density j found from the solution exactly satisfies equation div j = 0, if requirement V rot B ≡ 0 is fulfilled better than (5.2). Otherwise equation div j = 0 on the average throughout the volume is satisfied exactly, and at every point it is satisfied approximately.

Selection of function B, introduced in the calculation, is also determined by other considerations, the essence of which it is possible to explain from the example of the problem considered in Sections 2-4. In this problem of significance only is selection of the component of magnetic field $B_z(x, z)$ transverse to the flux. If in direction z the channel has relatively small width ($\delta/a > 1$), then within section $|z| < a$ it is possible to expect small change of B_z in comparison with the magnitude of $B_z(x, 0)$. Considering therefore $B_z(x, z) \approx B_z(x, 0) = B_0 b(x)$, we arrive at the formulation of the problem in Section 3. If however the ratio of transverse dimensions of the channel is the opposite ($\delta/a < 1$), although the whole system of the problem is close to two-dimensional, approximation $B_z(x, z) \approx B(x)$ can be unsuitable for not too great an extent of the zone of the magnetic field along the channel.

Solution of the problem, considering change of the magnetic field across the channel, is easily obtained from general forumulas of Section 1. Nonuniformity of the field, just as nonuniformity of velocity, leads to appearance of a transverse edge effect.

Let us note that there exist such fields for which $B_z(x, 0) < B_z(x, a)$ for small values of x and $B_z(x, 0) > B_z(x, a)$ for large x. In this case the transverse edge effect, caused by nonuniformity of velocity, will be weakened near the central section of the channel and will be strengthened far from it.

Submitted
12 March 1964

Literature

1. A. B. Vatazhin. Determining Joule dissipation in the channel of a magnetohydrodynamic generator. PMTF, 1962, No. 5.

2. A. B. Vatazhin. Certain two-dimensional problems of distribution of current in a conducting medium, moving in a channel in a magnetic field. PMTF, 1963, No. 3.

3. S. A. Regirer. Influence of boundary layer effect on distribution of current during flow of a conducting fluid in a channel. Collection: Problems of magnetohydrodynamics, Vol. 3, Riga, Publishing House of Academy of Sciences of Latvian SSR, 1963.

4. A. B. Vatzhin and S. A. Regirer. Approximate calculation of distribution during flow of a conducting fluid in a channel in magnetic field. PMM, 1962, Issue 3.

5. M. S. Longuet-Higgins. The electrical and magnetic effect of tidal streams. Month. Not. Roy. Astron. Soc., Geophys. suppl., 1949, Vol. 5, No. 8.

ON COOLING BY RADIATION OF GAS, FLOWING PAST A FLAT PLATE

A. F. Kurbatskiy and A. T. Onufriyev

(Novosibirsk)

In a number of problems of aerodynamics it is necessary to consider transfer of energy by radiation and thermal conduction through an absorbing medium. Finding the mutual influence of both forms of energy transfer is the subject of a number of works. In [1-3] there was considered the case of stationary one-dimensional transfer of energy between two plates. For flow in a laminar boundary layer the problem was considered in [4-8]; for turbulent flow, in [9]. For description of energy transfer by radiation there were used different approximations: one-dimensional, diffusional and of nonlinear thermal conduction. In the present work in the simple problem of a thermal boundary layer there is shown the influence of radiation on the magnitude of the energy flux, depending upon the parameter characterizing the relative magnitude of densities of energy fluxes caused by radiation and thermal conduction, and we compare different approximations.

Designations

q^1 – dimensionless magnitude of density of the energy flux, determined by radiation;

q^0 – the same, but determined by molecular thermal conduction;

q_*^1 – the same, but determined by radiation in the approximation of "nonlinear thermal conduction;"

q – the same for the total energy flux;

φ – dimensionless magnitude of density of energy of radiation;

Φ^0 — equilibrium density of energy of radiation;

c — velocity of light;

σ — Boltzmann's constant;

T — dimensionless temperature;

l — path length of radiation;

u — component of velocity of flow among axis x;

ρ — density of gas;

P — Prandtl number;

c_p — specific heat capacity at constant pressure;

x' — coordinate lengthwise along the plate;

y' — transverse coordinate;

ε — magnitude of the parameter, characterizing the relative role of molecular thermal conduction and radiation;

k — coefficient of molecular thermal conduction;

μ — coefficient of viscosity;

$I_n(x)$ — Bessel function of imaginary argument (n = 0.1);

$$q^1 = \frac{(q^1)'}{\sigma T_\infty^4}, \quad q^0 = \frac{(q^0)'}{\sigma T_\infty^4}, \quad q = q^0 + q^1, \quad \varphi = \frac{\Phi}{4\sigma T_\infty^4}, \quad A = \frac{\sigma T_\infty^4}{\rho u_\infty c_p T_\infty}$$

$$\Phi^0 = \frac{4\sigma T^4}{c}, \quad \varepsilon = \frac{3kT_\infty}{4l\sigma T_\infty^4}, \quad T = \frac{T'}{T_\infty}, \quad P = \frac{\mu c_p}{k}, \quad x = \frac{4x'A}{3l}, \quad y = \frac{y'}{l}.$$

1. The problem consists of finding the distribution of density of the energy flux the length of a semi-infinite ideal black plate during stationary flow past it of radiating hot gas. The plate is located along axis x. Gas flows parallel to the plate. We take the hypothesis of local thermodynamic equilibrium. The gas is gray. The process of energy transfer by radiation will be described in the diffusional approximation [10]

$$^4/_3 l \operatorname{div}(q^1)' = c\Phi^0 - c\Phi, \qquad (q^1)' = -{}^1/_3 l \operatorname{grad}(c\Phi)$$

Consider flow in the boudnary layer of an incompressible fluid during small changes of temperature for small Prandtl numbers P. In

this case there can be obtained a solution in final form. When $P \ll 1$ it remains to consider the problem of a thermal boundary layer, in which dissipation of energy due to viscosity will be ignored [6, 11]. Transfer of energy by radiation will basically occur in the direction to the plate with a value of parameter $A \ll 1$.

With these assumptions the problem is reduced to solution of system

$$\frac{\partial T}{\partial x} = \varepsilon \frac{\partial^2 T}{\partial y^2} + \frac{\partial^2 \varphi}{\partial y^2}, \qquad \frac{4}{9}\frac{\partial^2 \varphi}{\partial y^2} = \varphi - (4T - 3) \tag{1.1}$$

with boundary conditions

$$\begin{aligned} T &= T_1, \qquad {}^2/_3 \partial\varphi / \partial y = \varphi - (4T_1 - 3) \quad \text{when } y = 0 \\ T &= 1, \qquad \varphi = 1 \quad \text{when } y = \infty \end{aligned} \tag{1.2}$$

and with initial condition

$$x = 0, \qquad y > 0 \quad \text{when } T = 1$$

System of equations (1.1) can be reduced to an equation for the magnitude of the density of radiation energy

$$\varepsilon \frac{\partial^4 \varphi}{\partial y^4} - \frac{\partial^3 \varphi}{\partial x \partial y^2} - \frac{9}{4}(4 + \varepsilon)\frac{\partial^2 \varphi}{\partial y^2} + \frac{9}{4}\frac{\partial \varphi}{\partial x} = 0 \tag{1.3}$$

with boundary conditions

$$\frac{2}{3}\frac{\partial \varphi}{\partial y} = \frac{4}{9}\frac{\partial^2 \varphi}{\partial y^2} = \varphi - (4T_1 - 3) \quad \text{when } y = 0, \quad \varphi = 1 \quad \text{when } y = \infty \tag{1.4}$$

and with initial condition

$$\varphi = \varphi(0, y) \quad \text{when } x = 0 \tag{1.5}$$

Quantity $\varphi(0, y)$ satisfies the second equation when $T = 1$ (1.1).

Magnitudes of densities of energy fluxes are determined by

$$q^1 = -\frac{4}{3}\frac{\partial \varphi}{\partial y}, \qquad q^\circ = -\frac{4}{3}\varepsilon\frac{\partial T}{\partial y} = -\frac{\varepsilon}{3}\left[\frac{\partial \varphi}{\partial y} - \frac{4}{9}\frac{\partial^3 \varphi}{\partial y^3}\right]$$

Value of parameter $\varepsilon = \infty$ corresponds to the case of no radiation, and $\varepsilon = 0$ corresponds to the absence of thermal conduction. The

latter case was considered in [12]. The density of the energy flux on the wall when $\varepsilon = 0$ will be

$$q^1(0, x) = -4(1 - T_1)\, e^{-9/2x}\left[I_0(9/2x) + I_1(9/2x)\right] \tag{1.6}$$

2. Equation (1.3) with the corresponding boundary and initial conditions is solved with the help of the Laplace transform. For the transform of the density of the energy flux we obtain

$$q^+(0, s) = -4(1 - T_1)\left[\frac{(4 + \varepsilon + 4/3\sqrt{\varepsilon s} + 4/9\, s)^{1/2}}{3\sqrt{s}} - \frac{2}{9}\right] \tag{2.1}$$

$$q^{0+}(0, s) = -\frac{4(1 - T_1)\sqrt{\varepsilon}}{3\sqrt{s}} \tag{2.2}$$

Expression (2.1) on a plane with a cut along the negative semiaxis has only one singular point $s = 0$, and the complex integral in the expression for the original is reduced to an integral with respect to a real variable

$$q(0, x) = -\frac{4(1 - T_1)}{3\pi\sqrt{2}}\int_0^\infty \frac{e^{-xz}}{\sqrt{z}}\left[4 + \varepsilon - \frac{4z}{9} + \left[\left(4 + \varepsilon - \frac{4z}{9}\right)^2 + \frac{16\varepsilon z}{9}\right]^{1/2}\right]^{1/2} dz \tag{2.3}$$

$$q^0(0, x) = -\frac{4(1 - T_1)}{3\sqrt{\pi}}\frac{\sqrt{\varepsilon}}{\sqrt{x}} \tag{2.4}$$

From (2.4) it is clear that in the considered linear problem the density of energy flux, determined by molecular thermal conduction, does not experience the influence of radiation.

Quantity q^1 we find as the difference $q - q^0 = q^1$.

3. When $\varepsilon = 0$ the expression for density of the energy flux will be

$$q(0, x) = -\frac{8(1 - T_1)}{9\pi}\int_0^9 \frac{e^{-xz}}{\sqrt{z}}\,|9 - z|^{1/2}\, dz \tag{3.1}$$

Expression (3.1) can be converted to form (1.6). Correction to q^1 for small values of ε will be a quantity of the order of $\varepsilon^{1/2}$, which it is possible to see from series expansion of (2.3). As $\varepsilon \to \infty$ we obtain

$$q(0, x) \to -\frac{4(1 - T_1)}{3\sqrt{\pi}}\frac{\sqrt{\varepsilon}}{\sqrt{x}}$$

which corresponds to molecular energy transfer. The first term in q^1 corresponds to calculation of quantity

$$q_*^1(0, x) = -\int_0^\infty \frac{3}{2}[4T_1(y, x) - 3]\, e^{-3/4y}\, dy + (4T_1 - 3)$$

by the temperature profile, which is obtained from solution of the problem during allowance for thermal conduction alone; for large values of x:

$$q_*^1(0, x) \approx -\frac{8(1-T_1)}{3\sqrt{\pi e x}} \tag{3.2}$$

For large values of x we can obtain an asymptotic expression for density of the total flux of energy,

$$q(0, x) \approx -\frac{4(1-T_1)\sqrt{4+\varepsilon}}{3\sqrt{\pi x}}\left[1 - \frac{4}{9(4+\varepsilon)^2 x}\right] \tag{3.3}$$

and for the density of the flux of energy, determined by radiation,

$$q^1(0, x) \approx -\frac{4(1-T_1)}{3\sqrt{\pi x}}[\sqrt{4+\varepsilon} - \sqrt{\varepsilon}] \tag{3.4}$$

From (3.4) and (3.2) it is clear that the latter can be used for large values of ε, i.e., when thermal conduction plays a predominant role.

4. Approximation of "nonlinear thermal conduction" corresponds to the value of the effective coefficient of thermal conduction $k_x = k + (16/3)l\sigma T_\infty^3$.

The density of the energy flux is

$$q(0, x) = -\frac{4(1-T_1)\sqrt{4-\varepsilon}}{3\sqrt{\pi x}} \tag{4.1}$$

This quantity for large values of x coincides with the solution in diffusional approximation (3.3). But if we are interested in the radiation component in the energy flux, there is no coincidence [7, 13]; in this approximation we obtain that which should be compared with (3.4). As $l \to 0$,

$$q_{**}^{1} = -\frac{16(1-T_1)}{3\sqrt{\pi x}(1+\varepsilon)} \qquad (4.2)$$

we find that x is great, and $\varepsilon \to \infty$ and $q_{**}^{1}/q^{1} \to 2$. When l is small, but $k \to 0$, $\varepsilon \to 0$, and x is great, and $q_{**}^{1}/q^{1} \to 1$.

But in the molecular component of the density of the energy flux there is obtained here a great difference. When $l \to \infty$, but k is finite, $\varepsilon \to 0$ and $x \to 0$. Instead of (3.4) it is necessary to take (1.6), which gives $q^{1}(0, x) \to 1$ and $q_{**}^{1}/q^{1} \to \infty$.

5. Results of calculation of the magnitude of density of energy fluxes are given in the form of dependences on x of $q/(1 - T_1)$ in Fig. 1 for $\varepsilon = 10$, Fig. 2 for $\varepsilon = 1$ and Fig. 3 for $\varepsilon = 0.1$. In each figure curve 1 corresponds to density of total energy flux; curve 2, to density of energy flux determined by radiation; curve 3, to density of energy flux determined by thermal conduction; curve 4, to density of total energy flux, calculated in the approximation of "nonlinear thermal conduction"; the curve, marked by small crosses, corresponds to the quantity determined by (1.6); the curve, marked by circles, corresponds to q_{*}^{1}.

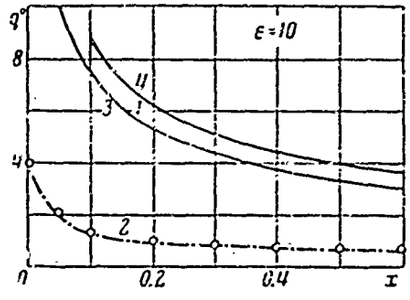

Fig. 1.

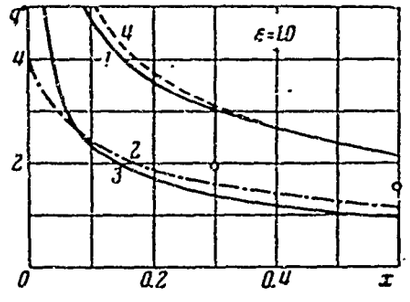

Fig. 2.

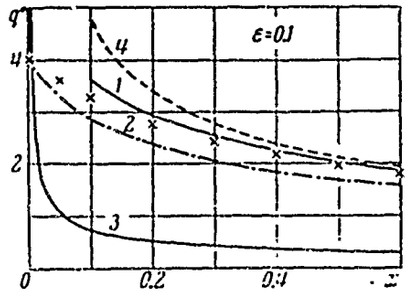

Fig. 3.

Comparison of curves shows that for small values of parameter ε the difference between results in the diffusional approximation and the approximation of nonlinear thermal conduction may be significant. From comparison of curves in Fig. 3 it is clear that the magnitude of density of the

total energy flux, determined by (1.6), when we completely ignored the action of thermal conduction, is close to the solution in diffusional approximation. When we allow for thermal conduction there occurs only a certain redistribution in energy fluxes.

This consideration of the linear problem allows to see the region of validity of different approximations utilized in describing the transfer of energy by radiation, which preserves it qualitative meaning in the more general case.

The authors thank V. P. Zamurayev and V. N. Vetlutskiy for useful discussions.

Submitted
13 January 1964

Literature

1. L. P. Filippov. Influence of radiation and absorption of a medium on process of heat transfer. Herald of Moscow State University, ser. of physical and mathematical sciences, 1954, No. 2.

2. I. V. Nemchinov and A. S. Fonarev. Couette flow taking into account heat transfer by radiation. PMTF, 1960, 3.

3. R. Viskanta and R. D. Grosh. Heat transfer by thermal conduction and radiation in an absorbing medium. Heat transfer, Russian trans. Journal of Heat Transfer, February Transactions of the ASME 1962, T. 84, ser. C, No. 1.

4. A. N. Rumynskiy. Boundary layer in radiating and absorbing media. News of AS of USSR, Mechanics and machine building, Dept. of Tech. Sci., 1960, No. 2.

5. G. N. Andreyev. Calculation of the radiation flux in a laminar boundary layer. News of AS of USSR, Dept. of Tech. Sci., 1960, No. 6.

6. Ye. A. Romishevskiy. Boundary layers and stabilized gas discharge with a diffusion character of radiation. Eng. Journal, 1962, Vol. 2, Issue 1.

7. R. Viskanta and R. J. Grosh. Boundary layer in thermal radiation absorbing and emitting media. Intern. J. Heat and Mass Transfer, 1962, Vol. 5, No. 9.

8. Koch and De Silva. Interaction between radiation and convection in the boundary layer of a flat plate at hypersonic speeds.

Rocket technology, Russian trans. of ARS Journal, 1962, Vol. 32, No. 5, pp. 103-105.

9. S. S. Kutateladze, A. I. Leont'yev and N. A. Rubtsov. Estimating the role of radiation during calculation of heat exchange in a turbulent boundary layer. PMTF, 1963, No. 4.

10. V. A. Ambartsumyan, E. R. Mustel', A. B. Severnyy, and V. V. Sobolev. Theoretical astrophysics. Gostekhteoritizdat, 1952.

11. M. N. Kogan. On flows with great thermal conduction. Reports of AS of USSR, 1959, Vol. 128, No. 3.

12. A. T. Onufriyev. On cooling by radiation of a semi-infinite volume of gas, PMTF, 1961, No. 2.

13. V. P. Zamurayev. Laminar boundary layer in a radiating-absorbing gas near a flat plate. PMTF, 1964, No. 3.

LAMINAR BOUNDARY LAYER IN A RADIATING-ABSORBING GAS NEAR A FLAT PLATE

V. P. Zamurayev

(Novosibirsk)

The stationary problem of laminar flow of a radiating-absorbing gas in a boundary layer near a flat plate was considered in a number of works [1-6]. However, due to assumptions made about radiation, the region of application of the obtained solutions is limited; for the same reason accuracy of the utilized methods of calculation of radiation is not known.

In the present work there is considered a laminar boundary layer near a plate with more exact description of the transfer of radiation. Heat transfer is carried out by normal thermal conduction and radiation. About radiation there are made a series of simplifying assumptions, utilized also in the works mentioned. Thus we take the hypothesis of local thermodynamic equilibrium — emissivity and the coefficient of absorptions are connected by Kirchhoff's law. The medium is assumed to be gray. Radiant fluxes along the plate will be disregarded in comparison with fluxes across it. This is permissible if change of temperature along the plate on the radiation path length is small. In radiant fluxes across a plate weak change of temperature along plate will show up in such a way that these fluxes will be determined by the temperature profile in the considered section. The wall is assumed ideal black. Physical properties of the medium can depend on temperature.

We show the character of asymptotic behavior of heat transfer far from the front point of the plate. For solution of the problem along the whole plate there is applied a differential method of solution of the system of partial differential equations with a complex integro-differential equation of energy. This method in its basic

features is similar to the differential method applied for solution of equations of the boundary layer without calculation of radiation [7-9]. In conclusion there are given results of calculations for one of the cases considered in [1]. Here, we show the character of heat transfer and the possibility of accounting for radiation in approximation of radiant thermal conduction.

1. We consider a stationary laminar boundary layer near a flat plate.

In variables x (longitudinal coordinate) and y (transverse coordinate) the problem at hand is described by system of equations

$$\frac{\partial \rho u}{\partial x} + \frac{\partial \rho v}{\partial y} = 0$$
$$\rho u \frac{\partial u}{\partial x} + \rho v \frac{\partial u}{\partial y} = \frac{\partial}{\partial y} \mu \frac{\partial u}{\partial y} \qquad (1.1)$$
$$\rho u c_p \frac{\partial T}{\partial x} + \rho v c_p \frac{\partial T}{\partial y} = -\frac{\partial q}{\partial y} + \mu \left(\frac{\partial u}{\partial y}\right)^2$$

Here u and v are components of velocity along and across the plate; T — temperature, ρ — density, μ — coefficient of viscosity, c_p — specific heat capacity at constant pressure, q — total flux of heat along y, equal to the sum of fluxes from normal thermal conduction q_m and from radiation q_r

$$q = q_m + q_r \qquad (1.2)$$

Flux of heat q_m is determined by usual method

$$q_m = -\lambda \partial T / \partial y \qquad (1.3)$$

where λ — coefficient of thermal conductivity.

The flux of heat from radiation q_r can be found by using its expression, obtained by integration with respect to the spectrum and solid angle of the intensity of radiation in the form of a formal solution of the transport equation, multiplied by the cosine of the angle between the direction of radiation and axis y, taking into account the assumption of grayness of the medium and ignoring change in temperature along x for several radiation path lengths:

$$q_r = 2\sigma T_0^4 E_3(\tau) + \int_0^{\tau} 2\sigma T^4 E_2(\tau - t)\,dt - \int_{\tau}^{\infty} 2\sigma T^4 E_2(t - \tau)\,dt \qquad (1.4)$$

Here σ — Stefan-Boltzmann constant; $E_n(\tau)$ — integral exponential function; τ — optical thickness of the layer of gas, determined by equation (l — radiation path length)

$$\tau = \int_0^y \frac{dy}{l} \qquad (1.5)$$

Subscript 0 characterizes values of parameters on the wall. Quantities ρ, μ, c_p, λ, l, in general, are functions of temperature.

Instead of continuity equation it is possible to consider two equivalent equations (ψ — stream function)

$$\rho u = \frac{\partial \psi}{\partial y}, \qquad \rho v = -\frac{\partial \psi}{\partial x} \qquad (1.6)$$

Solution of system of equations (1.1)-(1.5) is sought in region $x > 0$, $y \geq 0$ with boundary conditions:

$$u = v = 0, \quad T = T_0 \quad \text{when } y = 0; \qquad u = u_\infty, \quad T = T_\infty \quad \text{when } y = \infty \qquad (1.7)$$

2. The above problem is solved numerically. Here, the front point $x = y = 0$ is singular (stress of friction and flux of heat from normal thermal conduction behave in the vicinity of this point as $1/\sqrt{x}$), therefore for creation of a single algorithm of numerical calculation in all the region there are introduced new independent variables

$$\xi = \frac{2\sigma T_1^4}{\rho_1 u_\infty c_{p1} T_1} \frac{x}{l_1}, \qquad \eta = \left(\frac{\rho_1 u_\infty}{\mu_1 x}\right)^{1/2} \int_0^y \frac{\rho}{\rho_1}\,dy \qquad (2.1)$$

and instead of stream function $\psi(x, y)$ — we have a new function $f(\xi, \eta)$

$$\psi = \sqrt{\rho_1 u_\infty \mu_1 x}\, f \qquad (2.2)$$

As a result all derivatives in the equations of conservation become finite, and searched functions f, u and T in the new variables

vary slowly along the plate, thanks to which calculation with the same accuracy can be conducted with a larger step with respect to ξ.

Boundary conditions for $y = \infty$ should be considered at a certain finite distance from the plate, starting from which functions u and T differ from their limiting values u_∞ and T_∞ a magnitude, not exceeding errors of the difference diagram. In new variables the thickness of the boundary layer changes little, and the solution can be sought in standard region $\xi \geq 0$, $0 \leq \eta \leq \eta_\infty$.

We introduce dimensionless quantities

$$u' = \frac{u}{u_\infty}, \quad T' = \frac{T}{T_1}, \quad \rho' = \frac{\rho}{\rho_1}, \quad \mu' = \frac{\mu}{\mu_1}, \quad c_p' = \frac{c_p}{c_{p1}}, \quad \lambda' = \frac{\lambda}{\lambda_1}, \quad l' = \frac{l}{l_1}, \quad q' = \frac{q}{\sigma T_1^4} \tag{2.3}$$

where physical parameters, marked by index 1, are taken at temperature T_1. System of equations (1.1)-(1.6) with boundary conditions (1.7) in dimensionless quantities will take form

$$u' = \frac{\partial f}{\partial \eta} \tag{2.4}$$

$$\frac{\partial}{\partial \eta} \rho' \mu' \frac{\partial u'}{\partial \eta} + \frac{f}{2} \frac{\partial u'}{\partial \eta} + \xi \left(\frac{\partial f}{\partial \xi} \frac{\partial u'}{\partial \eta} - u' \frac{\partial u'}{\partial \xi} \right) = 0 \tag{2.5}$$

$$\frac{1}{P_1} \frac{\partial}{\partial \eta} \rho' \lambda' \frac{\partial T'}{\partial \eta} + \frac{f}{2} c_p' \frac{\partial T'}{\partial \eta} + \xi c_p' \left(\frac{\partial f}{\partial \xi} \frac{\partial T'}{\partial \eta} - u' \frac{\partial T'}{\partial \xi} \right) + \xi \Phi + \varepsilon_1 \rho' \mu' \left(\frac{\partial u'}{\partial \eta} \right)^2 = 0 \tag{2.6}$$

$$\Phi = -\frac{1}{2\sqrt{\xi \varepsilon}} \frac{\partial q_r'}{\partial \eta}, \qquad \rho' l' \Phi = (\theta_0^4 - T'^4) E_2(\tau) +$$

$$+ (\theta_\infty^4 - T'^4) E_2(\tau_\infty - \tau) + \int_0^{\tau_\infty} [T'^4(t) - T'^4] E_1(|\tau - t|)\, dt \tag{2.7}$$

$$\tau = \sqrt{\varepsilon \xi} \int_0^\eta \frac{d\eta}{\rho' l'} \tag{2.8}$$

Boundary conditions are

$$f = u' = 0, \quad T' = \theta_0 \quad \text{when } \eta = 0, \qquad u' = 1, \quad T' = \theta_\infty \quad \text{when } \eta = \eta_\infty \tag{2.9}$$

Here P_1 - is the Prandtl number;

$$P_1 = \frac{c_{p_1} \mu_1}{\lambda_1}, \qquad \varepsilon = \frac{\mu_1 c_{p_1} T_1}{2\sigma T_1^4 l_1}, \qquad \varepsilon_1 = \frac{u_\infty^2}{c_{p1} T_1} \tag{2.10}$$

The expression for Φ is obtained taking into account the fact that $T' = \theta_\infty$ when $\eta \geq \eta_\infty$. Fluxes of heat can be found according to the following formulas :

$$q_m' = -\frac{2\sqrt{\varepsilon}}{P_1\sqrt{\xi}}\rho'\lambda'\frac{\partial T'}{\partial \eta} \tag{2.11}$$

$$q_r' = 2\theta_0^4 E_3(\tau) - 2\theta_\infty^4 E_3(\tau_\infty - \tau) + 2\int_0^\tau T'^4 E_2(\tau - t)\,dt - 2\int_\tau^\infty T'^4 E_2(t - \tau)\,dt \tag{2.12}$$

3. From equation (2.8) it is clear that for small values of ξ the boundary layer is optically transparent, where the smaller ε, the longer it remains transparent. The term in energy equation (2.6), connected with radiation, is the product of ξ and bounded function Φ and for small ξ it is small in comparison with other terms of the equation. According to this the influence of radiation is small. When $\xi \to 0$ it disappears. The temperature profile here seeks a self-similar profile in the absence of radiation. However, singularity when $\xi = 0$ does not completely disappear. Being bounded, function Φ has unbounded derivatives with respect to ξ. Its first derivative behaves as $\xi^{-1/2} \ln \xi$. This is connected with the fact that the optical thickness of the boundary layer grows as $\sqrt{\xi}$ (for small ξ). As a result function Φ varies very sharply.

4. Integrating in the right part of equation (1.4) by parts and using (1.5), we can obtain an expression for q_r in dimensionless form

$$q_r' = -\frac{4}{3}\frac{1}{\sqrt{\varepsilon\xi}}\frac{\partial T'^4}{\partial x} + \frac{1}{\sqrt{\varepsilon\xi}}\frac{\partial T'^4}{\partial x}\Big|_{x=0} 2E_4(\sqrt{\varepsilon\xi}\,x) + \left(\alpha = \int_0^\alpha \frac{d\eta}{\rho' l'}\right)$$
$$+ \frac{2}{\sqrt{\varepsilon\xi}}\int_0^\alpha \frac{\partial^2 T'^4}{\partial t^2} E_4\left[\sqrt{\varepsilon\xi}\,(x - t)\right]dt - \frac{2}{\sqrt{\varepsilon\xi}}\int_x^\infty \frac{\partial^2 T'^4}{\partial t^2} E_4\left[\sqrt{\varepsilon\xi}\,(t - x)\right]dt \tag{4.1}$$

If $\sqrt{\varepsilon\xi} \to 0$, the integrands in (4.1) seek zero everywhere as $(\sqrt{\varepsilon\xi}|\alpha - t|)^{-1} \exp(-\sqrt{\varepsilon\xi}|\alpha - t|)$ with the exception of the vicinity of point $t = \alpha$, which seeks zero, where they are finite. As a result the corresponding terms have order $(\varepsilon\xi)^{-1}$. Therefore, when $\sqrt{\varepsilon\xi} \gg \alpha^{-1}$ instead of (2.12) for q_r' it is possible approximately to use expressi

$$q_r' = -\frac{4}{3}\frac{1}{\sqrt{\varepsilon\xi}}\rho' l'\frac{\partial T'^4}{\partial \eta} \quad \text{or} \quad q_r = -\frac{l}{3}\frac{\partial 4\sigma T^4}{\partial y} \tag{4.2}$$

Thus, for large values of $\varepsilon\xi$ the radiant flux outside the wall is obtained in the approximation of radiant thermal conduction.

The matter is different near the wall in a layer of thickness of several path lengths of radiation (thickness of this layer in variables η, ξ seeks zero as $1/\sqrt{\varepsilon\xi}$). Thus, when $l/L \to 0$, L — characteristic dimension of the problem (and, consequently, $1/\sqrt{\varepsilon\xi} \to 0$), for the radiant flux in this layer we obtain

$$q_r' = -\frac{4}{3}\left[1-\frac{3}{2}E_4(\tau)\right]\frac{1}{\sqrt{\varepsilon\xi}}\rho' l'\frac{\partial T'^4}{\partial \eta} \tag{4.3}$$

differing from (4.2) by factor $[1 - (3/2)E_4(\tau)]$, which changes from 0.5 on the wall to 1 in the gas flux (when $\tau = 4$ the difference of it from one constitutes less than 0.4%). The mutual portion of heat fluxes is determined correspondingly thus:

$$\frac{q_r}{q_m} = \frac{16}{3}\left[1-\frac{3}{2}E_4(\tau)\right]\frac{\sigma T^3 l}{\lambda}$$

Thus, for small l/L near the wall in a layer of gas of a thickness of several path lengths there is redistribution of the heat, transferred by radiation and by normal thermal conduction, in the direction of increase of the molecular thermal flux and corresponding decrease of the radiation flux (total thermal flux almost does not change). This is carried out by sharper lowering of temperature toward the wall. But the relative thickness of this layer is small. Therefore, considering radiation in the approximation of radiant thermal conduction, we can obtain the correct total thermal flux of heat; the radiation component of the thermal flux will be overstated a minimum of 2 times with change of parameter l/L from zero to infinity. In [1] this shortcoming of approximation of radiant thermal conduction to a certain extent is removed by introduction of a thin near-wall

layer, where the coefficient in the expression for the radiation thermal flux is less than in the remaining area by a factor of 2.

5. We solve system of equations (2.4)-(2.8) with boundary conditions (2.9) by the method of finite differences.

Region of flow $\xi \geq 0$, $0 \leq \eta \leq \eta_\infty = \text{const}$ is divided into characteristic strips of width h. We consider arithmetic mean values of the sought functions f_p ($f_p = f, u', T'$) on the left $(i-1)$-th and right i-th boundaries of the strip

$$f_p^\circ = {}^1/_2 (f_{p,\,i-1} + f_{p,i}) \tag{5.1}$$

Index i here means that the function is taken for ξ, equal to $\xi_i = ih$ $(i = 0, 1, 2, \ldots)$.

These mean values differ from exact values on the center line of the strip by a magnitude of the order of h^2.

System of equations (2.4)-(2.6) with boundary conditions (2.9) is written on the center line of the characteristic strip, where exact quantities are replaced by mean f_p°, and derivatives with respect to ξ are replaced by their differential analog

$$\frac{\partial f_p}{\partial \xi} \to \frac{f_p^\circ - f_{p,\,i-1}}{h/2} \tag{5.2}$$

In order not to resort to an iterative process, greatly increasing use of machine time, when radiation is present, and at the same time so as not to increase the error of approximation of the system, quantity Φ, describing radiation, and, simultaneously, $\rho'\mu'$, $\rho'\lambda'$, c_p' and velocity u' in (2.4), each of these quantities is replaced by a linear combination of its values on boundaries of the preceding strip, so that the error of approximation of the system remains of the order of h^2:

$$f_q \to f_q'' = (1 + {}^1/_2 b)\, f_{q,\,i-1} - {}^1/_2 b\, f_{q,\,i-2} \quad (b = h_2 / h_1) \tag{5.3}$$

where h_1 is the preceding step, and h_2 is the new step.

As a result the system of linear partial differential equations (2.4)-(2.6) is reduced to a system of ordinary linear differential equations

$$\frac{df^\circ}{d\eta} = u^\circ \tag{5.4}$$

$$\frac{d}{d\eta}(\rho\mu)^\circ \frac{du^\circ}{d\eta} + \frac{f^\circ}{2}\frac{du^\circ}{d\eta} + \xi^\circ\left(\frac{f^\circ - f_{i-1}}{h/2}\frac{du^\circ}{d\eta} - u^\circ\frac{u^\circ - u_{i-1}'}{h/2}\right) = 0 \tag{5.5}$$

$$\frac{1}{P_1}\frac{d}{d\eta}(\rho\lambda)^\circ\frac{dT^\circ}{d\eta} + \frac{f^\circ}{2}c_p^\circ\frac{dT^\circ}{d\eta} + \xi^\circ c_p^\circ\left(\frac{f^\circ - f_{i-1}}{h/2}\frac{dT^\circ}{d\eta} - u^\circ\frac{T^\circ - T_{i-1}'}{h/2}\right) + \xi^\circ\Phi^\circ + \varepsilon_1(\rho\mu)^\circ\left(\frac{du^\circ}{d\eta}\right)^2 = 0 \tag{5.6}$$

Boundary conditions are

$$f^\circ = u^\circ = 0, \quad T^\circ = \theta_0^\circ \text{ when } \eta = 0; \quad u^\circ = 1, \quad T^\circ = \theta_\infty^\circ \text{ when } \eta = \eta_\infty \tag{5.7}$$

This system is solved in this sequence. First, from equation (5.4) we find function $f^\circ(\eta)$. Then we solve equation (5.5) for $u^\circ(\eta)$. And, last, from equation (5.6) we find function $T^\circ(\eta)$.

After system (5.4)-(5.6) is solved, from algebraic relationships $f_{pi} = 2f_p^\circ - f_{p,i-1}$, a corollary of (5.1), we find values of the sought functions f, u' and T' for $\xi = \xi_i = ih$ with error of the order of h^2.

For solution of the linear system of ordinary differential equations (5.4)-(5.6) the region of flow in plane ξ, η is divided into n horizontal strips of width $\Delta = \eta_\infty/n$, and each of equations (5.4)-(5.7) is approximated by a difference equation of the second order of accuracy. As a result values of function $f^\circ(\eta)$ for $\eta = j\Delta$ are found by formula

$$f_j^\circ = f_{j-1} + \frac{\Delta}{2}(u_{j-1}^\circ + u_j^\circ), \qquad f_0' = 0 \quad (j = 1, 2, \ldots, n-1)$$

And instead of equations (5.5) and (5.6) we use, correspondingly, difference equations

$$[(\rho\mu)_j'' + (\rho\mu)_{j+1}'' + \frac{\Delta}{2} f_j^\circ + 2\xi^\circ \frac{\Delta}{h}(f_j^\circ - f_{i-1j})]\, u_{j+1}^\circ - [(\rho\mu)_{j-1}'' + 2(\rho\mu)_j'' +$$

$$+ (\rho\mu)_{j+1}'' + 4\xi^\circ \frac{\Delta^2}{h} u_j'']\, u_j^\circ + [(\rho\mu)_{j-1}'' + (\rho\mu)_j'' - \frac{\Delta}{2} f_j^\circ -$$

$$- 2\xi^\circ \frac{\Delta}{h}(f_j^\circ - f_{i-1j})]\, u_{j-1}^\circ + 4\xi^\circ \frac{\Delta^2}{h} u_j''\, u_{i-1j}' = 0 .$$

$$[(\rho\lambda)_j'' + (\rho\lambda)_{j+1}'' + \frac{\Delta}{2} P_1 f_j^\circ c_{pj}'' + 2\xi^\circ \frac{\Delta}{h} P_1 c_{pj}''(f_j^\circ - f_{i-1j})]\, T_{j+1}^\circ - [(\rho\lambda)_{j-1}'' +$$

$$+ 2(\rho\lambda)_j'' + (\rho\lambda)_{j+1}'' + 4\xi^\circ \frac{\Delta^2}{h} P_1 c_{pj}''\, u_j^\circ]\, T_j^\circ + [(\rho\lambda)_{j-1}'' + (\rho\lambda)_j'' - \frac{\Delta}{2} P_1 f_j^\circ c_{pj}'' -$$

$$- 2\xi^\circ \frac{\Delta}{h} P_1 c_{pj}''(f_j^\circ - f_{i-1j})]\, T_{j-1}^\circ + 4\xi^\circ \frac{\Delta^2}{h} P_1 c_{pj}''\, u_j^\circ T'_{i-1j} + 2\xi^\circ \Delta^2 P_1 \Phi_j'' +$$

$$+ \frac{\varepsilon_1}{2} P_1 (\rho\mu)_j''(u_{j+1}^\circ - u_{j-1}^\circ)^2 = 0$$

$$u_0^\circ = 0, \quad u_n^\circ = 1; \qquad T_0^\circ = \theta_0^\circ, \quad T_n^\circ = \theta_\infty^\circ.$$

Each of these equations is a second order equation with known values of the sought functions at different ends of the interval. They are solved by the method of successive approximations [?].*

Quantity $(\rho' l' \Phi)_{ij}$ is calculated by the formula

$$(\rho' l' \Phi)_{ij} = (\theta_0^4 - T'^4_{ij}) E_2(\tau_{ij}) + (\theta_\infty^4 - T'^4_{ij}) E_2(\tau_{\infty i} - \tau_{ij}) +$$

$$+ \sqrt{\varepsilon \xi_i}\, \frac{\Delta}{2} \sum_{k=1}^{n} (F_{ik-1j} + F_{ikj})$$

where

$$F_{ikj} = (T'^4_{ik} - T'^4_{ij}) E_1(|\tau_{ik} - \tau_{ij}|) \frac{1}{(\rho' l')_{ik}}$$

Optical thickness τ_{ij}, is calculated by a difference analog of equation (2.8):

$$\tau_{ij} = \tau_{ij-1} + \sqrt{\varepsilon \xi_i}\, \frac{\Delta}{2} \left[\frac{1}{(\rho' l')_{ij-1}} + \frac{1}{(\rho' l')_{ij}} \right] \qquad (j = 1, 2, \ldots, n)$$

$$\tau_{i0} = 0$$

In order to start computation, it is necessary to know profiles of velocity and temperature in the initial ($\xi = 0$) and the first ($\xi = h$) sections. Solution in these sections is sought by the method of successive approximations.

---

*Cyrillic "progonka" comes from a verbal root with the sense of "drive away" or "drive through" — hence it possibly implies successi e approximation [Tr. Ed. note].

6. Results of calculations are given for the case: $\theta_\infty = 1$, $\theta_0 = 0.1$, $\varepsilon = 0.2$, $P_1 = 1$, $\varepsilon_1 = 0$. Physical properties in this case are assumed constant — quantities $\rho'\mu'$, $\rho'\lambda'$, c_p', $\rho'l'$ were equated to one. All these conditions accurately correspond to one of the variants in [1].

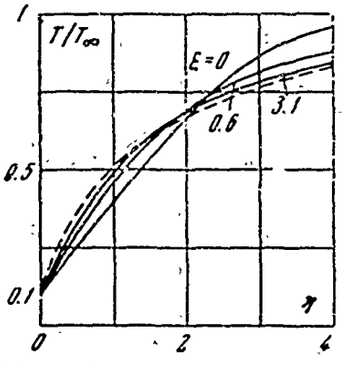

Fig. 1.

The problem was considered with step varying with respect to ξ. Accuracy was checked by calculating with other values of the step both with respect to ξ, and with respect to η. Initially calculation was made for the following values of the step with respect to ξ:

$h = 0.002$ when $0 \leqslant \xi \leqslant 0.008$
$h = 0.004$ when $0.008 \leqslant \xi \leqslant 0.02$
$h = 0.008$ when $0.02 \leqslant \xi \leqslant 0.06$
$h = 0.02$ when $0.06 \leqslant \xi \leqslant 0.3$
$h = 0.1$ when $0.3 \leqslant \xi \leqslant 5.1$

The step with respect to η in this case was equal to 0.4, and the value of η on the external boundary was 16. Calculation on a computer took 5 minutes.

Calculation was repeated up to $\xi = 3.1$ with values of the step half as large both with respect to ξ and with respect to η. The value of η_∞ to $\xi = 0.5$ was assumed equal to 13, and then it was increased to 16.

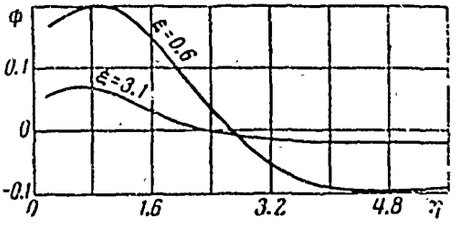

Fig. 2.

The maximum difference between the first and second calculation in values of temperature was 0.3%, and in thermal fluxes on the wall it was 0.7% (for $\xi = 3.1$). The difference in values of Φ reaches several percent.

Results of the calculation are presented in the form of curves. The dotted line plots corresponding curves from [1].

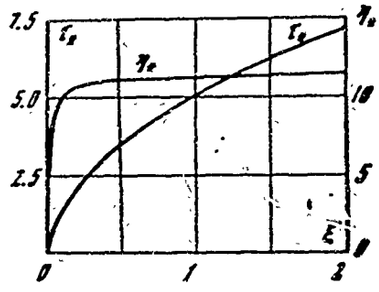

Fig. 3.

In Fig. 1 there are depicted temperature profiles with respect to variable η for different values of ξ. With growth of ξ the temperature profile is deformed from a self-similar one without radiation into a profile, corresponding to consideration of radiation in the approximation of nonlinear (radiant) thermal conduction. Deformation occurs in such a way that hot gas in the presence of radiation becomes cooler, and gas near wall becomes hotter. In the physical plane this corresponds to the hot gas cooling faster, and the gas near the wall cooling more slowly (in comparison with the case when radiation is not considered). This is explained by the fact that hot gas gives off heat not only by molecular thermal conduction, but also by radiation, while cold gas near the wall absorbs more than it radiates

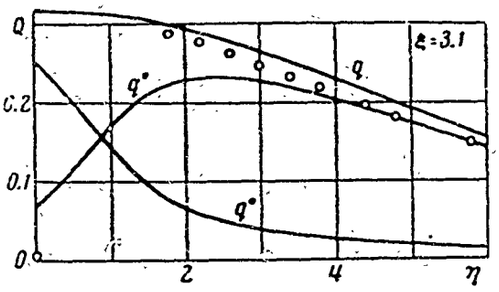

Fig. 4.

(Fig. 2), where for different values of ξ there is depicted the dependence on η of magnitude Φ, proportional to $-\partial q_r/\partial_\eta$).

In Fig. 3 the thickness of boundary layer η_* is constructed, calculated from a value of temperature, differing from the maximum by 1%. For small ξ there is observed very sharp thickening of boundary layer. Subsequently, thickness of the boundary layer with respect to η almost does not vary and is close to its maximum (as $\xi \to \infty$).

In the considered conditions deformation of the temperature profile for small values of ξ occurs sharply, which is connected with rapid growth of the optical thickness of the boundary layer (Fig. 3), where in the midst of the flux it occurs more rapidly.

The latter signifies the approximation of nonlinear thermal conduction for radiation becomes acceptable initially in the hottest region of the boundary layer. The same fact is seen from Fig. 4, where circles mark radiation thermal fluxes, calculated in the approximation of nonlinear thermal conduction from the non-self-similar temperature profile for $\xi = 3.1$.

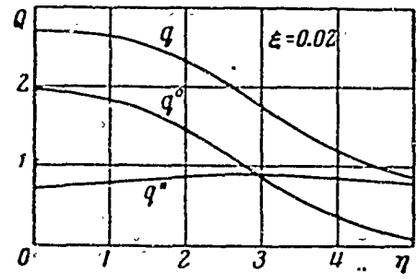

Fig. 5.

The region, where the temperature profile is close to linear, in the presence of radiation is narrowed with growth of ξ. This one may see directly from Fig. 1, and also by examining Figs. 4 and 5, where there are plotted thermal fluxes $Q = (q/\sigma)T_\infty^4$ because of radiation q^*, and normal thermal conduction q° and the total q, depending upon η for ξ equal to 0.02 and 3.1. For small values of ξ the molecular thermal flux near the wall decreases more slowly, and for large ξ, more rapidly. Since the thermal flux from normal thermal conduction is proportional to the slope of the temperature profile, curvature of the profile grows with growth of ξ.

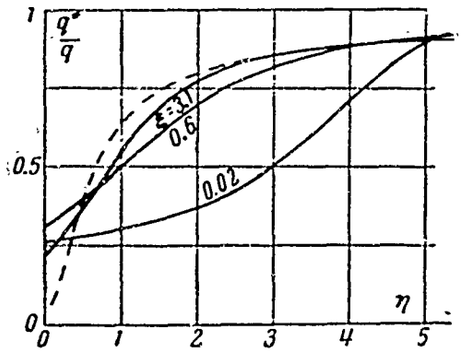

Fig. 6.

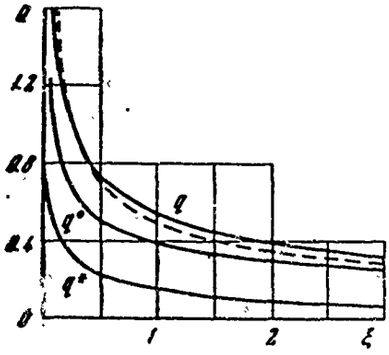

Fig. 7.

For small values of ξ the radiant flux changes slowly with thickness of the boundary layer (Fig. 6), since the boundary layer

is still optically transparent (Fig. 3). But at $\xi = 0.02$ in the considered case there clearly stands out a maximum of radiation flux, connected with the fact that heat is initially transferred by radiation, and only at the wall does there occur redistribution, and heat is also transmitted by molecular thermal conduction, where the total flux of heat almost does not change. For large ξ this effect is seen to a greater degree. This one may see well from Fig. 6, where there is depicted the portion of radiant flux which depends on ξ. In a rather wide region inside the boundary layer the share of radiant flux grows with growth of ξ, especially rapidly for small values of ξ. This growth of the share of radiation in heat transfer is connected with the fact that the temperature profile in this region becomes more gentle. Near the wall, conversely, steepness of profile grows, and the share of the radiant flux drops. (For small ξ the share of the radiant flux also grows near the wall due to sharp drop of the molecular flux).

In Fig. 7 we constructed the flux of heat on wall from radiation, the flux of heat from normal thermal conduction, and also the total flux. In the same place we plotted total fluxes of heat allowing for radiation in the approximation of nonlinear thermal conduction (from [1]). The difference in the considered conditions is somewhat greater than 10%. The difference in the radiation component of the thermal flux was greater (for $\xi = 3.1$ they differ in the considered conditions by a factor of 40).

In conclusion we thank A. T. Onufriyev for useful discussion of this work.

Submitted
17 February 1964

Literature

1. R. Viskanta and R. I. Grosh. Boundary layer in thermal radiation absorbing and emitting media. Int. J. Heat. and Mass Transfer, 1962, 5, 795-806.

2. Koch and De Silva. Interaction between radiation and convection in the boundary layer of a flat plate at hypersonic speeds. Rocket Technology, Russian. trans. of ARS Journal, 1962, Vol. 32, No. 5, 103-105.

3. A. F. Kurbatskiy and A. T. Onufriyev. On cooling by radiation of gas, flowing past a flat plate. PMTF, 1964, No. 3.

4. A. N. Rumynskiy. Boundary layer in radiating and absorbing media. News of AR of USSR, Dept of Tech. Sci., Mechanics and machinebuilding, 1960, No. 2, 47-53.

5. G. N. Andreyev. Calculation of the radiation flux in a laminar boundary layer. News of AS of USSR, Dept. of Tech. Sci., Mechanics and machinebuilding, 1960, No. 6, 109-111.

6. Ye. A. Romishevskiy. Boundary layers and stabilized gas discharge with diffusion character of radiation. Eng. Journal, 1962, Vol. 2, Issue 1, 170-174.

7. Liu Shên-Ch'üan. Calculation of the laminar boundary layer in an incompressible fluid with suction or in-blowing. Journal computational mathematics and mathematical physics, 1962, Vol. 2, No. 4, 666-683.

8. Numerical methods in gas dynamics. Coll. of works of Computational Center of Moscow State University, eds: G. S. Roslyakov and L. A. Chudov, Publishing House of Moscow State University, 1963, II.

9. V. G. Gromov. Application of a three-layer differential scheme for solution of boundary layer equations. News of AS of USSR, Dept. of Tech. Sci., Mechanics and machinebuilding, 1963, No. 5, 124-133.

MEASUREMENT OF PARAMETERS OF GAS FLUXES WITH THE HELP OF A BEAM OF FAST ELECTRONS

A. M. Trokhan

(Novosibirsk)

There is considered the possibility of using a thin beam of fast electrons as a probe for determination of parameters of gas fluxes: local velocity and density of gas, and also for local visualization of fluxes. To this end there are used fluorescence and x-radiation, excited during passage of a beam of electrons through a given region of the investigated flux.

Finding the local velocity of a gas, and also velocity fields in the investigated flux, is a necessary component part of most experimental gas dynamics problems. During work with rarefied gas fluxes the Pitot tube, usually utilized for this purpose, turns out to be far from satisfactory. For Reynolds numbers, smaller than two hundred (for conditions of a free flux and diameter of the probe), the pressure, given by the Pitot tube, deviates from ideal values, given by Rayleigh's formula, and for Reynolds numbers, smaller than several tens, the geometry of the probe begins to have a substantial effect. The influence of compressibility, slippage, and also delay of excitation of vibrational degrees of freedom of molecules of the gas still further complicate interpretation of the pressure, given by the Pitot tube, making it an independent very difficult problem. In view of this it becomes necessary to develop new means of measuring velocity, capable of giving reliable results during research of fast fluxes of rarefied gas.

Good results in this direction were attained during tracing of fluxes by ions, formed by means of pulse irradiation of a moving gas by a beam of fast electrons [1-3]. These methods have two valuable properties — they will be absolute, i.e., they do not require calibration and at the same time they do not require introduction in the flux of

external probes. However, tracing by ions allows us to find only a certain velocity averaged through the irradiated section, where the base of measurement in view of small directivity of electrodynamic detectors should be great. At the same time most valuable for most experimental problems is the possibility of finding the local velocity, the velocity "at a point," i.e., the base of measurement should be minimal. This problem can be solved, apparently, only by optical methods.

Designations

v — velocity of the medium;

A^+ — positive ion;

B^- — negative ion;

L — base of measurement of velocity;

β — image scale;

l, l' — distance from principal planes of the objective to conjugate planes;

F — focal length of objective;

N — particle density;

n — concentration of excited particles;

D — coefficient of diffusion;

P — density of excitation of particles;

Q — density of deactivation of particles;

τ — lifetime of excited state;

λ — wavelength;

ν — frequency;

h — Planck's constant;

c — velocity of light;

α — angle between line of observation and vector of velocity;

θ — angle between vertex of light-dividing wedge and axis of image of the spectral line.

1.1. Excitation of fluorescence of gas. Local feed of

energy to gas by a electric discharge or a flux of fast particles leads to corresponding local change of its parameters. Moreover, in the gas there appears a series of processes, leading to dispersion of the introduced energy. Some of these processes are accompanied by radiation of light. Most of them are very fast, in a time interval of the order of 10^{-9} to 10^{-8} sec, but individual processes have significantly greater duration, as a result of which upon cessation of feed of energy the glow does not cease instantly, but lasts for a certain time, called the time of afterglow. The duration of afterglow and its intensity in different gasses can vary within very wide limits. For instance, duration of afterglow of pure nitrogen under favorable conditions attains 5 to 5.5 hours [4]. This is the so-called Lewis-Rayleigh afterglow of active nitrogen, caused by triple collisions including atomic nitrogen in the ground state. At the same time nitrogen also has significantly brighter afterglow, lasting about 0.1 sec, determined by double collisions [5]. Argon has prolonged afterglow. It is determined both by recombination and luminiscence of metastable states. For instance, state $3P_0$ of argon has life duration of the order of 0.0005 sec, and state $3P_2$ has a duration 0.004 sec [6].

Afterglow of air has mainly a hemiluminescent nature and is determined by reaction

$$NO + O \rightarrow NO_2 + h\nu$$

giving a green continuum with luminscence duration of the order of 10^{-5} sec, and by

$$NO + O_3 \rightarrow NO_2 + O_2 + h\nu$$

giving a red continuum.

Furthermore, there is recombinational afterglow,

$$A^+ + B^- \rightarrow AB + h\nu$$

where A^+ is a positive ion, and B^- is a negative ion or electron.

A process, giving very prolonged (and correspondingly very weak) afterglow in air, is luminiscence of so-called atmospheric bands of molecular oxygen, connected with a metastable state. Its life attains 7 sec [7]. Sufficiently bright prolonged afterglow in air was observed, however, only during excitation by an electric discharge.

Spark discharge is a very simple and effective means of excitation of gas flow; however, it cannot be used at a pressure below several tens of millimeters, since with lowering of pressure the discharge loses its local character. For excitation of glow in fluxes of rarefied gas there can be used beams of artifically accelerated charged particles. The spectral composition and time of attenuation of afterglow in gasses practically do not depend on the kind of exciting particles, if only these particles are sufficiently fast [8, 9]. Apparently, the most convenient particle is the electron. Beams of artificially accelerated electrons are a very effective and flexible tool for local excitation of glow in a gas medium. The diameter of the electron beam can vary in wide limits, e.g., from 100 Å [10] to tens of millimeters. Density of current in the beam can be very great. Thus, there are obtained beams with current density of 200 amps/cm^2 [11]. The path length of the beam in gas is easily regulated by an accelerating voltage [12]. For the considered purposes very valuable also is the possibility of comparatively easy realization of modulation of the beam of electrons.

For drawing an intense beam of electrons from the vacuum, where it is formed, into the investigated gas medium there are used differential gas-dynamic* windows [13] with pump evacuation from

*For a description see S. T. Sinitsyn. Instrument for preserving a vacuum with an open reservoir aperture. Author's cert. No. 35903, class 21 d. 17, 31 March 1934.

intermediate chambers. With work which is not very prolonged the gas-dynamic window can be somewhat simplified by freezing of a special working gas.*

In examining different gases from the point of view of the given applied problems two factors are important: what is the brightness of glow and what is the duration of preservation of an excited state by the gas. Here, the considered gases can be divided into three groups:

1) gases, yielding a prolonged, bright afterglow;

2) gases, long preserving an excited state, but giving a weak afterglow;

3) gases, having a short afterglow.

Accordingly during research of gas fluxes there can be used different methods of measuring local velocity.

1.2. Method of fluorescent tracing. As an example of a gas, giving off a bright, prolonged afterglow, we can use helium. In Fig. 1 is given a photograph of a stream of helium, emerging from a nozzle with a cross-sectional diameter equal to 3 mm. In the photograph on the left the stream has subsonic velocity, on the right it is supersonic. The stream is intersected by a beam of electrons possessing an energy of 20 kev. The diameter of the beam is about 0.3 mm; current is 0.2 ma. As can

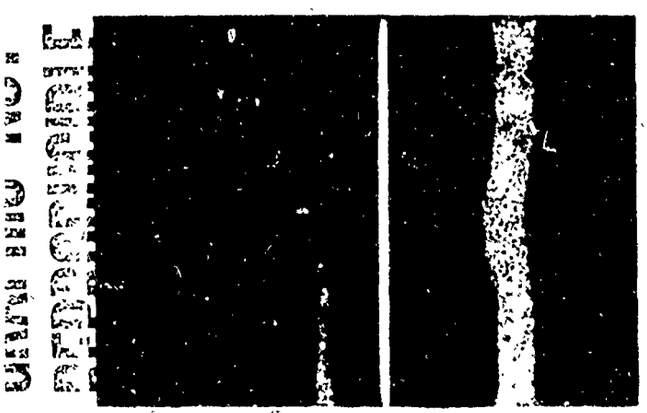

Fig. 1.

*For description see A. M. Trokhan. Method of gas-dynamic wind . , Author's cert. No. 128949, class 21 d. 35, 30 May 1959.

be seen from the photograph, from the place of intersection of the stream by the beam of electrons downstream there spreads a well-defined luminescent sheet.

The method of fluorescent tracing* consists in forming, by pulse irradiation by a narrow intense beam of fast electrons in the given region of the investigated flux, a luminescent plasma "trace." Thanks to the presence of afterglow the velocity of the trace, which is part of the flux, can be measured by optical methods by finding the time of its flight a given distance in the space of the flux. Turn to Fig. 2. Let us assume in a wind tunnel behind wall 1-1 there moves the investigated flux of gas. On the outer side of the wall there is located source 2, emitting a narrow beam of electrons 3-4, modulated in the form of short pulses. As a result of electron shocks a certain volume of gas, located along line 3-4, at the moment of passage of the current pulse starts to gleam, and there will be formed a luminescent gas column, moving together with the remaining flux. Perpendicular to the plane of the drawing there is located an optical system, consisting of objective 7 and diaphragm 8, having two small apertures. Behind diaphragm 8 is located photoelectric multiplier 9, coupled into a recording network. As a result of the presence of apertures in diaphragm 8 light reaches the cathode of the photomultiplier only

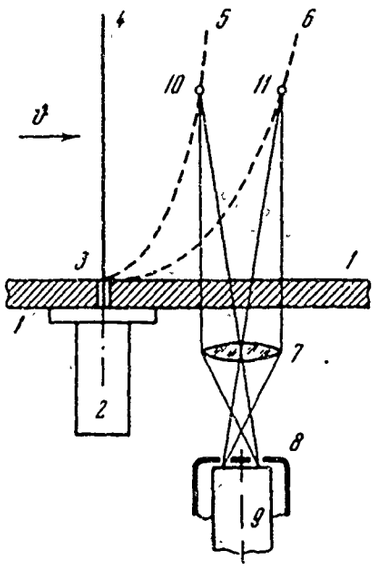

Fig. 2.

*For a description see A. M. Trokhan. Method of measuring the velocity of a gas flux. Author's cert. No. 131109, class 42o15, 30 December 1959.

from points of the flux, which are located along two straight lines, intersecting the plane of motion of the column at points 10 and 11. Thus, when the luminescent column at a certain moment of time, passing through point 10, occupies position 3-5, depending on the velocity profile, in the photomultiplier there appears a current pulse. A second pulse appears when the column, passing through point 11, occupies position 3-6. Knowing the distance between points 10 and 11 and determining the time between pulses, corresponding to moments of passage through them by the luminescent columm, we can find the average velocity of the flux along base 10-11.

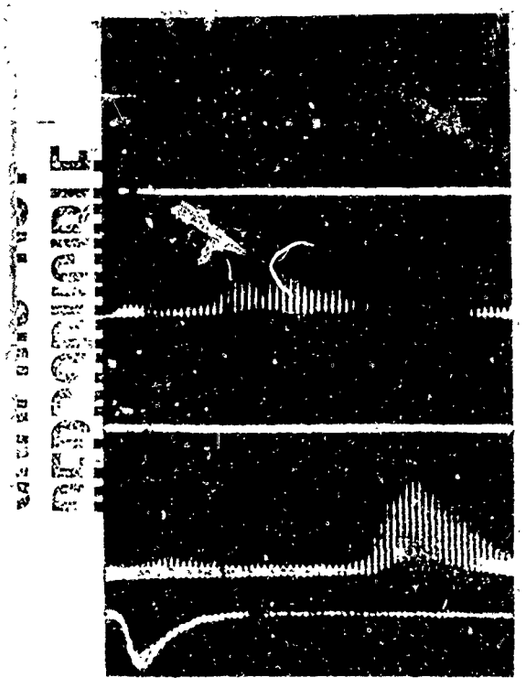

Fig. 3.

Typical oscillograms, obtained in this way, are presented in Fig. 3: in the upper part of each of the pairs of oscillograms there is given the signal from the photomultiplier; in the lower is the beam current; the value of time marks is 0.2 microseconds; width of apertures in the diaphragm is 0.4 mm (in the flux scale); the gas is helium; pressure in the chamber was 10 mm.

The upper oscillogram of Fig. 3 corresponds to a pulse value of current in the beam of 0.8 ma with accelerating voltage of 20 kv, and the middle oscillogram corresponds to a current of 0.1 ma; the base of measurement is 3 mm. As can be seen, decrease of signal level leads to the necessity of certain time-averagings of the results in view of the fluctuating nature of the signal.

As the detector in the present work we used an uncooled photomultiplier FEU-17A with objective Jupiter-3

During measurement by the given method the velocity of gas is found by determing the time of flight of the luminescent trace known distance, base L

$$L = L' \beta = L' l / l' \qquad (1)$$

Here β – image scale; L' – distance between diaphragm apertures; l, l' – distances from principal planes of the objective to conjugate planes, correspondingly to the object and to the diaphragm.

Maximum error in determining the base is determined by expression

$$\frac{\Delta L}{L} = \pm\left[\frac{\Delta L'}{L\beta} + \frac{\beta \Delta l}{(1 \mp \beta) F} + \frac{\Delta l'}{(1 \mp \beta) F}\right] \qquad (2)$$

Here F – focal length of the objective.

In the case of average accuracy of measurements maximum error in determining the base is of the order of one percent. Error can be lowered by one more order if one takes special measures, such as use of long-focal-length objectives and more precise diaphragms. Maximum error in finding the interval of time depends on the method of recording. When using a very simple method – linear oscillograph scanning – error of measurement is 1-5% depending upon the quality of the oscillograms.

Thus, maximum total error during measurement of velocity by the given method has a magnitude of the order of 2 to 6%. Let us note that perturbation of the flux by the measuring tool – the beam of electrons – is practically nonexistent, and accuracy of measurement is determined only by accuracy of determination of distance and time.

For measurement there can be used both single-channel and two-channel circuits. Application of a single-channel circuit (both signals move to one multiplier) is advisable when pulses do not overlap.

At the moment of irradiation under the action of scattered and secondary electrons a flash occurs in the whole volume of gas (intensity of flash drops approximately exponentially with distance from the beam axis); therefore, measurement of the flight time can be carried out also with a single-channel circuit with one aperture in the diaphragm.

In the lower part of Fig. 3 is given a typical oscillogram of this form. The base of measurement in this case is the distance from the axis of the beam to the investigated point.

Oscillography is the most graphic, but not always the most convenient means of measurement of flight time. In a number of cases, i.e., when the signal level is low and the Schottky effect of radiation begins to be substantial or when it is required to investigate statistical laws governing fluctuations of velocity, it is more expedient to use a delayed coincidence circuit.

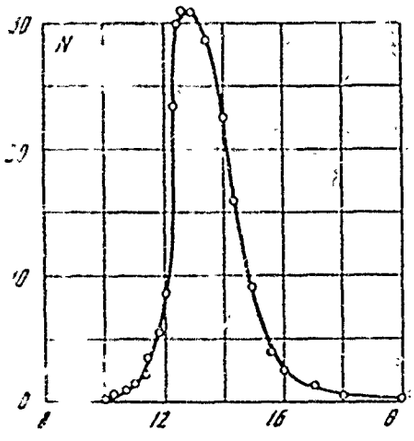

Fig. 4.

As an example, in Fig. 4 there is given the dependence of the number of coincidences of pulses in thousands of pulses per minute depending upon a delay in microseconds for two points, 9.6 mm downstream. Resolving time of the counter is 1 microsecond. The base is located along the axis of the stream. The presence of a more gentle trailing edge of the coincidences curve is caused, apparently, by the presence of a large velocity gradient along the line of observation, which is clear from Fig. 5, which gives the velocity profile in a cross section of the nucleus of the stream.

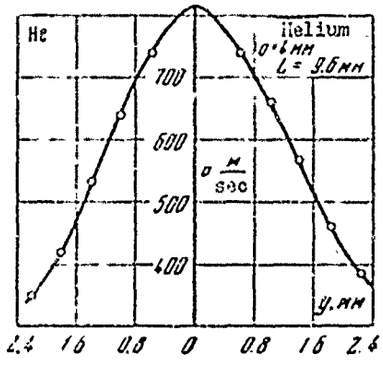

Fig. 5.

This curve is obtained with that same base of measurement L = 9.6 mm and at the same chamber pressure, equal to 4 mm, but by means of oscillographic recording.

Spatial resolution with respect to the position of the base in the space of the flux may be very high. Apparently, it is fully practicable to obtain a spatial resolution with respect to the position of the base of measurement in the space of the flux of the order of hundredths of a millimeter. Since the base is selected optically, change of its position can be realized practically as fast as one wishes, e.g., by means of introduction in the system of the necessary revolving prisms or mirrors.

Fully practicable will be obtaining of a base of measurement of the order of 1 mm or less.

The range of pressures, in which for a concrete gas we can use the given method, is determined first of all by the sensitivity of the recording system and power of the exciting beam. In our experiments with helium of industrial purity pressures varied from 0.8 to 50 mm. The lower limit was determined by sensitivity, the upper, by operation parameters of the installation. Under the considered experimental conditions the lower limit apparently can be improved by an order by means of introducing cooling of the multiplier and increasing the beam current.

Application of stroboscopic photographing of the motion of the fluorescent trace with the help of the electron-optical converters allows us to find the instantaneous velocity field in a gas flux.

1.3. Use of "blow-away" of fluorescence. In Fig. 1 on the left is given a photograph of glow, caused by a stationary electron beam, intersecting a subsonic stream of helium. Downstream from the point

of intersection by the beam there extends a tongue of luminescence. The length of the tongue is a function of a series of parameters, including velocity of the flux.

For the density of particles, excited in the moving gas medium by the electron beam, we can write the following equation:

$$\frac{\partial}{\partial x}\left(D\frac{\partial n}{\partial x}\right)+\frac{\partial}{\partial y}\left(D\frac{\partial n}{\partial y}\right)+\frac{\partial}{\partial z}\left(D\frac{\partial n}{\partial z}\right)-\frac{\partial}{\partial x_i}(nv_x)-$$
$$-\frac{\partial}{\partial y}(nv_y)-\frac{\partial}{\partial z}(nv_z)+P(x,y,z,n,N)-Q(n,N)=\frac{\partial n}{\partial t} \qquad (3)$$

Here n — density of excited particles; N — total particle density; D — coefficient of diffusion; v — velocity of the medium; P — density of xcitation (density of sources); Q — density of deactivation (density of drains).

For the very simple one-dimensional case of steady flow of an incompressible fluid, irradiated by a flat beam of electrons, assuming D = const, $n \ll N$, and also on the assumption of monomolecularness of the reaction of luminiscence, we obtain

$$D\frac{d^2n}{dx^2}-v\frac{dn}{dx}-\frac{n}{\tau}+q=0 \qquad \begin{matrix}(x<0,\ q=0)\\ (0\leqslant x\leqslant B,\ q=\text{const})\\ (B<x,\ q=0)\end{matrix} \qquad (4)$$

Here B — width of beam; q — density of excitation, τ — duration of excited state.

Solution has the following form

$$n=q\tau\frac{k_2}{k_1-k_2}(1-e^{k_1B})\,e^{k_1x} \qquad (x<0)$$
$$n=q\tau\left[\frac{k_2}{k_1-k_2}e^{k_1(x-B)}-\frac{k_1}{k_1-k_2}e^{k_2x}+1\right] \qquad (0\leqslant x\leqslant B) \qquad (5)$$
$$n=q\tau\frac{k_1}{k_2-k_1}(1-e^{-k_2B})\,e^{k_2x} \qquad (B<x)$$
$$\left(k_{1,2}=\frac{v}{2D}\pm\left(\frac{v^2}{4D^2}+\frac{1}{D\tau}\right)^{1/2}\right)$$

Thus, we have three regions of flow: region 3, irradiated by electrons; region 1, lying upstream; and region 2, lying downstream from region 3.

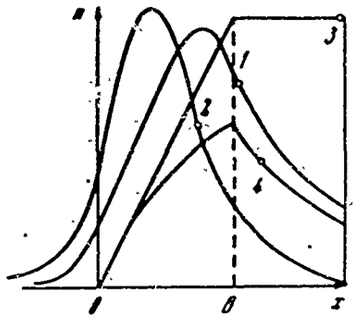

Fig. 6.

The solution is shown graphically in an arbitrary scale in Fig. 6 for the general case: (1) D, τ, $v \neq 0, \infty$; and three limiting cases: (2) $v = 0$, D, $\tau \neq 0, \infty$; (3) $\tau = \infty$, $D = 0$; $v \neq 0, \infty$; (4) $D = 0$; v, $\tau \neq 0, \infty$.

Geometrically roots k_1 and k_2 constitute quantities, the reciprocals of sections of axis x, lying in the corresponding regions, in which function $n = f(x)$ changes by a factor of e.

Experimentally, quantities $k_1 = 1/x_1$ and $k_2 = 1/x_2$ can be found easily by photometry. It is possible to write the following system, connecting three unknown magnitudes v, D, τ and the two magnitudes x_1 and x_2, found from experiment

$$v = D\frac{x_2 - x_1}{x_2 x_1}, \qquad v = \frac{1}{\tau}(x_2 - x_1) \tag{6}$$

Any additional condition, connecting unknowns or determining one of them, makes the system determinate.

Note that the velocity of the gas will, apparently, be far from the most important quantity yielded by this system. Measuring the velocity independently and finding thus the other two quantities, we probably can obtain information about the pressure and temperature of the gas.

In the conducted experiments what was said above found confirmation only qualitatively. Small dimensions of stream (3-5 mm) led to large gradients of velocity and density. The region of irradiation did not have sharp boundaries and had a rotational form, and not of a

parallelepiped. Furthermore, in view of the smallness of the investigated volume, and consequently, of the luminous fluxes, it turned out to be difficult to conduct monochromatization of radiation, as a consequence of which we measured the integral luminous flux, corresponding to different reactions. Taken together this substantially complicated calculation and hampered realization of exact quantitative measurements.

As an example of a gas, having a dim afterglow, but preserving excitation well for a prolonged time, we can use argon. For research of flows of such gases by the method of fluorescent tracing we can use an admixture to the basic gas of a certain amount of an auxiliary gas, which illuminates upon receiving excitation from the basic component. Thus, for instance, addition to argon of several percent of nitrogen sharply increases the brightness of afterglow. Adding as an admixture various gases, we can obtain afterglow in the required spectral region.

1.4. Use of luminescent probes. As a detector, perceiving excitation of gas in a fluorescent trace, we can also use usual solid phosphors, introduced in the flux by micro-probes.* The phosphor is illuminated as the result of energy transfer either when excited atoms, molecules, or ions strike it, or as the result of absorption of quanta of vacuum ultraviolet radiation, suspended in the gas. Here, the efficiency of the phosphors turns out to be very high. Thus, the quantum yield of willemite for shortwave radiation is greater than unity, constituting, for instance, during irradiation by light with λ = 1850 A a quantity of the order of 2-3 [14].

The very fact of use of a mechanical probe is undesirable in view of the inevitable perturbation of the flux. However, as compared

*For a description see A. M. Trokhan. Device for measurement of the velocity of a gas flux, Author's cert. No. 141018, class 42o15, 15 September 1960.

to other probe methods this method has this merit, that the dimensions of probe are minimal, measurement is absolute, and the base of measurement is located higher up the flux relative to the probe. Thanks to increase of signal level use of luminescent probes will allow us, apparently, to expand the area of applicability of fluorescent tracing in the direction of low pressures and small velocities of flow. In Fig. 7 there is given an oscillogram, obtained by a probe, covered with willemite, in a stream of argon.

Fig. 7.

For measurement of the velocity of gases with short afterglow one can use the Doppler shift of spectral lines. Determination of the Doppler shift is rather widely used for finding the velocity of fast fluxes of gas [15, 16]. Here, they use either natural radiation of the gas, or the glow of a specially introduced admixture, most frequently sodium. This method is applied only for gases whose temperature is sufficiently high for thermal excitation of radiation, or for gases directly in the area of electric discharge. The velocity found by them, will be a certain average magnitude for the flux along the line of observation, where error due to averaging may be very great.

1.5. Doppler shift of spectral lines. Use of a beam of fast electrons for excitation of local glow in a gas flux allows us to apply the Doppler shift method to research of fluxes of both weakly-luminescent, and also nonluminous cold gases.* Here it turns out to be

*For a description see A. M. Trokhan. Device for determining the velocity of gas. Author's cert. No. 134495, class 42o15, 29 February 1960.

possible to measure the local velocity of gas with the smallest possible spatial averaging.

A diagram of the instrument for measurement of local flux velocity by Doppler shift of spectral lines of radiation, caused by a beam of fast electrons, is shown in Fig. 8. Beam of electrons 1, emitted by electron gun 2, is introduced through the wall of wind tunnel 3 in the investigated region of the flux. Light, emitted by region 4, through objectives 5 and 6 and lightguide 7 moves to a spectrograph or monochromator 8.

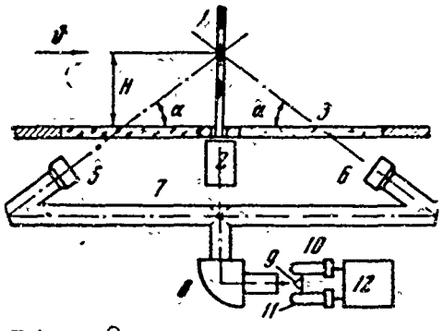

Fig. 8.

Here, light, emitted by region 4, strikes objective 5 at an angle α against the flux, and strikes objective 6 at an angle α with the flux. As a result radiation, passing through these two channels, should be shifted magnitude

$$\Delta\lambda = 2\lambda \frac{v}{c} \cos\alpha \qquad (7)$$

Here λ — wavelength of spectral line; v — velocity of the flux; c — velocity of light.

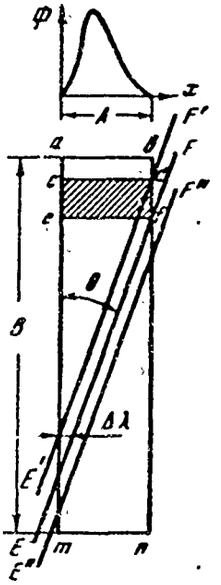

Fig. 9.

Leaving spectrograph 8 radiation of the given spectral line strikes a light-dividing wedge 9 and then proceeds to photomultipliers 10 and 11. Unbalancing of the multiplier, caused by displacement of the spectral line, is fixed by recording device 12.

The principle of recording shift of the wavelength of the spectral line is explained by Fig. 9. Let us assume that the image of spectral line in the plane of the exit slit of the monochromator is bounded by parallel lines ab and mn. Let us assume also that $\Phi(x)$ — the

distribution of intensity in cross section of the line — has a form which is arbitrary, but constant in all the height. The exit slit does not pass adjacent lines of radiation, and also does not cut off the investigated line. Width of the exit slit here is equal to A + 2Δx, where Δx is a quantity intentionally chosen larger than the magnitude of displacement of wavelength under the given conditions of the experiment. At an angle θ to the axis of the line there is fixed a light-dividing wedge with face EF. The whole luminous flux, passing through the plane of the exit slit above line EF, strikes one enlarger; the whole luminous flux, passing below EF strikes the other. Both multipliers have the same gain factor. Let us assume that at a certain moment we have radiation from a gas, not moving in the direction of the line of observation. We set EF in such a way that the luminous fluxes above and below the light-dividing wedge are equal:

$$\iint_{abjh} \Phi(x)\,ds = \iint_{hjnm} \Phi(x)\,ds = \frac{1}{2}\iint_{abnm} \Phi(x)\,ds = \frac{1}{2}\Phi \qquad (8)$$

Here Φ is the total luminous flux.

Let us assume now that as a result of motion of the medium the line is shifted along the x-axis a magnitude dΔλ. This is equivalent to line EF, with line Φ(x) fixed, shifting in height a distance $d\lambda/\mathrm{tg}\,\theta$, occupying position E'F'. The magnitude of luminous flux, passing in the channel, will vary here by magnitude

$$\Delta\Phi = \iint_{cdef} \Phi(x)\,ds = \frac{d\Delta\lambda\Phi}{B\,\mathrm{tg}\,\theta} \qquad (9)$$

Here d is linear dispersion of the spectrograph.

Thus, if glow of the gas medium is observed alternately, first with the flux, and then against it, the corresponding photocurrents of the multipliers will differ by the following magnitude:

$$I_1 - I_2 = 2\frac{d\lambda}{c}\,\frac{\cos\alpha}{\mathrm{tg}\,\theta}\,\frac{\Phi\gamma}{B}\,v = \mathrm{const}\;v \qquad (10)$$

Here γ — integral sensitivity of the multiplier. The result does not depend on the width and form of the spectral line. Difference of currents is greater, the less angle θ; however, here it is necessary that, shifting, line EF intersects only the lateral face of rectangle abnm. Absolute error in determination of velocity by Doppler shift of spectral lines constitutes 15-30 m/sec [15, 17]. Thus, the method can be used with success for measurement of high velocities. In Fig. 10 we give the spectrum of glow of industrial helium, argon and air (from top to bottom). Below is given the spectrum of an iron arc. Characteristically almost all the energy of radiation of air in the visible range was apportioned to one band of the molecular ion of nitrogen.

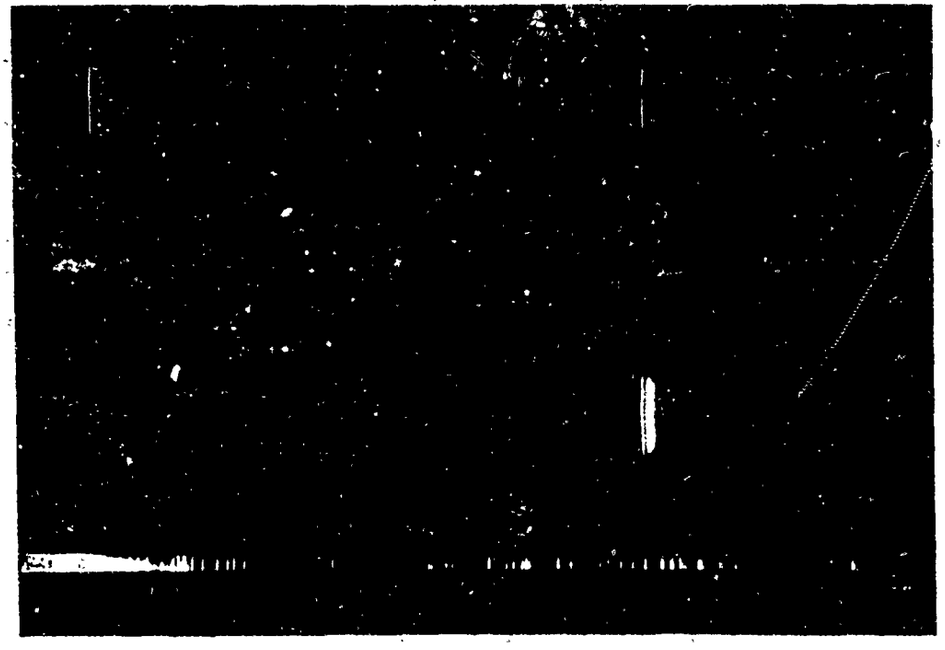

Fig. 10.

For recording it is also possible to use a Fabry-Perot etalon united, when necessary, to fast recording with an image converter. Since glow occurs in cold gas, Doppler broadening is minimal. At low pressures Stark broadening also is small. In view of this Doppler

shift can be measured with high accuracy.

2.0. Measurement of local density of a gas. Measurement of local density of rarefied gas can be realized by recording the glow, emitted by the gas under the influence of electronic impacts [18, 19]. During emanation of definite spectral lines the intensity of radiation emitted per unit volume of gas, other things being equal, turns out to be proportional to the local density of the gas.

Deficiencies of this method are:

1) Intensity of visible radiation, emitted by a given volume of gas, with identical conditions of irradiation depends not only on the density, but also on the temperature of the gas, which is caused by the presence of processes of quenching of fluorescence, which depend on temperature [20];

2) Measurements can be made only in the absence of natural radiation of the gas, and also in the absence of any outside sources of light, i.e., the method only is useful for research of cold fluxes.

In the present work there is considered the possibility of using x-radiation for determining the local density of gas emitted during slowing-down of fast electrons by it.

Measurement of the integral intensity of radiation, conducted by a gas-discharge counter through a mica window, showed that in wide limits there exists a linear dependence of the intensity of radiation on gas density.

In Fig. 11 are photographs of x-radiation in an argon medium at pressures, equal to 0.85, 1.7, 3.4, and 6.8 mm, excited by a beam of electrons with beam current of 0.7 ma and accelerating voltage 25 kv. Minimum exposure was 15 minutes. Exposure time was inversely proportional to pressures. Photometry of negatives showed that here within

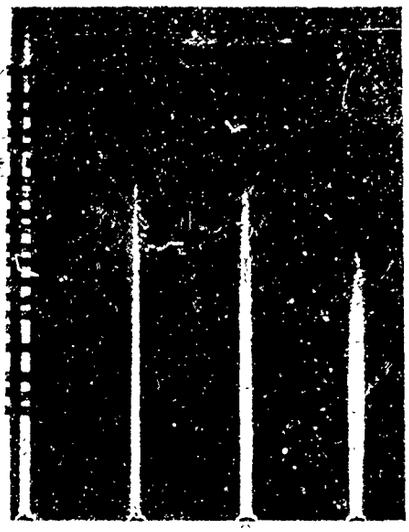

Fig. 11.

the limits of accuracy of the experiment blackening in the region of entrance of the beam into the gas is identical. For photographing we used a camera obscura, having a hole of diameter 0.2 mm in a lead shield, coated with aluminized mica. Distance from the screen to the beam axis was 100 mm. Photographing was on X-ray film of type RF-3. As can be seen from these photographs, brightness of radiation changes with distance from the place of entrance of the beam into the gas. However, if the density of gas is sufficiently low (accelerating voltage is sufficiently great), these changes are small. If in the path of the beam there are regions of increased or lowered density of the gas, these changes of density cause corresponding changes of local brightness of the X-ray glow.

Fig. 12.

Thus in Fig. 12 there is presented a photograph of a 25 kv beam of electrons intersecting a thin (diameter of approximately 3 mm) stream of argon at a pressure of 5 mm. In Fig. 3 the point of intersection is distinctly visible. The glow in the upper part of the photograph is caused by the impact of electrons on the surface of a copper collector. Brightness of the X-ray glow depends both on the kind of gas and its density, and on the power of the electron beam.

For diagnostic purposes it is expedient to use low-power beams; therefore, it is necessary to apply the most sensitive radiation detectors. In Fig. 13 is a diagram of one possible device for

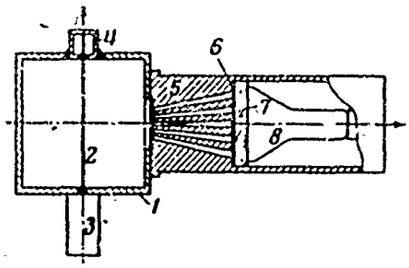

Fig. 13.

measuring gas density. Into chamber 1, containing the investigated gas flux, there is introduced a beam of fast electrons 2, emitted by electron gun 3 and trapped by collector 4. With the help of X-ray unit 5, consisting of a thick diaphragm with holes in the form of cones having a common vertex on the beam axis, from the whole volume, irradiated by electrons, there is separated a small region, radiation from which, passing through diaphragm 6, opague to visible light, reaches scintillator 7. Radiation of the scintillator is recorded by photomultiplier 8.

The described method of measurement can be used both for research of pulsations of gas density in a given region, and for measurement or visualization of density fields. Natural radiation of gas or light from outside sources does not affect results of measurements.

For research of unsteady flows it is necessary to use more powerful beams of electrons, and to photograph with the help of image converters.

3.0. Visualization of flows. Usual methods of visualization of flows of gas, using an interferometer, shadow and schlieren photography, turn out to be unfit for research at pressures below several mm. Therefore, for visualization of fluxes of rarefied gas we use either the afterglow evoked by a high-frequency discharge [21], the glow discharge directly in the investigated region [22], or absorption of ultraviolet radiation [23].

All these methods allow us to visualize the flux as a whole; to study the "fine" structure of the flux turns out to be difficult, with the exception of certain particular cases. The fact is that

all the methods are integrated, i.e., glow or absorption of light by a given region of a flux is part of the glow or absorption along the whole line of observation. If the region is small, then the share introduced by it to the overall quantity is small. This makes results more crude, and raises uncertainty about interpretation of them.

Use of beams of fast electrons allows us to solve this very important problem. Depending upon the duration of afterglow the solution may differ.

If we introduce a nonmodulated thin beam of fast electrons into a gas flux, possessing prolonged afterglow, downstream from the irradiated region there will spread a solid luminescent sheet. Afterglow in streams of a gas, irradiated by a beam of electrons, was first observed in [24]. Photographing the sheet, we can find the flow surface, passing through a given line (axis of the beam).

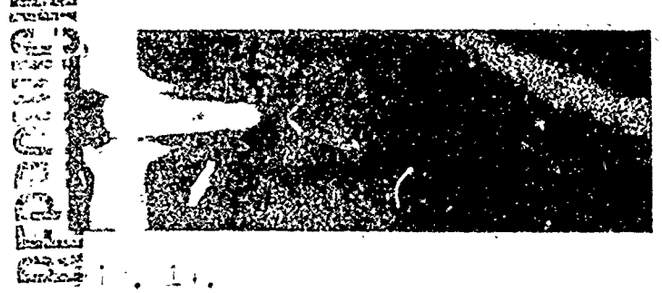

Fig. 14.

If we have two beams crossing in the flux, corresponding photography will allow us to find the spatial position of the flow line, passing through the point of intersection of the beams. Local brightness of the sheet of afterglow is a function of local density. Brighter regions correspond to denser gas. This allows us to visualize flow in the given flow surface. In Figs. 14-16 are examples

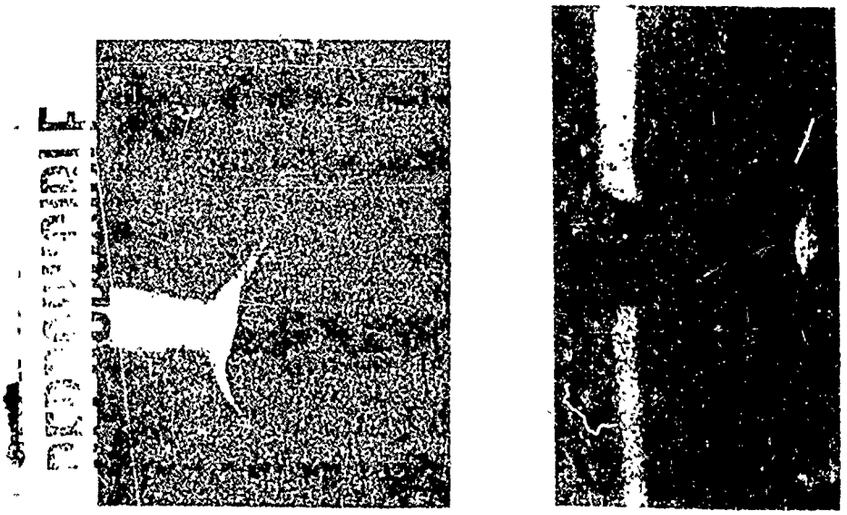

Fig. 16.

of visualization of flow past very simple models by a stream of helium: a wedge, a cylinder and a flat wall, normal to the flux. This method allows us to determine position of shock waves, the thickness of the boundary layer, the region of separation of the flow, etc. It should be noted that in the given method of research only visualization is possible; quantitative determination of local density, apparently, is impossible inasmuch as local brightness depends not only on local density, but also on change of density along the flow line from the point of excitation of glow to the considered one, i.e., on the prehistory of the flow.

This method is unsuitable for research in air, or in other gases which have weak afterglow. For visualization in this case we can use a flat beam of electrons. Since under identical conditions of irradiation the brightness of glow of gas inside the irradiated region is a linear function of density [18], it turns out to be possible not only to obtain visualization of the field of densities, but also to find its exact quantitative values. The beam can be arbitrarily oriented to the flow; therefore, it turns out to be possible to investigate the field of densities in any given plane of the flow.

3.1. Visualization by scanning of the beam. Introduction of flat beam in a gas is more difficult than introduction of a thin circular beam; in the present work we used a scanning beam. Scanning of the beam in the plane, parallel to the axis of flow, was carried out with the help of a small electromagnet, located at the entrance of the beam into the gas medium. The field strength was varied by sinusoidal law. In Fig. 17 is an example of visualization of flow, thus obtained. If

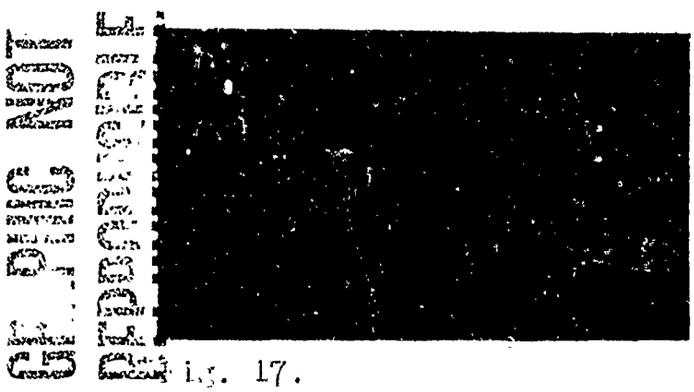

Fig. 17.

we need quantitative results, it is expedient to photograph in X-rays. To obtain quantitative values sinusoidal scanning is inconvenient. To ensure uniformity of the velocity of the beam, intensity of the deflecting field should change by sawtooth law.

The author is thankful to S. A. Khristianovich for attention paid to this work.

Submitted
17 December 1963

Literature

1. L. Glenn and Mellen. Gas-Flow Speedometer. Electronics, 1950, Vol. 23, No. 2, 80-81.

2. W. Kunkel and L. Talbot. Ion tracer technique for air speed measurements at low densities. NACA TN, 1954, No. 3177, 31 pp.

3. N. M. Baryshova and V. N. Ushakov. Measurement of the velocity of a stream, passing from the nozzle of a high-vacuum pump. PTE, Publishing House of Academy of Sciences of USSR, 1959, No. 5, 94-98.

4. J. Berkowitz, W. A. Chupka and G. B. Kistiakowsky. Mass-Spectrometric study of the kinetics of nitrogen afterglow. J. Chem. Phys., 1956, 25, No. 3, 457-466.

5. W. A. Kunkel. Short afterglow in nitrogen. Phys. Rev., 1953, Vol. 92, 534.

6. N. A. Kaptsov. Electrical phenomena in gasses and a vacuum. Energoizdat, 1950.

7. V. N. Kondrat'yev. Kinetics of chemical gas reactions. Publishing House of Academy of Sciences of USSR, 1958.

8. A. E. Grün. Die Fluoreszenz von Gasen bei der Abbremsung schneller Teilchen. Z. Naturforschg., 1954, 9a, 55-63.

9. C. Y. Fan. Emission spectra excited by electronic and ionic impact. Phys. Rev., 1956, Vol. 103, No. 6, 1740.

10. M. P. Davoine. Étude d'une sonde électronique fine Applications. J. Phys. et radium, 1954, 15, No. 12, 90-91.

11. G. R. Brewer. Formation of high-density electron beams. J. Appl. Phys., 1957, 28, No. 1, 7-15.

12. A. E. Grün. Lumineszenz-photometrische Messungen der Energieabgabe im Strahlungsfeld von Elektronenquellen Eindimensionaler Geometrie. Z. Naturforschg., 1957, 12a, No. 2, 89-95.

13. F. Schumacher. Dynamische Druckstufenstrecken für den Einschuss intensiver, monokinetischer Korpuskularsrahlbündel in Gase hohen Drucks. Optik, 1953, 10, 116-131.

14. F. A. Putayeva and V. A. Fabrikant. Sensitivity of phosphors for luminescent tubes in shortwave ultraviolet radiation. News of AS of USSR, Ser. Physics, 1957, 21, No. 4, 541-543.

15. S. E. Frish and Yu. M. Kagan. Spectroscopic study of the motion of ions in plasma, Journal of exper. and theor. physics, 1947, 17, No. 6, 577-584.

16. F. P. Bundy, H. M. Strong and A. B. Gregg. Measurement of velocity and pressure of gases in rocket flames by spectroscopic methods. J. Appl. Phys., 1951, 22, No. 8, 1069-1077.

17. J. A. Fusca. Speedometer proposed for space vehicle. Aviat. Week, 1950, 70, No. 25, 201-217.

18. A. E. Grün. On the fluorescence of air, excited by fast electrons, Canadian J. Phys., 1958, 36, No. 7, 858-862.

19. B. W. Schumacher and E. O. Gadamer. Electron beam fluorescence probe for measuring the local gas density in a wide field of observation. Canadian J. Phys., 1958, Vol. 36, No. 6, 659-671.

20. A. E. Grün and E. Schopper. Die Untersuchung von Energieaustausch – und Löschprozessen in Gasen durch Anregung mit schnellen Teilchen. Z. Naturforschg., 1954, 9a, No. 2, 134-147.

21. Kunkel and Hurlbat. Luminescent visualization of a flow in low pressure wind tunnels. Problems of rocketry, IL, 1958, No. 3.

22. H. J. Pomelburg. A new glow-discharge method for flow visualization in supersonic wind tunnels. J. Aero/Space Sci., 1958, 25, No. 11, 727-728.

23. Evans. New method of visualization in low density wind tunnels. Problems of rocketry, IL, 1958, No. 4.

24. A. E. Grün. Einige gasdynamische und spektroskopische Beobachtungen an angeregten Gasstrahlen. Z. Naturfroschg., 1954, 9a, No. 10, 833-836.

DETERMINING DENSITY FIELDS OF THREE-DIMENSIONAL GAS-DYNAMIC FLOWS ON THE BASIS OF OPTICAL METHODS

S. M. Belotserkovskiy, V. S. Sukhorukikh and V. S. Tatarenchik

(Moscow)

There are given certain results of research of three-dimensional gas-dynamic flows by optical methods. Integral values of density are determined directly, and local values are found from integral equations. In these equations density is a function of three space coordinates. One of the coordinates plays the role of the parameter. If from density, as a function of two coordinates, we can pass by some means to a dependence on one variable, the considered relationships will be ordinary integral equations. Such a transition is obvious in the case of flat and axisymmetric distribution of density.

For the shown reason in experimental gas dynamics optical methods up to now have been applied only for study of flat and axisymmetric flows [1]. The authors proposed a method of research of three-dimensional gas-dynamic flows on the basis of quantitative optical methods [2]. Its essence is as follows.

On the basis of preliminary information we select approximating functions, which describe the field of densities, including also the form of the surface of discontinuity. For determination of approximating functions there are used results of interference or shadow measurements, obtained for different directions of movement of light rays through the gas flux. The necessary quantity of directions depends on the form of investigated flow and is established in the process of research.

Designations

ρ_0 — density of gas in normal conditions;

n_0 — index of refraction of the gas in normal conditions;

ρ_∞ — density of gas in an undisturbed flux;

p — pressure on the surface of the body;

p_∞ — pressure of the undisturbed flux;

M — Mach number

α — angle of incidence;

ω_k — angle of half-aperture of the cone;

λ — wavelength of light;

λ_{max} — wavelength of light at maximum transmission of interference light filter;

$\Delta\lambda$ — half-width of transmission band of interference light filter.

§ 1. Basic relationships. In Fig. 1 is depicted one section of the investigated gas flux. The perturbed region is included between the contour of the body (1) and the external boundary (2). In supersonic flows this external boundary is a forward shock. The velocity of undisturbed flow is perpendicular to the plane of the drawing, and incident rays are parallel to it.

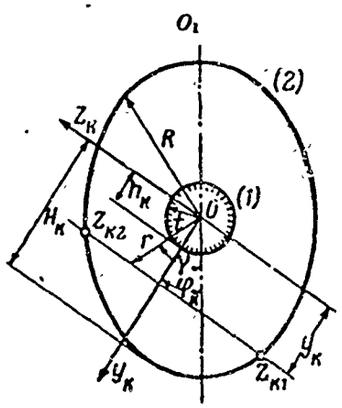

Fig. 1.

We introduce rectangular system of coordinates Oxy_kz_k, whose x-axis is directed along the velocity of undisturbed flow; axis z_k is directed along incident rays. By φ_k we designate the angle between a certain fixed plane OO_1 and axis y_k. In the given direction of radioscopy we obtain experimental data, corresponding to angles φ_k and $\varphi_k + \pi$, since change of the direction of rays to the opposite does not change the result.

These data are different, if axis z_k does not coincide with the plane of symmetry.

The contour of the body in the considered section x = const is described by equation $t = t(\gamma)$; the contour of the external boundary is given by equation $R = R(\gamma)$. The current point is defined by coordinates r and γ. By h_k and H_k we designate maximums of coordinate y_k on the contour of the body and on the external boundary.

Consider some ray, entering the perturbed region at a point with coordinates y_k, z_{k1}. Disregarding distortion of the ray, we take for its path in the perturbed region chord y_k = const. The point of departure of the ray from the perturbed region has coordinate y_k, z_{k2}.

Results of interference measurements will be distributions of functions $m_k(x, y_k)$, which express change of the optical path length of light passing through the perturbed region. Functions m_k are connected with the distribution of density along the light ray by relationship

$$\int_{z_{k1}}^{z_{k2}} (\rho^* - 1)\, dz_k = \varepsilon_k m_k (y_k)$$

$$\left(\rho^* = \frac{\rho}{\rho_\infty},\ \varepsilon_k = \frac{\rho_0 \lambda}{\rho_\infty (n_0 - 1)}\right) \qquad (1.1)$$

Here λ — wavelength of light; ρ_0, n_0 — density and index of refraction of gas in normal conditions; ρ_∞ — density in an undisturbed flow.

The result of shadow measurements will be changes $\Delta(dx/dz_k)$ and (dy_k/dz_k) of directions of light rays passing through the perturbed region. These magnitudes are connected as follows with distribution of components of the density gradient along the light ray:

$$\int_{z_{k1}}^{z_{k2}} \frac{\partial \rho^*}{\partial x} dz_k = (\mu_k + \rho_2^*)\,\Delta\left(\frac{dx}{dz_k}\right) + \left(\frac{dx}{dz_k}\right)_1 (\rho_2^* - \rho_1^*)$$

$$\int_{z_{k1}}^{z_{k2}} \frac{\partial \rho^*}{\partial y_k} dz_k = (\mu_k + \rho_2^*)\,\Delta\left(\frac{dy_k}{dz_k}\right) + \left(\frac{dy_k}{dz_k}\right)_1 (\rho_2^* - \rho_1^*) \qquad (1.2)$$

$$\int_{z_{k1}}^{z_{k2}} \frac{\partial \rho^*}{\partial z_k} dz_k = \rho_2^* - \rho_1^* \qquad \left(\mu_k = \frac{\rho_0}{\rho_\infty (n_0 - 1)}\right)$$

Here ρ_1^*, ρ_2^* – values of ρ^* at points of entrance and exit of the ray from the region.

§ 2. Solving integral equations. Let us turn to a cylindrical system of coordinates with the same direction of the x-axis and polar coordinates r, γ in plane x = const.

Density in the section x = const is considered a function of polar angle γ and a dimensionless radial coordinate

$$\xi = \frac{r - t}{R - t} \qquad (2.1)$$

On the body surface $\xi = 0$; on the boundary of the perturbed region $\xi = 1$. For definitiveness we assume that OO_1 is the plane of symmetry of the flow. We present periodic continuous dependence of density on the angle in the following form:

$$\rho(\xi, \gamma) = \sum_{m=0}^{q_\rho - 1} \rho_m(\xi) \cos^m \gamma \qquad (2.2)$$

Contours of the external boundary of the perturbed region and of the body in section x = const are approximated by expressions of the same type:

$$R(\gamma) = \sum_{m=0}^{q_R - 1} R_m \cos^m \gamma$$

$$t(\gamma) = \sum_{m=0}^{q_t - 1} t_m \cos^m \gamma \qquad (2.3)$$

where R_m and t_m — coefficients, determined according to measurements H_k and h_k.

The highest degree of polynomials (2.2) and (2.3) is selected in accordance with the expected character of the approximated functions; in process of treatment these numbers can be modified and definitized.

We designate by q the number of different measurements, determined by angles φ_k. If the z_k-axis does not coincide with the plane of symmetry of flow,

$$q = 2u$$

where u — number of directions of radioscopy. With coincidence of one of the directions of radioscopy with the plane of symmetry,

$$q = 2u - 1$$

Number q should not be less than the largest of numbers q_ρ, q_R, q_t. Substitution of expansions (2.2) and (2.3) in relationships (1.1) and (1.2) leads to system of integral equations for functions $\rho_m(\xi)$ or their derivatives.

For interference method when $q = q_\rho$ we have

$$\sum_{m=0}^{q_\rho - 1} \int_{z_{k1}}^{z_{k2}} \rho_m(\xi) \cos^m\gamma \, dz_k = z_{k2} - z_{k1} + \varepsilon_k m_k(\zeta)$$
$$\zeta = \frac{y_k - h_k}{H_k - h_k} \qquad (k = 1, 2, \ldots, \eta) \qquad (2.4)$$

System of integral equations (2.4) is solved numerically by means of division of range $0 \leq \xi \leq 1$ by dividing points ξ_i at N small intervals, within limits of which functions $\rho_m(\xi)$ are replaced by constants ρ_{mi}.

As a result of this the system of integral equations is turned into a system of linear equations for unknowns ρ_{ms}

$$\sum_{m=0}^{q-1} a_{ms}^{ks}\rho_{ms} =$$

$$= \Phi_{ks} - \sum_{i=1}^{s-1}\sum_{m=0}^{q-1} a_{mi}^{ks}\rho_{mi}$$

$$\begin{pmatrix} k = 1, 2, \ldots, q \\ s = 1, 2, \ldots, N \end{pmatrix} \qquad (2.5)$$

Here s is the largest odd number i for y_k = const.

When $q > q_\rho$ system (2.5) in accordance with the method of least squares takes form

$$\sum_{m=0}^{q_\rho-1} \rho_{ms}\left(\sum_{k=1}^{q} a_{ms}^{ks}a_{ns}^{ks}\right) =$$

$$= \sum_{k=1}^{q} \Phi_{ks}a_{ns}^{ks} -$$

$$- \sum_{i=1}^{s-1}\sum_{m=0}^{q_\rho-1} \rho_{mi}\left(\sum_{k=1}^{q} a_{mi}^{ks}a_{ns}^{ks}\right)$$

$$(n = 0, 1, \ldots, q_\rho - 1) \qquad (2.6)$$

Calculations were done on a digital computer. Details of calculations are not considered here.

§ 3. Examples. Results of determination of the field of densities near a cone with half-angle ω equal to 15° with an angle of incidence $\alpha = -7.5^\circ$ and values of Mach number M = 3.5 and M = 4.2 are given.

The experimental part of the work was executed on a four-mirror Mach-Zehnder interferometer with field of view 225 mm. As the light source we used a spark discharge between cadmium electrodes. Interference pictures were photographed simultaneously in white and in monochromatic light. Photographs in white light were used for measurement of the whole part of change of optical path length, expressed in the wavelength of light. To obtain photographs in

monochromatic light we applied an interference light filter (λ_{max} = = 644 mμ, $\Delta\lambda$ = 5 mμ).

The experiment was conducted for three and five values of angle φ_k(q = 3 and q = 5). Change of angle φ_k was carried out by turning the model about an axis, parallel to the velocity of the undisturbed flow. Data for angles φ_k and $\varphi_k + \pi$ were obtained in one blowing with a fixed position of the model. Values of q turned out to be odd due to the fact that one of the values of φ_k was equal to 1/2 π, and the flow had a plane of symmetry.

The obtained photographs in monochromatic light for M = 3.5 are presented in Figs. 2, 3, and 4. To them the correspond angles φ_k, equal to 0 and π (Fig. 2), (1/4)π and (3/4)π (Fig. 3) and (1/2)π (Fig. 4).

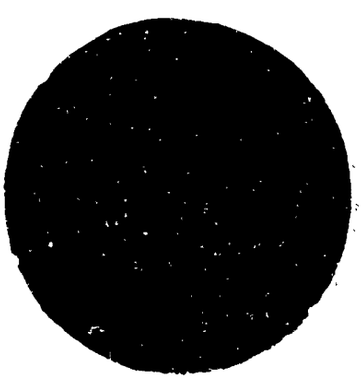

Fig. 2.

Fig. 3.

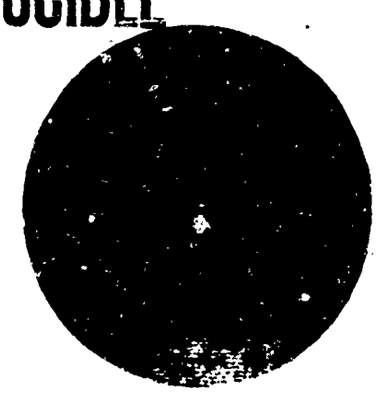

Fig. 4.

Results of analysis of the experiment by the above method are presented in Figs. 5 and 6 in the form of dependence $\rho/\rho_\omega = \rho^*(\xi, \gamma)$. Ray γ = 0 is located on windward side of the flow. Experimental values of ρ^* are given by points, and solid lines show results of numerical calculation of density according to method of [3]. Every curve has its own origin of coordinates with the same index as the number of the curve. The reading unit along the axis of ordinates is

is marked by a brace.

Experimental data in Fig. 5 correspond to values M = 3.5, q = 5 in Fig. 6 we have values M = 4.2 and q =3. Number of intervals N, into which the range $0 \leq \xi \leq 1$ is divided, in both cases was equal to 20. Due to this relationships (2.5) for the first case were reduced to 20 systems of 5 equations; for second they were reduced to 20 systems of 3 equations.

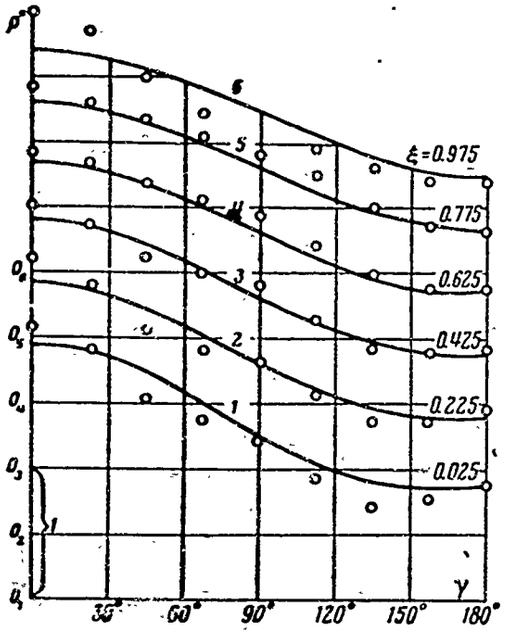

Fig. 5.

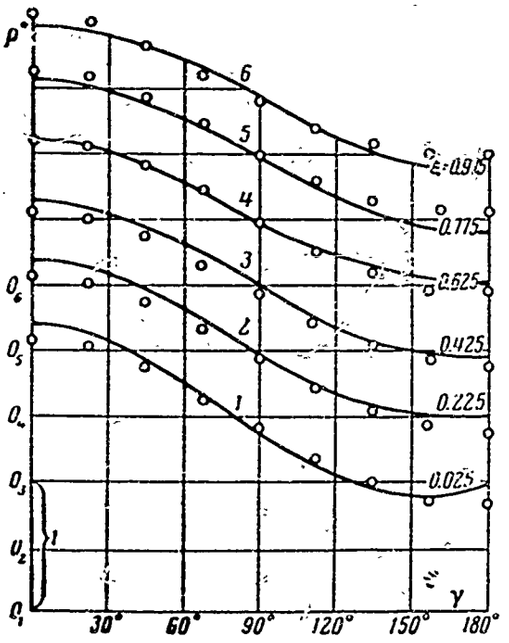

Fig. 6.

From the given data it is clear that during determination of density near a cone, flowed past at a small angle of incidence, it is possible to limit oneself to number q = 3.

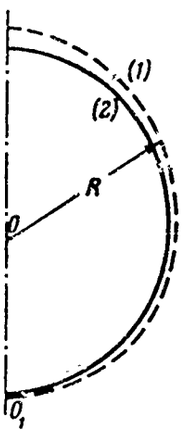

Fig. 7.

The shape of the shock wave for M = 3.5 is shown in Fig. 7. Curve (1) corresponds to the considered experiment; curve (2) is obtained by the method of [3].

In Fig. 8 are given results of recalculation of density in pressure p on the surface of the body ($\xi = 0$), on the assumption that on surface of the cone entropy function $\$^{\varkappa} = p/\rho^{\varkappa}$ is constant and is equal to its value on the windward side of the shock wave front. Pressure on the

undisturbed flux is designated p_∞; M = 3.5.

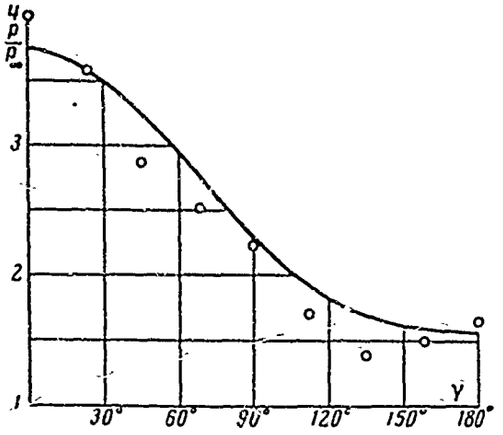

Fig. 8.

Submitted
29 February 1964

Literature

1. Physical measurements in gas dynamics and during burning, IL, 1957.

2. S. M. Belotserkovskiy, V. S. Sukhorukikh, and V. S. Tatarenchik. Research in three-dimensional gas-dynamic flows on the basis of quantitative optical methods. Report to Second All-Union Conference on Theoretical and Applied Mechanics. Annotations of reports, Academy of Sciences of USSR, 1964.

3. K. I. Babenko and G. P. Voskresenskiy. Numerical method of calculating three-dimensional flow past bodies by a supersonic flux. Journal of computer mathematics and mathematical physics, 1961, Vol. 1, No. 6.

ON MECHANISMS OF DISINTEGRATION OF A DROP MOVING IN A GAS FLOW

V. A. Borodin, Yu. F. Dityakin, and
V. I. Yagodkin

(Moscow)

In work [1] there was an attempt at theoretical study of unstable axisymmetric forms of perturbations of a spherical drop of an ideal fluid, flowed past by a flux of another ideal fluid, leading to its disintegration. For solution of this problem there was used the method of small perturbations.

We found the critical valuesof the Weber number and also forms of neutral perturbations. Below there is considered the case of increasing perturbations, and also their form for different values of the Weber number.

According to Rayleigh's hypothesis, of all possible forms of increasing perturbations, in reality there is realized the form having the biggest value of increment $Z = -a^3\rho_1\beta^2/T$, where a — radius of the drop, ρ_1 — density of the fluid of the drop, T — coefficient of surface tension, β in the given problem is the purely imaginary frequency of oscillations [1]; therefore, for determining the form of perturbation for a given value of Z from the equation of eigenvalues one should find the least value of the Weber number $W = \rho_2 aU^2/T$, since the values of Z monotonically increase with growth of W; here ρ_2 — density of the medium, U — relative velocity of the drop.

In [1] there is obtained the system of equations

$$a_n = \alpha_n a_{n-2} + \beta_n a_{n+2} \qquad (n=0, 1, 2, \ldots) \tag{1}$$

where

$$\alpha_n = -\frac{c_{n,\,n-2}}{c_{n,\,n}}, \qquad \beta_n = -\frac{c_{n,\,n+2}}{c_{n,\,n}}$$

$$c_{n,n} = Z + R_n - A_n W, \qquad c_{n,\,n-2} = C_{n-2} W, \qquad c_{n,\,n+2} = B_n W, \tag{2}$$

$$A_n = \frac{1}{2}\,\frac{n^2(n+1)(2n^2+n-2)}{(4n^2-1)(2n+3)}, \qquad C_{n-2} = \frac{9}{4}\,\frac{(n-1)^2(n-2)^2}{(2n-1)(2n-3)}$$

$$B_n = \frac{9}{4}\,\frac{(n+1)(n+2)^2(n+3)}{(2n+3)(2n+5)}, \qquad R_n = n(n-1)(n+2)$$

from which, after eliminating constants, we obtain an equation for eigenvalues of the problem.

System of equations (1) disintegrates into two systems:

$$\begin{array}{ll}
n = 2k \quad (k = 1, 2, \ldots), & n = 2k+1 \quad (k = 0, 1, 2, \ldots) \\
a_2 = \beta_2 a_4, & a_1 = \beta_1 a_3 \\
a_4 = \alpha_4 a_2 + \beta_4 a_6, & a_3 = \alpha_3 a_1 + \beta_3 a_5 \\
\ldots\ldots\ldots\ldots & \ldots\ldots\ldots\ldots \\
a_{2k} = \alpha_{2k} a_{2k-2} + \beta_{2k} a_{2k+2}, & a_{2k+1} = \alpha_{2k+1} a_{2k-1} + \beta_{2k+1} a_{2k+3}
\end{array} \tag{3}$$

The equation, corresponding to k = 0, can be rejected, since $\alpha_2 = 0$, and the equation of nodal lines on the perturbed drop surface does not include a_0. The remaining coefficients are defined simply in terms of a_2.

We introduce designations

$$\frac{a_{2k+1}}{a_1} = \alpha_3\alpha_5 \ldots \alpha_{2k+1}s_{2k+1}, \qquad \gamma_{2k+1} = \alpha_{2k+1}\beta_{2k-1} \qquad (k = 0, 1, 2, \ldots)$$

$$\frac{a_{2k}}{a_2} = \alpha_4\alpha_6 \ldots \alpha_{2k}s_{2k}, \qquad \gamma_{2k} = \alpha_{2k}\beta_{2k-2} \qquad (k = 1, 2, 3, \ldots) \tag{4}$$

Then we present system (3) in the following form:

$$\begin{array}{ll}
1 = \gamma_3 s_3, & 1 = \gamma_4 s_4 \\
s_3 = 1 + \gamma_5 s_5, & s_4 = 1 + \gamma_6 s_6 \\
s_5 = s_3 + \gamma_7 s_7, & s_6 = s_4 + \gamma_8 s_8 \\
\ldots\ldots\ldots\ldots & \ldots\ldots\ldots\ldots \\
s_{2k+1} = s_{2k-1} + \gamma_{2k+3} s_{2k+3}, & s_{2k} = s_{2k-2} + \gamma_{2k+2} s_{2k+2}
\end{array} \tag{5}$$

Quantities γ_{2k+3} and γ_{2k+2} with increase of k, how calculations showed, rapidly diminish; therefore, to facilitate calculations it is convenient to apply continued fractions.

In equations (5) for a certain sufficiently large k we set $\gamma_{2k+3} = 0$, $\gamma_{2k+2} = 0$. Then for s_3 and s_4 we obtain expressions in the form of continued fractions

$$s_3 = \frac{1}{1} - \frac{\gamma_5}{1} - \frac{\gamma_7}{1} - \ldots, \qquad s_4 = \frac{1}{1} - \frac{\gamma_6}{1} - \frac{\gamma_8}{1} - \ldots \tag{6}$$

The general solutions of systems (5) in continued fractions have the form

$$\begin{aligned} s_{2k+1} &= s_{2k-1}\left(\frac{1}{1} - \frac{\gamma_{2k+3}}{1} - \frac{\gamma_{2k+5}}{1} - \ldots\right) \\ s_{2k} &= s_{2k-2}\left(\frac{1}{1} - \frac{\gamma_{2k+2}}{1} - \frac{\gamma_{2k+4}}{1} - \ldots\right) \end{aligned} \tag{7}$$

Determining s_3 and s_4 from the first equations of systems (5) and substituting them in equations (6), we obtain equations of eigenvalues of the problem, written in continued fractions

$$1 = \frac{\gamma_3}{1} - \frac{\gamma_5}{1} - \frac{\gamma_7}{1} - \ldots, \qquad 1 = \frac{\gamma_4}{1} - \frac{\gamma_6}{1} - \frac{\gamma_8}{1} - \ldots \tag{8}$$

From equations (2) and (3) we easily obtain expressions for γ_j:

$$\begin{aligned} \gamma_{2k+1} &= \frac{B_{2k+1} C_{2k+1} W^2}{(Z + R_{2k+1} - A_{2k+1} W)(Z + R_{2k-1} - A_{2k-1} W)} \\ \gamma_{2k} &= \frac{B_{2k-2} C_{2k-2} W^2}{(Z + R_{2k} - A_{2k} W)(Z + R_{2k-2} - A_{2k-2} W)} \end{aligned} \tag{9}$$

Assigning values of dimensionless increment Z and finding the value of the least roots W of equations (8), we can establish the dependence of least roots W on Z for both systems of equations of (3). These calculations gave the dependences depicted in Fig. 1 in logarithmic coordinates. In Fig. 2 are given forms of perturbations, corresponding to the calculated values of W and Z.

Then we carried out calculations of forms of perturbations, which

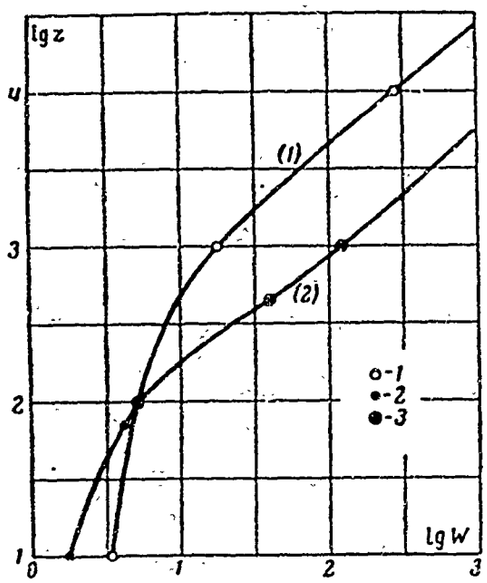

Fig. 1.

have the largest increment, for different values of W by the formula of the rate of lifting of the surface of the drop [1]

$$v_{r_1} = \frac{1}{a}\sum_{n=0}^{\infty} n a_n P_n(x) e^{-i\omega t} \qquad (10)$$

Coefficients of the equations were calculated by formulas (4)-(7).

As can be seen from Figs. 1 and 2, for values of the Weber number $1.63 < W < 1000$ three forms of increasing perturbations are possible. For $1.63 < W < 4$ there appears a form with two nodal lines (here n is even).

When $4 < W < 5$ there occurs a transition from the shown form to a form with four nodal lines. Last, for $W > 5$ the most rapidly growing form of perturbations will be the form with one nodal line (n is odd).

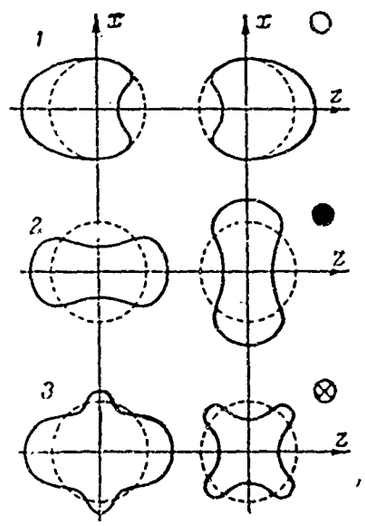

Fig. 2.

The form with two nodal lines, apparently, can lead to formation of two drops in the direction of flow or one torus. The critical value of W for this form will be W = 1.63, which is confirmed by [2].

The form with four nodal lines can exist in a narrow interval of values of the Weber number, and, therefore, the probability of its real appearance is minute. This form could lead to the formation of two drops and a torus or two tori.

The form with one nodal line may, apparently, lead to formation

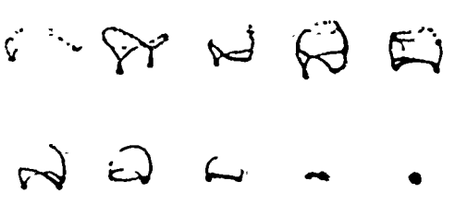

Fig. 3.

of a "pocket." Actually, such forms were observed (photographs in Fig. 3) immediately at $W \geq 5$ in [3].

Duality of theoretical forms (Fig. 2) follows from the fact that linear formulation of the problem gives a solution with an arbitrary factor of indefinite sign. In fact deformation of the drop should occur in such a manner that energy of the drop is increased at the expense of energy of the flow. For this, it is necessary that at points of the surface of the drop where pressure is maximum the velocity of deformation is directed into the drop. Then there is realized the form depicted in Fig. 2 on the right for the case of even n. For n, odd in the framework of the theory of an ideal fluid, both forms are equivalent (corollary of the D'Alembert-Euler paradox). However, in fact, pressure on the front side of the drop is greater, and this should lead to formation of a "pocket," stretched along the flow (Fig. 3).

Thus, from these conclusions concerning different forms of perturbations, appearing during motion of a fluid spherical drop in a medium of another fluid, it becomes evident that oscillation and breaking phenomena in part of a fluid torus should play an essential role in the process of disintegration of such a drop.

The form with one nodal line leads to such a ring with a "pocket" of very thin film (Fig. 3), which subsequently breaks into a great number of small drops, and the ring is turned into a torus, divisible into two big drops and many small ones.

The form with two nodal lines also leads to a torus, but without an enclosing "pocket."

In Fig. 4 are consecutive slides of the motion of a drop of ink,

dropped into water (photographs were taken from above). It is clear that from the drop of ink there appears a torus, in which there further form antinodes, and it breaks into drops, and each again turns into a torus, in which there again appear antinodes, etc.

Fig. 4.

It is necessary to note that the number of antinodes appearing in the torus may be two, three, or more; it decreases with decrease of the diameter of the torus.

The problem of oscillations and breaking of a fluid torus is considered, apparently, only by S. Oka [4]. He made the very complex calculation of the number of drops, into which a motionless torus disintegrates, depending upon the ratio of the torus radius R

to the radius of its cross section r only for values $R/r \geq 5$; in [4] there are given following values:

$R/r =$	5	6	7	8	9	10	11	12
$m =$	3	4	5	6	6	7	8	8

From the formula given in the same place it follows that when $R/r = 3$ to 4, $m = 2$.

These results can be obtained from the following elementary considerations.

If ratio R/r is great, splitting of the torus can be considered splitting of a rectilinear cylindrical stream of round section under the condition that in length $2\pi R$ there are packed a whole number of waves m.

Since, according to Rayleigh [5] the maximum of instability corresponds to $2\pi R/\lambda = 0.697$, with condition $m\lambda = 2\pi R$ we obtain

$$m = \{0.697\, R/r\} \tag{11}$$

Here symbol {x} signifies the integer nearest to x. Formula (11) gives all the above-cited values of m, and also values m = 2 and 3 for $R/r = 3$ and 4. This shows that allowance for toroidalness does not influence the number of drops formed from the torus. It is easy to see that the torus can be divided:

into two drops with fulfillment of inequalities

$$R/r \geqslant 2/0.697 = 2.87 \quad \text{or} \quad R/a > 1.2 \tag{12}$$

into three drops with fulfillment of inequalities

$$R/r > 3/0.697 = 4.3 \quad \text{or} \quad R/a > 1.58 \tag{13}$$

Here a – radius of initial drop.

Comparison of these results with the above experiments can be made only for very slowly moving tori. Thus, in Fig. 4c it is clear

that ratio R/a for the case of division of a torus into three drops is approximately equal to two. The circumstance that in experiments ratio R/a is significantly larger than it is according to formulas (12) and (13), apparently, is explained by the influence of transverse flow past of a filament the length of the maximum growing perturbation.

Submitted
16 December 1963

Literature

1. V. A. Borodin, Yu. F. Dityakin and V. I. Yagodkin. On splitting of a spherical drop in a gas flow. PMTF, 1962, No. 1.

2. S. V. Bukhman. Experimental research of disintegration of drops. News of Academy of Sciences of Kazakh Soviet Socialist Republic, 1954, No. 11.

3. W. R. Lane. Shatter of Drops in streams of Air. Ind. Eng. Chem., 1951, Vol. 43, No. 6.

4. S. Oka. On the Instability and Breaking up of a Ring of Liquid into small Drops Proc. Phys-Math. Soc. Japan, Third ser., 1936, Vol. 18, No. 9.

5. G. Lamb. Hydrodynamics. United Government Publishing House of Technical and Theoretical Literature, M-L, 1947.

INFLUENCE OF THE RELATIVE VELOCITY OF A GAS BUBBLE IN A LIQUID ON CHANGE OF ITS DIMENSIONS

Yu. N. Kalashnikov

(Leningrad)

During research of the bubbly form of cavitation the basic problem is to find dependences characterizing change of dimensions of cavitational bubbles in the liquid. Principal attention here is usually allotted to mechanical processes caused by disturbance of the equilibrium of force on the boundary of the bubble, since these processes determine such known phenomena of cavitation as cavitational noise and erosion of the surface of the flowed-past body. At the same time during flow past sufficiently extended bodies or motion of liquid in closed channels, e.g., cavitational tubes, appearance and development of the indicated form of cavitation is greatly influenced by diffusion of the gas dissolved in the liquid. Due to disturbance of diffusion equilibrium on its boundary, the bubble changes it dimensions (even in the presence of an equilibrium of forces on the boundary) either due to dissolution of gases contained in it, or due to liberation in it of gases dissolved in the liquid. This process, called bubbly gas cavitation, has been investigated by many authors, and for the case of a bubble, motionless relative to the liquid, there were found equations which describe change of its dimensions. Results of calculations by these equations sufficiently well agree with results of measurements of dimensions of growing or dissolving gas bubbles [1].

At the same time, for bubbles moving in liquid such coordination up to now has not been obtained, possibly, because of the sufficient complexity of experiment with respect to measurement of the dimensions of these bubbles.

In the book of V. G. Levich [2] there is a solution of the problem of diffusion in liquid, containing a moving drop of another liquid. According to this solution, and also similar

solutions for solid particles [3], the diffusion flow of gas into a bubble moving relative to the liquid should be proportional to the relative velocity to a certain degree. However, measurements conducted by Liebermann during surfacing of bubbles in a field of hydrostatic pressure [3] did not show dependence of the degree of intensification of diffusion on the velocity of surfacing.

Below there are derived equations of state of a gas bubble moving in liquid, taking into account diffusion of the gas; for comparison there are given certain results of experimental research into the influence of the relative velocity of the bubble in a liquid on change of its dimensions.

1. Let us consider the diffusion flow of gas in a bubble flowed past by a liquid. We consider that motion of the gas bubble in the liquid takes place with Péclet numbers $N_{pe} \gg 1$. For water solutions of gases contained in the air, the Prandtl number N_{Pr} will be of the order of 10^3; therefore, the indicated condition will take place for Reynolds numbers $N_{Re} > 10^{-2}$, which corresponds to dimensions of bubbles, surfacing in water under the action of the hydrostatic pressure gradient, $R > 10^{-5}$ m:

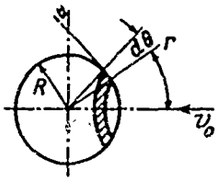

Fig. 1. Spherical system of coordinates.

$$\left(N_{\mathrm{Pe}}=\frac{v_0R}{k},\ N_{\mathrm{Re}}=\frac{v_0R}{\nu},\ N_{\mathrm{Pr}}=\frac{N_{\mathrm{Pe}}}{N_{\mathrm{Re}}}\right)$$

We connect the spherical system of coordinates with the center of the moving bubble (Fig. 1). Considering axial symmetry of problem, we have the equation of steady diffusion of gas in the liquid:

$$v_r\frac{\partial c}{\partial r}+v_\theta\frac{1}{r}\frac{\partial c}{\partial\theta}=k\left[\frac{\partial^2 c}{\partial r^2}+\frac{2}{r}\frac{\partial c}{\partial r}+\frac{1}{r^2\sin\theta}\frac{\partial}{\partial\theta}\left(\sin\theta\frac{\partial c}{\partial\theta}\right)\right] \qquad (1.1)$$

with boundary conditions

$$c=c_s \text{ when } r=R, \qquad c=c_0 \text{ when } r\to\infty$$

Here c — concentration of gas dissolved in the liquid; v_r and v_ϑ — components of velocity of the liquid on axes of the spherical system of coordinates; k — coefficient of molecular diffusion of gas

in the liquid; R — radius of the bubble; c_s — saturation concentration on the bubble boundary.

Since the bubble is flowed past by liquid with $N_{Pe} \gg 1$, on its surface there will form a thin diffusion layer, in which there occurs a sharp change of concentration from c_s on the boundary of the bubble to almost c_0 on the boundary of the layer. In this case derivatives of concentration with respect to the angular coordinate are small as compared with derivatives with respect to the radius vector and, furthermore, for values of r close to R we have

$$\frac{2}{R}\frac{\partial c}{\partial r} \ll \frac{\partial^2 c}{\partial r^2}$$

Accordingly, equation (1.1) will be simplified:

$$v_r \frac{\partial c}{\partial r} + v_\theta \frac{1}{r}\frac{\partial c}{\partial \theta} = k\frac{\partial^2 c}{\partial r^2} \tag{1.2}$$

We will introduce stream function ψ, connected with v_r and v_θ by relationships

$$v_\theta = -\frac{1}{r\sin\theta}\frac{\partial \psi}{\partial r}, \qquad v_r = \frac{1}{r^2\sin\theta}\frac{\partial \psi}{\partial \theta} \tag{1.3}$$

and turn to new variables ψ and θ. Such a change of variables will allow us to transform (1.2) into an equation of thermal conduction type:

$$\frac{\partial c}{\partial r} = \frac{\partial c}{\partial \psi}\frac{\partial \psi}{\partial r} = -r\sin\theta\, v_\theta \frac{\partial c}{\partial \psi}$$

$$\frac{\partial^2 c}{\partial r^2} = \frac{\partial}{\partial r}\left(\frac{\partial c}{\partial r}\right) = \frac{\partial \psi}{\partial r}\frac{\partial}{\partial \psi}\left(-r\sin\theta v_\theta \frac{\partial c}{\partial \psi}\right) = r^2\sin^2\theta v_\theta^2 \frac{\partial^2 c}{\partial \psi^2}$$

$$\left(\frac{\partial c}{\partial \theta}\right)_r = \left(\frac{\partial c}{\partial \theta}\right)_\psi + \frac{\partial c}{\partial \psi}\frac{\partial \psi}{\partial \theta} = \left(\frac{\partial c}{\partial \theta}\right)_\psi + r^2\sin\theta v_r \frac{\partial c}{\partial \psi}$$

Substituting values of derivatives with respect to concentration in (1.2), we have

$$\frac{\partial c}{\partial \theta} = kr^3\sin^2\theta v_\theta \frac{\partial^2 c}{\partial \psi^2} \tag{1.4}$$

Since equation (1.4) is valid in the diffusion boundary layer, it is possible to present $r = R + \varepsilon$, where $\varepsilon \ll R$ and changes from

zero to the thickness of the diffusion boundary layer. Then r = $= R(1 + \varepsilon/R)$, and r^3 is approximately equal to R^3.

In distinction from motion of a solid sphere in liquid, tangential velocity on the boundary of the bubble is not equal to zero, but according to [2], it is

$$(v_\theta)_{r=R} = v_1 \sin\theta \tag{1.5}$$

where v_1 – absolute value of velocity on the boundary of bubble when $\theta = 90^\circ$. Velocity v_1, depending upon hydrodynamic conditions of motion of the bubble, varies from $(1/2)v_0$ for $N_{Re} \ll 1$ (the solution of Rybchinskiy-Adamar [2]) to $(3/2)v_0$ for very large Reynolds numbers (when $N_{Re} \gg 1$ distribution of velocities on surface of the bubble becomes close to that in the case of flow past a solid sphere by an ideal fluid).

Tangential velocity in a diffusion boundary layer differs little from (1.5) due to the fact that thickness of the diffusion layer on order is less than the thickness of the hydrodynamic boundary layer by $N_{Pr}^{1/3}$.

Taking these assumptions into account we give equation (1.4) the form

$$\frac{\partial c}{\partial \vartheta} = kR^3 v_1 \sin^3\theta \frac{\partial^2 c}{\partial \psi^2} \tag{1.6}$$

where the value of $\partial^2 c/\partial\psi^2$ is taken for small values of ε, when the following approximate expression for the stream function, obtained by integration of (1.3), is valid:

$$\psi = -Rv_1 \sin^3\theta\varepsilon$$

We introduce the new variable

$$s = kR^3 v_1 \int \sin^3\theta\, d\theta = kR^3 v_1 \left(\frac{\cos^3\theta}{3} - \cos\theta\right) + A$$

where the integration constant A is selected from the condition that $s = 0$ when $\theta = 0$. Consequently, $A = (2/3)kR^3v_1$. As a result of this, equation (1.6) will become

$$\frac{\partial c}{\partial s} = \frac{\partial^2 c}{\partial \psi^2} \tag{1.7}$$

with boundary conditions

$$c = c_s \quad \text{when } \psi = 0 (\varepsilon = 0), \qquad c = c_0 \quad \text{when } \psi = \infty$$

To this we should add one more condition, namely, in the front critical point of the bubble ($r = R$, $\theta = 0$) concentration of the incident flux should be the same as at infinity, which corresponds to $c = c_0$ when $s = 0$.

Equation (1.7) is easily solved by operation method. Its integral is equal to

$$c = \frac{2}{\sqrt{\pi}}(c_s - c_0)\int_0^u e^{-x^2}\,dx$$

where

$$u = \frac{\psi}{2\sqrt{s}} = \frac{Rv_1 \sin^2\theta\varepsilon}{2\sqrt{kR^3v_1(1/3\cos^3\theta - \cos\theta + 2/3)}}$$

The gradient of concentration on the bubble boundary is

$$\left(\frac{\partial c}{\partial \varepsilon}\right)_{\varepsilon=0} = \frac{2c_s - c_0}{\sqrt{\pi}}\frac{\partial}{\partial u}\left(\int_0^u e^{-x^2}\,dx\right)\frac{\partial u}{\partial \varepsilon}\Big|_{\varepsilon=0} = \frac{v_1 \sin^2\theta\,(c_0 - c_s)}{\sqrt{\pi kRv_1(1/3\cos\theta - \cos\theta + 2/3}} \tag{1.8}$$

From this we find, according to Fick's law, the flow of mass of the gas from the bubble per unit time (Fig. 1).

$$\frac{dm}{dt} = -\int_0^\pi 2\pi R\sin\theta R\,d\theta k\left(\frac{\partial c}{\partial \varepsilon}\right)_{\varepsilon=0} = \frac{2\pi R^2 kv_1(c_0 - c_s)}{\sqrt{\pi kv_1 R}}\int_0^\pi \varphi(\theta)\,d\theta$$

$$\varphi(\theta) = \frac{\sin^3\theta}{\sqrt{1/3\cos^3\theta - \cos\theta + 2/3}}$$

In Fig. 2 is a graph of integrand $\varphi = \varphi(\theta)$. Calculation gives for the integral a value, equal to 2.30. Considering $v_1 = (1/2)\,v_0$,

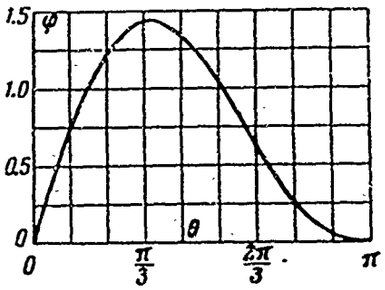

Fig. 2. Graph of function $\varphi(\theta)$.

we have

$$\frac{dm}{dt} = 5.78\, R \sqrt{kR v_0}\,(c_0 - c_s) \qquad (1.9)$$

In the case of a motionless bubble [4],

$$\frac{dm}{dt} = 4\pi R k\,(c_0 - c_s) \qquad (1.10)$$

Thus, increase of the intensity of diffusion of gas from the bubble due to flow past it of a liquid is equal to

$$\lambda = \frac{(dm/dt)_1}{(dm/dt)_0} = 0.46\left(\frac{Rv_0}{k}\right)^{1/2} = 0.46\,(N_{pe})^{1/2} \qquad (1.11)$$

Here, subscript 1 signifies the value of the derivative for $N_{pe} \gg 0$, and subscript 0 is the value for $N_{pe} = 0$.

This result allows us to consider a bubble moving in liquid motionless, for which the gas diffusion coefficient is increased, as it were, by a factor of λ.

It is obvious that the value of λ for small numbers N_{Pe} will lie between one and the value given by (1.11). Therefore, for these numbers N_{Pe} it is possible to write an interpolation formula

$$\frac{dm}{dt} = 4\pi kR\,(1 + 0.46 N_{Pe}^{1/2})\,(c_0 - c_s) \qquad (1.12)$$

which for $N_{Pe} \gg 1$ passes into (1.9), and for $N_{Pe} = 0$, into (1.10).

Expression (1.9) was obtained on the assumption of constancy of the bubble radius R.

In reality, with growth or dissolution of the bubble its radius changes. This circumstance raises the necessity when solving a problem on diffusion to satisfy boundary conditions on a mobile boundary, which is a complex problem.

For small values of the velocity of the bubble wall, occurring in processes of gas cavitation, expression (1.9) can be used,

obviously, also in the case of a bubble radius varying in time, considering the phenomenon quasi-stationary.

2. Expression (1.12) obtained in the preceding section allows us to obtain equation of state of a spherical gas bubble, using the equation of equilibrium of forces on its boundary

$$p(t)_i = p_g + p_d - \frac{2\sigma}{R} \tag{2.1}$$

Here p(t) – pressure in the liquid; p_g – pressure of gas in the bubble; p_d – pressure of saturated vapors of the liquid; σ – constant of surface tension.

The mass of gas in the bubble is

$$m = {}^4/_3\pi R^3 \rho_g \qquad \left(\rho_g = \frac{\rho_{ga}}{p_a} p_g\right)$$

where ρ_g – density of gas in the bubble, determined by the Boyle-Mariotte equation; ρ_{ga}, in turn, is density of gas at atmospheric pressure p_a. Consequently,

$$m = \frac{4}{3}\pi R^3 \frac{\rho_{ga}}{p_a}\left[p(t) - p_d + \frac{2\sigma}{R}\right] \tag{2.2}$$

Differentiating (2.2) with respect to time and comparing with (1.12), we have

$$\frac{dR}{dt} = \frac{1}{p(t) - p_d + {}^4/_3\sigma/R}\left(\frac{kp_a(1 + 0.46\,N_{Pe}^{1/2})}{\rho_{ga}R}(c_0 - c_s) - \frac{R}{3}\frac{dp(t)}{dt}\right) \tag{2.3}$$

The saturation concentration on the bubble boundary in accordance with Henry's law can be expressed as follows:

$$c_s = \frac{p_g}{p_a} c_{sa} \tag{2.4}$$

Here c_{sa} – concentration of saturation at atmospheric pressure, determined for the given temperature from known tables.

Substituting (2.4) in (2.3) and designating $\alpha = c/\rho_{ga}$, where

α – volume of gas reduced to atmospheric pressure, dissolved in a unit volume of water, taking into account (2.1), we finally obtain

$$\frac{dR}{dt} = \frac{1}{p(t) - p_d + 4\sigma/3R}\left\{k\alpha_{sa}\left[\frac{\alpha_0}{\alpha_{sa}}p_a - p(t) + p_d - \frac{2\sigma}{R}\right]\times\right.$$
$$\left.\times\left(\frac{1}{R} + 0.46\frac{\sqrt{v_0}}{\sqrt{kR}}\right) - \frac{R}{3}\frac{dp(t)}{dt}\right\} \qquad (2.5)$$

with initial condition $R = R_0$ for $t = 0$.

With constant pressure in the liquid, equation (2.5) can be integrated. We introduce dimensionless quantities

$$R^\circ = \frac{R}{R_0}, \quad \tau = \frac{k}{R_0^2}t, \quad \alpha^\circ = \frac{\alpha_0}{\alpha_{sa}}, \quad p^\circ = \frac{p - p_d}{p_a}$$
$$\gamma = \frac{2\sigma}{R_0 p_a}, \quad \delta = \frac{p^\circ}{p^\circ - \alpha^\circ}, \quad \varphi = \frac{\gamma}{p^\circ - \alpha^\circ}, \quad \lambda = 0.46\left(\frac{R_0 p_a}{k}\right)^{1/2} \qquad (2.6)$$

In this case $dp/dt = 0$; therefore, it is possible to reduce equation (2.5) to form

$$\frac{dR^\circ}{d\tau} = -\alpha_{sa}\left(\frac{1}{R^2} + \frac{\lambda}{\sqrt{R^3}}\right)\left(1 + \frac{\varphi}{R^3}\right)\left(\delta + \frac{2}{3}\frac{\varphi}{R^3}\right)^{-1} \qquad (2.7)$$

with initial condition $R = 1$ for $\tau = 0$.

Designating $\sqrt{R^\circ} = \omega$, we rewrite (2.7) as follows:

$$\frac{2\omega^3(\delta\omega^3 + 2/3\,\varphi)\,d\omega}{(\omega^3 + \varphi)(\lambda\omega + 1)} = -\alpha_{sa}\,d\tau$$

Integrating this equation and returning to the old variable, we have

$$\frac{\alpha_{sa}}{2}\tau = \frac{\delta}{3\lambda}(1 - \sqrt{R^{\circ 3}}) - \frac{\delta}{2\lambda^2}(1 - R^\circ) + \left(\frac{\delta}{\lambda^3} + \frac{2}{3}\frac{\varphi}{\lambda} - \frac{\delta\varphi}{\lambda}\right)(1 - \sqrt{R^\circ}) +$$
$$+ \frac{\lambda^{-2}\delta\varphi + 2/3\,\varphi^2 - \delta\varphi^2}{\lambda^2\varphi + 1}\left[\frac{1}{2}\ln\frac{R^\circ + \varphi}{1 + \varphi} + \lambda\sqrt{\varphi}\left(\operatorname{arc\,tg}\frac{\sqrt{R^\circ}}{\sqrt{\varphi}} - \operatorname{arc\,tg}\frac{1}{\sqrt{\varphi}}\right)\right] +$$
$$+ \frac{\lambda^{-2}\delta + 2/3\,\varphi - \delta\varphi}{\lambda^3(\lambda^2\varphi + 1)}\ln\frac{\lambda\sqrt{R^\circ} + 1}{\lambda + 1} \qquad (2.8)$$

for $\varphi > 0$, which corresponds to dissolving bubbles, and

$$\frac{\alpha_{sa}}{2}\tau = \frac{\delta}{3\lambda}(1-\sqrt{R^{\circ 3}}) - \frac{\delta}{2\lambda^2}(1-R^{\circ}) + \left(\frac{\delta}{\lambda^3} + \frac{2}{3}\frac{\varphi}{\lambda} - \frac{\delta\varphi}{\lambda}\right)(1-\sqrt{R^{\circ}}) + \\ + \frac{\lambda^{-2}\delta\varphi + {}^2/_3\varphi^2 - \delta\varphi^2}{2(\lambda^2\varphi+1)}\left[\ln\frac{R^{\circ}+\varphi}{1+\varphi} + \lambda\sqrt{|\varphi|}\ln\frac{(\sqrt{R^{\circ}}-\sqrt{|\varphi|})(1+\sqrt{|\varphi|})}{(\sqrt{R^{\circ}}+\sqrt{|\varphi|})(1-\sqrt{|\varphi|})}\right] + \\ + \frac{\lambda^{-2}\delta + {}^2/_2\varphi - \delta\varphi}{\lambda^2(\lambda^2\varphi+1)}\ln\frac{\lambda\sqrt{R^{\circ}}+1}{\lambda+1} \qquad (2.9)$$

for $\varphi < 0$, which corresponds to growing bubbles.

Considering in (2.8) $R^{\circ} = 0$, we obtain the following relationship for determining the time T of total dissolution of the gas bubbles

$$\frac{k\alpha_{sa}}{2R_0^2}T = \frac{\delta}{6\lambda}\left(2 - \frac{3}{\lambda} + \frac{6}{\lambda^3} + \frac{4\varphi}{\delta} - 6\varphi\right) + \\ + \frac{\lambda^{-2}\delta\varphi + {}^2/_3\varphi^2 - \delta\varphi^2}{\lambda^2\varphi+1}\left(\frac{1}{2}\ln\frac{\varphi}{1+\varphi} - \lambda\sqrt{\varphi}\,\mathrm{arc\,tg}\,\frac{1}{\sqrt{\varphi}}\right) + \\ + \frac{\lambda^{-2}\delta + {}^2/_2\varphi - \delta\varphi}{\lambda^2(\lambda^2\varphi+1)}\ln\frac{1}{1+\lambda} \qquad (2.10)$$

Expression (2.10) allows us to calculate the time during which for certain conditions a gas bubble will be completely dissolved, and to compare it with the experimental value.

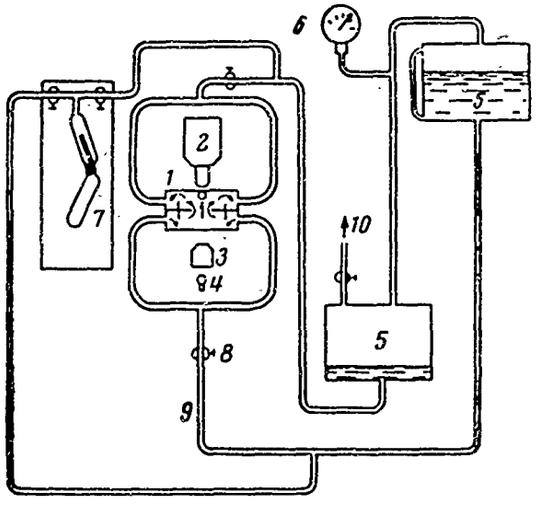

Fig. 3. Fundamental scheme of the experimental installation. 1 – vessel; 2 – microscope with movie camera; 3– system of condensers; 4 – source of light; 5 – tanks; 6 – vacuum manometer; 7 – instrument for determining air-content of the water; 8 – clamps; 9 – connecting hoses; 10 – feed to compresser and vacuum pump.

3. The fundamental diagram of the experimental installation is shown in Fig. 3. Vessel 1 for observing the bubble is a round vessel, made of organic glass (Fig. 4). In the upper part of the vessel is a window of thick plate glass, which ensured small deviations of form of bubbles from the spherical (organic glass is hardly moistened by water, and on it bubbles have a flattened form). Water flowed into the radial gap between the outer wall of the vessel and the inner circular partition. From gap through holes in the partition water reached the lower central part of the vessel, and then through a hole of diameter 10 mm in a diaphragm it enters the upper central part and through upper holes in the circular partition and radial clearance it leaves the vessel. Such a labyrinth is created in order to ensure the most exact flow of water to the center of the lower surface of the inspection window, in which the gas bubble is located, since with small deflection the bubble is easily carried off by the water.

Fig. 4. Vessel for observation of bubbles.

The flow of water was created by the difference of water levels in two tanks. The velocity of the flow of water through the hole in diaphragm of the vessel was determined by the flow rate and could be regulated by the relative location of tanks in height. In the tanks, with the help of a vacuum pump and compressor, it was possible to assign any pressure from deep rarefaction to 4 atm (abs).

Observation and filming of bubbles were produced on a microfilming installation of type MKU-1, which allows us to obtain a 100-power magnification on film.

With return movement the water was passed through an instrument

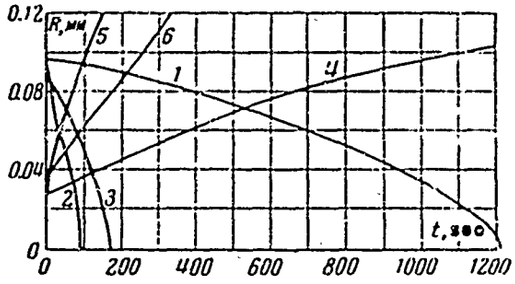

Fig. 5. Influence of the velocity of flow past an air bubble U, cm/sec, by water on its growth and dissolution. Temperature of water is 20°C; α_0 = 1.79%. Curve 1 — U = 0; 2 — = U = 27 at p = = 10750 kg/m^2; curve 3 — U = 16 at p = 10250 kg/m^2; curve 4 — U = 0; 5 — U = 13; 6 — U = 2.6 at p = 6850 kg/m^2.

for determining the gas-content of the liquid, and we measured the quantity of air dissolved in the water.

On the described installation we conducted a large number of experiments in observation of the growth and dissolution of air bubbles with different velocities of flow past them by water. In Fig. 5 there are shown some of the experimental curves of change of radii of dissolved and growing bubbles in motionless water and with different velocities of flow past them by water, and in Figs. 6 and 7 are photographs of these bubbles.

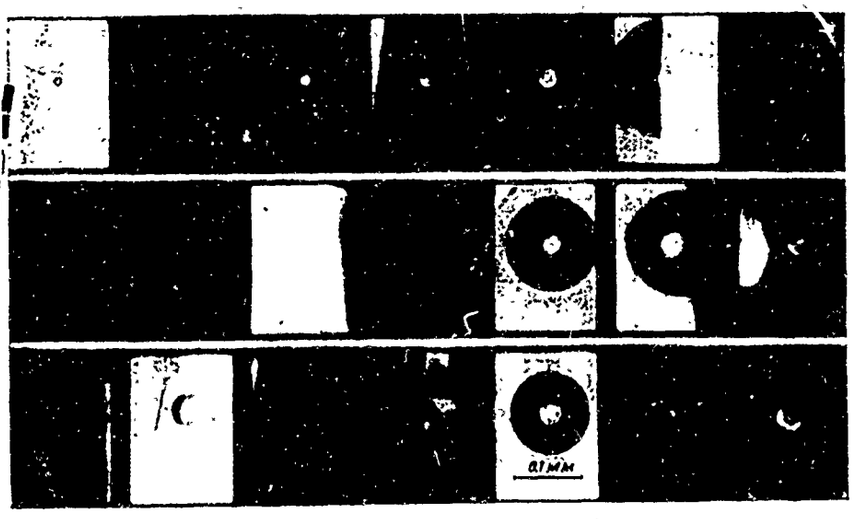

Fig. 6. Sequential photographs of dissolving bubbles: 200 sec; U = 0; 30 sec, U = 16 cm/sec; 15 sec, U = 27 cm/sec.

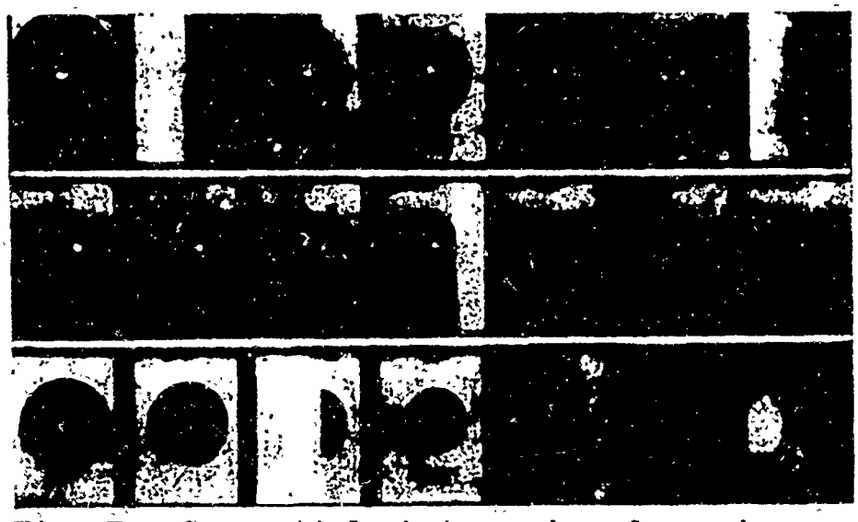

Fig. 7. Sequential photographs of growing bubbles: 120 sec, U = 0; 30 sec, U = 2.6 cm/sec^{-1}; 30 sec, U = 13 cm/sec^{-1}.

From experiment the velocity of flow past a free bubble by liquid remains unknown, which is embodied in expression (1.12), although we know the rate of flow of water through the hole in the diaphragm of the vessel. Therefore, it would have been possible to try to find this velocity from one experiment, solving for this purpose equation (2.8) for λ, and, by determining the ratio of the velocity of flow past a free bubble to the velocity of flow through the diaphragm hole, to calculate from the same (2.8) the time of growth or dissolution of the bubble for another experiment and to compare this time with its experimental value. It is somewhat unclear, here, what magnitude of the coefficient of diffusion to put in the calculation, since in motionless liquid during contact of a spherical bubble against a flat wall the intensity of diffusion decreases by a factor of ln 2 [3].

We shall consider the intensity of diffusion the same as in the case of an infinite fluid, since with such a scheme of flow past a bubble the influence of the wall on diffusion of gas through sections of the surface of the bubble turned toward the flow should be small,

and flow of gas through these sections, as can be seen from Fig. 2, constitutes the prevailing part in the total flux across the whole surface of the bubble. Obviously, with decrease of the velocity of flow past the bubble the influence of the wall on intensity of diffusion should increase.

To this purpose, for conditions corresponding to curve 2 of Fig. 5, we graphically solved equation (2.10), as a result of which we obtained $\lambda = 9.60$, and, consequently, $U/V_0 = 24$, where U – velocity of flow through the hole in the diaphragm.

Thus, for a bubble, change of whose dimensions is depicted by curve 3 of Fig. 5, we have $V_0 = 5.7$ mm/sec and $\lambda = 7.26$. From equation (2.10) we obtain T = 150 sec; the experimental value of the time of total dissolution of this bubble, as can be seen from Fig. 5, is equal to 170 sec.

Matching should be considered satisfactory, considering inevitable errors in determination of conditions of the experiment and a certain influence of the wall on diffusion.

Thus intensity of diffusion of gas into a gas bubble during its relative motion in a liquid increases proportionally to the velocity of flow past the bubble to the 1/2 power. Even with sufficiently small relative velocities, with which bubbles at a dimension of the order of 0.1 mm surface, intensity of diffusion is increased by an order or more as compared to the case of a motionless bubble.

Results of experimental research confirm our theoretical conclusions.

Submitted
20 September 1963

Literature

1. A. D. Pernik. Problems of cavitation. Sudpromgiz, 1963.

2. V. G. Levich. Physico-chemical hydrodynamics. Fizmatgiz, 1959

3. L. Liebermann. Air Bubbles in Water. J. Appl. Phys., 1957, Vol. 28, No. 2.

4. P. S. Epstein and M. S. Plesset. On the Stability of Gas Bubbles in Liquid-Gas Solutions. J. Chem. Phys., 1950, Vol. 18, No. 11.

ON THE STABILITY OF A COLLAPSING GAS CAVITY IN ROTATING LIQUID

V. K. Kedrinskiy and G. M. Pigolkin

(Novosibirsk)

This work, basically, is devoted to experimental research of the stability of the shape of a collapsing gas cavity, formed by a rotating liquid volume and filled with air or a mixture of acetylene and oxygen. In the latter case we determined the influence of ignition of the mixture at the moment of maximum compression on stability of the cavity shape during its subsequent expansion. At the end there is an attempt to construct certain diagrams of the observed phenomena.

Experiments were conducted on installation presented in Fig. 1. The working chamber was cylinder 1 with transparent walls 2, filled with water. High-pressure chamber 3 with a 50% mixture of acetylene and oxygen was separated from the working chamber by a diaphragm.

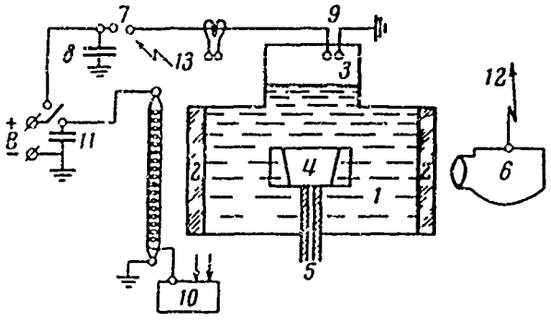

Fig. 1.

The basic working part of the installation – a "rotator" – consisting of two parallel plates, rigidly fastened by four thin ribs. The lower plate rests on shaft 5 with a hole for admission of gas. During supplying of gas through the hole in the shaft during rotation between the plates there will form

cavity 4. Motion of the cavity walls was fixed by high-speed photorecorder 6. At the moment of opening of the shutter of the photorecorder a synchronizing pulse ignites air gap 7 in the circuit of capacitor 8, which, discharging in gap 9, ignites the mixture. During discharge of capacitor 8 a Rogovsky strip placed in the circuit of this capacitor, starts pulse transformer 10, which, in turn, starts the pulse tube, standing in the circuit of capacitor 11.

In Fig. 2a is a typical photograph of pulsation of the gas cavity. Scanning of the process is downward, cavity is somewhat skewed on a cone. The moment of collapse is clearly seen in the nineteenth frame. The cavity at the moment of maximum compression is a cylinder overcompressed at its center. Compression is unstable, and during the following expansion of the cavity it is significantly eroded. In this photograph is the case of compression of a cavity, filled with a mixture of acetylene and oxygen (the moment of igniting is seen well in the eighteenth and nineteenth frames). The fact of ignition of the gas is determined by the self-glow, fixed at the moment of maximum compression without illumination of the process. Repetition of the above experiment for the case of a cavity filled with air showed that the influence of ignition of the mixture inside the cavity essentially does not affect subsequent expansion. Figure 2b depicts the final moment of collapse and subsequent expansion of the air cavity (the initial radius in this case is somewhat less than the preceding). As can be seen from the photograph, instability in this case is stronger. The cause is the decrease of the minimum radius and, as a result, strong disturbance of centering at the moment of maximum compression. In such cases we always see total destruction of the cavity.

Location of the "rotator" in a transparent hollow cylinder permitted us to achieve significant improvement of stability (Fig. 2c).

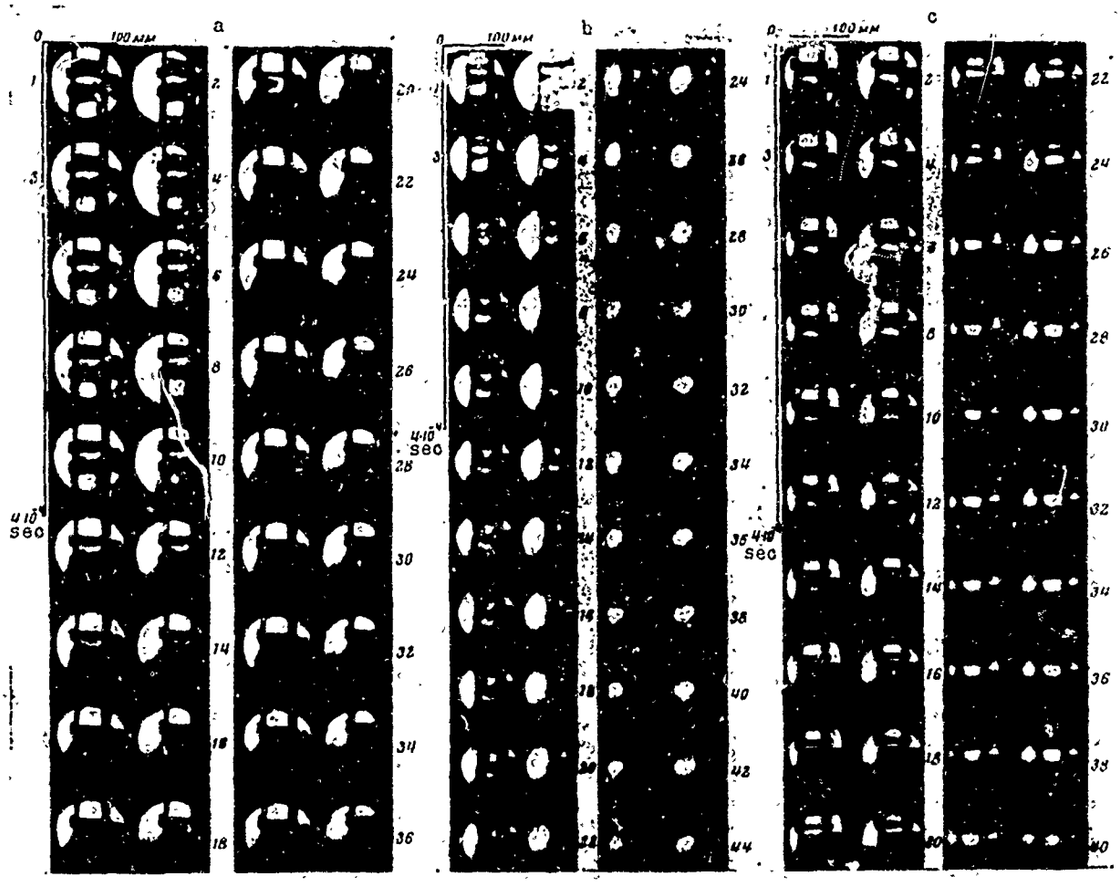

Fig. 2.

However, the above scheme of the experiment did not give a possibility of improving the stability by increasing of the rate of rotation of the liquid due to the appearing eddies. Installation above the "rotator" of a lattice allowed us only slightly to increase the rate, since appearance of small eddies led to instability of the initial shape of the gas cavity.

We succeeded in significantly increasing the rate of rotation and freeing ourselves from eddies by rotation of the whole "vessel—liquid" system and introduction of a piston (Fig. 3). Instead of the "rotator" there is established a transparent cylinder 1 with piston 2.

Between the piston and the bottom of cylinder we filled in water. Regulating the admission of gas under piston during rotation of the cylinder, we obtained cavity 3 of the desired dimensions. The rate of rotation of the cylinder was in the order of 30 rev/sec; initial pressure of the mixture in the explosion chamber varied from 200 to 500 mm, the height of the cavity was 10-80 mm; diameter of cavity was 40-70 mm. In Fig. 4a is a typical photograph of compression of the cavity by a solid (along the diameter of the cylinder) piston. Compression occurs in two ways: by radius and by height. This, one may see especially distinctly in Fig. 4b. In the direction of motion of the piston on the surface of the cavity there moves a compression wave, reminiscent of "bora" in low water. Naturally, with such very unstable compression expansion of the cavity leads to its total destruction. Obviously, for stability it is necessary to preserve the height of the cavity during compression. For this the solid piston is replaced by an annular one (Fig. 5). In this case the cavity is compressed symmetrically; the shape of the cavity remains during pulsation close to cylindrical; the surface waves are insignificant (Fig. 4c).

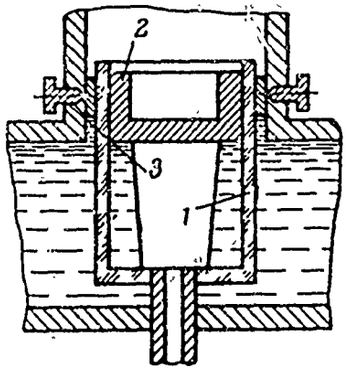

Fig. 3.

As a result of experimental research there is revealed the basic possibility of obtaining sufficient stability of walls during collapse.

Let us consider briefly certain diagrams of axially symmetric flow of an initially twirled liquid with a free surface.

The liquid revolves together with a cylindrical vessel of radius R, as a solid with constant angular velocity ω. During rotation inside

the liquid there will form [illegible], close to cylindrical. Disregarding viscosity, we consider [illegible] preserves a moment of momentum N about the axis of the cylinder. [illegible] equicyclical the surfaces, whose generatrices [illegible] equation

$$\Lambda(r, x, t) = \text{const}$$

where r and x are radial and axial coordinates, respectively. If generatrices of equicyclical surfaces have a small slope to the axis and weakly depend on time, then the approximate solution is analogous to that which is obtained in the theory of long water, where

$$c = \omega \frac{r_0^2}{2} \left(\frac{R^2}{r_0^2} - 1 \right)^{1/2}$$

Here c — velocity of [illegible] disturbances, analogous to the velocity of sound in gas dynamics; r and r_0 — current and initial radii of cavity, respectively; R — internal radius of the vessel.

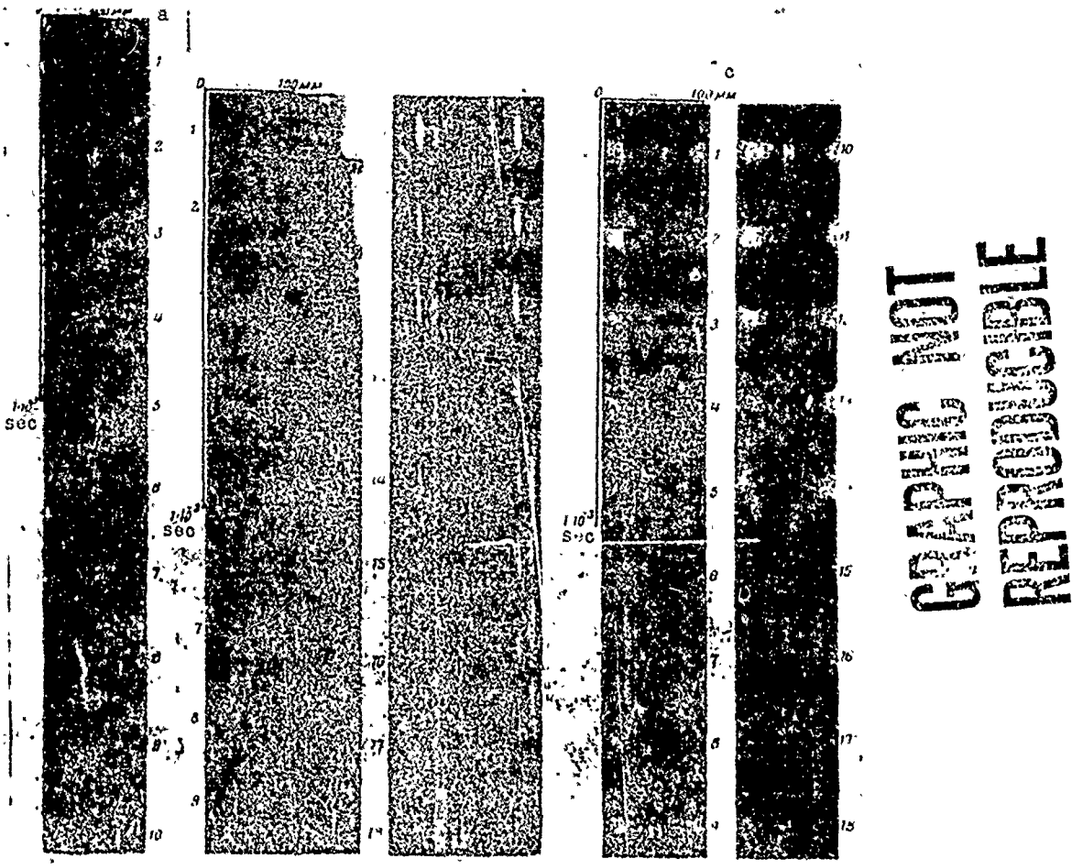

Fig. 4.

This solution gives a simple wave, leading to formation of a shock. Flow, illustrated by Fig. 4a and b, is reminiscent of flow with a shock. The equation of motion in the axially symmetric case is satisfied when

$$u = \text{const}, \qquad r = 0, \qquad N = N(t, t)$$

where u and v — axial and radial velocities, respectively. Consequently, flow with a shock is theoretically possible. However, integral relationships in our case do not give the possibility of determining the velocity of the shock as depending on its amplitude and parameters of motion before the shock.

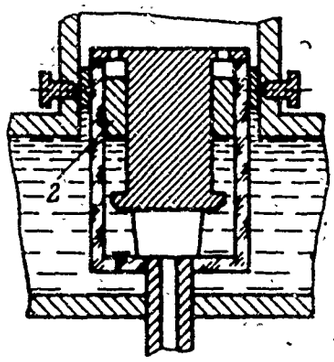

Fig. 5.

Study of experimental data showed that, in distinction from discontinuous flows in shallow water, here we have a free surface without any traces of turbulation. However, it is easy to show that flow, in which at infinity the free surface has various values of radius, cannot everywhere satisfy Euler's equations.

Consequently, the zone of turbulent motion should exist somewhere inside the liquid, so that the free surface does not become turbulent.

Let us assume that the turbulent zone adjoins the zone of regular flow. The shock moves here toward the zone of regular flow. On the free surface contact can be realized only on a circumference of minimum radius. Taking all these assumptions, we obtain absence of turbulence on the free surface and the expression for the velocity of the shock is

$$D = \omega \frac{r_0}{\xi_0} \frac{R^2 - \xi_0^2}{\sqrt{2R^2 - r_0^2 - \xi_0^2}}$$

where D — velocity of the shock, ξ_0 — minimum radius of the free surface. Axial velocity after the shock is determined from the condition of conservation of mass of the liquid

$$(u - D)(R^2 - \xi_0^2) = -D(R^2 - r_0^2)$$

The question of the existence of the mentioned regular flow has encountered significant difficulties and remains open.

Thus, for the case with a solid piston the criterion of stability of shape of the cavity during compression is analogous to the condition of adiabaticity of compression of a gas volume

$$u \ll C$$

where u — velocity of the piston. When u ~ C (Fig. 4a and b) u ≈ C ≈ ≈ 4 m/sec we obtain unstable motion with a shock.

In the case with an annular piston the collapsing cavity is the most stable in shape. However, the authors did not manage to find a physically acceptable model of motion, calculation of which would be sufficiently simple and at the same time, gave satisfactory explanation of stability of cavity shape.

The authors are grateful to B. V. Voytsekhovskiy and R. I. Soloukhin for their attention to this work.

A THEORY OF THERMAL EXPLOSION IN UNSTEADY STATE

V. V. Barzykin, V. T. Gontkovskaya,
A. G. Merzhanov, and B. I. Khudyayev

(Moscow)

With the help of computers we analyze and give a solution of the system of equations of thermal explosion in partial derivatives for a reaction of the zero and first order during conductive heat transfer in the reaction zone and Newtonian heat exchange on the boundary.

We definitize determination of basic characteristics of thermal explosion. The obtained results are presented in the form of approximate formulas, relating characteristics of thermal explosion with all parameters of the problem in a wide range of their variation.

We give the criterion of applicability of the equation averaged by volume for calculation of the period of induction in the case of conductive heat transfer in a reaction volume. We offer a method of averaging the system of equations of thermal explosion.

1. The unsteady-state system of equations on the assumption of conductive heat transfer in a reaction volume and of constancy of thermophysical coefficients in dimensionless variables has the following form (see, e.g., [1]):

heat-conduction equation

$$\frac{\partial\theta}{\partial\tau} = \varphi(\eta)\exp\frac{\theta}{1+\beta\theta} + \frac{1}{\delta}\left(\frac{\partial^2\theta}{\partial\xi^2} + \frac{n}{\xi}\frac{\partial\theta}{\partial\xi}\right) \tag{1.1}$$

equation of chemical kinetics

$$\frac{\partial \eta}{\partial \tau} = \gamma \varphi(\eta) \exp \frac{\theta}{1 + \beta\theta}$$

$$\theta = \frac{E}{RT_0^2}(T - T_0), \qquad \tau = \frac{QEk_0 t}{c\rho RT_0^2} \exp\left(-\frac{E}{RT_0}\right), \qquad \xi = \frac{r}{r}$$

$$\delta = \frac{QEr^2 k_0}{\lambda RT_0^2} \exp\left(-\frac{E}{RT_0}\right), \qquad \gamma = \frac{c\rho RT_0^2}{QE}, \qquad \beta = \frac{RT_0}{E} \tag{1.2}$$

Here, θ – heating up, τ – time; ξ – coordinate, δ – Frank-Kamenetskiy criterion, $n = 0$, 1, and 2 correspondingly for plane-parallel, cylindrical and spherical vessels, η – the degree of conversion. The variables with dimensions are: $T(x, t)$ – temperature in reaction volume, T_0 – ambient temperature, Q – thermal effect of the reaction, k_0 – preexponent, E – activation energy, λ – coefficient of thermal conductivity, c – specific heat capacity, ρ – density, R – universal gas constant, r – radius of vessel (for a plane-parallel one, half the thickness).

This system was not investigated in detail. In the theory of thermal explosion in unsteady state [2-7] various simplifications are reaction volume, decomposition of the exponential factor, etc).

Below there are described results of solution of system (1.1)-(1.2) for the case of a reaction of the zero and first order ($\varphi(\eta)$ correspondingly is equal to 1 and $(1 - n)$). The system was solved for the following initial and boundary conditions:

$$\begin{aligned} &\theta = 0, \quad \eta = 0 \quad \text{when } \tau = 0 \\ &\frac{\partial \theta}{\partial \xi} = 0 \quad \text{when } \xi = 0 \\ &\frac{\partial \theta}{\partial \xi} = -B\theta \quad \text{when } \xi = 1 \left(B = \frac{\alpha r}{\lambda}\right) \end{aligned} \tag{1.3}$$

Here B – Biot criterion, α – coefficient of heat transfer from the charge surface. Case $B \to \infty$ corresponds to assignment on the surface of a constant temperature ($\xi = 1$, $\theta = 0$).

Solution was carried out on a computer. We found functions $\theta(\xi, \tau)$ and $\eta(\xi, \tau)$ for different values of parameters n, δ, B, γ, β. The

basic purpose of calculations was to determine,

the critical condition

$$\delta_* = \delta_* (n, B, \gamma, \beta) \tag{1.4}$$

and the period of induction

$$\tau_0 = \tau_0 (\delta, n, B, \gamma, \beta) \quad \text{when} \quad \delta > \delta_* \tag{1.5}$$

Calculations were conducted in the following ranges of variation of parameters:

$$0.5\delta_* \leqslant \delta \leqslant 10\delta_*, \quad 0.001 \leqslant B < \infty$$
$$0 \leqslant \gamma \leqslant 0.01, \quad 0 \leqslant \beta \leqslant 0.05$$

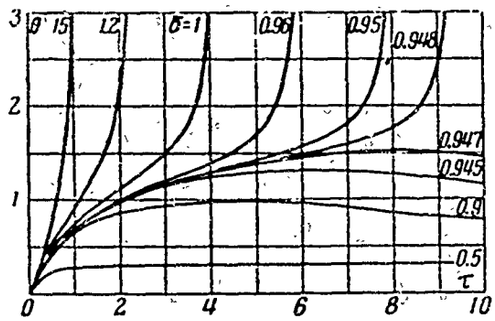

Fig. 1. Dependence $\theta(\tau)$ when $n = 0$, $\beta = 0$, $\gamma = 0.005$, $B = \infty$.

2. Before passing to presentation of quantitative regularities of thermal explosion, we shall emphasize certain aspects of the physical picture of the phenomenon and definitize determinations of basic characteristics.

As it is known, a distinctive feature of thermal explosion is the presence of two clearly expressed regimes. For small δ the reaction flows almost steadily with small heating up; for large δ there is observed progressive thermal self-acceleration of the reaction, leading to explosion. For a reaction of zero order* change of regimes during change of parameter δ takes place with a discontinuity at $\delta = \delta_*$; here there exists the largest value of steady heating up.

Analysis shows that with burning out of the substance ($\gamma \neq 0$) a mathematical discontinuity, dividing these two conditions, does not exist. Transition from one regime to the other during change of δ (or of other parameters) occurs continuously, where the greater the

*So that system (1.1)-(1.2) describes the behavior of a reaction of zero order, it is sufficient in the second equation to formally set $\gamma = 0$.

burning out (the greater γ), the wider the transitional region [2]. By the actual meaning of the phenomenon, a thermal explosion corresponds to a narrow transitional region, which is observed usually for γ of the order of 10^{-2}-10^{-3}. In Fig. 1 is a typical picture of $\theta(\tau)$ for different δ. The presence of a transitional region leads to the necessity of certain more precise definitions of determinations of basic characteristics of a thermal explosion.

1°. Preexplosion heating up — a characteristic, obtained in steady-state theory for reaction of zero order (maximum steady-state heating up of a system). According to steady-state theory [1, 8, 9] we have $1 \leq \theta_* \leq 1.6$. From analysis of an unsteady-state system of equations with allowance for burning out it follows that such a characteristic, strictly speaking, does not exist. The magnitude of the maximum value of heating up $\theta_m(\xi, \tau)$ with increase of δ continuously increases (Fig. 2) and here becomes larger than θ_*. However, heatings up $\theta_m > \theta_*$ occur in a very narrow range of variation of parameter δ and in concrete cases are realized comparatively rarely. In this connection observation of maximum heatings during experimental research of thermal explosion and comparison of them with preexplosion heatings, determined by steady-state theory, are always useful. Thus, for instance, systematic observation of excessive heating during research of the thermal explosion of Tetryl in a melted state allowed us to establish complex convection mechanism of heat transfer in the reaction zone, caused by mixing of the liquid phase by bubbles of the products of decomposition [10].

2°. Critical criterion (or limit of self-ignition) is relationship between parameters of the system $\delta_*(n, B, \gamma, \beta)$, separating two regimes of the reaction. Since transition from one regime to the

other occurs continuously, as δ_* it is possible to select a value of δ, corresponding to the bend in curve $\theta_m(\delta)$ (Fig. 2).

3°. Induction period. In the literature there is upheld the definition according to which by the induction period we understand the time of achieving of preexplosion heating up (see, e.g., [2, 5, 6]). Here, it is assumed that the time of flow of a process when $\theta > \theta_*$ is considerably less than the induction period. This definition is inaccurate, since, first, preexplosion heating up, as such, does not exist, and therefore, the time of its achievement θ_* will not be a characteristic quantity, and second, the time of the process when $\theta > \theta_*$ cannot be ignored (Fig. 1, Table 1).

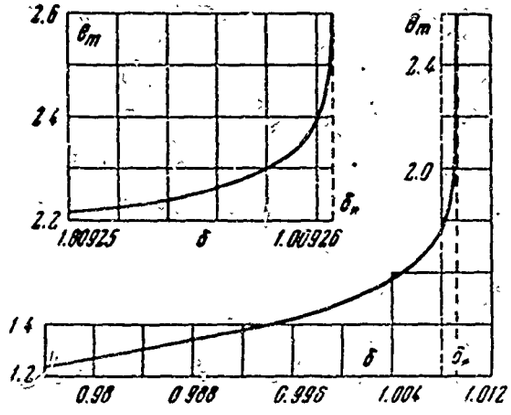

Fig. 2. Dependence $\theta_m(\delta)$ when $n = 1$, $\beta = 0.03$, $\gamma = 0.005$, $B = 2$.

It is more correct to characterize induction period by time τ_0 of achievement of the maximum velocity of nonisothermal reaction. Such a definition* allows us to trace the rules of change of the induction period in transition conditions (Fig. 3). Dependence $\tau_0(\delta)$ has a maximum, corresponding to δ_*. When $\delta \to \delta_*$ (from both sides) τ_0 sharply increases, seeking its maximum value τ_*. Quantity τ_* strongly depends on γ and when $\gamma = 0$ (zero order of reaction), as noted by D. A. Frank-Kamenetskiy** [3], $\tau_* \to \infty$.

---

*When $\delta > \delta_*$ in the interval of change of γ shown above, for τ_0 with error not worse than 1-2% it is possible to take a time of achievement $\theta = 5$, convenient for practical computation.

**In works [2, 4] they incorrectly obtained finite values τ_* for a reaction of zero order.

It is necessary to note that in the considered case of simple non-self-accelerated reactions τ_* is not a convenient characteristic of thermal explosion, since during experimental research, thanks to the very sharp dependence $\tau_0(\delta)$ near the limit, it is practically impossible to find τ_*.

Table 1. Difference $\Delta\tau$ Between Time of Achieving $\theta = 5$ and $\theta = 1.2$ Depending upon δ for $n = 0$; $\gamma = 0.005$, $B = \infty$.

δ	τ_5	$\tau_{1.2}$	$\Delta\tau$, %
1.5	1.02	0.7	31
1	1.1	0.74	33
0.95	4.1	2.31	44
0.948	8	3.4	57
0.948	9.3	3.45	63

4°. Degree of preexplosion reaction is a conditional characteristic, sometimes introduced in consideration for estimating burning out of the substance during the induction period, which near the limit, as can be seen from Fig. 4, can attain comparatively great values. Let us note that the degree of preexplosion reaction, as a characteristic, has clear meaning in the framework of the theory of quasi-steady thermal explosion [11].

3. Dependence of δ_* on all parameters (1.4) with a degree of accuracy* fully sufficient for practical calculations (±10%) can be presented in the form

$$\delta_* = \delta_0 \varphi_1(B)\,\varphi_2(\gamma)\,\varphi_3(\beta)$$

$$\varphi_1(B) = \frac{B}{2}\left(\sqrt{B^2+4} - B\right)\exp\frac{\sqrt{B^2+4}-B-2}{B} \qquad (3.1)$$

$$\varphi_2(\gamma) = 1 + 2.4\gamma^{1/2}, \qquad \varphi_3(\beta) = 1 + \beta$$

Here δ_0 is the value δ_*, obtained by D. A. Frank-Kamenetskiy in steady-state theory ($n = 0$, $\delta_0 = 0.88$; $n = 1$, $\delta_0 = 2.00$; $n = 2$, $\delta_0 = 3.32$).

Function φ_1 is obtained from the steady-state boundary value

*Determination of δ_* with the help of a computer was conducted with error, not exceeding 5%.

problem [9]; function φ_2 expresses correction for burning out during the induction period; the form of this function was approximately obtained by D. A. Frank-Kamenetskiy [3]; as a result of solution of system (1.1)-(1.2) the coefficient before γ was somewhat definitized (2.4 instead of 1.39); function φ_3 was obtained by the authors as a result of reworking the calculations of Parks [12]. Dependence (3.1) is checked in a large number of variants (more than 50); part of them is given in Table 2.

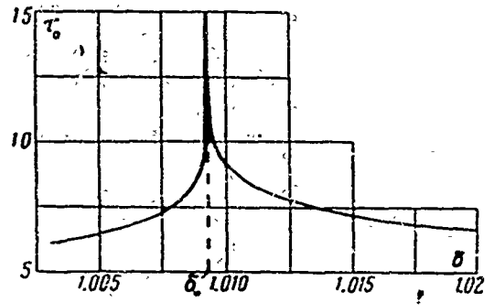

Fig. 3. Dependence $\tau_0(\delta)$ when n = 1, β = 0.03, γ = 0.005, B = 2.

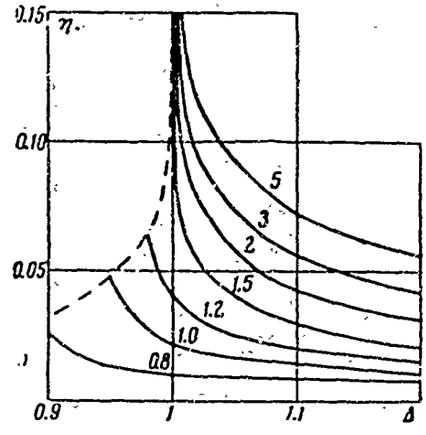

Fig. 4. Degree of conversion η, corresponding to different temperatures depending upon Δ. Dotted curve — η, corresponding to maximum of temperature.

Table 2. Dependence of δ_* on Different Parameters.

n	B	$\gamma \cdot 10^3$	$\beta \cdot 10^3$	δ_* (per 3.1)	δ_* (computer)	Error %
0	0.001	5	0	0.00035	0.00037	5.4
0	0.5	5	0	0.15	0.16	6.3
0	2	1	3	0.43	0.43	0
0	10	10	5	0.85	0.87	2.3
0	20	5	0	0.85	0.84	1.2
0	∞	1	3	0.93	0.92	1.1
0	∞	5	0	0.94	0.94	0
0	∞	10	5	1.03	1.04	1
1	0.01	5	0	0.0078	0.0079	1.3
1	0.05	5	0	0.039	0.039	0
1	0.1	5	0	0.077	0.077	0
1	1	10	3	0.66	0.67	1.5
1	5	1	5	1.5	1.48	1.3
1	20	0	1	1.83	1.80	1.7
1	∞	1	5	2.15	2.14	0.5
1	∞	5	0	2.14	2.15	0.5
1	∞	10	3	2.29	2.31	1
2	0.01	5	0	0.013	0.012	8.3
2	0.1	5	0	0.12	0.11	9
2	1	5	0	1.0	0.93	7.5
2	2	10	1	1.7	1.60	6.2
2	10	1	3	2.9	2.93	1
2	∞	0	5	3.5	3.45	1.5
2	∞	1	3	3.5	3.42	2
2	∞	5	0	3.6	3.54	1.8
2	∞	10	1	3.7	3.66	1.1

Thus, the influence of different parameters on the critical criterion with shown accuracy can be considered independent, which is very convenient for concrete calculations.

4. On the basis of numerical solutions of equations (1.1)-(1.2) we analyzed the dependence of τ_0 on all parameters of problem (1.5) in the shown range of variation of them. The character of this dependence is rather complicated: in this connection, to show the whole picture, it was necessary to conduct a rather large number of calculations. Part of them is given in Tables 3-6.

Table 3. Dependence of τ_0 on γ for Different $\Delta = \delta/\delta_*$ for $n = 1$, $\beta = 0$, $B = 0.01$.

Δ	$\gamma=0$	0.001	0.005	0,01
1.1	4.52	4.04	3.56	3.22
1.2	3.17	2.98	2.74	2.57
1.5	2.07	2.01	1.94	1.88
2.5	1.42	1.40	1.39	1.38
4	1.22	1.22	1.21	1.21
6	1.14	1.14	1.13	1.13
10	1.08	1.08	1.08	1.08

Table 4. Dependence of τ_0 on n for Different Values of Δ for $\beta = 0$, $B = \infty$, $\gamma = 0.005$.

Δ	$n=0$	1	2
1.1	3.35	3.07	2.81
1.2	2.57	2.35	2.15
1.5	1.80	1.65	1.51
2.5	1.28	1.19	1.12
4	1.12	1.06	1.03
6	1.06	1.02	1.01
10	1.02	1.01	1.01

Table 5. Dependence of τ_0 on B for Different Δ for $\gamma = 0.005$, $n = 1$, $\beta = 0$.

Δ	$B=0.01$	0.1	0.5	1	5	10	∞
1.1	3.56	3.56	3.53	3.4	3.1	3.07	3.07
1.2	2.74	2.74	2.71	2.63	2.36	2.35	2.35
1.5	1.94	1.94	1.91	1.85	1.66	1.65	1.65
2.5	1.39	1.38	1.36	1.32	1.20	1.19	1.19
4	1.21	1.21	1.18	1.14	1.07	1.06	1.06
6	1.13	1.13	1.10	1.07	1.03	1.03	1.02
10	1.08	1.08	1.05	1.03	1.15	1.01	1.01

From the tables it is clear that the induction period is most strongly influenced by parameter δ. The influence of the other parameters is significantly weaker. We shall discuss the influence of each of the parameters.

The dependence of τ_0 on δ. The form of dependence $\tau_0(\delta)$ was known long ago. As follows from the works of Todes [2], with increase of δ, τ_0 drops, approaching its least value — the induction period in

adiabatic conditions τ_a. Dependence $\tau_0(\delta)$ is conveniently presented in form $\tau_0(\Delta)$, where $\Delta = \delta/\delta_* -$ relative distance from the limit of self-ignition. With such a presentation it is easier to comprehend the character of the influence of other parameters, and also to select approximate formulas.

The dependence of τ_0 on γ is especially noticeable near the limit. With increase of δ it weakens and when $\Delta > 7$ it is practicall absent.

The dependence of τ_0 on β in accordance with the concepts of D. A. Frank-Kamenetskiy is weak and has a purely correcting character.

The dependence of τ_0 on n and B. Solution of system of equations (1.1)-(1.2) in partial derivatives allows us to consider the question of the dependence of τ_0 on the shape of the vessel and conditions of heat exchange on the surface, which in principle was impossible in theories using the assumption of the absence of distribution of temperature in the reaction zone. From Fig. 5 and Table 5 it is clear that dependence $\tau_0(B)$ has two limiting cases as $B \to 0$ and as $B \to \infty$. With identical distance from the limit (Δ = const) the induction period is less; the more intense the heat transfer. The shape of the vessel affects the induction period analogously. The larger the surface-to-volume ratio, the more intense (for identical B) the heat removal, and the less the induction period. Minimum τ_0, other things being equal, is obtained in a spherical vessel. For large Δ, when (just as for small B) temperature distribution is insignificant, the dependence of τ_0 on n and on B disappears.

Table 6. Dependence of τ_0 on β When γ = = 0, n = 1, B = ∞.

β	$\Delta = 2$	∞
0	1.34	1
0.01	1.37	1.02
0.03	1.42	1.07
0.05	1.49	1.11

Calculations of the induction period were conducted with error, not exceeding 5%. All obtained results in interval $1.1 \leq \Delta \leq 10$ could be described with the same accuracy by approximate formula

$$\tau_0 = \tau_a(\beta) f_1(\Delta, \gamma) f_2(n, B, \Delta), \qquad \tau_a(\beta) \quad 1 \quad 23 \tag{4.1}$$

Here τ_a – adiabatic induction period, practically not depending on γ in the selected range of variation of γ. Function

$$f_1(\Delta, \gamma) = 1 - 0.62 \frac{1 - 4\Delta^{-2}\sqrt{\gamma}}{(\Delta - 0.95)^{0.9}} \tag{4.2}$$

does not depend on n and B and describes basic variation of τ_0 from Δ in limiting case $B \to 0$ for different γ; function

$$f_2(n, B, \Delta) = 1 - \frac{[1 + 1.5(1 - 0.1\Delta)n]B}{16(1 + B)} \tag{4.3}$$

describes change of the induction period due to shape and heat exchange. The dependence on Δ here has a corrective character.

5. In connection with these results the question of the possibility of using the well-known ([2, 3, 4, 6] and others) system of equations, written on the assumption of constancy of temperature in the reaction volume is of interest. Such a system of equations in the designations used here has the form

$$\frac{d\theta}{d\tau} = \varphi(\eta) \exp \frac{\theta}{1 + \beta\theta} - C\theta, \qquad \frac{d\eta}{d\tau} = \gamma\varphi(\eta) \exp \frac{\theta}{1 + \beta\theta} \tag{5.1}$$

When using this system two approaches are possible. Either it is assumed that temperature distribution in the system is lacking for physical reasons (for instance, purely convective heat transfer in the substance, weak heat emission) and then notation of equations (5.1) does not contain additional assumptions, and constant C is expressed through the coefficient of heat transfer α, which has the clear meaning of the coefficient of heat emission from the surface of the reaction volume to the environment, and other parameters are as follows: $C = \frac{\alpha S R T_0^2}{Q E V k_0} \exp \frac{E}{R T_0}$

Here S – surface, and V – volume.

Or the notation of system (5.1) is treated as a certain approximation (averaging by volume), i.e., the mathematical method for facilitating solution of system (1.1)-(1.2). In this case with the following definition of averaging

$$\langle \psi \rangle = \int_0^1 \psi \xi^n d\xi$$

we imply two assumptions

$$\left\langle \varphi(\eta) \exp \frac{\theta}{1+\beta\theta} \right\rangle = \varphi(\langle\eta\rangle) \exp \frac{\langle\theta\rangle}{1+\beta\langle\theta\rangle}, \qquad \left(\frac{\partial\theta}{\partial\xi}\right)_{\xi=1} = C_1\langle\theta\rangle$$

Furthermore, it is necessary from independent considerations to determine the constant. Frank-Kamenetskiy offered [1] a method of finding constant C_1 by using findings of the steady-state theory of thermal explosion, namely

$$C_1 = c\delta_0$$

It is obvious that the solution of system (5.1) for finding which it is necessary to assign only the initial condition, should completely coincide with the solution of system (1.1)-(1.2) with the same initial conditions and for $B \to 0$ in boundary condition (1.3). For comparison we solved system (5.1) and system (1.1), (1.2) for $B = 0.01$. Coincidence of solutions in a wide range of variation of different parameters is within the limits of accuracy of calculation.

The structure of formula (4.1) for the induction period, in connection with this, can be treated as follows.

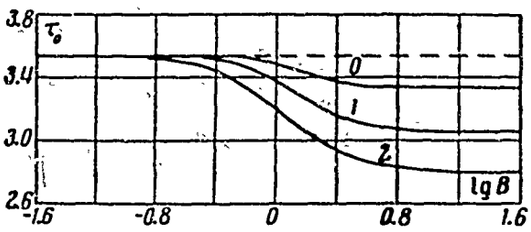

Fig. 5. Dependence $\tau_0(B)$ for three vessel shapes (n = 0, 1, 2) when $\Delta = 1.1$, $\beta = 0$, $\gamma = 0.005$.

Function $\tau_0 = \tau_a(\beta) f_1(\Delta, \gamma)$ (see (4.1), (4.2)) can be considered the result, obtained from solution of averaged system (5.1), and function $K = f_2(n, B, \Delta)$ (see (4.3)) constitutes a factor, showing how much τ_0, calculated

from the averaged system, is larger than τ_0 obtained from the system of partial differential equations, and is in point of fact the criterion of possibility of use of the averaged system for calculations of the induction period. As can be seen from (4.3) and Fig. 5, the biggest divergence is attained at $n = 2$, $B \to \infty$, and $\Delta \to 1$.

It is possible to offer another method of averaging system (1.1)-(1.2), containing only one assumption and free of the necessity of using findings of steady-state theory — the so-called weighted averaging.

Let us consider this method in the example of a reaction of zero order for $\beta = 0$.

Equation (1.1) for arbitrary three-dimensional region G with surface S will be written as follows:

$$\frac{\partial \theta}{\partial \tau} = \exp \theta + \frac{1}{\delta} \nabla^2 \theta \qquad (5.2)$$

The initial condition is $\tau = 0$, $\theta = 0$; the boundary condition is $\partial\theta/\partial n = -B\theta$ on surface S.

We average equation (5.2) with weight $(\xi_1; \xi_2; \xi_3)$ ($\xi_1; \xi_2; \xi_3$ — coordinates); u_0 will be the first eigenfunction of equation $\nabla^2 u + \lambda u = 0$ with boundary conditions on surface S $du/dn = -Bu$. We normalize u_0 so that

$$\int_{(G)} u_0 \, dV = 1 \quad (dV \text{ — an element of the volume}).$$

The law of averaging will be written as follows

$$\langle \theta(\tau) \rangle = \int_{(G)} \theta(\xi_1; \xi_2; \xi_3; \tau) \, u_0 dV$$

After simple computations, averaging equation (5.2), we obtain

$$\frac{d\langle \theta \rangle}{d\tau} = \int_{(G)} u_0 \exp \theta dV - \frac{\lambda_0}{\delta} \langle \theta \rangle$$

where λ_0 — corresponding eigenvalue. Function $\exp \theta$ — convex function,

and $\exp\theta \geq (1 + \theta - \langle\theta\rangle)\exp\langle\theta\rangle$; therefore, assuming

$$\int_V u_0 \exp\theta\, dV = \exp\langle\theta\rangle \qquad (5.3)$$

we obtain averaged equation

$$\frac{d\langle\theta\rangle}{d\tau} = \exp\langle\theta\rangle - \frac{\lambda_0}{\delta}\langle\theta\rangle$$

with initial condition $\langle\theta(0)\rangle = 0$. Here there is error of the order of

$$\int_{(G)} \frac{(\theta - \langle\theta\rangle)^2}{2} \exp\langle\theta\rangle\, dV$$

The critical criterion in this case, obviously, is written $\langle\delta_*\rangle = \lambda_0/e$ (the sign of averaging $\langle\ \rangle$ means that δ_* is obtained from the averaged system); $\langle\delta_*\rangle$ is somewhat overstated, since by assumption (5.3) the source is somewhat weakened. For greater detail on such estimates see [13]. Let us note that if we analyze results on induction periods in the form $\tau_0(\Delta)$, the values of τ_0 obtained from both methods of averaging coincide.

It is possible to show that averaging of equations in the problem taking into account burning out and also for $\beta \neq 0$ requires no new assumptions.

Submitted
23 January 1964

Literature

1. D. A. Frank-Kamenetskiy. Distribution of temperatures in a reaction vessel and the steady-state theory of thermal explosion. Journal physical chemistry, 1939, Vol. 13, Issue 6.

2. O. M. Todes. Theory of thermal explosion. Journal of phys. chem., 1939, Vol. 13, Issue 7; O. M. Todes and A. V. Melent'yev. Theory of thermal explosion, II. Journal of phys. chem., 1939, Vol. 13, Issue 11.

3. D. A. Frank-Kamenetskiy. A non-steady-state theory of thermal explosion. Journal of phys. chem., 1946, Vol. 20, Issue 2.

4. P. Gray and M. J. Harper. Thermal explosions. Trans. Far. Soc., 1959, Vol. 55.

5. T. Kinbara and K. Akita. An approximate solution of the equation for self-ignition. Combustion and Flame, 1960, 4, p. 173.

6. P. H. Thomas. Effect of reactant consumption on the induction period and critical condition for a thermal explosion. Proc. Roy. Soc., 1961, A 262, p. 192.

7. J. Zinn and C. I. Mader. Thermal Initiation of explosives. J. Appl. Phys., 1960, Vol. 31, No. 2.

8. N. N. Semenov. Thermal theory of burning and explosions. Progress of physical sciences, 1940, Vol. 23, Issue 3.

9. V. V. Barzykin and A. G. Merzhanov. Boundary value problem in the theory of thermal explosion. Reports of Academy of Sciences of USSR, 1958, Vol. 120, Issue 6.

10. A. G. Merzhanov, V. G. Abramov, and F. I. Dubovitskiy. Critical conditions of thermal explosion of Tetryl. Reports of Academy of Sciences of USSR, 1959, Vol. 128, Issue. 6.

11. A. G. Merzhanov and F. I. Dubovitskiy. Quasi-steady-state theory of thermal explosion of self-accelerated reactions. Journal of phys. chem., 1960, Vol. 34, Issue 10.

12. J. R. Parks. Criticality criteria for various Configuration of Self-heating Chemical as Function of activation Energy and Temperature of Assembly. J. Chem. Phys., 1961, Vol. 34, Issue 1.

13. S. I. Khudyayev. Boundary value problems for certain quasi-linear elliptic equations. Reports of Academy of Sciences of USSR, 1964, Vol. 154, Issue 4.

THE BURNING VELOCITY OF POWDER UNDER VARIABLE PRESSURE*

Ya. B. Zel'dovich

(Moscow)

With a powder burning in solid phase there will form a heated layer; thickness of the layer depends on the burning velocity; in turn the burning velocity is connected with the temperature profile in the heated layer. One can expect that during rapid change of pressure the heated layer can not reconstruct itself in time, and the burning velocity turns out to depend not only on the instantaneous pressure, but also on the curve of its change. We trace the dependence of burning velocity on pressure during rapid changes of pressure for certain cases.

In the theory of burning of powder, developed since 1942 [1], it was shown that the relaxation time of processes occurring in a gas is minute compared to the relaxation time (time of change) of distribution of heat in powder. Therefore, if we limit our consideration to intervals of time, significant as compared to the relaxation time of processes in a gas, we can assume that the state of the gas layer nearest to the surface, in which the chemical reaction is concentrated, each moment is in accordance with the thermal state of the thin layer of the k-phase (powder) nearest to the interface; distribution of temperature in deeper layers does not have a direct influence on the process occurring at the surface. If, furthermore, we assume that the zone of gasification of the solid substance is very narrow and that gasification occurs with constant temperature (this corresponds to a reaction with very great activation energy), the relaxation time of the zone of gasification of powder also can be ignored, and we can relate the zone of gasification to the layer of gas above the surface

*Published from materials of a report to the Institute of Chemical Physics, Academy of Sciences of USSR in 1944.

of the powder. The thermal state of the part of the heated layer nearest to the surface of the powder here should be completely determined by only one magnitude — the temperature gradient at the surface. This quantity characterizes the transfer of heat from the gas and the zone of gasification into the heated layer of powder. Thus, at each moment the burning velocity is determined by the current value of pressure above the surface of the powder and the magnitude of the temperature gradient at the surface φ:

$$u = u(p, \varphi) \tag{0.1}$$

Quantity φ, just as the whole distribution of temperature in the powder, depends on those actions, which the powder experienced up to the considered moment; this distribution we find by solving the problem of thermal conduction for a body, extended in one direction and limited in the other direction by a surface of given temperature T_k (temperature of gasification), moving by a given law

$$x = x(t), \qquad dx/dt = u(t) \tag{0.2}$$

§ 1. Steady-state regime and the limit. In the frequent, most important case, when the burning velocity is kept constant for a prolonged interval of time, quantity φ seeks a definite limit, depending on the burning velocity and the initial temperature of the powder T_0

$$\varphi_c = \varphi_c(u, T_0) = \frac{u}{\varkappa}(T_k - T_0) \tag{1.1}$$

where $\varkappa$ — coefficient of thermal diffusivity of the powder.

Substituting this expression for φ in (0.1), we obtain an expression for determining that unique value of velocity, for a given pressure and initial temperature, which should be realized during prolonged maintenance of a given pressure: this state of burning we call a steady-state regime and we denote quantities pertaining to it by subscript c:

$$u_c = u[p, \varphi_c(u, T_0)] \tag{1.2}$$

$$u_c = u_c(p, T_0) \tag{1.3}$$

The steady-state regime obeys simple relationships, which follow from equations of conservation; therefore, $u_c(p, T_0)$ can be directly expressed through p and T_0, thermal and kinetic properties of the

powder and products of its gasification without the help of equations (0.1), (1.1), and (1.2).

Dependence (1.3) we shall subsequently consider fixed by the corresponding experiments, in which burning velocity was measured at constant or sufficiently slowly changing pressure and with different values of T_0. We shall use this dependence of u on p and T_0, fixed by experiment, in order to determine the dependence of velocity u on pressure and the temperature gradient φ (see formula (0.1)); the temperature of gasification T_k we consider known and constant.

In reality measurement or calculation of T_k is a difficult problem. For its solution it is necessary to investigate the thermal decomposition of powder at high temperature, when this decomposition proceeds with great velocity. Constancy of T_k also, strictly speaking, does not occur. Quantity T_k should be such that it ensures a velocity of gasification which is equal to the burning velocity. However, due to the very strong dependence of the gasification velocity on temp rature with high activation energies (doubling of velocity during change of T_k by $\sim 5^\circ$), significant change of the burning velocity causes only small change of T_k, due to which it is possible to consider T_k constant.

Having a table of measured values of $u_c(p, T_0)$ for different p and T_0, by formula (1.1) we calculated for each pair of values of p and T_0 the magnitude of gradient φ; comparing quantities u, p and φ pertaining to this experiment, we obtain a table, expressing dependence (0.1).

For T_0, close to T_k, the burning velocity seeks a definite limit u_k; magnitude φ_c, according to (1.1), here is close to zero.

Direct observation of u_k is hindered by the rapid decomposition of powder at a temperature, close to T_k; quantity u_k can be found by extrapolation to T_k of the dependence of u on T_0, measured at lower temperatures. Both theoretical considerations, and also, experimental material shows that the burning velocity does not increase without limit as T_0 approaches T_k.

With decrease of T_0 there occurs growth of φ due to increase of $T_k - T_0$; this growth is delayed by simultaneous drop of velocity u. (Lowering of T_0 decreases the temperature of burning of the powder T_b; burning velocity depends on T_b as exp $(-E/2RT_b)$.) That value of T_0 at which φ reaches a maximum is the natural limit of steady-state burning; this condition is easily formulated mathematically (all derivatives are at constant pressure)

$$\frac{\partial \varphi_c}{\partial T_0} = \frac{T_k - T_0}{\varkappa}\left(\frac{\partial u_c}{\partial T_0}\right)_p - \frac{u_c}{\varkappa} = 0, \quad \frac{1}{u_c}\left(\frac{\partial u_c}{\partial T_0}\right)_p = \frac{1}{T_k - T_0} \tag{1.4}$$

In [1] the theory of a limit was considered with definite assumptions about the form of dependence $u_c(p, T_0)$, connected with chemical kinetics of a burning reaction. The advantage of formulation (1.4) will be the use of only one constant T_k in addition to the experimentally studied dependence $u_c(p, T_0)$.

Subsequently, we shall assume that we are above the limit, with such a T_0 at which steady-state burning at constant pressure is stable and possible, for which we should have inequality

$$\frac{1}{u_c}\left(\frac{\partial u_c}{\partial T_0}\right)_p < \frac{1}{T_k - T_0} \tag{1.5}$$

Simultaneously, formula (1.4) allows us to determine the actual maximum value of φ at which (at a given pressure) burning in the gas phase is possible; for that we put the value of T_0, found from (1.4),

and the corresponding u_c in formula (1.1). This maximum value of the gradient, earlier [1] designated φ_B, plays an important role: for ignition of powder it is necessary to heat it in such a manner that at surface temperature T_k the gradient is less than φ_B. Conversely, if in the course of burning we reach gradient $\varphi > \varphi_B$ (for instance, due to a drop in pressure, causing decrease of φ_B), there occurs extinguishing of the powder, and burning ceases. Expression (1.5) is general. Considering constant the derivative

$$\frac{1}{u_c}\left(\frac{\partial u_c}{\partial T_0}\right)_p = \left(\frac{\partial \ln u_c}{\partial T_0}\right)_p = \beta \tag{1.6}$$

we find the dependence of u_c on T_0 by integrating (1.6)

$$u_c(T_0) = \text{const}\, e^{\beta T_0} \tag{1.7}$$

Inequality (1.5) in this case we can rewrite as

$$\beta (T_k - T_0) < 1 \tag{1.8}$$

$$u_k/u_c = e^{\beta (T_k - T_0)} < e \tag{1.9}$$

$$u_c > u_k/e = 0.37 u_k \tag{1.10}$$

In the latter form the condition of stability of burning was also found in [1] with certain assumptions about the kinetics of the reaction of burning, which approximately led to a dependence of form (1.7).

Substituting expressions T_0 and u_c at the limit of stability in (1.1), we determine the critical value of the gradient:

$$\varphi_B = \frac{u_k}{3xe} \tag{1.11}$$

The ratio of the critical gradient φ_B to the steady-state one at a given pressure depends on the product $\beta(T_k - T_0)$, determining the "margin of steadiness" of burning

$$\frac{\varphi_B}{\varphi_c} = \frac{1}{\beta (T_k - T_0)} e^{[\beta (T_k - T_0) - 1]} \tag{1.12}$$

§ 2. Very rapid change of pressure. Formula (1.3) for constant T_0 gives the dependence of burning velocity on pressure for very slow change of pressure and complete reconstruction of the layer. In the opposite extreme case of very rapid change of pressure the layer absolutely does not succeed in being reconstructed; thus, the sought dependence of u on p for very rapid changes of p is given by function $u(p, \varphi)$ (formula (0.1)) for constant φ. The method of transition from $u_c(p, T_0)$ to $u(p, \varphi)$ described in the preceding section in principle completely solves this problem. Along with the functional dependence, of great interest is comparison of partial derivatives

$$\left(\frac{\partial u_c}{\partial p}\right)_{T_0}, \quad \left(\frac{\partial u_r}{\partial p}\right)_{\varphi}$$

We compose the expression of the total differential of (1.3) and (1.1)

$$du = \left(\frac{\partial u}{\partial p}\right)_{T_0} dp + \left(\frac{\partial u}{\partial T_0}\right)_p dT_0 = \nu \frac{u}{p} dp + \beta u dT_0 \tag{2.1}$$

$$d\varphi = \frac{T_k - T_0}{\varkappa} du - \frac{u}{\varkappa} dT_0 = \frac{\varphi}{u} du - \frac{\varphi}{T_k - T_0} dT_0$$

$$= \nu \frac{\varphi}{p} dp - \left(\frac{1}{T_k - T_0} - \beta\right) \varphi dT_0 \tag{2.2}$$

Here the following designations are introduced:

$$\nu = \frac{p}{u}\left(\frac{\partial u}{\partial p}\right)_{T_0} \quad \left(\frac{\partial \ln u}{\partial \ln p}\right)_{T_0} \tag{2.3}$$

$$\beta = \frac{1}{u}\left(\frac{\partial u}{\partial T_0}\right)_p \quad \left(\frac{\partial \ln u}{\partial T_0}\right)_p \tag{2.4}$$

Quantity ν constitutes the value of the exponent in the exponential law of burning: considering

$$u = u_1 p^{\nu} \tag{2.5}$$

we directly obtain the equation written above for ν. However, the calculation is not based on the special assumption of correctness of the exponential law of burning, since the assumption that ν is constant is not obligatory; expression (2.3) for ν we can write for any law with this difference only, that with a law of burning, differing from (2.5), exponent ν is variable. Thus for a linear law we find

$$u \quad a + bp, \qquad v \cdot \frac{p}{u}\frac{\partial u}{\partial p} = \frac{bp}{a+bp} \tag{2.6}$$

Magnitude of the temperature coefficient of the burning velocity β we also do not consider constant, and, thus, we are not limited to a particular case of any definite dependence of u on T_0.

With the help of (2.2) we express dT_0 by dp and $d\varphi$ and substitute in (2.1). We find, after simple transformations,

$$du = \frac{v}{1-\beta(T_k-T_0)}\frac{u}{p}dp - \frac{\beta(T_k-T_0)}{1-\beta(T_k-T_0)}\frac{u}{\varphi}d\varphi \tag{2.7}$$

Comparing (2.7) with the expression of the total differential

$$du = \left(\frac{\partial u}{\partial p}\right)_\varphi dp + \left(\frac{\partial u}{\partial \varphi}\right)_p d\varphi \tag{2.8}$$

we find

$$\left(\frac{\partial u}{\partial p}\right)_\varphi = \frac{v}{1-\beta(T_k-T_0)}\frac{u}{p} \tag{2.9}$$

or

$$\left(\frac{\partial \ln u}{\partial \ln p}\right)_\varphi \quad \frac{p}{u}\left(\frac{\partial u}{\partial p}\right)_\varphi \quad \frac{v}{1-\beta(T_k-T_0)} \tag{2.10}$$

$$\left(\frac{\partial u}{\partial \varphi}\right)_p \quad -\frac{\beta(T_k-T_0)}{1-\beta(T_k-T_0)}\frac{u}{\varphi} \tag{2.11}$$

Formulas (2.9) and (2.10) respond to the question of the law of change of burning velocity during very rapid change of pressure; in this case, for constant φ, the derivative of velocity with respect to pressure turns out to be larger with respect to $1/[1 - \beta(T_k - T_0)]$ as compared to the derivative of velocity with respect to pressure during slow change of pressure. In that same respect the effective value of the exponent in the exponential law during rapid change of pressure also increases. As can be seen from the formulas, quantity $\beta(T_k - T_0)$, which we encounter in the theory of the limit of stability of burning (formulas (1.5)-(1.8)), also plays a role here. The closer to the limit the system is — condition of limit $\beta(T_k - T_0) = 1$ — the more labile it is, and the greater the changes of velocity caused

by rapid change of pressure.

As we know, in the internal ballistics of reactive systems the value of the exponent of the law of burning has greatest significance; for the possibility of steady burning in a semiclosed volume it is necessary that $\nu < 1$. From what has been said it is clear that powder, satisfying this condition during slow change of pressure, may, during rapid change of pressure, give an effective exponent larger than one.

In a semiclosed volume under conditions which allow rapid change of pressure it is possible to expect unsteady burning. Steadiness of the burning regime of powder in the chamber of a missile was considered in detail by the author using the method of small perturbations [2]. In this work we also obtained formulas (2.7)-(2.11).

Finally, on the assumption of a constant temperature coefficient of burning velocity β and constant exponent ν, we find how many times pressure should instantaneously drop so that extinguishing occurs.

From this we formulate such a condition: gradient $\varphi(p_1)$, which corresponds to steady-state burning with initial pressure p_1, should be equal or larger than the critical gradient $\varphi_B(p_2)$, causing extinguishing at pressure p_2. Using (1.12), (1.1), and (2.5), we find

$$\left(\frac{p_1}{p_2}\right)^{\nu} = \frac{1}{\beta(T_k - T_0)} e^{\beta(T_k - T_0)-1} \qquad (2.12)$$

We give ratio p_1/p_2, calculated on the assumption that $\nu = 2/3$, for different values of $\beta(T_k - T_0)$:

$\beta(T_k - T_0)$	0	0.2	0.4	0.6	0.8	1.0
$(p_1/p_2)^{\nu}$	∞	2.25	1.38	1.12	1.025	1.0
p_1/p_2	∞	3.40	1.62	1.18	1.04	1.0

§ 3. Graphic presentation of relationships of the preceding paragraphs. The relationship derived above can be illustrated by diagrams, which facilitate understanding of the qualitative aspect of the matter.

In Fig. 1 is the distribution of temperature at the surface of the powder. Temperature gradient φ depends on the angle of inclination α of the tangent to the curve at point A($x = 0$, $T = T_k$, $\varphi = \operatorname{tg} \alpha$). In this figure there are shown two methods of determining the thickness of the layer. Strictly speaking, temperature only asymptotically seeks T_0 with increase of x, so that even at point E, far from the surface, the temperature, although slight, differs from T_0; therefore, we can speak about the thickness of the layer only conditionally. The first method of determining the conditional thickness consists in passing through point A a tangent and finding the point of intersection of C with line BCE, on which $T = T_0$($\Delta x_1 = (T_k - T_0)/\varphi$). The second method consists in constructing rectangle ABCD in such a manner that its area is equal to the area ABCE, bounded by curve T(x) and line $T = T_0$:

$$\Delta x_2 = \int_0^\infty \frac{(T - T_0)}{T_k - T_0} dx$$

In the considered case with temperature distribution (4.1) both definitions of Δx coincide and give $\Delta x = \varkappa/u$.

The distribution of temperature (Fig. 1) is obtained for prolonged maintenance of constant pressure and for a given constant temperature in the depth of the powder T_0. At the same pressure, but with a different temperature T_0', the powder will burn with another velocity, the distribution of temperature and the magnitude of gradient φ will be different. In Fig. 2 curves (a) and (b) give, accordingly,

dependences $u(T_0)$ and $\varphi(T_0)$ pressure-constant, corresponding to steady-state burning.

To bring T_0 to T_k is practically impossible due to the fact that the powder is rapidly decomposed already at a lower temperature; therefore, corresponding parts of the curves are shown by a dotted line.*

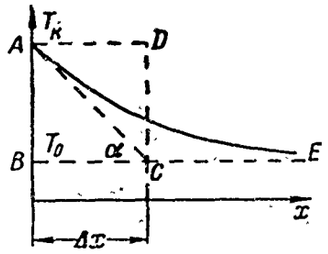

Fig. 1.

The value of velocity extrapolated to T_k is designated u_k.

Curve $\varphi_c(T_0)$ passes through a maximum with coordinates T_B, φ_B. The value of velocity corresponding to T_B is designated $u_B = u_c(T_B)$.

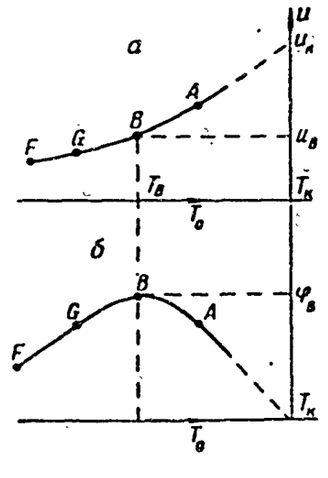

Fig. 2.

Let us construct a graph of u depending upon φ for a given pressure (Fig. 3); for that we take various values of T_0 and plot in plane uφ the corresponding $u(T_0)$ and $\varphi(T_0)$. This process is easily traced by points A, G, B. General considerations of theory show that the dependence of u on φ for a given pressure should be the same, regardless of whether the process as a whole is steady-state, i.e., regardless of the distribution of temperature in deeper layers of the powder and regardless of whether, in the course of burning, φ is kept constant. Figure 3 graphically shows that: 1) for $\varphi > \varphi_B$ there is no corresponding velocity, i.e., burning is impossible; and 2) for $\varphi < \varphi_B$ to each φ there corresponds two possible burning velocities (see, e.g., points A and G). Segment BG of the curves of Fig. 3 in reality is not realized and should be rejected. Consequently,

*We can get closer to temperature T_k during the study of burning of low boiling secondary explosives, e.g., methylnitrate.

steady-state burning is also impossible at temperature $T_0 < T_B$ (in Fig. 2 corresponding parts of curves BGF are obtained by extrapolation or calculation). How is one to conceive of this impossibility?

In Figs. 4 and 5 solid lines give the distributions of temperatures, corresponding to points A and G, at which φ are identical for different T_0 and u.

In regime A, to which Figure 4 corresponds, steady burning is stable; with passage of time the distribution as a whole shifts into the depth of the powder, and the width of the thermal layer and gradient φ are kept without change — see dotted curves of Fig. 4. In regime G steady burning would be possible, if it occurred with low velocity. But to gradient φ in this regime there also corresponds a second possible velocity — such as in regime A — since gradients are identical. There will be realized just this, high velocity; but distribution of temperature is not in accordance with high velocity, with burning the deep layers are not sufficiently heated, distribution becomes steeper and gradient φ grows. When it reaches φ_B, burning ceases. Thus, if one were to prepare a powder of very low temperature T_G for corresponding slow burning, creating for that a very deep heated layer (Fig. 5), in fact, instead of slow burning there will occur a fast flash, the heated layer will be expended, and the powder will extinguish.

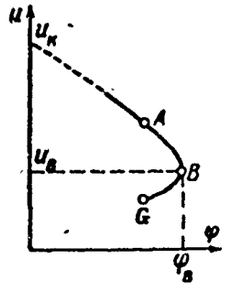

Fig. 3.

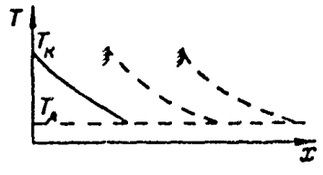

Fig. 4.

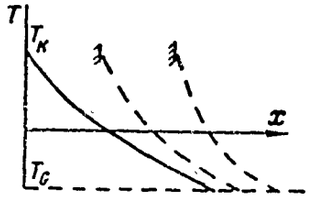

Fig. 5.

We plot on the same graph curves of $u(\varphi)$, pertaining to different pressures (Fig. 6); here, we depict only the practically realizable upper part of each curve.

Considering T_k constant, as we did in all calculations, we note that points describing steady burning at different pressures, but at one and the same initial temperature of the powder T_0, are located on straight lines, emanating from the origin of coordinates; from (1.1) it follows that ratio

$$\frac{u_c}{\varphi_c} = \frac{\varkappa}{T_k - T_0}$$

is constant on lines $T_0 = \text{const}$.

If, e.g., at a temperature of the powder T_0' pressure slowly increases from p_2 to p_1, the powder burns steadily at each pressure. In Fig. 6 the point depicting the regime of burning shifts from M to S (slow — slow change of pressure); increase of pressure is accompanied by growth of burning velocity and reconstruction of the layer, causing increase in the temperature gradient φ. Rapid change of pressure is accomplished without reconstruction of the layer, with constant φ; change of velocity is depicted by segment MR (rapid — rapid change of pressure). As can be seen from Fig. 6, increase of velocity here is great. At pressure p_1 in the first moment the powder burns as if its temperature is higher than it is in fact. The difference between change of velocity along a ray ($T_0 = \text{const}$) and along the vertical ($\varphi = \text{const}$) is minimal at T_0, close to T_k (ray $T_0 = T_k$ in Fig. 6 coincides with the axis of ordinates) and increases as we near the limit ($T_0 \to T_B$) in accordance with formula (2.10).

With decrease of pressure change (decrease) of velocity is also greater in the case of the rapid process than in the case of the

slow one. As can be seen from Fig. 6, during rapid pressure decay, for instance, from p_2 (point M) to p_4, we will find no solution; that φ, which was steady for p_2, exceeds maximum φ_B at pressure p_4. During slow change of pressure we cross at point L, corresponding to a steady-state regime of burning at pressure p_4. Thus, Fig. 6 explains extinguishing of powder with rapid pressure decay.

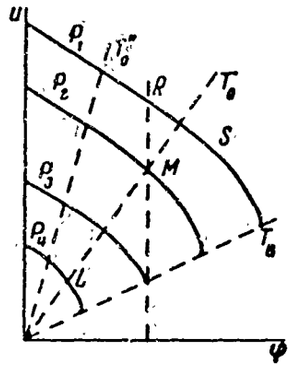

Fig. 6.

As can be seen from the figure, the higher the initial temperature of the powder, the lower should be the final pressure to achieve extinguishing (compare with data of § 2).

§ 4. Small changes of pressure. We formulate the problem of the law of change of burning velocity during arbitrary small changes of pressure. In this case change of the burning velocity and change of temperature distribution in the powder can also be considered small and we can limit ourselves to the first terms of the series of expansions.

With a constant burning velocity the temperature distribution in the heated layer of the powder (the examination is conducted in a system of coordinates, in which the surface of the powder shifts with constant velocity – burning velocity u_0) has the form

$$T = T_0 + (T_k - T_0)\exp\left[-\frac{u_0}{\varkappa}(x - u_0 t)\right] \qquad (4.1)$$

We find now the temperature distribution, which differs by a small component from distribution (4.1). The additional small component we also take in the form Ae^{mx+nt}. From heat conduction equation

$$\frac{\partial T}{\partial t} = \varkappa \frac{\partial^2 T}{\partial x^2} \qquad (4.2)$$

and boundary condition $T = T_0$ as $x \to \infty$ we find $n = \varkappa m^2$, $m < 0$.

Assigning the position of the surface of the burning powder as the surface on which $T = T_k$, we determine the law of motion of the burning surface (we consider A small):

$$x|_{T=T_k} = u_0 t + \frac{A}{T_k - T_0} \frac{\varkappa}{u_0} e^{(mu_0 + \varkappa m^2) t} \tag{4.3}$$

The burning velocity of the powder is

$$u = \frac{dx}{dt}\bigg|_{t=T_k} = u_0 + (mu_0 + \varkappa m^2) \frac{A}{T_k - T_0} \frac{\varkappa}{u_0} e^{(mu_0 + \varkappa m^2) t} \tag{4.4}$$

The temperature gradient at the surface of the powder is

$$\varphi = -\frac{dT}{dx}\bigg|_{T=T_k} = \frac{u_0}{\varkappa}(T_k - T_0) - A\left(\frac{u_0}{\varkappa} + m\right) e^{(mu_0 + \varkappa m^2) t} \tag{4.5}$$

Relationships (4.3)-(4.5) were also obtained in work [2], devoted to research of stability of burning of powder in a thrust chamber.

We denote by p_0, that pressure at which we have

$$u = u_0 \quad \text{when} \quad \varphi = \varphi_0 = \frac{u_0}{\varkappa}(T_k - T_0) \tag{4.6}$$

Then with the help of (2.8), (2.9), and (2.11) we find the law of change of pressure, substituting

$$du = \left(\frac{\partial u}{\partial \varphi}\right)_p d\varphi + \left(\frac{\partial u}{\partial p}\right)_\varphi dp, \qquad dp = \frac{du - (\partial u / \partial \varphi)_T d\varphi}{(\partial u / \partial p)_\varphi} \tag{4.7}$$

$$p - p_0 = \frac{u - u_0 - (\partial u / \partial \varphi)_T (\varphi - \varphi_0)}{(\partial u / \partial p)_\varphi}$$

$$p = p_0 + \frac{p_0}{u_0 \nu} \frac{\varkappa}{T_k - T_0} \left\{ m + \frac{\varkappa m^2}{u_0} [1 - \beta (T_k - T_0)] - \right. \tag{4.8}$$

$$\left. - \beta (T_k - T_0) \left(\frac{u_0}{\varkappa} + 2m \right) \right\} A \exp [(mu_0 + \varkappa m^2) t]$$

If we set

$$p = p_0 + Pe^{\omega t} \tag{4.9}$$

and express m and A in terms of ω and P, for velocity we find

$$u = u_0 + \frac{\nu u_0}{p_0} \frac{Pe^{\omega t}}{1 - \beta (T_k - T_0) (2\Omega + 1 - \sqrt{1 + 4\Omega})\ 2\Omega} \qquad \left(\Omega = \frac{\omega \varkappa}{u_0^2}\right) \tag{4.10}$$

Formula (4.10) is valid for any values, including complex or purely imaginary, of Ω; here the complex ratio of change of velocity to change of pressure indicates a phase shift between variations of

pressure and variations of burning velocity caused by them.

Formula (4.10) contains the limiting cases considered earlier:

$$u - u_0 = \nu \frac{u_0}{p_0}(p - p_0) \quad \text{when } \omega \to 0 \tag{4.11}$$

$$u - u_0 = \frac{\nu u_0 (p - p_0)}{p_0 [1 - \beta (T_k - T_0)]} \quad \text{when } \omega \to \infty \tag{4.12}$$

in accordance with (2.8)-(2.11).

Considering ω small,

$$\omega \ll \frac{u_0^2}{\varkappa}, \quad \Omega \ll 1 \tag{4.13}$$

we expand (4.10) in a series and remove the term, containing ω.

We find

$$u = u_0 + \frac{\nu u_0}{p} P e^{\omega t} + \frac{\nu u_0}{p_0} \frac{\omega \varkappa}{u_0^2} \beta (T_k - T_0) P e^{\omega t} \tag{4.14}$$

Noting that

$$u_0 + \frac{\nu u_0}{p_0} P e^{\omega t} = u_c (p), \qquad \frac{\nu u_0}{p} = \left(\frac{\partial u_c}{\partial p}\right)_{T_0}, \qquad \omega P e^{\omega t} = \frac{dp}{dt} \tag{4.15}$$

we rewrite (4.14) in final form

$$u = u_c (p) + \left(\frac{\partial u_c}{\partial p}\right)_{T_0} \beta (T_k - T_0) \frac{\varkappa}{u_c^2} \frac{dp}{dt} \tag{4.16}$$

or, substituting expression β in form (2.4),

$$u = u_c (p) + \left(\frac{\partial u_c}{\partial p}\right)_{T_0} \left(\frac{\partial u_c}{\partial T_0}\right)_p \frac{\varkappa (T_k - T_0)}{u_c^3} \frac{dp}{dt} \tag{4.17}$$

Formulas (4.16)-(4.17) give an answer to the question of deviation of velocity $u_c(p)$, obtained at the same pressure if we continue to keep this pressure constant. This deviation is proportional to the derivative of pressure with respect to time. It is easy to show that the formulas are applicable not only for a simple exponential (or harmonic, in the case of an imaginary ω) law of change of pressure in time, but also for any law p(t), since it is always possible to present it in form

$$p(t) = p_0 + \Sigma P_n e^{\omega_n t}$$

By virtue of linearity, each component in pressure gives a corresponding component in velocity. We recall, however, that all

calculations of this section are performed on the assumption that changes of pressure, velocity, and other variables are small, and in deriving (4.16)-(4.17) we were limited to the same low frequencies. Thus, formulas (4.16)-(4.17) are applicable only to a smooth curve of the pressure-time relationship, not containing high-frequency components (see condition (4.13)).

§ 5. Burning and extinguishing during dropping pressure. Solution of the problem of burning with variable pressure for any law of dependence $p(t)$ in the preceding section we found on the assumption of small changes.

Let us find by dimensional theory a criterion, determining the role of unsteady phenomena for any changes of pressure. On this criterion there should depend not only deviation of velocity from its steady-state value, but also the presence or absence of extinguishing of the powder, occurring with sufficiently rapid and deep pressure decay. The sought criterion should reflect the relationship between the rate of change of pressure and that time which is necessary in order that, after change of pressure, the thermal layer can be reconstructed in accordance with the new conditions of burning, i.e., the relaxation time.

The relaxation time τ of a heated layer of powder can be determined if we know its thickness Δx, the time during which a layer of such thickness $\tau = \Delta x/u$ burns, or the time of levelling off of temperature in a layer of given thickness $\tau = (\Delta x)^2/\varkappa$. Substituting expression $\Delta x = \varkappa/u$, which follows from the solution of thermal problem (4.1), one can prove that both determinations of relaxation time τ, given above, coincide and give

$$\tau = \frac{\varkappa}{u^2} \qquad (5.1)$$

The rate of change of pressure is characterized, obviously, by derivative dp/dt. In order to construct the dimensionless criterion, we compose the relative change of pressure for the relaxation time

$$B = \frac{\tau}{p}\frac{dp}{dt} = \frac{\varkappa}{u_c^2 p}\frac{dp}{dt} \tag{5.2}$$

Assuming we have an exponential law of burning $u_c = u_1 p^{\nu}$, we obtain another expression of the criterion:

$$B = \frac{\varkappa}{u_1^2}p^{-1-2\nu}\frac{dp}{dt} = -\frac{\varkappa}{2\nu}\frac{d(u_c^{-2})}{dt} \tag{5.3}$$

This criterion, and also dimensionless constants of the powder ν and $\beta(T_k - T_0)$ determine for unsteady phenomena the change of velocity and spontaneous combustion or extinguishing of the powder.

Derived above for small and slow changes of pressure, formula (4.16) can be recorded by the criterion B in the form

$$\frac{u}{u_c} = 1 + \nu\beta(T_k - T_0)B, \qquad |B| \ll 1 \tag{5.4}$$

For the case of falling pressure ($B < 0$) we solve the problem, considering any B (not small). Given a definite value of B, we should expect that

$$\frac{u}{u_c} = \psi(B) \tag{5.5}$$

will be a constant quantity, which it is necessary to determine. Constant B corresponds to a definite law of change of pressure, which we obtain by integration of (5.3)

$$p^{-2\nu} = -\frac{2\nu u_1^2 B}{\varkappa}t \tag{5.6}$$

From this we find the law of change of burning velocity

$$u = u_1 p^{\nu}\psi = \frac{\psi}{\sqrt{-2\nu B}}\sqrt{\frac{\varkappa}{t}} \tag{5.7}$$

and the law of motion of the burning surface

$$x = \int u\,dt = \frac{2\psi}{\sqrt{-2\nu B}}\sqrt{\varkappa t} = 2C\sqrt{\varkappa t} \qquad \left(C \equiv \frac{\psi(B)}{\sqrt{-2\nu B}}\right) \tag{5.8}$$

Thus, a constant negative value of B corresponds to motion of the burning surface in which the path covered is proportional to the square root of the time of motion. Solution of the equation of thermal conduction, in which temperature depends on ratio $x/\sqrt{\varkappa t}$ (in particular $T = T_k$ when $x/\sqrt{\varkappa t} = 2C$), we easily find by substituting $T = T(x/\sqrt{\varkappa t})$ in equation (4.2). Here (4.2) will turn into an ordinary differential equation. Solving the latter, we find

$$T = T_0 + D\left[1 - \operatorname{erf}\left(\frac{x}{2\sqrt{\varkappa t}}\right)\right] \qquad \left(\operatorname{erf} z = \frac{2}{\sqrt{\pi}}\int_0^z e^{-\zeta^2} d\zeta\right) \tag{5.9}$$

We determine constant of integration D from condition

$$x = 2C\sqrt{\varkappa t}; \quad T = T_k = T_0 + D\left[1 - \operatorname{erf}\left(\frac{x}{2\sqrt{\varkappa t}}\right)\right], \quad D = \frac{T_k - T_0}{1 - \operatorname{erf} C} \tag{5.10}$$

For the gradient of temperature at the surface we obtain

$$\varphi = -\left(\frac{\partial T}{\partial x}\right)_{T_k} = \frac{2}{\sqrt{\pi}} D \frac{e^{-C^2}}{2\sqrt{\varkappa t}} = \frac{T_k - T_0}{\sqrt{\varkappa t}} \frac{e^{-C^2}}{\sqrt{\pi}(1 - \operatorname{erf} C)} \tag{5.11}$$

The three magnitudes u, p, and φ are connected by the one equation of the dependence of burning velocity on the pressure and the gradient of temperature (0.1). If the velocity of steady burning of the powder is connected with initial temperature T_0 and pressure p by formulas (1.7) and (2.5), for dependence (0.1), using the method described in § 1, we can obtain

$$\frac{u}{u_c} = \exp\left[\beta(T_k - T_0)\left(1 - \frac{\varphi}{\varphi_c(p)}\frac{u_c(p)}{u}\right)\right] \tag{5.12}$$

Substituting for u and φ their expression (5.7) and (5.11), we obtain an equation, solution of which gives the change of velocity ψ depending upon the rate of pressure decay, which is characterized by B, and on constants of the powder ν, $\beta(T_k - T_0)$

$$\psi = \exp\left[\beta(T_k - T_0)\left(1 - \frac{e^{-C^2}}{\sqrt{\pi} C(1 - \operatorname{erf} C)}\right)\right], \quad C = \frac{\Psi(B)}{\sqrt{-2\nu B}} \tag{5.13}$$

As one would expect, for small values of B the solution of (5.13) coincides with expression (5.4), derived earlier by another method.

More interesting is the question of the rate of pressure decay, causing extinguishing and corresponding to the value of B. For its determination we use the expression of burning velocity u_B at the limit of stability of burning and compare it with the steady velocity for the given pressure (see (1.9)-(1.10)):

$$u_B = \frac{u_k}{e}, \qquad u_c = u_k e^{-\beta(T_k - T_0)}, \qquad \psi_B = \frac{u_B}{u_c} = e^{\beta(T_k - T_0) - 1} \tag{5.14}$$

Substituting this expression in (5.13) we obtain an equation whose solution gives the critical value of B_B, leading to extinguishing:

$$\exp[\beta(T_k - T_0) - 1] = \exp\left[\beta(T_k - T_0)\left(1 - \frac{\exp(-C^2)}{\sqrt{\pi}\, C(1 - \operatorname{erf} C)}\right)\right] \tag{5.15}$$

Hence

$$\beta(T_k - T_0)\exp(-C^2) = \sqrt{\pi}\, C(1 - \operatorname{erf} C) \tag{5.16}$$

Given different values of auxiliary quantity C, we obtain corresponding values of $\beta(T_k - T_0)$, ψ, and B. Calculations give

C	0	0.2	0.5	1.0	1.5	∞
$\beta(T_k - T_0)$	0	0.285	0.55	0.76	0.855	1.0
$-\nu B_B$	∞	3.0	0.82	0.31	0.167	0.0

As can be seen from equations and the obtained data, for the burning velocity and the condition of extinguishing product νB is essential; the greater the dependence of burning velocity on pressure, the lower the rate of drop of pressure B which causes an equal action.

§ 6. Comparison with experiment. One of the conclusions of the developed theory of burning of powders and condensed explosives [1] is the conclusion that stable steady burning of powder is possible only if dimensionless magnitude $\beta(T_k - T_0)$ is less than or equal to one. Experiments of K. K. Andreyev on burning of nitroglycol at low temperatures, evidently, confirm this. There are, however, experimental data, indicating that the criterion of stability of burning is not

always satisfied. We give, for instance, data on quantity $\beta(T_k - T_0)$ for powder H. For that we use values of the temperature coefficient of the burning velocity of this powder obtained in [3] and the magnitude of the temperature of the surface of the powder according to data of A. A. Zenin. Below in the table we give these data for various pressures:

p_{atm}	10	20	50
$\beta \cdot 10^3$	5.1	8.2	8.2
$T_k - T_0$	300	360	400
$\beta(T_k - T_0)$	1.53	2.88	3.28

Divergence of theory and experiment bears witness to the limited nature of the theory, the cause of which lies in idealization of the mechanism of burning of the powder. In particular, in theory we used an idealized concept of the zone of gasification of powder; it was assumed that the activation energy of the gasification reaction is very great, so that the reaction occurs in a narrow inertialess zone at a constant temperature, not depending on the burning velocity. In reality, the zone of reaction has finite thickness and inertia; the temperature of the surface, although it changes little with change of the burning velocity, can substantially affect the gradient of temperature at the surface. These factors affect the magnitude of the criterion of stability of burning. From physical considerations it is possible to assume that complete allowance for the reaction in the condensed phase will lead to easing of unsteady effects and to increase of stability of burning of the powder.

Of interest are experiments in interruption of burning of powder.

In the experiments of G. A. Barskiy and O. I. Leypunskiy, performed at the Institute of Chemical Physics of the Academy of Sciences of the USSR in the 1940's, a charge burned in a chamber with nozzle equipped with a deflecting flap. Impact of the incident load on the

hook freed the flap. Pressure fell from 100-200 kg/cm^2 to atmospheric in time Δt less than 0.1 sec. Burning velocity of the powder at atmospheric pressure was near 0.04 cm/sec. Substituting these values in the expression (5.6) of the law of change of pressure for constant B, we find (we take $\varkappa = 2 \cdot 10^{-3}$ cm^2/sec)

$$-Bv = \frac{\varkappa (p_{00}^{-2\nu} - p_0^{-2\nu})}{2a_1^2 \Delta t} = \frac{2 \cdot 10^{-3} \cdot 1}{2 \cdot 0.04^2 \cdot 0.1} \approx 6 \qquad (6.1)$$

Here p_0 — initial pressure; p_{00} — final pressure.

According to data of § 5, such a rate of pressure decay by several times exceeds that necessary for extinguishing the powder (when $\beta(T_k - T_0) = 0.5 - B\nu \approx 1$). This conclusion agrees with the fact that in experiments of G. A. Barskiy and O. I. Leypunskiy there was indeed attained cessation of burning.

Certain information about experiments in extinguishing of powder has been published recently [4, 5]. In the experiments of Price [4] it was found that the depth of pressure drop, necessary for extinguishing, grows with increase of initial pressure in the combustion chamber. This result agrees with formula (2.12). In the work of Ciepluch [5] there was studied interruption of burning of a mixture powder (ν = = 0.337). The rate of pressure decay, dp/dt, required for extinguishing turned out to be roughly proportional to initial pressure. This also is in qualitative agreement with theory (see formula (5.3)).

After extinguishing repeated ignition of the powder from contact of the surface with hot gasses or from heat supplied by radiation is possible. If the powder is heated by hot gas by means of conductive thermal conduction, then it is easy to prove that heating of the surface of the powder will be small. As is known from the theory of thermal conduction [6] (p. 88), temperature on the interface of two

media 1 and 2, having initially temperatures T_1 and T_2, constant throughout the mass, during propagation of heat remains constant and is equal to

$$T_k = \frac{T_2 + T_1 \sqrt{(\lambda \rho c_p)_1 / (\lambda \rho c_p)_2}}{1 + \sqrt{(\lambda \rho c_p)_1 / (\lambda \rho c_p)_2}} \qquad (6.2)$$

(λ, c_p, ρ — correspondingly thermal conductivity, heat capacity and density of the media). Assume that medium 1 is a gas; the temperature of the gas is equal to the temperature of burning of the powder T_1 = = 2400°K; and medium 2 is a powder; the temperature of the powder is equal to initial temperature T_2 = 300°K. The ratio of density of the gas to density of the powder we consider equal to $4 \cdot 10^{-3}$, which corresponds to pressure in the combustion chamber of ~50 atm. Heat capacity of the powder c_{p_2} = 0.36 cal/(g·deg), of the gas c_{p_1} = = 0.40 cal/(g·deg); thermal conductivity of the powder $\lambda_2 = 5 \cdot 10^{-4}$ cal/(cm·sec·deg), of the gas $\lambda_1 = 2 \cdot 10^{-4}$ cal/(cm·sec·deg). In this case the temperature of the surface of the powder, calculated by formula (6.2), will be equal to 377°K, which is insufficient for ignition.

However, if there is convective supply of heat to the powder (hot gasses blow over its surface) or if there is heat transfer by radiation from heated parts of chamber (intensity of radiation of which slowly decreases in time), then repeated ignition of the powder is possible.

In conclusion I take this opportunity to express sincere gratitude to K. K. Andreyev, O. I. Leypunskiy, I. P. Grave, M. Ye. Serebryakov, and I. M. Shapiro for their interest in my work. I am very grateful to Yu. B. Khariton who turned my attention in connection with work [1] to the phenomenon of extinguishing of powder in the

barrel of an artillery piece after firing of the shell. I also thank V. B. Librovich for help in preparation of the article for publication.

Submitted
29 February 1964

Literature

1. Ya. B. Zel'dovich. The theory of burning of powders and explosives. Journal of exper. and theor. physics, 1942, Vol. 12, Issues 11-12.

2. Ya. B. Zel'dovich. Stability of burning of powder in a semi-closed volume. PMTF, 1963, No. 1.

3. P. F. Pokhil, O. I. Nefedova, and A. D. Margolin. On the anomalous dependence of the burning velocity of powder on initial temperature. Reports of Acad. of Sci. of USSR, Vol. 145, No. 4, 1962.

4. E. W. Price. "Analysis of results of combustion instability research of solid propellants," presented at solid propellant rocket research conf., Princeton, N. J., Jan 28-29, 1960 (ARS reprint, No. 1058-60).

5. C. C. Ciepluch. Effect of rapid pressure decay on solid propellant combustion. ARS Journal, Vol. 31, No. 11, 1961.

6. H. S. Carslaw and J. C. Jaeger. Conduction of heat in solids. Oxford Press, 1959.

AN APPROXIMATE METHOD IN THE THEORY OF UNSTEADY BURNING VELOCITY OF POWDER

A. G. Istratov, V. B. Librovich, and
B. V. Novozhilov

(Moscow)

During change of pressure the burning velocity of powder changes. If change of pressure is slow, so that the temperature profile in the heated layer of the powder can reflect the varying pressure, there are quasi-stationary conditions of burning. During fast change of pressure the temperature profile in the powder will lag behind the pressure, and the burning velocity of the powder therefore, differs from quasi-stationary.

Unsteady conditions of burning of powder were considered in the works of Ya. B. Zel'dovich [1, 2]. In [3] there was conducted numerical calculation of transient processes from steady-state conditions of burning at one pressure to steady-state conditions at another pressure on an electronic computer. In it there are investigated cases of a sharp rise of pressure and rapid narrowing of nozzle in the combustion chamber of a powder-propellant rocket engine. The influence of instantaneous rise of pressure on the burning velocity of powder was also considered in [4], in which there were used assumptions about the mechanism of burning of powder, differing in many respects from those in [1-3].

Below, with the help of the method of approximation of integral relationships [5-7] we derive analytic expressions of the unsteady burning velocity for a model of powder, whose burning velocity is determined only by pressure and the temperature gradient at the surface of the condensed phase. We consider cases of instantaneous and exponential change of pressure. We obtain conditions of extinguishing of powder during decrease of pressure. We make a comparison with results of numerical calculation [3]. We investigate cases of linear and exponential dependences of steady burning velocity of powder on its initial temperature.

§ 1. Fundamental equations. Application of the method of integral relationships. In steady-state conditions the burning velocity of a powder

$$u^\circ = Bp^\nu f(T_0)$$

is determined by its initial temperature T_0 and pressure p.

As it is known [1], during steady burning there is a simple relationship between initial temperature and the temperature gradient on the boundary of the condensed phase,

$$\varphi = \left|\frac{\partial T}{\partial x}\right|_0 = \frac{u^\circ}{\varkappa}(T_1 - T_0) \tag{1.1}$$

where $\varkappa$ — coefficient of thermal diffusivity and T_1 — temperature of the surface of the powder. Expressing from (1.1) temperature T_0 as a function of φ and p, it is possible to present burning velocity in the form $u = F(p, \varphi)$. This dependence will also be valid for unsteady burning, which was shown by Ya. B. Zel'dovich [1]. However, in this case relationship (1.1) no longer will be satisfied, and for determination of φ it is necessary to solve the heat-conduction equation in the solid phase.

Before formulating the problem, let us turn to the following dimensionless variables

$$\theta = \frac{T - T_0}{T_1 - T_0}, \quad \tau = \frac{u_0^2}{\varkappa} t, \quad \xi = \frac{u_0}{\varkappa} x,$$
$$z = \left(\frac{p}{p_0}\right)^\nu, \quad w = \frac{u}{u_0} \tag{1.2}$$

Here x — space coordinate ($x > 0$, $x = 0$ — surface of the powder), t — time, u — burning velocity, u_0 — initial value of burning velocity (when $t = 0$), p_0 — initial pressure.

The problem consists of finding functions $w(\tau)$, $\theta(\tau, \xi)$, which determine the unsteady burning velocity and distribution of temperatures in the solid phase from heat-conduction equation

$$\frac{\partial \theta}{\partial \tau} = \frac{\partial}{\partial \xi}\left(\frac{\partial \theta}{\partial \xi} + w\theta\right) \tag{1.3}$$

the law of burning

$$w = F\left(z, \left|\frac{\partial \theta}{\partial \xi}\right|_0\right) \tag{1.4}$$

and the given dependence of pressure on time $z(\tau)$ during transition from one steady-state regime

$$z(0) = 1, \qquad w(0) = 1, \qquad \theta(0, \xi) = e^{-\xi} \tag{1.5}$$

to another

$$z(\infty) = z_1, \qquad w(\infty) = w_1 = z_1, \qquad \theta(\infty, \xi) = e^{-w_1 \xi} \tag{1.6}$$

with boundary conditions

$$\theta(\tau, 0) = 1, \qquad \left(\frac{\partial \theta}{\partial \xi}\right)_\infty = 0 \tag{1.7}$$

In [3, 4] solution of the thermal conduction equation (1.3) was produced numerically on an electronic computer. In this work the solution is found by the method of approximation of integral relationships [5-7]. This method was first applied by Karman and Pohlhausen in boundary layer theory.

The method consists of seeking, instead of the solution of the thermal conduction equation, the solution of the integral relationship obtained from (1.3) by integration with respect to ξ from $\xi = 0$ to $\xi = \infty$:

$$\frac{d}{d\tau}\int_0^\infty \theta\, d\xi = -w - \left(\frac{\partial \theta}{\partial \xi}\right)_{\xi=0} \tag{1.8}$$

The integral relationship is solved if we are given the distribution of $\theta(\xi)$, depending on a certain parameter. The approximate solution should satisfy boundary conditions and qualitatively correctly describe the character of temperature distribution. In our case it was expedient to select the following temperature distribution:

$$\theta(\tau, \xi) = [1 - f(\tau)]\, e^{-\xi} + f(\tau)\, e^{-w_1 \xi} \tag{1.9}$$

where $f(\tau)$ — a function, changing from zero (for $\tau = 0$) to one (when $\tau = \infty$).

Substituting (1.9) in (1.8), we obtain an ordinary differential equation for determining dependence $f(\tau)$:

$$\frac{w_1-1}{w_1}\frac{df}{d\tau}=w-1-(w_1-1)f \qquad (1.10)$$

The dimensionless temperature gradient of the surface is expressed in the form

$$\left|\frac{\partial\theta}{\partial\xi}\right|_0=1+(w_1-1)f \qquad (1.11)$$

For final solution of the problem it is necessary to make the law of burning (1.4) more concrete and give function $z(\tau)$.

§ 2. Unsteady burning velocity for linear dependence of burning velocity of powder on initial temperature. If the velocity of steady burning of powder depends linearly on initial temperature T_0 ($u^0 = Bp^\nu(1 + \alpha T_0)$), law of burning (1.4) in dimensionless variables has the form [3]

$$w=z\frac{1+\beta}{2}\left[1+\left(1-\frac{43}{z(1+\beta)^2}\left|\frac{\partial\theta}{\partial\xi}\right|_0\right)^{1/2}\right],\qquad \beta=\frac{\alpha(T_1-T_0)}{1+\alpha T_0} \qquad (2.1)$$

In [3] there is used another quantity $\eta = 2/(1 + \beta)$.

Relationship (2.1) together with (1.11) allows us, instead of an equation for f (1.10), to write an equation for velocity w

$$\frac{1}{w}\left(1+\beta-2\frac{w}{z}\right)\frac{dw}{d\tau}+\frac{w}{z^2}\frac{dz}{d\tau}=w_1\left(\frac{w}{z}-1\right) \qquad (2.2)$$

It is convenient to introduce a new function $W = w/z$. It has a simple meaning. During steady burning $W = 1$; deviation of W from one characterizes the degree of unsteadiness of burning. For this function from (2.2) we obtain equation

$$\frac{(1+\beta-2W)}{W}\frac{dW}{d\tau}+(1+\beta-W)\frac{1}{z}\frac{dz}{d\tau}=w_1(W-1) \qquad (2.3)$$

Let us investigate the transient process from steady-state conditions $w = z = 1$ to steady-state conditions $w_1 = z_1$ with the following

dependence of pressure on time:

$$z = e^{-\gamma\tau} \quad \text{when } 0 < \tau < \tau_0$$
$$z - z_1 = w_1 = e^{-\gamma\tau_0} = \text{const} \quad \text{when } \tau_0 < \tau < \infty \tag{2.4}$$

Using initial condition W = 1 for τ = 0, we obtain

$$\tau = \frac{1}{\gamma(1+\beta) - w_1}\left[(1+\beta)\ln W - \frac{\gamma(1+\beta) - w_1(1-\beta)}{w_1 - \gamma} \times \right.$$
$$\left. \times \ln\left(1 + \frac{(\gamma - w_1)(1-W)}{\gamma\beta}\right)\right] \quad (\tau < \tau_0) \tag{2.5}$$

$$\tau = \tau_0 + \frac{1}{w_1}\left[(1-\beta)\ln\frac{W_0 - 1}{W - 1} + (1+\beta)\ln\frac{W_0}{W}\right] \quad (\tau > \tau_0) \tag{2.6}$$

where W_0 – value of W when $\tau = \tau_0$, determined from (2.5).

With infinitely fast change of pressure ($\gamma = \pm\infty$) the solution comes from expression (2.6) for $\tau_0 = 0$. In order to determine W_0 in this case it is necessary to consider the limit of (2.5) as $\gamma \to \pm\infty$ with condition $\gamma\tau_0 = -\ln w_1$, or more simply, set $z = z_1 = w_1$ in (2.1) on the condition that $\left|\partial\theta/\partial\xi\right|_0 = 1$. For W_0 we obtained expression

$$W_0 = \frac{1+\beta}{2}\left[1 + \left(1 - \frac{4\beta}{z_1(1+\beta)^2}\right)^{1/2}\right] \tag{2.7}$$

Function $f(\tau)$, necessary for finding the temperature distribution of the solid phase, we express from (2.1) and (1.11) through W and z:

$$f = \frac{zW(1+\beta-W) - \beta}{\beta(z_1 - 1)} \tag{2.8}$$

The given solution is valid both for decrease of pressure ($\gamma > 0$, $z_1 < 1$), and for increase of pressure ($\gamma < 0$, $z_1 > 1$).

For illustration of the results obtained in Fig. 1 we give the dependence of unsteady burning velocity w on time for share (1) and exponential (2) pressure decay. The dotted line shows steady velocity (or pressure to power ν). Curves correspond to the following parameters: $\beta = 0.6$, $w_1 = 0.95$, $\gamma = \infty$, $\gamma = 0.25$. It is clear that the burning velocity differs more from steady burning velocity the sharper the pressure decay. The velocity of steady burning is greater than that of unsteady due to the fact that the latter occurs with a

less heated surface layer of the powder. In Fig. 2 the dotted lines depict the dependences of burning velocity W on time with a sharp rise when $p_1/p_0 = 10$ and $p_1/p_0 = 200$ ($\nu = 2/3$, $\beta = 0.74$). Solid lines in this figure give the same dependences taken from [3], which were obtained by numerical integration of the equation on an electronic computer. It is clear that the method of approximation gives satisfactory agreement with results of exact calculation.

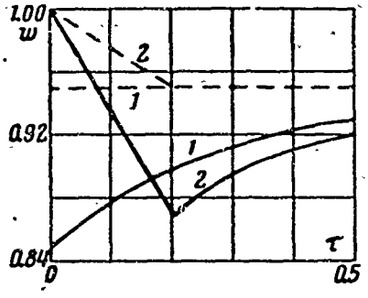

Fig. 1.

In Fig. 3 are profiles of temperature in powder, calculated by formulas (1.9), (2.6), and (2.8) for two different moments of time (dotted curves), and there also are plotted the results of exact calculation, taken from [3] (solid curves 1, 2, 3, 4 correspond to $\tau = 0.0$, 0.16, 0.237, ∞ when $\beta = 0.74$, $p_1/p_0 = 10$). Also there is observed satisfactory coincidence of results.

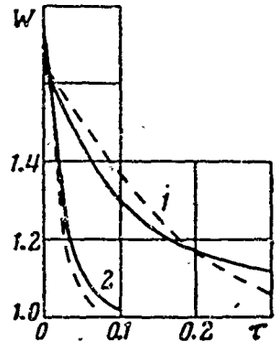

Fig. 2.

In Fig. 4 is a comparison of dependences, obtained by approximate formulas and by exact calculation, for $p_1/p_0 = 10$, $\nu = 2/3$ for different values of β: $\beta = 0.905$ (curve 1) and $\beta = 0.6$ (curve 2). It is clear that as β approaches one (the criterion of stability of burning of powder according to Ya. B. Zel'dovich [1] is condition $\beta < 1$) accuracy of approximate calculation lowers.

With sufficiently rapid pressure decay there can occur extinguishing of the powder. For instantaneous change of pressure this can be seen from formula (2.7). If

$$z_1 < \frac{4\beta}{(1+\beta)^3}$$

the expression under the radical is negative, and a solution does not exist.

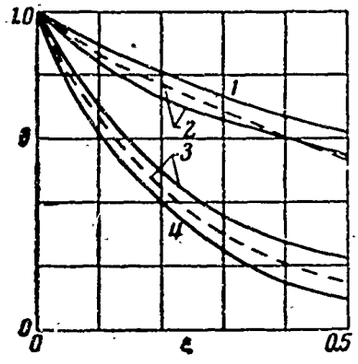

Fig. 3.

The temperature gradient at the surface of the powder, produced under the initial pressure, is equal in this case to the critical gradient, with which, as we know from the theory of Ya. B. Zel'dovich [1, 2], there still can exist a flame above the surface of the powder. With great decrease of pressure the gradient exceeds the critical.

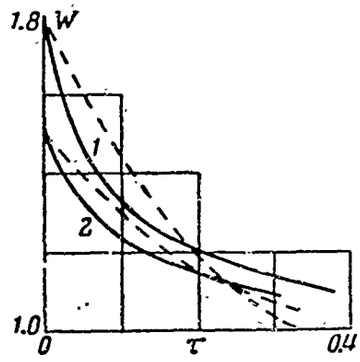

Fig. 4.

With smooth change of pressure it is necessary to investigate the more general formula (2.1), from which it is clear that the critical value of W is $1/2(1 + \beta)$. A smaller value of W, in principle, cannot be attained. When $W^* = 1/2(1 + \beta)$, which corresponds to achievement of the critical gradient, there occurs extinguishing of the powder. From equation (2.3) it follows that under this condition $dW/d\tau$ becomes an infinitely large negative quantity.

If we are given a finite value of z_1, two cases are possible. For small values of γ (weak unsteadiness) W is always greater than W^*, and the powder is not extinguished. For large values of γ, W at a certain moment attains W^*, and there occurs cessation of burning.

We obtain the critical value of γ^* (for a given z_1), if we set $W = W^*$ in the moment most dangerous for extinguishing, i.e., at $\tau = \tau_0$.

Here, $z_1 = \exp(-\gamma\tau_0)$, $W = 1/2(1 + \beta)$. Then from (2.5) for dependence $z_1 = z_1(\gamma^*)$ we obtain transcendental equation

$$z_1 = \exp\frac{1}{r-(1+\beta)}\left\{(1+\beta)\ln\frac{1+\beta}{2} - \right.$$
$$\left. - \frac{(1+\beta)-r(1-\beta)}{r-1}\ln\left[1+\frac{(1-r)(1-\beta)}{2\beta}\right]\right\}, \qquad r = \frac{z_1}{\gamma^*} \tag{2.9}$$

Hence

$$z_{1\infty} = \frac{4\beta}{(1+\beta)^2} \quad \text{as} \quad \gamma^* \to \infty$$

$$z_1 \approx \frac{4\beta}{(1+\beta)^2}\left[1 - \frac{4\beta}{(1+\beta)^3\gamma^*}\left(\ln\frac{1+\beta}{2} + (1+2\beta)\ln\frac{1+\beta}{2\beta} - (1-\beta)\right)\right] \tag{2.10}$$
$$\text{as} \quad \gamma^* \gg 1$$

For sufficiently small values of γ there is no extinguishing for any values of z_1. In this case $dW/d\tau$ becomes equal to zero before W attains value W*. The point of termination of the extinguishing curve $z_1(\gamma^*)$ is determined from the condition of equality to zero of the second term in braces in expression (2.9). Its coordinates are

$$z_1^* = \left(\frac{1+\beta}{2}\right)^{\frac{1+\beta}{\beta}}, \qquad r^* = \frac{1+\beta}{1-\beta} \tag{2.11}$$

In Fig. 5 are curves 1-5 of dependence $z_1(\gamma^*)$ when β = 1.0, 0.7, 0.5, and 0.3.0. The dotted line shows the locus of points of termination of the extinguishing curve.

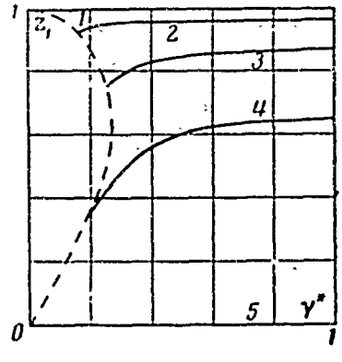

Fig. 5.

§ 3. Unsteady burning velocity with an exponential dependence of the burning velocity of powder on initial temperature. Absolutely analogously to the preceding case it is possible to investigate unsteady burning of powder, the velocity of which depends on T_0 exponentially ($u^0 = Bp^\nu e^{\alpha T_0}$). Dimensionless burning velocity is related to z and the temperature gradient by the relationship

$$w = z\exp\beta\left(1 - \frac{1}{w}\left|\frac{\partial\theta}{\partial\xi}\right|_w\right), \qquad \beta = \alpha(T_1 - T_0) \tag{3.1}$$

For determination of w we have equation

$$(\beta - 1 - \Lambda)\frac{d\Lambda}{d\tau} + (\beta - \Lambda)\frac{1}{z}\frac{dz}{d\tau} = w_1\Lambda \qquad \left(\Lambda \equiv \ln\frac{w}{z}\right) \tag{3.2}$$

It is easy to show that for $\beta \ll 1$ relationships (2.1) and (3.1) and equations (2.3) and (3.2) change into one another, as it should be, since a linear law is obtained from exponential under just this condition.

If pressure depends on time according to law (2.5), the solution of equation (3.2) will be

$$\tau = \frac{\gamma - w_1(1-\beta)}{(w_1-\gamma)^2} \ln\left[1 + \frac{(w_1-\gamma)\Lambda}{\gamma\beta}\right] - \frac{\Lambda}{w_1-\gamma} \qquad (\tau < \tau_0) \qquad (3.3)$$

$$\tau = \tau_0 + \frac{1}{w_1}\left[(1-\beta)\ln\frac{\Lambda_0}{\Lambda} + (\Lambda_0 - \Lambda)\right] \qquad (\tau > \tau_0) \qquad (3.4)$$

With instantaneous change of pressure Λ_0 is determined from equation

$$\Lambda_0 = -\ln w_1(1 - \Lambda_0\beta) \qquad (3.5)$$

Minimum possible $\Lambda_0 = \beta - 1$, and the critical value of pressure, at which powder extinguishing occurs [2] as $\gamma \to \infty$

$$z_{1\infty} = \beta e^{1-\beta} \qquad (3.6)$$

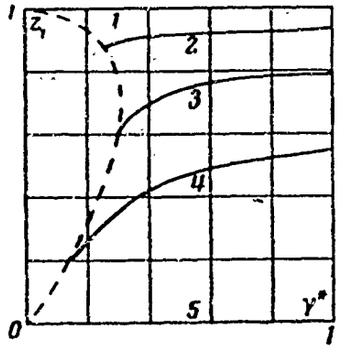

Fig. 6.

The curve of extinguishing is sought from transcendental equation

$$z_1 = \exp\frac{1}{1-r}\left\{1 - \beta - \frac{1-r}{1-r}(1-\beta)\ln\left[1 + \frac{(1-\beta)(1-r)}{\beta}\right]\right\} \qquad (3.7)$$

When $\gamma^* \gg 1$

$$z_1 \approx \beta e^{1-\beta}\left\{1 - \frac{\beta e^{1-\beta}}{\gamma^*}\left[(1+\beta)\ln\frac{1}{\beta} - 2(1-\beta)\right]\right\} \qquad (3.8)$$

The point of termination of the curve of extinguishing is determined by relationships

$$z_1^* = \exp\left[-\frac{(1-\beta)^2}{\beta}\right], \qquad r^* \quad \frac{1}{1-\beta} \qquad (3.9)$$

In Fig. 6 are curves 1, 2, 3, 4, 5 built by formula (3.7), correspondingly for values β = 1, 0.7, 0.5, 0.3, and 0.

In conclusion we thank O. I. Leypunskiy and G. I. Barenblatt for discussion of the work and valuable advice.

Submitted
6 March 1964

Literature

1. Ya. B. Zel'dovich. The theory of burning of powders and explosives. Journal of exper. and theor. physics, 1942, Vol. 12, Issues 11-12.

2. Ya. B. Zel'dovich. The burning velocity of powder with variable pressure. PMTF, 1964, No. 3.

3. B. V. Novozhilov. Transient processes during burning of powders. PMTF, 1962, No. 5.

4. E. M. Landsbaum. The effect of a shock wave on a burning solid propellant. Advances Aeronaut. Sci., Vol. 3, Oxford — London — New York — Paris. Pergamon Press, 1962, pp. 497-511.

5. G. I. Barenblatt. Certain methods of approximation in the theory of unsteady filtration in elastic conditions. News of AS of USSR, Dept. of Tech. Sciences, 1954, No. 9.

6. G. I. Barenblatt. Approximate solution of problems of one-dimensional filtration in a porous medium. PMM, 1954, Vol. 18, No. 3.

7. V. B. Librovich. Ignition of powders and explosives. PMTF, 1963, No. 6.

INFLUENCE OF PRESSURE ON THE NORMAL VELOCITY OF THE FLAME OF A METHANE-AIR MIXTURE

V. S. Babkin, L. S. Kozachenko, and I. L. Kuznetsov

(Novosibirsk)

The influence of pressure and temperature on the normal velocity of the flame in a methane-air mixture is studied with the help of a bomb of constant volume in the pressure range 1-60 atm (abs.) and temperature range 16-220°C. The apparent velocity was determined in the initial section by means of high-speed filming using an optical schlieren system. Normal velocity was calculated as the result of division of apparent velocity by the calculated coefficient of expansion. In the pressure range 3-60 atm (abs.) the normal velocity obeys dependence $S_u \sim p^{-0.5}$.

1. Study of the influence of high pressure on the normal velocity of a flame began relatively recently on the basis of methods developed for measurements of normal velocities at low pressures (0.1-3 atm (abs.)). The method of a bomb of constant volume was used by Yampol'skiy and Price [1] for research of explosions of hydrogen-air mixtures up to 900 atm (abs.). Smith and Agnew [2] used this method to determine the velocity of the flame with initial pressures up to 20 atm (abs.) in methane-oxygen-nitrogen mixtures. A modified method of a bomb of constant pressure was successfully applied by Strauss and Edse [3] for a series of fuel-air and fuel-oxygen mixtures, burning under a pressure of up to 90 atm (abs.). In a wide range of pressures

up to 40 atm (abs.) the Bunsen-burner method was applied by Diederichsen and Wolfhard for methane-air mixtures [4]. The influence of pressure on the velocity of the flame of mixtures of methane, propane, ethylene and propylene with air in the range of 0.5-9 atm (abs.) was studied by the tube method by Egerton and Lefebre [5].

During transition to increased pressures application of the above-enumerated methods encountered certain difficulties. As Diederichsen and Wolfhard show, application of a Bunsen burner with a pressure chamber at high pressures requires a decrease of the diameters of the burner to very small dimensions (in their experiments at 20 atm (abs.) the diameter of burner was 1.7 mm) which to significant extent hampers observation of the flames. On the other hand, this leads to the necessity of measurement of minute consumptions of gas, which is connected with increase of error. In the experiments of Diederichsen and Wolfhard, with a stoichiometric relationship in the mixture and 20 atm (abs.) pressure, the consumption of methane was about 0.1 ml/sec. In [4] there is also indicated the difficulty of stabilization of the flame on Bunsen burners.

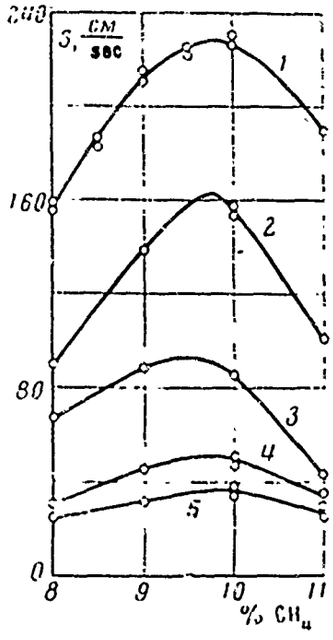

Fig. 1.

The method of a bomb of constant volume with application of pressure-time recording, although an old method, does not allow us to obtain reliable values of normal velocities of a flame, since different authors offered contradictory equations for their determination [6, 7].

Strauss and Edse [3], working with high pressures with a soap bubble, noted the difficulty of registration of boundaries of the bubble; therefore, instead of the coefficient of expansion

of products of burning usually determined experimentally, they used its thermodynamic computed value.

A very successful attempt at determination of the normal velocity of a flame is the method with application of ionization transducers, used by Smith and Agnew [2], in combination with measurements of apparent velocity of the flame by means of these transducers in the early stages of burning, when the process of flame propagation in a closed bomb can be considered a process* under constant pressure [8].

In this work there is undertaken a further study of the influence of pressure on the normal velocity of the flame of methane-air mixtures with initial pressures of up to 60 atm (abs.) and its dependence on temperature up to 220°C at atmospheric pressure. Measurements of normal velocity were conducted in a closed spherical bomb with central ignition in the initial section of flame propagation, with application of filming by the schlieren-method.

2. Description of experiments. The closed spherical bomb was a thick-walled steel vessel with a working cavity of 183 mm, equipped with inspection windows on opposite sides of the bomb of optical glass of 72 mm diameter and 48 mm thickness. The bomb was equipped with steel regulated electrodes for igniting the mixture by a centered spark and high-pressure valves for filling the bomb with the fuel mixture and evacuation. Recording of the flame was produced by means of high-speed filming using an optical schlieren system and a serial spark discharge as the source of light. A typical schlieren system

*In 1960, D. G. Nikitin investigated by the method of a bomb of constant volume with application of ionization transducers for registration of the flame the dependence of the normal velocity of flame propagation on pressure for mixtures of certain hydrocarbons with air during change of initial pressure from 1 to 8 atm (abs.) (cand. diss. Institute of Chemical Physics of Academy of Sciences of USSR, M, 1950).

with two long-focal objectives of type Telemar-2, where the bomb was located in the parallel beam of light between these objectives.

Propagation of flame was studied in the initial section of its motion, when the radius of the spherical flame does not exceed 1/4 the radius of the bomb. Here, increase of pressure in the bomb was not more than 1.5%, and, thus, it is possible to consider that propagation of the flame occurs at constant pressure, equal to the initial pressure. Analysis shows that the principal error in determination of normal flame velocity, caused by this approximation, also does not exceed 1.5% and, in general, can be allowed for. The section of flame formation directly after spark ignition was excluded from consideration, since spark energy and curvature of the front of the flame have a strong influence in this section on the apparent velocity.

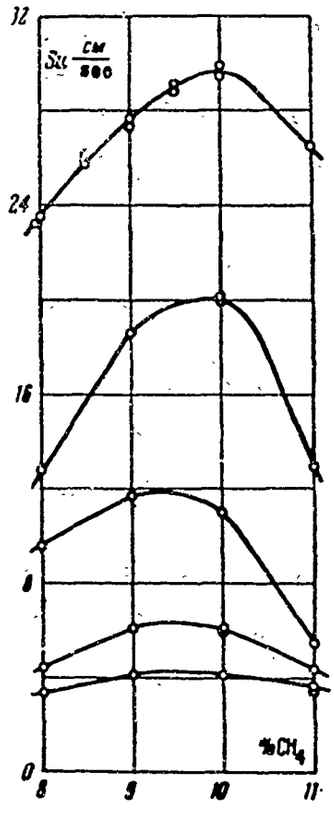

Fig. 2.

This last circumstance allowed us easily to determine the extent of this section directly by photographic recording of the flame.

Later stages of the process of propagation of flame are connected with significant increase of pressure in the bomb, which with sufficiently high initial pressure can lead to destruction of the installation. To prevent this during expansion of the range of initial pressures the bomb was equipped with a safety diaphragm of pure copper foil, which sustained the initial pressure, and then, bursting, ensured drop of the heightened pressure after the process of flame propagation in the initial section was already fixed. With comparatively

low initial pressures, of the order of 10 atm (abs.), when there was no danger of destruction of the bomb, the safety diaphragm was replaced by a steel diaphragm, which was not destroyed after the explosion.

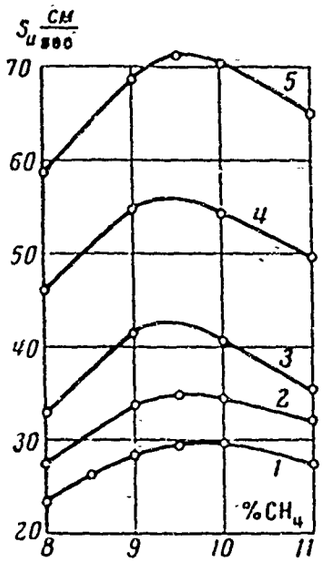

Fig. 3.

Change of the initial temperature of the mixture was attained by heating the bomb by electrical heaters. Evenness of preheating is ensured by the great mass of the bomb.

3. Results of experiments. As a result of analysis of motion picture records we determined the apparent velocity of the flame S, and normal velocity S_u was found from relationship $S_u = S/E$, where E is the coefficient of expansion of products during burning in conditions of constant pressure. The latter was calculated from thermodynamic relationships taking into account dissociation. Apparent velocity was determined by the slope of the straight line, tangent to flame developing in time spheres. Although, as was indicated, the state of the fresh mixture before the flame front and the state of products of burning changed with development of the process, nonetheless, the apparent velocity of the flame remained constant in the considered section with accuracy up to error of measurement. As was noted, the energy of the igniting spark renders a certain influence on formation of the flame; therefore, for ignition of the mixture we used a spark with minimum energy. Such a spark was selected experimentally. Special measurements of energy of the spark were not conducted.

It is necessary to note that in certain experiments there formed nonspherical flames and, although in the given method, rigorous

sphericalness of the flame is not obligatory, nonetheless such motion picture records were not analyzed.*

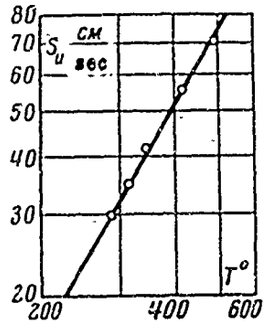

Fig. 4.

In all experiments we investigated flame propagation in mixtures of methane with air. Chromatographic analysis of the methane showed its composition to be the following: 98.2% CH_4, 1.33% N_2, 0.32% CO_2, 0.033% O_2, unknown component — 0.117%. For the given methane a stoichiometric mixture with air corresponds to 9.65% methane and 90.35% air.

In Fig. 1 are given dependences of apparent velocity S (cm/sec) of flame propagation on volume content (in %) of methane in the mixture: curves 1, ..., 5 correspond to values of initial pressure p_0 = 1.0, 3.5, 10, 36, and 60 atm (abs.). Initial temperature of the mixture for these measurements was 16°C. On the basis of these experimental data and relationship $S_u = S/E$ we built dependences of the normal velocity of the flame on the volume contents of methane in the mixture for different pressures (Fig. 2) and the dependence of the normal velocity of the flame on pressure for a mixture of stoichiometric composition (solid line in Fig. 5). The dependence of normal velocity S_u (cm/sec) of the flame on the content of methane for different initial temperatures T_0 is presented in Fig. 3, where curves 1, 2, 3, 4, 5 correspond to values of T_0 = 16, 40, 70, 140, 220°C. These experiments were conducted at atmospheric pressure. In Fig. 4 in logarithmic coordinates there is given the dependence of normal velocity of the flame on temperature for a stoichiometric mixture.

---

*At heightened pressures in methane-air mixtures there is observed a tendency toward formation of anisotropic spherical flames. Such flames were taken into consideration.

4. Discussion of results. The influence of pressure on the normal velocity of a flame in methane-air mixtures at low pressures probably has been given more diverse study than any other fuel mixtures. However, the contradictory nature of published data testifies to the difficulty of exact determination of this influence. As for high pressures, information on the dependence of normal velocity on pressure is very limited. In Fig. 5 there is given in logarithmic scale a summary of data on the dependence of normal velocity of a flame on initial pressure for a stoichiometric methane-air mixture from certain published works, and also results of this work (points 7). Such a presentation of experimental results allows us to analyze the dependence on pressure in the form

$$S_u = \text{const}\, p^{-n}$$

From Fig. 5 it is clear that normal velocities of a flame, obtained in this work in the range from 3 to 60 atm (abs.), lie mostly along a straight line, corresponding to n = 0.5. In this range flame velocity can be expressed by dependence $S_u = 37.4/\sqrt{P}$. Below 3 atm (abs.) there is observed a tendency toward lowering of n. An analogous behavior of the dependence is noted in the work of Diederichsen and Wolfhard [4], the curve of point 1. In this work there is a break in the line at 2 atm (abs.), where the line from 3 to 40 atm (abs.) corresponds to $n \approx 0.53$, and from 0.1 to 1 atm (abs.) to $n \approx 0.2$. In good conformity with results of the authors both in magnitude of the exponent, and in absolute values of S_u are the results of Lefebre and Egerton [5], the curve of point 2, in the pressure range from 3 to 9 atm (abs.). The mentioned tendency of the dependence of normal velocity at low and high pressures can be traced in work [3], the curve of point 3, and in [8], the curve of point 4. If the dependence

on pressure in these works is considered in the above form, it is pos-

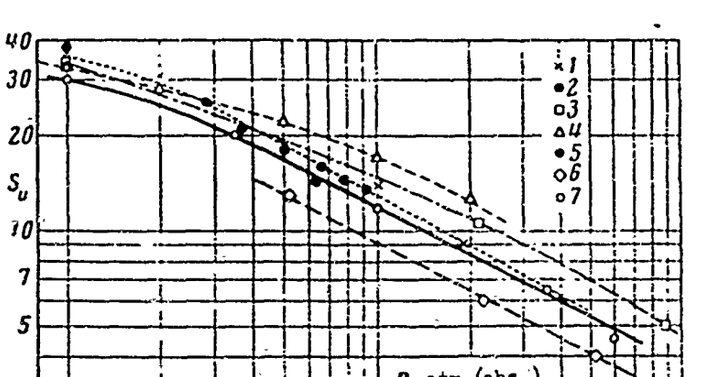

Fig. 5.

sible to see that n constantly increases for Agnew and Graiff [8] in the range from 0.2 to 20 atm (abs.), for Strauss and Edse [3] from 1 to 90 atm (abs.). In Fig. 5, point 5 in [9] matches well with the data of this work, and point 6 (data of Strauss and Edse, obtained by burner method [8]) agrees in exponent n.

Regarding pressure lower than atmospheric, analysis of experimental results in [4, 8-10] shows that for mixtures, close in composition to stoichiometric, exponent n lies between 0.1 and 0.2. In lean methane-air mixtures there is obtained the value n = 0.49 [11]. Thus, it seems, by a dependence of form $S_u = \text{const} \cdot p^{-n}$ it is possible satisfactorily to describe the influence of pressure in a wide range, say from 0.1 to 100 atm (abs.).

Very contradictory are the maxima of normal velocities of flame at atmospheric pressure. Here velocities vary from 28 to 40 cm/sec. Here the experimental values are concentrated in two regions: from 32 to 34 cm/sec [3, 8, 9, 12] and from 37 to 40 cm/sec [2, 4, 10, 13, 14]. With respect to [2, 10] it is possible to note that here normal

velocities may be overstated due to understating of the local expansion coefficient [7], in particular for a stoichiometric mixture, by a magnitude of the order of 8%.

In this work at atmospheric pressure maximum normal velocity of flame is equal to 30 cm/sec. This is partially justified by the low initial temperature of the mixture (16°C). Divergence in normal velocities, possibly, originates also from divergences in calculated coefficients of expansion; therefore, in the present work along with normal velocities we also give apparent velocities of the flame (Fig. 1). Thus, for a mixture of stoichiometric composition of methane with air as in [8] the value of apparent velocity is about 235 cm/sec, which is very close to this work — 231 cm/sec. Regarding error in normal velocities due to the possible disequilibrium state of products of combustion, this question still remains open to debate.

Submitted
15 July 1963

Literature

1. Zh. Yampol'skiy and S. Price. Explosions of hydrogen-air mixtures in a closed vessel at high pressure. IV Symposium (International) Questions of Combustion and Detonation Waves. Oborongiz, M, 1958.

2. D. Smith and J. T. Agnew. The effect of pressure on the laminar burning velocity of methane-oxygen-nitrogen mixtures. VI Symposium (International) on Combustion, New York, London, 1957.

3. W. A. Strauss and R. Edse. Burning velocity measurements by the constant-pressure bomb method. VII Symposium (International) on Combustion, London, 1959.

4. J. Diederichsen and H. G. Wolfhard. The burning velocity of methane flames at high pressure. Trans. Faraday Soc., 1956, Vol. 52, Part 8.

5. A. C. Egerton and A. H. Lefebre. Flame propagation: the effect of pressure variation on burning velocities. Proc. Roy. Soc., 1954, A, Vol. 222, No. 1149.

6. C. J. Rallis and G. E. B. Tremeer. Equations for the determination of burning velocity in a spherical constant volume vessel. Combustion and Flame, 1963, Vol. 7, No. 1.

7. V. S. Babkin, L. S. Kozachenko, and I. L. Kuznetsov. Measurement of the propagation velocity of flame by the constant-volume bomb method. PMTF, 1963, No. 6.

8. J. T. Agnew and L. B. Graiff. The pressure dependence of laminar burning velocity by the spherical bomb method. Combustion and Flame, 1961, Vol. 5, No. 3.

9. K. Wohl and N. M. Kapp. Flame stability at variable pressures. Project Meteor Rep., No. UAC-42, United Aircraft Corp., 1949.

10. J. Manton and B. B. Milliken. Study of pressure dependence of burning velocity by the spherical vessel method. Proceedings of the gas dynamics symposium on aerothermochemistry, Northwestern University, Evanston, Illinois, 1956.

11. A. Egerton and D. Sen [?]. Propagation of flame. Influences of pressure on the propagation velocity of a flat flame front. IV Symposium (International) on Questions of Combustion and Detonation Waves. Oborongiz, M, 1958.

12. B. Lewis and G. von Elbe. Combustion, Flames and Explosions of Gases. Academic Press, INC, New York and London, 1961.

13. T. G. Scholte and P. B. Vaags. The burning velocity of hydrogen-air mixtures and mixtures of some hydrocarbons with air. Combustion and Flame, 1959, Vol. 3, No. 4.

14. J. M. Singer, J. Grumer, and E. B. Cook. Burning velocities by the Bunsen-burner method. Proceedings of the gas dynamics symposium on aerothermochemistry, Northwestern University, Evanston, Illinois, 1956.

DEPENDENCE OF THE BURNING VELOCITY OF VARIOUS FUEL SYSTEMS ON INITIAL TEMPERATURE

A. D. Margolin, O. N. Nefedova, and P. F. Pokhil

(Moscow)

There is conducted experimental study of the dependence of the burning velocity of representatives (hexogene, mixture of potassium perchlorate with tungsten, zirconium and potassium benzoate) of various groups of fuel systems on initial temperature (from -140 to +150°). In the experiments we varied the relationships of components of the mixture, discharge density and pressure of the inert gas in which burning was produced.

Experiments showed that the logarithm of the burning velocity u(lg u) of hexogene and of mixtures of potassium perchlorate with metals is linearly connected with the initial temperature of the substance T_0. The dependence $\lg u = f(T_0)$ of the mixture of potassium perchlorate with potassium benzoate has a discontinuity.

Results of experiments are compared with the hypothesis of transition of the leading stage, determining burning velocity, with growth of temperature from one spatial stage of burning to another.

Study of the dependence of the burning velocity of explosives on initial temperature is of great value for combustion theory [1, 2].

Earlier [3, 4] it was shown that the dependence of burning velocity u of powder H on initial temperature T_0 has an anomalous character (a discontinuity in the curve at coordinates T_0 and lg u). On the basis of available ideas on the mechanism of burning of powders [5] there was advanced the hypothesis [6] that in the region of the discontinuity the leading role passes from one spatial stage of burning to another. Here, the higher the discontinuity temperature, the more likely that the dominating role is played by burning in the reaction layer of the condensed phase; and the lower the discontinuity point, the more likely predominance of burning above the surface of the condensed phase (in the smoke-gas and gas phases).

To check the mentioned hypothesis we conducted an experimental study of the dependence of burning velocity on initial temperature (from -140 to + 150°C) for various classes of fuel systems: hexogene, which according to known data* burns in the gas phase [5]; mixtures of potassium perchlorate with tungsten and zirconium, during burning of which reactions in the gas phase, apparently, practically do not affect burning velocity; and the mixture of potassium perchlorate with potassium benzoate. During experiments we varied the composition of the mixture, density of substance ρ and initial pressure p. Experiments were conducted by the method described in [4]. Samples of the studied fuel systems of 5 mm diameter and 10 mm height were prepared by bilateral extrusion. Samples of lesser density were prepared by batch extrusion in Plexiglas pipes with internal diameter 5 mm and height 20 mm. For burning velocity in this article, we take mm/sec dimension.

The dependence of the mass burning velocity ρu of hexogene on initial temperature at a pressure of 5 atm(gage) is presented in

*A. F. Belyayev. The mechanism of burning of explosives. Doctoral dissertation, Moscow, 1946.

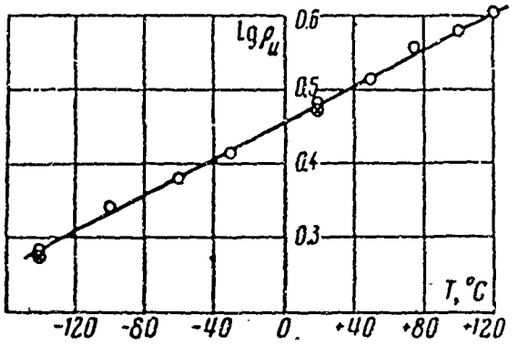

Fig. 1.

Fig. 1. Points show the mass burning velocity of charges with density 1.72 g/cm^3, and points with crosses indicate the burning velocity of charges with density 1.20 g/cm^3. In Fig. 2 is shown the dependence of the burning velocity of hexogene, having a density of 1.72 g/cm^3, on temperature at pressures of 50, 60, and 100 atm(gage) (curves 1, 2, and 3, respectively). By these experimental data we determined the value of the temperature coefficient of burning velocity $\beta = d \ln u/dT_0$.

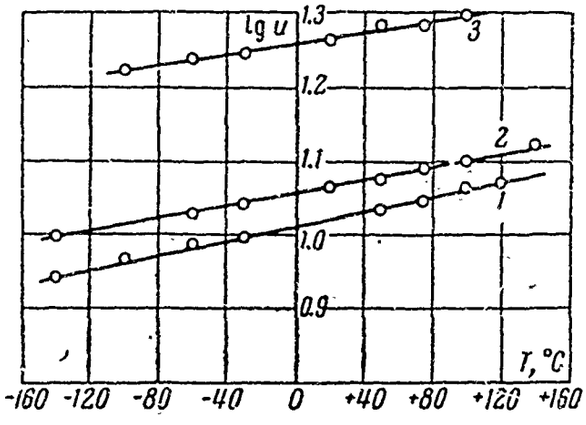

Fig. 2.

The dependence of the logarithm of the burning velocity of hexogene on initial temperature in the whole studied range of temperature from -140 to +150°C and the pressure range from 5 to 100 atm(gage) is rectilinear and can, with sufficient accuracy, be described by a constant temperature coefficient. At a pressure of 5 atm, $\beta = 2.8 \times \times 10^{-3}$ deg^{-1}; at a pressure of 50 atm, $\beta = 1.17 \cdot 10^{-3}$ deg^{-1}; at 60 atm(gage), $\beta = 1.0 \cdot 10^{-3}$ deg^{-1}; and finally at 100 atm(gage) $\beta = 0.7 \cdot 10^{-3}$ deg^{-1}. In accordance with literature data, with growth of pressure the temperature coefficient decreases [1].

As can be seen from Figs. 1, 2, the process of burning of hexogene does not change qualitatively with increase of temperature.

Under the conditions studied here the burning velocity of hexogene is best determined by reactions above the surface of the condensed phase, by the mechanism discussed by A. F. Belyayev. That

burning of hexogene occurs basically in the gas phase is also indicated by the independence of the mass burning velocity from initial density ([1] and Fig. 1 of the present work).

Earlier it was shown that hexogene in a vacuum does not burn, which also indicates the important role of the gas phase during burning of this substance [5].

In Fig. 3 there is shown the dependence of the burning velocity of a mixture of 57% Zr + 43% $KClO_4$ on the initial temperature at atmospheric pressure; in Fig. 4 there is shown the same dependence at pressure 5 atm(gage) for a mixture of 50% W + 50% $KClO_4$; and in Fig. 5

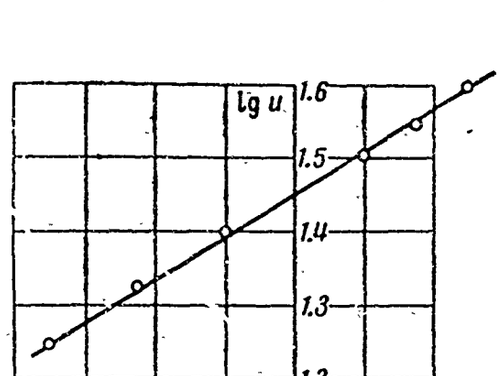

Fig. 3.

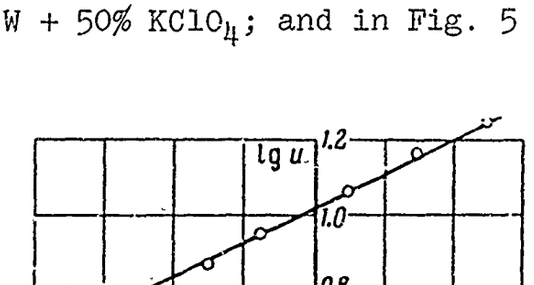

Fig. 4.

at atmospheric pressure for the mixture 74% W + 26% $KClO_4$ (lines 1 and 2 correspond to density $\rho = 5.59$ g/cm^3 and $\rho = 3.60$ g/cm^3).

From Figs. 3, 4, 5, and Table 1 it is clear that the dependence of the burning velocity of mixtures of potassium perchlorate with metals — tungsten and zirconium — on the initial temperature with sufficient accuracy is described by a constant temperature coefficient.

The mixture 50% W + 50% $KClO_4$ at atmospheric pressure burns unstably (at a temperature +20° the ignited mixture goes out, at -140° the mixture cannot be ignited).

Since experimental dependence $\lg u = f(T_0)$ is smooth, without a break, it may be concluded that the mechanism of burning does not change qualitatively with increase of initial temperature. Components of the mixtures studied — the metals tungsten and zirconium — at the temperature of the surface layer of burning of the condensed phase practically do not evaporate; the oxidizer potassium perchlorate is not capable of independent burning. Experiments, conducted by P. F. Pokhil and L. D. Romodanova, showed that these mixtures burn in a vacuum ($p \sim 10^{-2}$ mm Hg) with flameless burning without preheating, i.e., in the reaction layer of the condensed phase of such mixtures there are intense exothermic reactions, capable of supporting combustion.

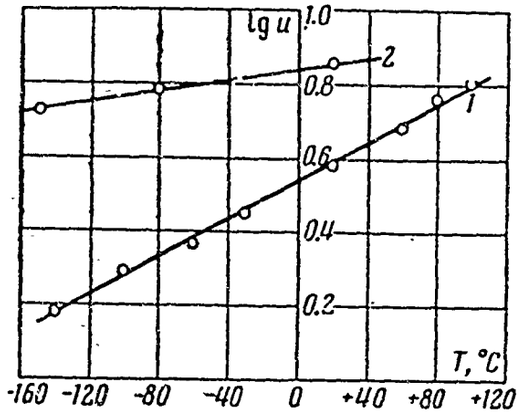

Fig. 5.

Table 1

Composition, wt. %,	ρ, g/cm^3	p, kg/cm^2	β, deg^{-1}
74% W + 26% $KClO_4$ (stoichiometry)	5.59	1	$5.7 \cdot 10^{-3}$
74% W + 26% $KClO_4$	3.69	1	$1.9 \cdot 10^{-3}$
50% W + 50% $KClO_4$	4.21	6	$4.9 \cdot 10^{-3}$
57% Zr + 43% $KClO_4$	3.09	1	$3.4 \cdot 10^{-3}$

On the basis of what has been presented it is possible to consider that in conditions of the conducted experiments the leading stage, determining the burning velocity of these mixtures, is in the reaction layer of the condensed phase in the whole temperature range studied.

With decrease of density of the mixture of potassium perchlorate with tungsten the mass burning velocity increases, and the temperature coefficient decreases (Fig. 5). It is possible that this effect is connected with anomalies in the reaction layer of the condensed phase. Not excluded is the possibility that there also occurred a jump of combustion in pores of a low-density mixture.

More complicated was the dependence of burning velocity on the initial temperature of a mixture of potassium perchlorate with organic fuel – potassium benzoate. This dependence at atmospheric pressure is shown in Fig. 6. Curve 1 pertains to a mixture of potassium benzoate with potassium perchlorate with a weight relationship of components 30% + 70% and with density 1.39 g/cm^3. Curves 2, 3, and 4 describe burning of mixtures with a relationship of components 30% + 70%, 15% + 85%, and 40% + 60% and with a density 2.16, 2.38, and 2.04 g/cm^3, respectively.

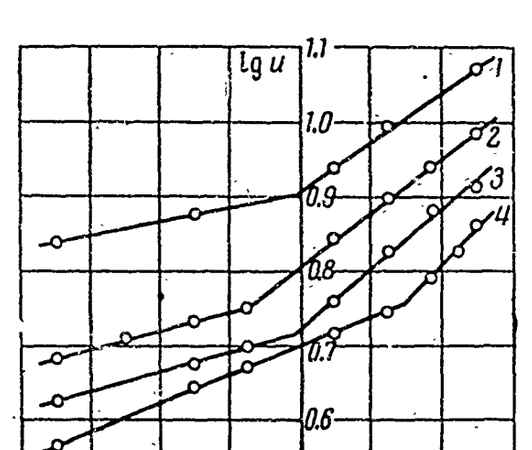

Fig. 6.

As can be seen from Fig. 6, this dependence cannot be described by a coefficient of burning velocity constant in the whole temperature range. Such anomalous dependences, characterized by a sharp change of the temperature coefficient in a narrow interval of initial temperatures, were observed earlier only during burning of nitroglycerine powder [1, 3, 4].

In Table 2 there are given temperature coefficients β^- below the point of discontinuity and β^+ above the point of discontinuity of a mixture of potassium perchlorate with potassium benzoate and the temperature at the point of discontinuity of the curve at coordinates T_0 and lg u. From Fig. 6 it is clear that temperature at the point of discontinuity T_0 decreases as the composition of the mixture approaches stoichiometric.

Table 2

Composition, wt. %	ρ, g/cm^3	T, C°	$\beta-$, deg^{-1}	$\beta+$, deg^{-1}
70% $KClO_4$ + 30 C_6H_5COOK	2.16	—30	$1.4 \cdot 10^{-3}$	$4.3 \cdot 10^{-3}$
30% CH_5COOK + 70% $KClO_4$	1.39	0	$1.4 \cdot 10^{-3}$	$4.1 \cdot 10^{-3}$
85% $KClO_4$ + 15% C_6H_5COOK	2.38	0	$2.1 \cdot 10^{-3}$	$4.3 \cdot 10^{-3}$
60% $KClO_4$ + 40% C_6H_5COOK	2.04	+60	$2.3 \cdot 10^{-3}$	$5.8 \cdot 10^{-3}$

The anomalous dependence of burning velocity of the mixture of potassium perchlorate and potassium benzoate from the point of view of our hypothesis is explained by the fact that at temperatures below the region of discontinuity the leading role is played by reactions in one spatial stage of burning, and above the break, in another. It is possible to consider that the leading stage of burning below the region of discontinuity are processes in the gas and smoke-gas phases, and above it, in the reaction layer of the condensed phase.

To check this hypothesis we conducted experiments with a mixture of different density, since when the leading stage of burning is in the gas phase the initial density should affect the mass burning velocity little [1, 7], and when the leading stage of burning is in the reaction layer of the condensed phase it is possible to expect that the mass burning velocity will increase with increase of density, first, due to increase of thermal conductivity and, second, due to the reacting particles of the oxidizer and fuel coming close to one another. Experiment showed that at high initial temperatures mass velocities will differ by approximately 20%, and at low initial temperatures they will differ by 10%. These values differ little from one another, so that by these data we can confidently judge a change of the mechanism of combustion.

It is necessary to note that potassium perchlorate in the reaction layer of the condensed phase is in a melted state, which conceals the influence of density.

Data of G. K. Oranskaya [1] show that at 18°C the mass burning velocity of pyroxylin does not depend on density, and at 98°C the mass burning velocity increases with increase of density above 0.5 g/cm^3 (experiments at atmospheric pressure). Apparently, this result is explained by the fact that with increase of initial temperature the role of the reaction layer of the condensed phase increases in accordance with our hypothesis. (Let us remember that according to A. I. Korotkov and O. I. Leypunskiy [3], the break of the curve at coordinates T_0 and lg u for nitroglycerine powder H, consisting of more than half pyroxylin, occurs at a temperature of 20-40°C.)

It would be interesting to determine the temperature of the leading stage of a reaction by the value of the temperature coefficient, as this is done, e.g., in [2]. However, in our work we basically investigated mixtures whose kinetics have not been studied. Furthermore, the temperature of the surface of the reaction layer of the condensed phase in many cases changes not additively to change of the initial temperature of the mixture [8].

Indeed, our experiments showed that the temperature on the surface of the pyroxylin powder burning without flame (pressure p ~ ~ 10^{-2} mm Hg), heated to 90°C, is equal to ~300°C, and of powder heated to 140°C is equal to ~320°C.

Using these values of initial temperatures and temperatures on the surface, and also values of burning velocity u = 0.7 mm/sec at 90°C and u = 1.4 mm/sec at 140°C, given in [5], by the formula of Zel'dovich [7] we calculated the activation energy of pyroxylin E = = 40,000 cal/mole and preexponent B = $10^{17.7}$ sec^{-1} (the coefficient of thermal diffusivity of the powder is taken equal to 10^{-3} cm^2/sec). The values of E and B obtained here are close to the kinetic data of

B. S. Samsonov [1], who, for slow decomposition of pyroxylin in vacuum, obtained E = 44,600 cal/mole and B = $10^{17 \cdot 8}$ sec^{-1}.

Measurement of the surface temperature during flameless burning showed that heat, liberated in the reaction layer of the condensed phase, with increase of initial temperature of the pyroxylin powder from 90 to 140°C decreases by 15% (from 84 to 72 cal/g). Heat capacity of the products of the generated smoke-gas mixture and powder was consider equal to 0.4 cal/g·deg.

The authors thank N. N. Mikhaylov for the design and manufacture of the installation for cooling the samples.

Submitted
23 November 1963

Literature

1. K. K. Andreyev. Thermal decomposition and burning of explosives. State power engineering publishing house, 1957.

2. A. F. Belyayev and G. V. Lukashenya. The pressure dependence of the temperature coefficient of burning velocity of VV [explosives] and powders. Reports of Academy of Sciences of USSR, 1963, Vol. 148, No. 6.

3. A. I. Korotkov and O. I. Leypunskiy. Temperature dependence of the temperature coefficient of burning velocity of powder at atmospheric pressure. Coll: Explosion physics, Publishing house of AS USSR, 1953, No. 2.

4. P. F. Pokhil, O. I. Nefedova, and A. D. Margolin. The anomalous dependence of the burning velocity of powder on initial temperature. Reports of Academy of Sciences of USSR, 1962, Vol. 145, No. 4.

5. P. F. Pokhil. The mechanism of burning of smokefree powders. Coll: Explosion physics, Publishing house of AS USSR, 1953, No. 2; 1954, No. 3.

6. A. D. Margolin. The leading stage of burning. Reports of Academy of Sciences of USSR, 1961, 141, No. 5.

7. Ya. B. Zel'dovich. Theory of burning of powders. Journal of exper. and theor. physics, 1942, Vol. 12, No. 12.

8. A. D. Margolin and P. F. Pokhil. Influence of pressure on the velocity of processes in the reaction layer of the condensed phase of a burning powder. Reports of Academy of Sciences of USSR, 1963, Vol. 150, No. 6.

STUDY OF THE TEMPERATURE DISTRIBUTION DURING BURNING OF AMMONIUM PERCHLORATE

V. K. Bobolev, A. P. Glazkova, A. A. Zenin, and O. I. Leypunskiy

(Moscow)

Study of the laws of burning of ammonium perchlorate is of interest in connection with the anomalies revealed during the study of its burning. Friedman, Nugent, et al. [1] discovered the phenomenon of an upper and lower limit of burning with respect to pressure, and also measured by thermocouples (junction ~50 μ) the maximum temperature of the flame, which turned out to be equal to 930°C and weakly grew with increase of pressure up to 150 atm. Subsequently, Levy and Friedman [2] established that application of an asbestos shell removes the upper limit. However, experiments of one of the authors of the present article [3] showed that burning of perchlorate is very sensitive to change of experimental conditions and, in particular, of the shell; for unarmored charges 7 mm in diameter in the pressure range above 150 atm, in distinction from charges 4 mm in diameter used by Friedman, burning takes place, but it proceeds unstably, with pulsations, and the dependence of burning velocity on pressure has an unusual form, depicted in Fig. 1, from which it is

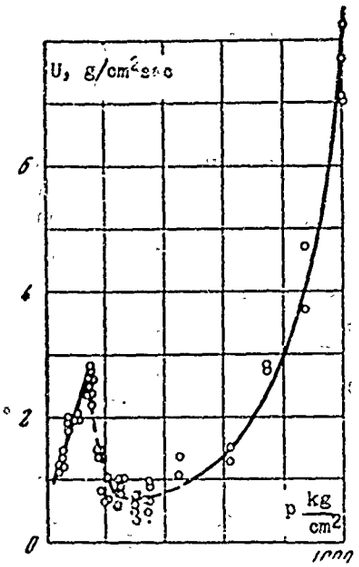

Fig. 1. Pressure dependence of burning velocity for unarmored 7-millimeter samples of ammonium perchlorate according to experiments of Glaskova.

clear that increase of pressure above 150 atm entails a drop of burning velocity. Drop of burning velocity with pressure was also observed for samples 12 mm in diameter, which is significantly larger than the critical diameter of burning in these conditions (see [3]).

Drop of burning velocity with pressure was observed also in the experiments of A. F. Belyayev and A. I. Korotkov [1] for potassium picrate. This phenomenon is unusual and is therefore of special interest. One proposed explanation of this phenomenon was expressed by K. K. Andreyev and Sung Ts'üan-Ts'ai,* connected with phase conversion of perchlorate at 240°C (at this temperature there occurs conversion of orthorhombic modification to cubic, which, by data of Bircumshaw [5], decomposes with considerably less velocity).

Temperature measurements during research of burning (surface temperature T_s, maximum flame temperature T_{max}, temperature gradient at the surface φ_s, etc.) are one of the most effective means in clarification of the mechanism of burning. Arden, Powling, and Smith [6] attempted to determine T_s of burning perchlorate by an infrared pyrometer and T_{max} by thermocouples (see [1]). They found that at atmospheric pressure $T_s = 450 \pm 30°C$ does not depend on burning velocity and the nature of the combustible addition, and T_{max} increases

*K. K. Andreyev and Sung Ts'üan-Ts'ai. Research of thermal decomposition of ammonium perchlorate and certain mixtures based on it. Dissertation, Moscow, 1961.

with increase of pressure. Based on constancy of T_s and increase of T_{max}, they stated the hypothesis that the temperature gradient at the surface increases with growth of pressure, and that the foremost mechanism during burning is sublimation. Subsequently, Powling and Smith [7], investigating burning of heated ammonium perchlorate (pure and with small additions of fuel) at pressures less than atmospheric, by the same method, arrived at the conclusion that burning velocity is limited by the equilibrium endothermic decomposition of NH_4ClO_4 into NH_3 and $HClO_4$. However, analysis of data given in that work for the temperature distribution in the zone of burning shows that on the surface of burning perchlorate there is an exothermic process.

In the present work we studied the temperature distribution during burning of ammonium perchlorate by the method of thin thermocouples, developed by A. A. Zenin* (see also [8]).

For measurements we applied П-shaped thermocouples W + Re-W + Re (5 and 20% Re), round ones of diameter 15 and 30 μ and laminar ones, 3, 5, and 7 μ thick, respectively. Experiments were set up with 7-millimeter samples of unsifted perchlorate (pressed to a density, close to its specific gravity – 1.93 to 1.94 g/cm^3) for which the phenomenon of a drop of burning velocity with pressure appears most sharply. Experiments were conducted in the pressure range 40-350 atm in a nitrogen atmosphere.

The method of embedding the thermocouples was developed in two variants. By the first we first molded columns of perchlorate 10 mm high and in them at an angle of ~45° at a distance of ~5 mm from the upper face we drilled holes 250 μ in diameter, through which there was inserted a П-shaped thermocouple, after which the sample was placed in a die of somewhat larger diameter, where there was preliminarily

*A. A. Zenin. Study of temperature distribution during burning of condensed substances. Dissertation, Moscow, 1962.

poured a portion of perchlorate, and it was pressed at a pressure of 3000-3500 kg/cm^2. In the second variant a П-shaped thermocouple was inserted between two portions of powdery perchlorate and pressing was performed in one step. To obtain transparent samples it was required to maintain them at this pressure for some 15-20 minutes. Simultaneously with recording of the temperature distribution on a loop oscillograph N-700 (thermocouples were connected through a preamplifier) there was recorded the velocity and nature of burning by a photorecorder. This allowed us to study the nature of burning in the region of drop of burning velocity with pressure in more detail. In particular, it was found that along with stops of burning there are regular oscillations of temperature in the gas phase with a period ~50 milliseconds and amplitude of oscillation up to 500° (1000 - 500°). Oscillations in temperature of the flame and the plateau on the temperature recording agree well with decrease of brightness of glow and with stops on the photographs of burning. This gave us grounds to call the region of pressures 160-350 atm the region of unstable burning.

In accordance with dependence $u_b = f(p)$ obtained earlier [3] (where u_b – mass burning velocity in g/cm^{2}sec, p – pressure in kg/cm^2) oscillograms of the temperature distribution have a different character. In the region of stable burning (below 150 atm) they have normal form, similar to that obtained earlier, e.g., for powder H. In Fig. 2 there are presented the most characteristic oscillograms of stable and unstable burning (160-350 atm). Oscillograms in the region of unstable burning are characterized by the presence in most oscillograms of a "plateau" with a stable temperature ~270°C and pulsation of temperatures in the flame. A typical oscillogram with oscillations of temperature in the gas phase with a period ~50 milliseconds is

presented in Fig. 2b. In the upper part of the given oscillograms are seen time marks with a frequency of 50 cps. At present final analysis of oscillograms during unstable burning is not possible; they will be analyzed after additional experiments, in which simultaneously with temperature we will more exactly record oscillations in burning velocities by height of the sample (e.g., with the help of a high-speed movie camera).

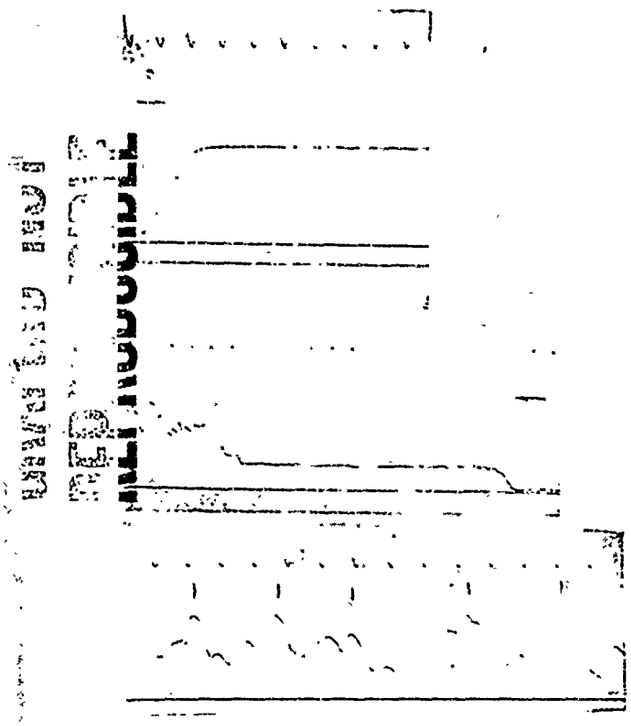

Fig. 2. Typical oscillograms of burning: a) in the stable region, p = 50 atm; b) in the unstable region, p = 250 atm; c) oscillogram, illustrating oscillations of temperature in the gas phase at p = 250 atm.

Let us note that in certain experiments burning went out upon reaching the thermocouple; in all these cases the surface of the extinguishing discharge was strictly horizontal and even, and the maximum recorded temperature was, on the average, ~270°C, which was taken as the surface temperature.

In the region of stable burning surface temperature was determined both by the method cited above — by peak intensity of heat emission in the condensed phase in analysis of oscillograms — and also by direct measurements by the method offered by P. F. Pokhil [ ]. For this, in a cylindrical column of perchlorate a distance of 2-3 mm we drilled longitudinal holes 250-300 μ in diameter for the thermocouple, from whose ends we suspended weights of 4-6 g; the column was ignited by a tablet of perchlorate, and when burning reached the thermocouple, under the weight of the weights it moved over the surface and recorded its temperature.

Analysis of oscillograms in the region of stable burning allowed us to obtain the temperature distribution in the zone of burning ($l > 0$ — gas phase, $l < 0$ — condensed phase), and analysis of temperature profiles gave us the distribution in the zone of the intensity of heat emission Φ. These results are shown in Fig. 3. In the graph of Fig. 4 are shown the pressure dependences of total heat emission, heat emission in the condensed and gas phases, and also the heat increment from the gas phase (q).

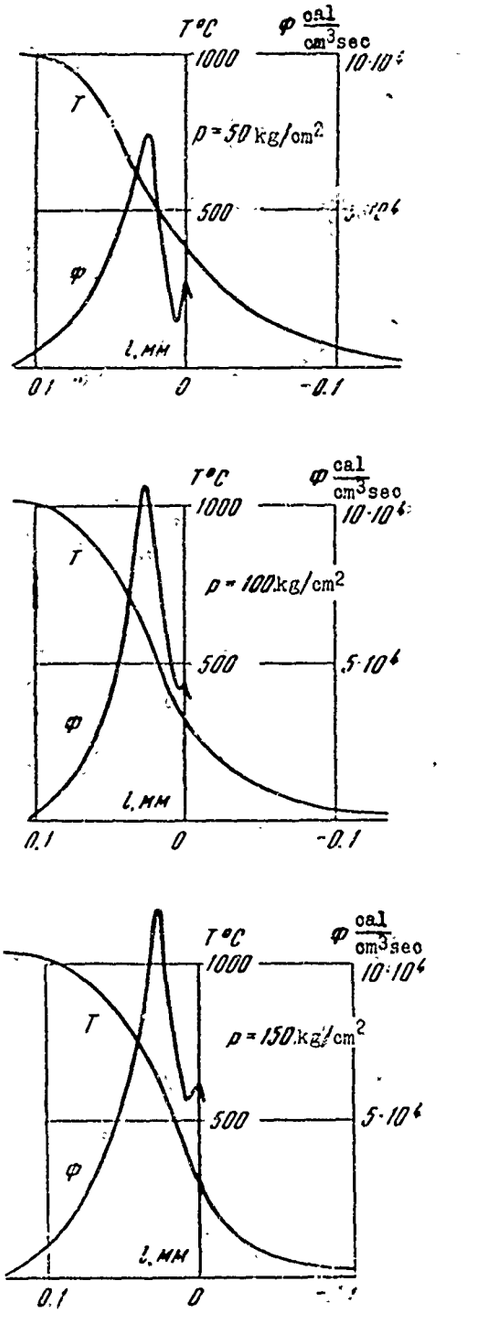

Fig. 3. Temperature profiles and distribution of the rate of emission of heat during burning of ammonium perchlorate in the stable region.

In pressure range 40-150 atm (stable conditions) there is observed an increase

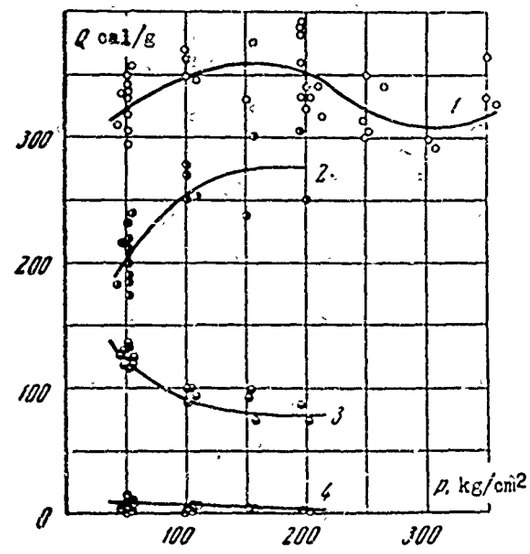

Fig. 4. Pressure dependence of total heat emission 1, heat emission in the gas 2 and condensed 3 phases, and also the heat increment from the gas phase 4 during burning of ammonium perchlorate on pressure.

of total heat emission 1, which is connected with its strong growth in gas phase 2, while heat emission in condensed phase 3 drops with

increase of pressure. However, it would be incorrect to consider that growth of burning velocity is caused only by growth of heat emission in the gas phase, since the supply of heat from gas phase 4 is small and changes little with pressure, and heat emission in the condensed phase, although higher by one order, sharply drops with pressure, and therefore one cannot explain the observed growth of burning velocity with pressure by the usual thermal mechanism.

The cause of increase of burning velocity with pressure one should seek, probably, in the nature of chemical reactions occurring here, the mechanism of which can vary with pressure (for another hypothesis of one of the authors, see below).

In principle there is also possible sharp increase of dispersion, which may cause an increase of burning velocity. This hypothesis requires experimental proof. Dispersion, undoubtedly, occurs during burning of ammonium perchlorate;* however, the quantity of unburned particles carried into the flame zone and precipitated on walls of the protective glass at a height, sometimes exceeding the height of the sample by 2-3 times, was larger for a lower burning velocity (at 50, 250-350 atm).

Possible also is growth of burning velocity due to change of surface structure; this too requires experimental proof. However, at present it is difficult to imagine the reason why the surface of perchlorate would be less friable at a higher surface temperature, e.g., 425°C at 50 atm, and more friable at lower surface temperature (325°C at 150 atm), which differs less from the temperature of phase transition, possibly also accompanied by loosening.

---

*P. F. Pokhil in this connection noted that, apparently, to burning of ammonium perchlorate it is possible to extend the mechanism of burning of ballistite powders, i.e., burning with participation of dispersion and formation of a smoke-gas phase and significant heat emission in the condensed phase.

A number of authors [6, 7] consider that during burning of ammonium perchlorate on its surface there occurs either sublimation, or endothermic decomposition of perchlorate. Levy and Friedman [2] calculated the width of the reaction zone in the gas phase, proceeding from the endothermic character of the process on the surface. It turned out to be equal to 0.1 μ for 100 atm.

Profiles obtained by us show that the width of the reaction zone in the gas phase is 1000 times greater than that calculated by Friedman and Levy. Moreover, from our results it follows that in the

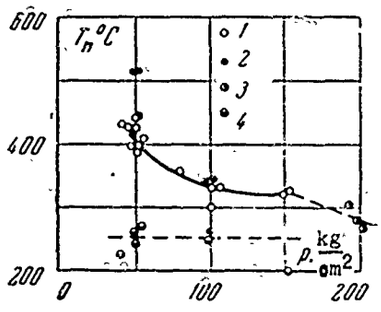

Fig. 5. Pressure dependence of temperature on surface of burning ammonium perchlorate: 1 — surface temperatures, determined by splash on oscillogram; 2 — surface temperatures, determined with the help of thermocouple with loads; 3 — surface temperatures at 200 atm are obtained during stable burning of preliminarily heated (to 40-50°) samples; 4 — temperatures of the break in the temperature distribution in the condensed phase in certain experiments during burning of ammonium perchlorate.

condensed phase during burning of ammonium perchlorate there is liberated a significant quantity of heat (80-120 cal/g) (Fig. 4). Furthermore, during sublimation or equilibrium decomposition T_s should grow with pressure, and not conversely as this follows from our experiments, presented in the graph of Fig. 5.

It is necessary to remind one also that Bircumshaw and Newman [5] could not detect a noticeable quantity of sublimated perchlorate during heating of it for 4.5 hours at 260°C at atmospheric pressure. In our experiments pressures were significantly higher.

The presented facts force us to doubt the validity of the hypotheses of works [6, 7], at least for the studied pressure range.

As can be seen from the graph of Fig. 5, surface temperature of burning ammonium perchlorate drops with growth of pressure and in

the region of unstable burning nears the phase transition temperature. Incidentally, one should note that in certain oscillograms in the region of temperatures of the order of 250°C there was observed a small break with a practically thermoneutral effect, which, possibly, is connected with the temperature of phase transition and weakly depends on pressure, as follows from the graph of Fig. 5.

Above it was noted (see Fig. 4) that heat emission in the condensed phase drops with increase of pressure. This phenomenon was not observed earlier for any of the studied substances.

Upon approximation of T_s to the temperature of phase transition during growth of pressure, heat emission in the condensed phase should drop more rapidly, since phase transition occurs with absorption of heat. This circumstance may be the reason for the drop of velocity, and in separate, unfavorable cases, the reason for extinguishing of burning. Incidentally, one should note that one of the possible factors supporting burning during pulsating conditions may be heat emission during reverse phase transition of cubic modification into orthorhombic with decrease of surface temperature to the temperature of phase transition.

Results of Fig. 5 in interval 50-150 atm are surprising not only in the drop of surface temperature with increase of pressure (i.e., according to Fig. 1, with increase of burning velocity), but also the low value of temperature. Known data on the kinetics of decomposition of perchlorate, obtained at a temperature of up to 280°C and extrapolated to 420°C, give a rate of gasification of perchlorate several orders smaller than the measured rate of decrease of the quantity of perchlorate during burning. Apparently, the kinetics and mechanism of gasification at relatively low temperature in experiments on the

decomposition of perchlorate differ from the kinetic and mechanism of gasification of perchlorate occurring at the same or higher temperature on the surface of burning perchlorate. One of the authors expressed the hypothesis that, perhaps, during burning there occurs catalysis of the decomposition of perchlorate on the surface by products of reaction and by active centers, proceeding from the flame zone to the surface of the condensed phase. The fact is that the presence of a flow of heat from the flame zone to the surface of the condensed phase automatically signifies the presence of diffusion of molecules (including radicals) from the flame zone to the surface. These active products of reaction can render effective catalytical action.

This hypothesis pertains, naturally, not only to burning of perchlorate, but also to burning of any condensed system, in which there exists a flow of heat from the reaction zone in the gas phase to the surface of the condensed phase, since thermal conduction in gas is carried out by means of diffusion of "hot" molecules (including active ones). This hypothesis, obviously, also contains in itself a possible mechanism by which the gas phase governs decomposition of the condensed phase. The significance of this mechanism would be especially substantial in those cases when the heat increment from the gas phase is small, and heat emission in the condensed phase is great and almost ensures maintenance of the surface temperature.

On the graph of Fig. 6 there is shown the pressure dependence of T_{max}; it passes through its maximum values, 1060°C, at 100-150 atm, and then starts to drop, although pressure is increased.

With the help of the previously developed method by distribution of temperature in the gas phase we calculated curves of the dependence

of the rate of heat emission in the burning zone. Calculation was conducted by the method of finite differences with an interval of 10 μ. By curves of the intensity of heat emission we calculated total activation energies and reaction orders in the gas phase. The obtained magnitudes E and n, although having a formal character, can be of unquestioned interest for establishment of the mechanism of burning.

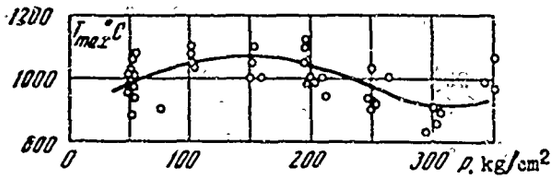

Fig. 6. Pressure dependence of maximum temperature of burning of ammonium perchlorate.

The reaction order was calculated by the pressure dependence of the intensity of heat emission for a fixed temperature by the formula $\Phi^* = B + n \lg p$, where Φ^* — intensity of heat emission at fixed temperature, B — constant (equal to $\lg Ae^{-E/RT}$), n = the reaction order, p — pressure.

For temperatures 500-600°, corresponding to the region of peak intensity of heat emission in the gas phase, the reaction order is ~1. Activation energy was calculated by the formula $u \sim p^{n/2} e^{-E/2RT_m}$, where u — burning velocity, E — activation energy, T_m — temperature corresponding to peak intensity of heat emission. Effective activation energy in interval of pressures 30-150 atm turned out to be equal to 10-15 kcal/mole. Calculation of activation energy of reactions in the condensed phase we plan to conduct in the future by experiments, where for fixed pressure we will change initial temperature of the sample and, as a result of this, the burning velocity and surface temperature.

Small changes of initial temperature of samples, sometimes occurring in our experiments, led to a change of burning velocity,

and with it of surface temperature. They permitted us to roughly estimate total activation energy of reactions in the condensed phase at 50 atm, which turned out to be of the order of 20-30 kcal/mole.

Conclusions. 1. We obtained temperature profiles in region of pressures 40-350 atm, which show the presence of two regimes of burning of ammonium perchlorate, stable (40-150 atm) and unstable (160-350 atm).

2. We fixed anomalous pressure dependences of surface temperature and heat emission in the condensed phase — a drop with growth of the latter.

3. We expressed a hypothesis about change of the mechanism of burning of ammonium perchlorate with growth of pressure and about the catalytical influence of products, diffusing from the reaction zone in the gas phase to the surface, on the reaction of gasification of the condensed phase.

4. We expressed a hypothesis about the cause of the drop of burning velocity of ammonium perchlorate with growth of pressure at $p > 150$ atm.

5. We ascertained the fact of significant divergence between kinetics of thermal decomposition and kinetics of gasification of perchlorate during burning.

Submitted
15 April 1963

Literature

1. R. Friedman, R. G. Nugent, K. E. Rumbel, and A. C. Scurlok. Deflagration of Ammonium Perchlorate. VI Symposium on Combustion, 1957, 612.

2. G. B. Levy and R. Friedman. Further Studies of Pure Ammonium Perchlorate Deflagration. VIII Symposium on Combustion, 1960, 663.

3. A. P. Glazkova. Pressure dependence of burning velocity of ammonium perchlorate. PMFT, 1963, No. 5, p. 121.

4. A. F. Belyayev and A. I. Korotkov. Burning of mercury fulminate and potassium picrate at heightened pressures. Explosion physics, 1952, No. 1.

5. L. L. Bircumshaw and B. H. Newman. The Thermal Decomposition of Ammonium Perchlorate. Proc. Roy. Soc., 1954, A 227, 115, 228.

6. E. A. Arden, I. Powling, and W. A. W. Smith. Observations on the Burning of Ammonium Perchlorate. Combustion and Flame, 1963, Vol. 6, No. 1, 21.

7. I. Powling and W. A. W. Smith. The Surface Temperature of Burning Ammonium Perchlorate. Combustion and Flame, 1963, Vol. 7, No. 3.

8. A. A. Zenin. Heat exchange of microthermocouples in conditions of burning of condensed substances. PMFT, 1963, No. 5.

9. P. F. Pokhil, L. D. Romodanova, and M. M. Belov. The mechanism of burning of smokeless powders. Explosion physics, 1955, No. 3.

EXPLOSION ON THE SURFACE OF A LIQUID

V. F. Minin

(Novosibirsk)

In work [1] there is considered a formulation of the problem of the motion of an ideal incompressible and weightless liquid of infinite depth, caused by an explosion on its surface. As the basic parameter, characterizing the effect of the explosion on the liquid, there is taken the momentum acquired by the liquid. In this case during self-simulating motion the graph of the time-dependence of the size of the funnel, built in logarithmic scale, for a cylindrical explosion should be a straight line with angular slope, equal to 1/3, which is confirmed by experiments given in work [1]. Below are results of experimental research devoted to this question.

1. Cylindrical explosion. Explosion was produced by means of discharge of a battery of 50 μf capacitors, charged to voltage of 3 kv through Nichrome wire 40 mm long and 0.09 mm in diameter. Discharges were produced in a tank with hard walls of dimensions 1100 × × 550 × 20 mm. Plexiglas windows 40 mm thick, built into walls of the tank, allowed us to produce optical registration of the phenomenon. The wire was established perpendicular to the long edges of the tank. The initial level of the free surface of the liquid was fixed by a line on the tank window. Motion of liquid after the explosion was recorded by high-speed filming on camera SFR-1 in the beginning of

the process, but more recently by camera Pentazet 16. Speed of filming during experiment was monitored and was strictly constant during the time of registration of the phenomenon, which allowed one to analyze experiments, considering one frame to be the unit of time.

As a result of analysis of experiments of the initial stage of explosion (filming speed $2 \cdot 10^5$ frames per sec) in Fig. 1 there is constructed the dependence of diameter d (mm) of the funnel at the level of the free surface on time t (sec) (in logarithmic coordinates, Fig. 1a [sic]); experimental points lie along line 1; in a later stage of explosion (filming 3000 frames per sec) up to a time, equal to 10^{-2} sec, dependence also is close to straight line 2. Angular slope of straight lines, obtained from the experiment, varies from 0.45 to 0.48, with mean value for 20 experiments 0.47.

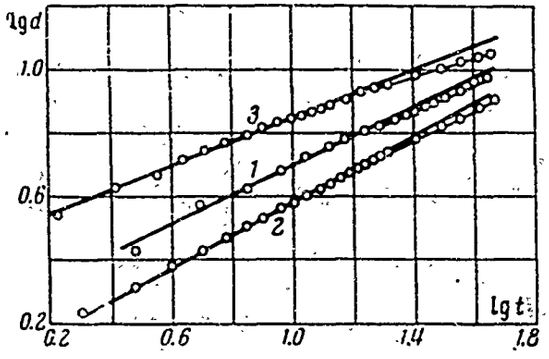

Fig. 1.

After 10^{-2} sec experimental points deviate downwards from a straight line. Acceleration a of the funnel wall on the level of the free surface, determined after the explosion, turned out to be equal to

$$a = 11\,g \text{ when } t = 1 \cdot 10^{-2};\ a = 5.5\,g \text{ when } t = 1.5 \cdot 10^{-2} \text{ sec};$$
$$a = 3\,g \text{ when } t = 2 \cdot 10^{-2} \text{ sec}.$$

Therefore, fully evident is the fact that starting from times, greater than 0.01 sec, the funnel ceases to be geometrically similar in the process of motion (Fig. 2, where d and r are in mm). Thus, further motion of the liquid is substantially influenced by acceleration due to gravity, which was not considered in work [1], where in conditions of the experiment described here, experimental points li

on a straight line with slope 1/3, starting from time of approximately $5 \cdot 10^{-2}$ sec, i.e., in region where weight is substantial.

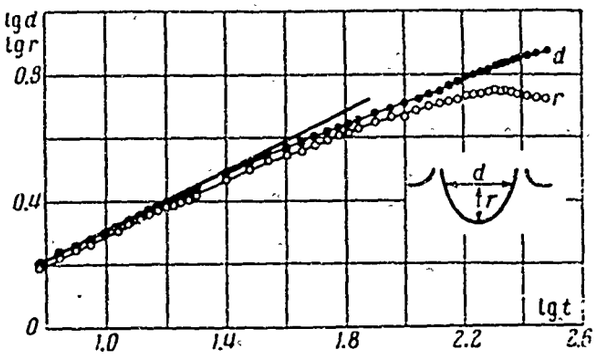

Fig. 2.

This regularity is stable relative to slight variation of immersion of the wire. In our proof we produced explosions both above the free surface and beneath it. Essential distinctions in motion of liquid here were not detected; furthermore, which [sic] during explosion above the surface the size of the funnel at a fixed moment of time is several times less than with immersion of the wire, which is obvious. In order to trace the motion of liquid for a larger interval of time than 0.01 sec, in the absence of gravity, there was built an experimental installation, consisting of a falling platform with a tank of the dimensions 560 × 300 × × 20 mm and a movie camera set on it. This device allowed us to record motion of weightless liquid for 0.3 sec; in Fig. 3 this case corresponds to curve 1, and for comparison there is given curve 2, obtained in analogous conditions to curve 1, but with weight. In experiments filming speed was 2000 frames per sec. Curve 1 to moment of time 0.02 sec turned out to be also close to a straight line with angular coefficient 0.47.

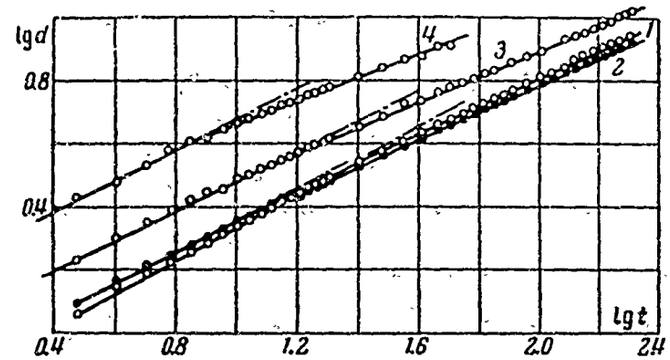

Fig. 3.

During experiments with different energies of the explosion produced on the surface of weightless liquid, it was found that, starting

from a certain funnel size motion of the liquid essentially depends on dimensions of the tank. This can be illustrated by curves 1, 3, and 4 in Fig. 3, where it is clear that a break in the curves occurs at the same funnel size, approximately 1/8 the size of the tank. To check the assumption we performed experiments in a tank 260 mm long and with explosion energy corresponding to the explosion presented in Fig. 3 by curve 1. Here, it turned out that the break of the curve starts earlier and corresponds to moments of time, when the funnel size is approximately 1/8 the size of the tank.

Thus, to study the motion of an infinite weightless liquid, caused by an explosion on its surface, for a time, greater than 0.02 sec, with existing tank sizes did not seem possible.

For a plane explosion on the surface of a liquid it was possible to obtain in an experiment the velocity field in liquid at different fixed moments of time, which was done as follows.

Water in the bath was replaced by a salt solution, in which there were mixed particles of rosin of the dimension 0.1-0.3 mm. Concentration of salt in water was selected in such a way that the specific weight of the solution and of rosin were identical. After explosion the liquid was illuminated by pulse tube IFK-120, and was photographed by a camera with open shutter on a photographic plate of dimensions 18 × 24 cm. Moment of time of filming was set in the following manner.

Upon supply of voltage to detonated wire there was started square wave generator GIP-2, which formed single square pulse of predetermined duration. After differentiation of this pulse there was trimmed a signal, corresponding to the leading edge of the front, and by a signal from the trailing edge there was started a thyratron, working on a pulse transformer, which ignited the flashbulb. Thus, the moment of filming was determined by duration of the square pulse and could be selected

from 10^{-6} to $5 \cdot 10^{-2}$ sec. Response time of the circuit did not exceed 10^{-7} sec. Exposure during photographing, upon desire, could be changed from 10^{-4} to $5 \cdot 10^{-3}$ sec, by changing parameters of the shaping line, composed of inductances and capacitances and feeding the pulse tube.

However, in the given experiments exposure remained constant and equal to 10^{-3} sec. Filming of the velocity field was produced up to time 10^{-2} sec, i.e., in range, where weight is still not essential, and energy of explosion was selected such that influence of the tank walls could be disregarded.

In Fig. 4 there is given a photograph of the velocity field with time from the beginning of the explosion to the beginning of the exposure of the photograph 2.5 msec, which was obtained during an explosion on the surface. On the photograph there are drawn lines, passed in such a way that the paths of rosin particles, photographed on the photographic plate, are tangent to these lines at every point. Considering the time of exposure of the photograph to be small, it is possible to speak of the given curves as flow lines, which, of course, will be a certain approximation. Experiments showed that, as one should have been led to expect, the family of flow lines, taken at different moments of time with a time interval of 1 msec in the time, passed from the beginning of explosion to 10^{-2} sec, i.e., during the time, when in our conditions liquid can still be considered weightless, remains geometrically similar with precision obtained in development of the photograph.

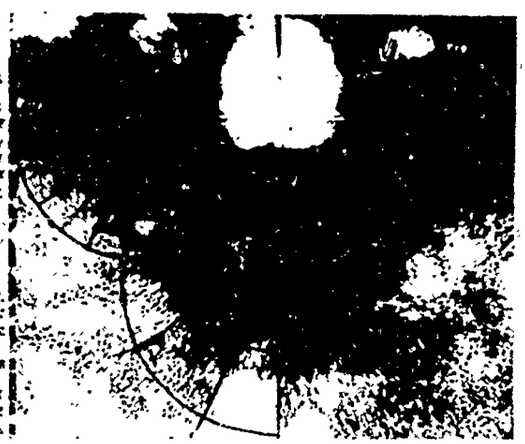

Fig. 4.

This fact does not pertain to a sputtering stream, i.e., to that region of flow where continuity of the liquid is disturbed.

From these photographs of velocity field it is possible to judge the potential realized during motion of the liquid. It turned out that the form of potential in a fairly rough approximation is near to that which is given by a source placed in the center of an explosion, and two flows of half intensity placed symmetrically relative to the source at an angle of 45° to the free surface, a distance of 1.75r from the center of the explosion, where r — depth of the funnel.

It is necessary to note that this form of potential of flow does not pretend to be an exact description of motion of the liquid and in a certain sense has more of a qualitative than quantitative character.

In Fig. 4 is shown the form of a free surface realized during an explosion.

The interior of the funnel, below the initial level of the liquid, is close in form to a circular semicylinder with ratio of diameter to depth from 2.2 to 2.36.

2. Point explosion on a water surface. An explosion was produced in a Plexiglas tank, having dimensions 600 × 500 × 400 mm. The battery of capacitors in this case was charged to 3 kv and was discharged through a flat spiral 3 mm in diameter, made from wire 0.09 mm in diameter. Such a flat charge was established exactly on the surface of the liquid. Registration of the phenomenon was produced with the help of high-speed filming with rate of filming 2000 frames per sec.

Results of experiments were formulated in graphs with the coordinates indicated above. One of these experiments is represented in Fig. 1 (curve 3), where it is clear that experimental points lie on a

straight line with slope close to 0.4 up to time of $6.6 \cdot 10^{-3}$ sec. Average slope for 20 experiments is equal to 0.38, which also is not compatible with the pulse formulation of the problem, from which it follows that for the case of a point explosion slope should be 0.25.

Thus, from these experiments it may be concluded that motion of a weightless liquid, caused by an explosion on its surface, with the exception of sputtering streams, is close to self-simulating with an index of self-similation $\alpha = 0.47$ for cylindrical explosion and $\alpha = 0.38$ for a point explosion.

The experimental law of motion of a funnel, given in work [1], does not correspond to motion of weightless liquid.

Submitted
23 October 19 3

Literature

1. A. A. Deribas and S. I. Pokhozhayev. Formulation of problem of a strong explosion on the surface of a liquid. Reports of Academy of Sciences of USSR, 1962, Vol. 144, No. 3.

REMARK ON SCATTERING OF A GAS CLOUD IN A VACUUM

Yu. P. Rayzer

(Moscow)

In a number of works [1-3], in which the process of expansion of gas into a vacuum is considered, it is assumed that in sperically symmetric free-molecular scattering particles of gas have a Maxwellian velocity distribution. Such concepts must sometimes be dealt with during discussion of closely related questions.

Here one should turn attention to the fact that in order that during scattering of a gas cloud into a vacuum asymptotic velocity distribution of particles be Maxwellian, corresponding to the initial temperature of gas, we need very special initial conditions, almost unrealizable in practice. If the final distribution also has general features of Maxwelliam distribution, this analogy in most practical cases is deprived of any physical content.

Particles of gas, expanded into a vacuum, have Maxwellian velocity distribution

$$f(v)\,dv = \text{const}\; v^2 e^{-\beta v^2}\,dv \qquad (\beta = m/2kT_0) \tag{1}$$

only when a gas, having temperature T_0 and occupying some volume, say a sphere of radius R_0, from the very beginning expands without collisions. In this case upon the expiration of sufficient time, we

the basic mass of gas has scattered distances $r \gg R_0$, in space there is established a linear velocity distribution and Gaussian distribution of particle density by radius:

$$v = \frac{r}{t}, \qquad n = \frac{f(v)\,dv}{4\pi r^2 dr} = \frac{\text{const}}{t^3} e^{-\beta r^2/t^2} \tag{2}$$

However, so that collisions from the very beginning do not play a role, it is necessary that particle path length l_0 at the initial moment is of the order of or larger than dimensions of cloud R_0

$$R_0 / l_0 = n_0 \sigma R_0 \lesssim 1 \tag{3}$$

Here n_0 – average initial density of particles, σ – effective collision cross section. Let us note that it is possible to present (3) in the form $M \lesssim \frac{4}{3}\pi R_0^2 m/\sigma$, where M – mass. For instance, for atomic weight 15 and $\sigma \sim 10^{-15}$ cm^2 we have $M \lesssim 10^{-7} R_0^2$ (M in g, R_0 in cm).

In practice the most important object for application of the idealized problem of scattering of a gas sphere into a vacuum is the process caused by an explosion-like heating and transformation into gas of a certain quantity of solid matter, in a rarefied medium.

Taking into account the fact that in this case $n_0 \sim 10^{22}$-10^{23} cm^3, and section σ in order of magnitude is at least 10^{-15}-10^{-16} cm^2, we find that for satisfaction of condition (3) dimensions of the body should not exceed $\sim 10^{-7}$ cm, i.e., a magnitude of the order of several atomic diameters. If, however, e.g., the mass of the body is of the order of several grams, $R \approx 1$ cm, and on the length of the initial gas cloud there are included $\sim 10^7$ free path lengths!

Running through all possible values of initial parameters of the cloud: density n_0, radius R_0, and mass $M = n_0 m \frac{4}{3}\pi R_0^3$, and considering that to talk of scattering into a vacuum has meaning only in those cases when density n_0 is many orders larger than the density of the environment (an absolute vacuum does not exist), it is easy to prove

that relationship (3), with perhaps rare exceptions, is never satisfied in cases of physical or practical interest.

In real conditions, when $l_0 \ll R_0$, expansion of the gas cloud always starts with a gas-dynamic stage, where the final velocity distribution of particles is formed, as a rule, in the process of motion of a "solid" medium, even before onset of the stage of free-molecular scattering. And namely, velocities of particles approximately attain their final values when the initial thermal energy of the gas to a significant degree passes into kinetic energy of hydrodynamic motion, i.e., chaotic velocities of particles become small as compared to ordered radial velocities. Here, there almost ceases the action of forces of pressure, and scattering of gas obtains an inertial character.

Let us compare tentative moments of establishment of final velocities and of ceasing of collisions. During adiabatic expansion internal energy of gas E_T decreases approximately as

$$E_T \approx E_0 (R_0 / R)^{3(\gamma-1)}$$

where E_0 — total energy, which initial internal energy approximates, R — effective radius of sphere, γ — effective adiabatic index. Considering a highly heated dense gas, it is possible to assume for estimation that $\gamma = \frac{4}{3}$ and $E_T/E_0 \approx R_0/R$. Scattering becomes almost inertial, we say, with $E_T/E_0 = 0.1$ when $R_1 \approx 10 R_0$ (velocities here on an average attain 0.95 of their final values). The average mass velocity of scattering becomes equal approximately to $u \approx \sqrt{2(E_0/M)}$, and the radius of the sphere (with accuracy up to a coefficient of the order of unity) changes in time as $R \approx ut$.

The average number of collisions which an atom will experience from moment t to infinity in order of magnitude is

$$w \approx \int_t^\infty n V \sigma \, dt \qquad \left(V \approx \left(\frac{E_T}{M}\right)^{1/2},\ n \sim \frac{1}{R^3} \sim \frac{1}{t^3}\right)$$

Here V – average chaotic (thermal) velocity, n – average density in the sphere. Integrating, we find with accuracy up to a numerical coefficient of the order of unity $w \approx nV\sigma t$, where all quantities in the right part pertain to moment t.

For the moment of ceasing of collisions it is possible tentatively to take such moment starting from which an atom for all time to infinity will experience only one collision. This moment t_2 is determined from equation

$$(n V \sigma t)_{t=t_2} \sim 1$$

Using approximate relationships

$$\frac{n}{n_0} = \left(\frac{R_0}{R}\right)^3, \qquad \frac{V}{u} \approx \left(\frac{E_T}{E_0}\right)^{1/2} \approx \left(\frac{R_0}{R}\right)^{1/2}, \qquad t = \frac{R}{u}$$

we find the radius of a sphere R_2, at which collisions cease

$$R_2 \approx R_0 (R_0 / l_0)^{2/5} \tag{4}$$

(if $R_0 \lesssim l_0$, collisions are absent from the very beginning, in accordance with condition (3)).

Thus, if $R_1 \approx 10$, $R_0 < R_2$, i.e., if $R_0/l_0 > 300$, scattering becomes inertial even before collisions cease. This condition is satisfied in most cases of practical interest, and, consequently, the final velocity distribution of particles in these cases is established already in the gas-dynamic stage. It is determined by the asymptotic density profile, which at the limit $t \to \infty$ is kept unvaried $n \sim t^{-3} F \times$ $\times (r/t)$. Asymptotic velocity distribution during inertial scattering is $v = r/t$; therefore, final velocity distribution of particles is determined by function

$$f(v)\,dv = n\,4\pi r^2\,dr \sim r^2 F(v)\,dv$$

The asymptotic density profile depends on initial distributions of gas-dynamic quantities. There exists an unlimited number of such

initial distributions, for which function F has nothing in common with the Gaussian, and $v^2F(v)$ has nothing in common with Maxwellian. There is, for instance, the class of one-dimensional self-similar motions shown by L. I. Sedov [4] in which $v = r\varphi(t)$, and pressure p and density ρ are connected by relationship $\partial p/\partial r = -\rho r(\varphi^2 + d\varphi/dt)$. If initial distributions of gas-dynamic quantities satisfy this condition the density profile $F(r/t)$ by virtue of self-similarity is kept unvaried from the very beginning, and this profile, and consequently, also the asymptotic velocity distribution of particles $v^2F(v)$ can be given arbitrarily (see [5]).

It is clear that in many practically important cases the density profile formed in the stage when forces of pressure still act has common features with the Gaussian curve, and final velocity distribution has common features with the Maxwellian. However, this is nothing more than a convenient approximation, and here there is no physical connection with the initial Maxwellian distribution of heated gas. It is sufficient to say that "temperature" in the interpolational Maxwellian law may be several times greater than the initial temperature of gas, since to kinetic energy of radial motion there passes not only the initial energy of chaotic motion of particles, but also the energy of internal degrees of freedom, ionizing energy, initial thermal energy of free electrons, which in the process of adiabatic expansion and cooling recombine with ions, etc. For more detail on this see [5].

Submitted
5 March 1964

Literature

1. P. Molmud. Expansion of a gas cloud into a vacuum. Phys. Fluids, 1960, 3, 362.

2. R. Narasimha. Expansion of gases into a vacuum without collisions. J. Fluid Mech., 1962, 12, 294; Coll. trans. "Mechanics," 1963, No. 2.

3. A. Ya. Pressman. Flow of rarefied gas into a vacuum from a point source. Reports of Academy of Science of USSR, 1961, Vol. 138, 1305.

4. L. I. Sedov. Methods of similarity and dimensionality in mechanics. Gostekhizdat, 1957.

5. Ya. B. Zel'dovich and Yu. P. Rayzer. Physics of shock waves and high-temperature hydrodynamic phenomena, Fizmatgiz, 1963.

EQUATIONS OF STEADY AXISYMMETRIC FLOWS OF GAS IN VARIABLES "PRESSURE-STREAM FUNCTION"

V. G. Dulov

(Novosibirsk)

Equations of steady axisymmetric flows of an inviscid and non-heat-conducting gas with an arbitrary equation of state will be converted to such form when pressure and the stream function can be considered independent variables. The sought function of these variables is introduced so that dynamic equations are satisfied identically, and from the continuity equation for this function there is obtained the Monge-Ampere equation. The sought function itself constitutes a flow of momentum through a line of constant pressure in the direction of the axis of symmetry. Through values of this function we simply express the drag coefficient of a solid of revolution with a generatrix in the form of an arbitrarily taken flow line. There are examples of calculations. In the first there is considered the problem of external flow by supersonic flow past a body with an arbitrary generatrix. Approximation of change of the desired function along an isobar by a polynomial from the stream function allows us to reduce the problem to a system of ordinary differential equations. In the second problem we approximately find the distribution of parameters

between the shock wave and the surface of a blunt body in a hypersonic flow. The solution has relatively low accuracy, but is recorded in elementary form, useful for rapid calculations.

1. Below we use the following designations: x, y — geometric coordinates in the plane of the axial section, p — pressure, ρ — density, i — enthalpy per unit mass, ψ — stream function, w — modulus of velocity, u and v — projections of velocity on x and y axis, respectively, M — Mach number, ϑ — angle of inclination of velocity vector to axis of symmetry, S — entropy, a — speed of sound, index ∞ is used for designation of parameters of incident flow. All measured magnitudes refer to parameters of undisturbed flow. Enthalpy i we consider a given function of pressure and entropy (equation of state), $i = i(p, S)$.

We introduce as independent variables pressure p and stream function ψ. Then

$$d\psi = \rho y\,(u\,dy - v\,dx) = \rho y\,[u\,(y_p\,dp + y_\psi\,d\psi) - v\,(x_p\,dp + x_\psi\,d\psi)]$$

or

$$(\rho y u y_\psi - \rho y v x_\psi - 1)\,d\psi = (\rho y v x_p - \rho y u y_p)\,dp, \qquad 1/\rho = i_p$$

In view of independence of dp and $d\psi$ there follow from this the relationships

$$yy_\psi - vx_\psi = i_p y, \qquad vx_p - uy_p = 0 \tag{1.1}$$

Let us consider dynamic equations for an inviscid and nonheat-conducting gas

$$u\frac{\partial u}{\partial x} + v\frac{\partial u}{\partial y} + \frac{1}{\rho}\frac{\partial p}{\partial x} = 0 \tag{1.2}$$

$$S = S(\psi), \qquad {}^1/_2(u^2 + v^2) + i = i_m = \text{const} \tag{1.3}$$

Subsequently, we shall consider dimensionless enthalpy related to magnitude w_∞^2. In (1.2) let us turn to independent variables ψ and y; we obtain

$$p_\psi = u_y/y, \quad \text{or} \quad y_\psi = -u_p/y \tag{1.4}$$

In the latter case y is considered the sought function, and pressure is the independent variable.

Equations (1.1) and (1.4) can be useful for numerical calculations, since the form of their recording is superficially similar to the system of equations in characteristic variables: two of the obtained equations contain derivatives of the sought functions only in one direction. However, equations (1.1) and (1.4) cannot be considered as a system of independent equations.

Using isoenergetic relationship (1.3) for partial derivatives, we have

$$\tfrac{1}{2}y^2 = c_p, \qquad u = -\sigma_\psi \tag{1.5}$$

Equation (1.4) will be satisfied identically, if we assume that

$$x_p = (u/v)\, y_p, \qquad x_\psi = (v\rho/y) \tag{1.6}$$

where $\sigma = \sigma(p, \psi)$ — arbitrary function. Eliminating x, by cross-differentiation from (5) we can obtain an equation, containing only one function of σ

$$2(i_m - i)(\sigma_{p\psi}^2 - \sigma_{pp}\sigma_{\psi\psi}) - \left[i_s S'(\psi)\sigma_\psi + i_p \frac{2(i_m - i) - \sigma_\psi^2}{2\sigma_p} \right] \sigma_{pp} + \\ + 2i_p \sigma_\psi \sigma_{p\psi} + i_p^2 + [2(i_m - i) - \sigma_\psi^2]\, i_{pp} = 0 \tag{1.7}$$

For $\Delta > 0$ equation (1.7) will be an equation of hyperbolic type; for $\Delta < 0$ it is an elliptic equation, i.e., hyperbolicness occurs at supersonic speeds, and ellipticity at subsonic. From theory of Monge-Ampere equations it is known that if a coefficient in a non-linear combination of higher derivatives does not turn into zero, the boundary problem in the region of ellipticity for such an equation has two different solutions. If there is a point where this coefficient turns into zero, the solution will be unique. In equation (1.7) this coefficient will be the square of the modulus of velocity.

Consequently, when in a flow there is a critical point (for instance, in problems about external flow past bodies) there should be a unique solution. If, in the flow there are local subsonic regions, but total stagnation of the flow is absent (for instance, in supersonic gas jets), there can exist two solutions.

We shall clarify the gas-dynamic meaning of the introduced function $\sigma(p, \psi)$. The second of equalities (6) gives

$$\sigma = -\int u\, d\psi$$

Here the integral in the right part is taken along the isobar. It follows from this that σ constitutes the flow of momentum through line p = const in the direction of the axis of symmetry. We fix a certain surface of rotation with a generatrix in the form of a flow line. The projection X in the direction of the axis of symmetry of the force of total pressure on such a surface is calculated as follows:

$$X = 2\pi \int p y\, y_p\, dp = 2\pi (p\sigma_p - \sigma)$$

In particular, if X is determined for flow line $\psi = 0$ (surface of the solid), this last expression will give the magnitude of the drag force, where quantity $2\sigma_p \pi = \pi y^2$ for $\psi = 0$ is equal to the base area of the flowed-past body. Thus, to determine the drag coefficient of the body, it is necessary to know the value of function σ only at one point, corresponding to the trailing edge of the body.

2. Let us assume that solution of equation (1.7) in the vicinity of a certain line $\psi = \varphi(p)$ in plane $p\psi$ can be expanded into a series of form

$$\sigma(p, \psi) = \sigma^\circ(p) + \sigma_\psi^\circ [\psi - \varphi(p)] + \tfrac{1}{2}\sigma_{\psi\psi}^\circ [\psi - \varphi(p)]^2 + \ldots \qquad (2.1)$$

Here, index $^\circ$ designates values of the corresponding quantities on line $\psi = \varphi(p)$. If, we assume $\sigma \equiv \sigma^\circ(p)$, then, according to (1.6), we have $w \cos \vartheta = -\sigma_\psi \equiv 0$ or $\vartheta \equiv \frac{1}{2}\pi$. From equation (1.7) we find the

form of function $\sigma^{\circ}(p)$ which describes the degenerate case of axisymmetric flow — a two-dimensional gas source. Let us assume relationship $\psi = \varphi(p)$ determines the front line of the shock wave in plane (p, ψ). From mechanical conditions of compatibility we determine values of derivatives of σ°_{p} and σ°_{ψ} on this line (flow in front of the front is considered uniform; σ is related to p_{∞}):

$$\sigma_p^{\circ} = \psi, \qquad \sigma_{\psi}^{\circ} = p - 1 - kM_{\infty}^2, \qquad k = \frac{p_{\infty}\rho_{\infty}^2}{p_{\infty}} \tag{2.2}$$

It is possible to calculate values of function σ on the front line of the shock wave:

$$\sigma^{\circ}(p) = \int [\varphi(p) + (p - 1 - kM_{\infty}^2)\varphi'(p)]\,dp \tag{2.3}$$

Retaining the first two terms in expansion (2.1), by means of differentiation with respect to p and ψ, we prove that relationships (2.2) are satisfied everywhere behind the shock wave front. This is possible only for zero thickness of the shock layer, i.e., such a presentation of function σ corresponds to the Newtonian approximation.

Let us consider the case when expansion (2.1) is performed to members of the second order. Differentiating with respect to p and ψ, we obtain

$$\begin{gathered}\sigma_p = \psi - x^{\circ}_{\psi\psi}\varphi'(p)[\psi - \varphi(p)] + \frac{1}{2}\frac{dx^{\circ}_{\psi\psi}}{dp}[\psi - \varphi(p)]^2 \\ x_{\psi} = p - 1 - kM_{\infty}^2 + x^{\circ}_{\psi\psi}[\psi - \varphi(p)]\end{gathered} \tag{2.4}$$

Thus, in this approximation function σ_p along lines of constant pressure is approximated by a quadratic dependence on ψ, and the axial component of velocity is considered linearly related to the stream function.

In formulas (2.4) there are two unknown functions of pressure, $\sigma^{\circ}_{\psi\psi}$ and $\varphi(p)$. To find them we use the condition on the surface of the body and equation (1.7). The equation of the contour of the surface we consider given in the form $y^2 = f(\cos\vartheta)$, which, by virtue

of formulas (2.4), gives

$$\frac{d}{dp}\left[\sigma^{\circ}_{\psi\psi}\varphi^{2}(p)\right] = f\left\{\frac{1+kM_{\infty}^{2}-p+\sigma^{\circ}_{\psi\psi}\varphi(p)}{kM_{\infty}^{2}\sqrt{2(i_{m}-i)}}\right\} \tag{2.5}$$

Further, we assume that density ρ, speed of sound a, and consequently, quantity $\gamma = a^2\rho/p$ are known functions of pressure on the line of the shock wave front. With the help of conditions of compatibility in a shock wave, we can express values of all coefficients in equation (1.7) behind the wave front in terms of p, ρ, and γ. Differentiating (2.2) along line $\psi = \varphi(p)$, we eliminate derivatives of $\sigma^{\circ}_{\psi\psi}$ and $\sigma^{\circ}_{p\psi}$; we obtain

$$A(p) + \sigma^{\circ}_{\psi\psi}\left[B(p)\varphi(p) + C(p)\varphi'(p)\right] = 0 \tag{2.6}$$

where

$$\begin{aligned} A(p) &= 2\left(1-\frac{1}{\rho}-\frac{p-1}{\gamma p\rho}\right)\left(1-\frac{1}{\rho}-\frac{p-1}{kM_{\infty}^{2}}\right) \\ B(p) &= \frac{(3+\rho^{-1})(p-1)}{kM_{\infty}^{2}} - 3\left(1-\frac{1}{\rho}\right) - (p-1)\left(\frac{p-1}{kM_{\infty}^{2}}-1\right)\frac{d}{dp}\left(\frac{1}{\rho}\right) \\ C(p) &= -2\frac{p-1}{\rho}\left(1-\frac{1}{\rho}-\frac{p-1}{kM_{\infty}^{2}}\right) \end{aligned} \tag{2.7}$$

Functions $\sigma^{\circ}_{\psi\psi}$ and $\varphi(p)$ are the solution of a system of two nonlinear first order equations, (2.5) and (2.6).

If in (2.1) we retain members of the third order, similar calculations lead to a system of three nonlinear first order equations.

3. Let us assume that the relationship between pressure on the surface of the flowed-past body and the local angle of inclination of the surface, $\cos\theta = F(p)$ for $\psi = 0$ is given.

Introducing expression $\cos\theta$ in (2.5) and (2.4), we obtain

$$\frac{d}{dl}\left[\sigma^{\circ}_{\psi\psi}\varphi^{2}(p)\right] = f\left[F(p)\right]$$

$$\sigma^{\circ}_{\psi\psi}\varphi(p) = p-1-kM_{\infty}^{2}+kM_{\infty}^{2}\sqrt{2(i_{m}-i)}\,F(p)$$

If flow is past a blunt body, the first equation is integrated taking into account the fact that at the point of intersection of the shock wave with the axis of symmetry, i.e., at p, equal to the pressure

behind the direct shock wave front p_m, $\varphi(p_m) = 0$.

Then, from (2.7) we find

$$\sigma_{\psi\psi}^{\circ}\varphi(p) = \int_{p_m}^{p} f[F(p)]\,dp, \qquad \varphi(p) = \frac{1}{N}\int_{p}^{p_m} f[F(p)]\,dp \tag{2.8}$$

$$N = 1 + kM_\infty^2 - p - kM_\infty^2\sqrt{2(i_\infty - i)}\,F(p)$$

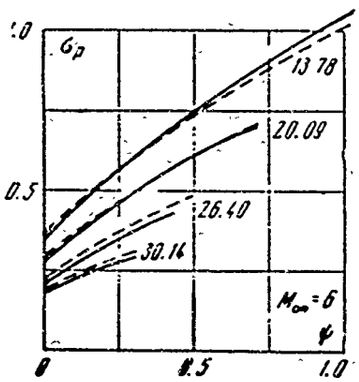

Fig. 1.

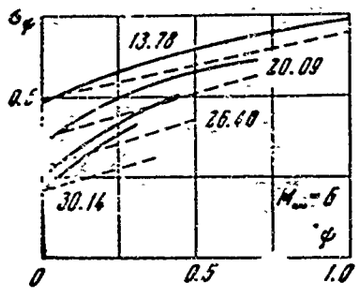

Fig. 2.

In Figs. 1 and 2 are results of calculations of distribution of parameters between the surface of a body and the shock wave by formulas (2.4) and (2.8) for the case of spherical blunting. Distribution of pressure on the surface was calculated by a modified formula of Newton, i.e., we assumed that

$$\cos\theta = \sqrt{1 + k^{-1}M_\infty^{-2}}\,\sqrt{1 - p/p_0}$$

where p_0 – stagnation pressure. Gas was considered ideal with constant ratio of thermal capacities, equal to 1.4. In Figs. 1 and 2 results of approximate calculations (dotted lines) are compared with numerical calculations taken from tables [1] (solid curves). Figures show values of dimensionless pressure on corresponding isobars. Fully analogous results of comparison were obtained for blunting in the form of spheroids at Mach numbers M_∞ from 3 to ∞.

Submitted
26 December 1963

Literature

1. O. M. Belotserkovskiy. Calculation of flow past axisymmetric bodies with a departing shock wave (calculating formulas and tables of flow fields). Comput. Center of Academy of Science of USSR, 1961.

EVOLUTION OF A WAVE PACKET IN HYDRODYNAMICS WITH DISPERSION OF SOUND

V. Ye. Zakharov

(Novosibirsk)

As it is known, in many cases for description of wave motions of plasma they apply hydrodynamic models. However, in distinction from usual hydrodynamics, in these models it is necessary to consider effects of wave dispersion, especially noticeable for motions with large spatial gradients. Such are models of "hydrodynamics of ion sound*" [1], of "hydrodynamics with ion dispersion" [2] and models describing propagation of sound in cold plasma across a magnetic field. To hydrodynamics with dispersion we also reduce problems of wave propagation in channels of finite depth. In these models there exist stationary waves of finite amplitude with a dimension of the order of the dispersion length [1, 2].

For each of these models there may be posed the question of evolution of an arbitrary wave packet. At first glance it seems that if one were to take the amplitude of the packet sufficiently small, it is possible to disregard the influence of nonlinear terms and to

*"Ion sound" may refer to propagation waves below ion cyclotron frequency [Tr. Ed. note].

consider that evolution of the packet is described by its propagation resulting from dispersion.

However, it is possible to show that such a consideration is valid only for very severe limitations on the shape of the packet, and that for the general case the influence of nonlinearity should be taken into account for even the smallest packet amplitude.

Let us consider a simple one-dimensional hydrodynamic model of plasma — model of ion sound. It is assumed that $T_e >> T_i$ and there is no magnetic field. Then plasma is described by velocity v and density n of ions and by the electrostatic potential φ. For these variables system of equations [3] is valid (m — mass of ions, $T_e = T$ — temperature of electrons, n_0 — undisturbed density of plasma)

$$\frac{\partial v}{\partial t} + v\frac{\partial v}{\partial x} = -\frac{e}{m}\frac{\partial \varphi}{\partial x}, \qquad \frac{\partial n}{\partial t} + \frac{\partial}{\partial x}(nv) = 0, \qquad -\frac{\partial^2 \varphi}{\partial x^2} = 4\pi e\left(n - n_0 \exp\frac{e\varphi}{T}\right) \tag{1}$$

Henceforth, we assume that we are considereing motions for which

$$\frac{1}{v}\frac{\partial v}{\partial x} \ll \frac{1}{r_d} \qquad \left(r_d = \left(\frac{T}{8\pi e^2 n_0}\right)^{1/2} \text{ — Debye radius of the plasma}\right)$$

so that dispersion effects are small. We shall, furthermore, consider that the amplitude of the wave is small (M - 1 < 1). Using these assumptions (M — Mach number), it is possible from the last equation to express the gradient of potential approximately:

$$e\frac{\partial \varphi}{\partial x} = T\frac{n'}{n} + 2Tr_d^2\frac{1}{n_0}\frac{\partial^2 n}{\partial x^2}$$

Then we introduce $\delta n = n - n_0$ and pass to a reference system, moving to the right with the speed of sound

$$z = x - ct, \qquad \tau = t \tag{2}$$

The system of equations taken on the form

$$\begin{gathered}\frac{\partial v}{\partial \tau} - c\frac{\partial v}{\partial z} + v\frac{\partial v}{\partial z} = -\frac{c^2}{n_0}\left(\frac{\partial \delta n}{\partial z} - \frac{\delta n}{n_0}\frac{\partial \delta n}{\partial z} + r_d^2\frac{\partial^3 \delta n}{\partial z^3}\right) \\ \frac{\partial \delta n}{\partial \tau} - c\frac{\partial \delta n}{\partial z} - n_0\frac{\partial v}{\partial z} + \delta n\frac{\partial v}{\partial z} + v\frac{\partial \delta n}{\partial z} = 0\end{gathered} \tag{3}$$

Now, due to the fact that effects of nonlinearity and dispersion are assumed small, it is possible to look for solutions for which

derivatives with respect to τ are small. This corresponds to consideration of waves running to the right and slowly evolving under the action of nonlinearity and dispersion.

The second of equations (3) also allows us to approximately obtain

$$\delta n \approx \frac{n_0}{c} v, \qquad \frac{\partial \delta n}{\partial z} \approx \frac{n_0}{c} \frac{\partial v}{\partial z} + \frac{2n_0}{c^2} v \frac{\partial v}{\partial z} + \frac{n_0}{c^2} \frac{\partial v}{\partial \tau} \tag{4}$$

Substituting expressions (4) in the first of equations (3), we finally obtain

$$\frac{\partial v}{\partial \tau} + v \frac{\partial v}{\partial z} = c r_d^2 \frac{\partial^3 v}{\partial z^3}, \qquad \mu = c r_d^2 \tag{5}$$

Equation (5) was obtained for waves on the surface of water and was applied in [3] for hydrodynamics with ion dispersion. Depending upon the law of dispersion we obtained different signs of μ.

Equation (5) allows us to estimate the relative magnitude of the nonlinear term and of the term with the highest order derivative. Let the characteristic amplitude of the packet be A, and a be its characteristic length. From equation (5) it is clear that integral of vdz is preserved. The nonlinear term has the order A^2/a, and dispersion has the order $\mu A/a^3$.

Since $Aa \sim E$, it is possible to record them, respectively, by E^2/a^3 and $\mu E/a^4$. It follows from this that with propagation of the packet a will increase, and the relative role of the nonlinear term increases.

The nonlinear and dispersion terms are compared at length $a_* \sim \mu/E$. In the considered model stationary solitary waves have exactly this length.

This consideration shows that only evolution of sufficiently narrow packets ($a < a_*$) can be considered in the frames of a linearized equation.

We shall now obtain stricter conditions on the form of the wave packet, for which evolution is determined basically by linear terms. For that, in equation (5) we replace variables

$$y = z - ut, \qquad \tau = t \tag{6}$$

equation (5) here takes the form

$$\frac{\partial v}{\partial \tau} = \mu \frac{\partial}{\partial y} \frac{1}{1 + \tau v_y} \frac{\partial}{\partial y} \frac{1}{1 + \tau v_y} v_y$$
$$v_y = \frac{\partial v}{\partial y} = \frac{\partial u / \partial z}{1 - \tau \partial u / \partial z}, \qquad \frac{\partial u}{\partial z} = \frac{v_y}{1 + \tau v_y} \tag{7}$$

From the last relationship it is clear that if $1 + \tau v_y = 0$, $\partial u/\partial z$ turns into infinity, which corresponds to "inversion of the front."

From the equation one can also see that in the description of the initial stage of evolution of the packet, when τ is small, it i possible to replace equation (7) by linear equation

$$\frac{\partial v}{\partial \tau} = \mu \frac{\partial^3 v}{\partial y^3} \tag{8}$$

If evolution of the packet for all values of τ is described by equation (9), it differs little qualitatively from linear spreading. For satisfaction of this it is necessary that

$$\left| \tau \frac{\partial v}{\partial y} \right| \ll 1 \tag{9}$$

The solution of equation (8) is expressed in Airy functions:

$$v(y, \tau) = \frac{1}{\mu \tau^{1/3}} \int v_0(y') \Phi\left(\frac{y - y'}{\mu \tau^{1/3}} \right) dy' \qquad (v_0(y) = v(y, 0)) \tag{10}$$

Let us note that y = z when t = 0.

We expand $v_0(y)$ in a series of derivatives of δ-function

$$v_0(y) = \sum_{n=0}^{\infty} \frac{A_n}{n!} \delta^{(n)}(y - y') \quad \left(\begin{array}{l} A - \text{n-th moment} \\ \text{of function } v_0(y) \end{array} \right) \tag{11}$$

Substituting (10) and (11) in condition (7), we obtain

$$\left| \frac{\tau^{1/3}}{\mu} \left(\frac{A_0}{\mu \tau^{1/3}} \Phi'\left(\frac{y}{\mu \tau^{1/3}} \right) + \frac{A_1}{2 \mu^2 \tau^{1/3}} \Phi''\left(\frac{y}{\mu \tau^{1/3}} \right) + \ldots + \frac{A_n}{(n+1)! (\mu \tau^{1/3})^{n+1}} \Phi^{(n+1)}\left(\frac{y}{\mu \tau^{1/3}} \right) \right) \right| < 1 \tag{12}$$

As $\tau \to \infty$ the main role is played by the first terms of series (12). For satisfaction of condition (12) it is necessary, in any

case, that

$$A_0 = 0, \qquad |A_1| < 2\mu^3 \tag{13}$$

Then condition (12) is satisfied for $|y| < \mu\tau^{1/3}$. For larger values of y it will still be necessary to consider nonlinear terms due to growth of derivatives of Airy functions as $y \to \infty$. If the first $(k - 1)$ moments of function v_0 are equal to zero, as $\tau \to \infty$ condition (12) has the form

$$|y| < \left(\frac{(k+1)!}{A_k}\right)^{\frac{4}{k+2}} \left(\mu^{2}\tau^{-\frac{1}{3}}\right)^{\frac{4}{k+2}} \mu^{\frac{3}{2}} \tau^{\frac{1}{3}} \tag{14}$$

Let us now estimate from expression (10) the width of the wave packet as $\tau \to \infty$. Let us assume that λ is the characteristic dimension, on which function $v_0(y)$ strongly changes. Then $v(y, \tau)$ decreases, starting from those y_* for which function Φ accomplishes several oscillations on length λ. If $v_0(y)$ differs from zero for $|y| < y_0$, then $y_* \gg y_0$ for larger values of τ.

Then

$$\Phi\left(\frac{y - y'}{\mu\tau^{1/3}}\right) \approx \left(\frac{y}{\mu\tau^{1/3}}\right)^{-1/4} \sin\left(\frac{2}{3}\left(\frac{y}{\mu\tau^{1/3}}\right)^{3/2} + \frac{\pi}{4}\right)$$

Characteristic "frequency" of the Airy function is $y^{1/2}\mu^{-3/2}\tau^{-1/2}$; from this follows the estimate

$$y_* \sim \frac{\tau\mu^3}{\lambda^2} \tag{15}$$

Approximately at these distances we compared various terms of series (12).

Comparison of estimates (14) and (15) shows that although one A_n differs from zero, there exists a region where it is necessary to consider nonlinear effects, although the width of this region decreases with growth of n.

It is possible that there exist initial conditions of specific form such that all $A_n = 0$, for which linear spreading of the packet

occurs for all τ and z.

Recently in [3] there were found self-similar solutions of equation (5), evolving according to a law, close to linear. Analysis of these solutions shows that they satisfy conditions (13).

In conclusion the author thanks R. Z. Sagdeyev for discussion of the work.

Submitted
23 January 1964

Literature

1. A. A. Vedenov, Ye. P. Velikhov, and R. Z. Sagdeyev. Nonlinear oscillations in rarefied plasma. Nuclear fusion, 1961, No. 1.

2. V. I. Karpman. Structure of the front of a shock wave, propagating at an angle to magnetic field in rarefied plasma. Journal tech. physics, 1963, Vol. 33, No. 8.

3. Yu. A. Berezin and V. I. Karpman. A theory of nonstationary waves of finite amplitude in rarefied plasma. Journal exper. and theoretical physics (going to press).

APPROXIMATE METHOD OF CALCULATION OF OPTIMUM SUCTION OF FLUID FROM THE BOUNDARY LAYER OF WING PROFILES WITH A POROUS SURFACE

L. F. Kozlov

(Leningrad)

By optimum suction of fluid from a boundary layer through the porous surface of a wing profile we mean such distribution of the normal component of velocity on the surface where in every section of the boundary layer the local Reynolds' number is equal to its lower critical value.

The problem of optimum suction of fluid from the boundary layer of a porous plate by numerical integration of the equation of L. Prandtl was first solved in [1]. An approximate solution of this problem in quadratures was obtained by the author [2].

The works of Wieghardt and Wortmann [3, 4] are devoted to approximate solution of an analogous problem for a boundary layer with a longitudinal drop of pressures on the external boundary. Both works are based on simultaneous use of equations of momentum and energy for a boundary layer. In the method of Wieghardt for every particular case it is proposed to integrate the basic system of differential equations by the very laborious numerical method of finite differences.

In the derivation of final formulas for optimum suction Wortmann used functions calculated with application of Schlichting profiles, very roughly approximating the real change of velocities in the boundary layer on a porous surface, especially near the breakaway point.

Below, for calculation of optimum suction of fluid from the boundary layer of wing profiles with a porous surface in an incompressible fluid, there is used a system of equations of zero and second "moments" [5]. The offered method is fairly precise and free from the deficiencies inherent in the methods of Wieghardt and Wortmann. It is necessary to note that for solution of boundary layer problems, a system of equations of "moments" was first proposed by L. G. Loytsyanskiy [6].

Designations

x – coordinate along surface of wing profile,

x_0 – coordinate of point of loss of stability without suction,

U_0 – incident flow velocity,

U – longitudinal velocity on external boundary of boundary layer,

v_0 – local velocity of suction of liquid through porous profile surface,

f – parameter of boundary layer,

i^{**} – parameter of suction from boundary layer through the surface,

R_x – Reynolds number,

R^{**} – local Reynolds number,

R_0^{**} – lower value of local critical Reynolds number without suction of fluid,

R_*^{**} – lower value of local critical Reynolds number during suction of fluid,

H – shape parameter of boundary layer,

δ^{**} – thickness of loss of momentum,

δ^* – thickness of displacement flow,

ν – kinematic coefficient of viscosity of the fluid,

$$a = 0.44,\ b = 5.48,\ B = 1.12,\ c = 9.54,\ H_0 = 2.59,\ H_1 = 4,\ A_1 = 26.3,\ B_1 = 8$$

$$f = \frac{U'\delta^{**2}}{\nu},\quad i^{**} = \frac{v_0\delta^{**}}{\nu},\quad R_x = \frac{U_0 x}{\nu},\quad R^{**} = \frac{U\delta^{**}}{\nu},\quad H = \frac{\delta^*}{\delta^{**}}$$

Using approximate interpolation formulas for the coefficient of friction and shape parameter H, we convert the equation of zero moment

to linear form:

$$\frac{df}{dx} = \frac{U''}{U'} f + \frac{U'}{U} [a + (B-2)\, t^{**} - bf] \tag{1}$$

Differentiating the parameter

$$f = \frac{U'\delta^{**2}}{\nu} = \frac{\nu U'}{U^2} R^{**2} \qquad \left(R^{**} = \frac{U\delta^{**}}{\nu}\right) \tag{2}$$

we find that

$$\frac{df}{dx} = \frac{\nu U''}{U^3} R^{**2} - \frac{2\nu U'^2}{U^3} R^{**2} + \frac{\nu U'}{U^2} \frac{dR^{**2}}{dx} \tag{3}$$

Substituting formulas (2) and (3) in equation (1), we obtain

$$\frac{\nu}{U} \frac{dR^{**2}}{dx} + \frac{\nu U'}{U^2} (b-2) R^{**2} - (B-2) \frac{r_0}{U} R^{**} - a = 0 \qquad \left(t^{**} = \frac{r_0}{U} R^{**}\right) \tag{4}$$

Equation of the second moment we use in the following form:

$$\frac{df}{dx} = \frac{U''}{U'} f + \frac{U'}{U} \frac{a}{H_0} (H - H_4 t^{**} - H_0 f) \tag{5}$$

After substitution of formulas (2) and (3) in equation (5) and the necessary algebraic transformations, we have

$$\frac{\nu}{U} \frac{dR^{**2}}{dx} + \frac{\nu U'}{U^2} (ac-2) R^{**2} + a \frac{H_4}{H_0} \frac{r_0}{U} R^{**} - a \frac{H}{H_0} = 0 \tag{6}$$

Eliminating from equations (4) and (6) quantity v_0/U, we obtain a differential equation for calculation of the local Reynolds number

$$R^{**2} = \exp\left[-k_0 \ln \frac{U(x)}{U(x_0)}\right] \left\{ \frac{a}{\nu [H_0 (B-2) + aH_4]} \times \right. \tag{7}$$
$$\left. \times \int_{x_0}^{x} [aH_4 + (B-2) H] U \exp\left[k_0 \ln \frac{U(x)}{U(x_0)}\right] dx \right\} + R_0^{**2}$$

Integrating (7) for boundary condition $R^{**} = R_0^{**}$ with $x = x_0$, we find

$$\frac{dR^{**2}}{dx} + \frac{U'}{U} k_0 R^{**2} - \left[\frac{a}{H_0}\left(\frac{aH_4}{B-2} - H\right)\right]\left[\frac{\nu}{U}\left(1 + \frac{a}{B-2}\frac{H_4}{H_0}\right)\right]^{-1} = 0$$
$$k_0 = \left[(ac-2) + \frac{a(b-2)}{B-2}\frac{H_4}{H_0}\right]\left(1 + \frac{a}{B-2}\frac{H_4}{H_0}\right)^{-1} \tag{8}$$

Calculations of optimum suction of fluid from the boundary layer start from the value of the Reynolds number R_0^{**} at the point of loss

of stability of the layer, up to which without suction of fluid the flow in the layer is stable to small disturbances. For known velocity distribution on the external boundary of the layer of a wing profile U(x) and given values of shape parameter H by formula (8) we calculate R^{**}. Obtaining family of curves $R^{**}(x, H)$ and knowing local critical Reynolds numbers, corresponding to every value of shape parameter H, we graphically determine relationship $R_*^{**}(x)$.

The lower values of the local critical Reynolds number R_*^{**} are calculated by research using the method of small disturbances of hydrodynamic stability of flow of liquid in a laminar boundary layer. It is known that hydrodynamic stability of flow basically depends on the degree of fullness of the velocity profile across the layer, to significant extent determined by shape parameter H. Therefore, it is natural that the value of the lower critical Reynolds number R_*^{**} simply depends on shape parameter H. As proposed in work [3], in subsequent calculations it is recommended to determine values of $R_*^{**}(H)$, using the following approximate formula:

$$R_*^{**} = \exp(A_1 - B_1 H) \tag{9}$$

From the zero moment equation (4) we obtain a formula for calculation of the optimum distribution of the velocity of suction of fluid:

$$\frac{v_0}{U} = \frac{\nu}{U}\frac{1}{B-2}\frac{1}{R^{**}}\frac{dR^{**2}}{dx} + \frac{\nu U'}{U^2}\frac{(b-2)}{(B-2)}R^{**} - \frac{a}{B-2}\frac{1}{R^{**}} \tag{10}$$

The first term in formula (10) we find from differential equation (7). After transformations we have

$$\frac{\nu}{U}\frac{1}{B-2}\frac{1}{R^{**}}\frac{dR^{**2}}{dx} = -\frac{\nu U'}{U^2}\frac{k_0}{B-2}R^{**} + \frac{a}{B-2}\frac{[aH_4 + H(B-2)]}{[H_0(B-2) + aH_3]}\frac{1}{R^{**}} \tag{11}$$

Substituting this expression in equation (10) and producing necessary calculations, in final form we find the formula for determining optimum distribution along a chord of a wing profile of the

velocity of suction of fluid from the boundary layer

$$\frac{v_0}{U} = \frac{\nu U'}{U^2}\frac{(b-2-k_0)}{B-2}R^{**} + \frac{a(H-H_0)}{[H_0(B-2)+aH_1]}\frac{1}{R^{**}} \qquad (12)$$

Determining, by formula (12), optimum distribution of velocity of suction by the method of approximation offered in work [5], it is possible to calculate all characteristics of the boundary layer and of friction drag of a wing profile.

For the particular case of a porous plate expressions (8) and (12) are reduced to an integral exponential function. Comparison of relationships obtained by various authors for velocity of optimum suction on a porous plate v_0/U for different Reynolds numbers R_x is shown in Fig. 1. On this graph there are plotted results of calculations by the proposed formula (12) (curve 1), and also according to [3, 4] (curves 2 and 3, respectively). Comparison shows satisfactory coincidence of results of calculations by the offered formula with corresponding data from [4]. Obtained results also allow us to conclude that distribution of optimum velocity of suction of fluid from a boundary layer to a significant extent depends on the Reynolds number.

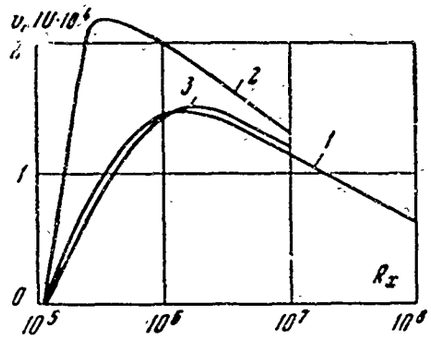

Fig. 1.

Submitted
7 November 1963

Literature

1. J. Pretsch. Die Leistungserparins durch Grenzschichtbeeinflussung beim Schleppen einer ebenen Platte. Deutsche Luftfahrtforschung, 1943, UM, No. 3048.

2. L. F. Kozlov. Optimum suction of the boundary layer on a porous plate in an incompressible fluid. Eng-physics journal, 1963, Vol. VI, No. 10.

3. K. Wieghardt. Zur Berechnung ebener und drehsymmetrischer Grenzschichten mit kontinuierlicher Absaugung. Ing.-Archiv, 1954, 22, 368.

4. F. Wortmann. Grenzschicht — Absaugung. Grenzschicht — forschung, Symposium Freiburg, Springer — Verlag, 1958.

5. L. F. Kozlov. Approximate integration of equations of a laminar boundary layer on a porous surface in an incompressible fluid. PMFT, 1962, No. 5.

6. L. G. Loytsyanskiy. Method of approximation for integration of equations of a laminar boundary layer in an incompressible fluid. PMM, 1949, Vol. XIII, Issue 5.

RESEARCH OF SPEED OF SOUND IN LIQUID AND GASEOUS ARGON

I. S. Radovskiy

(Moscow)

In [1] there were given certain results of measurements of the speed of sound in the vapor and liquid phases of argon on a saturation curve. Construction of an ultrasonic interferometer, created for research at low temperatures, is described in [2].

Below are results of systematic measurements of the speed of sound in gaseous and liquid argon in the range of temperatures 84-175 K and pressures 1-60 bar, including the critical region.

Measurements were taken by isochores, where simultaneously with measurement of the speed of sound there was also determined the density of argon — in the same experiments and on the same installation without additional complications of its construction. Strictly speaking, due to the presence of "ballast" volume (valves, connecting capillaries, etc.), and also due to thermal expansion the process of change of state of gas in the interferometer differed somewhat from isochoric, i.e., was quasi-isochoric.

The value of density for every experimental point was determined by means of introduction of corrections for ballast volume and thermal

expansion of the interferometer. Maximum total value of both corrections constituted 3%, and for most experiments did not exceed 1-2%. Accuracy of determination of corrections themselves was in any case not worse than 3-5%. Consequently, error introduced by corrections did not exceed 0.1%.

As a result of the conducted measurements there were derived more than 30 isochores, there were obtained about 200 experimental values of the speed of sound in gaseous and liquid argon and 100 values of the density of gaseous argon.

By means of extrapolation of isochores to intersection with the line of saturation, we also determined density of saturated vapors of argon in range of temperatures 87-146°K.

The data obtained on the speed of sound were compared with calculated data of Hilsenrath [3], which are only for gaseous argon at low pressures (in the investigated phase region there are no experimental data on the speed of sound in argon).

Divergence with data of Hilsenrath constitutes 0.1-0.2%. Near the line of saturation it reaches 0.45%.

Results of determination of density of argon were compared with data of Michels [4] along the line of saturation (divergence is about 0.5%) and isotherms 133 and 153°K (divergence of 0.2-0.3%).

In Fig. 1 are isochores (solid lines) and isotherms (dotted lines) of the speed of sound in gaseous argon; in Fig. 2, the same in liquid argon; black points correspond to the line of saturation. Isotherms were obtained by means of graphic analysis of experimental isochores. Furthermore, in Fig. 1 are plotted calculated data of Hilsenrath on isotherms (half blackened points).

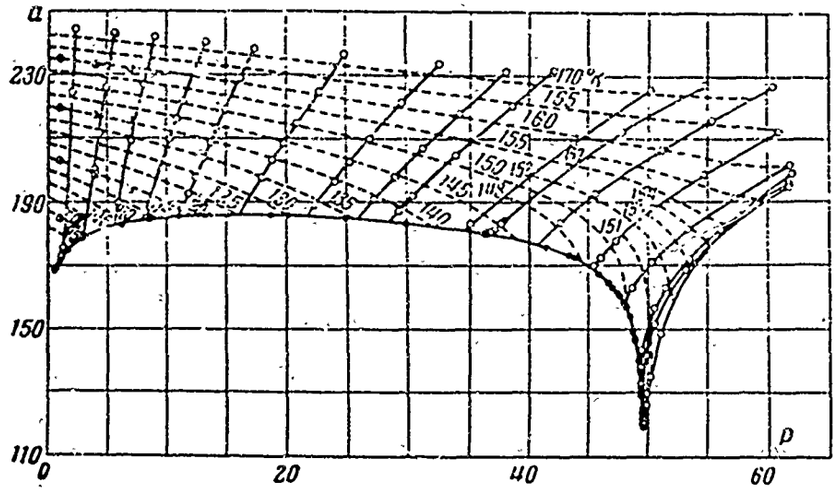

Fig. 1.

Isotherms of the speed of sound were extrapolated to pressure p = 0. The obtained values of the speed of sound were compared with those calculated by the formula for an ideal gas

$$a_0 = \sqrt{5/3\,RT}$$

Divergence between experimental and theoretical values of a_0 is within ±0.2%.

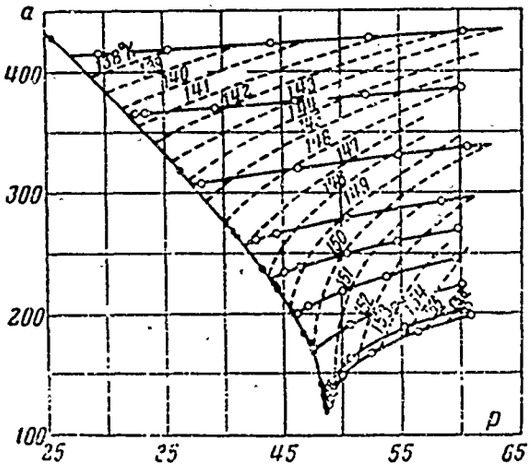

Fig. 2.

Results of measurements of the speed of sound ($msec^{-1}$) are also given in Tables 1 and 2 for whole values of temperature and pressure.

In the critical region, where the speed of sound strongly depends on temperature and pressure, we conducted more detailed measurements. Isotherms of the speed of sound in the critical region, including the critical isotherm (150.63°K), are presented in Table 3.

Results of determination of density (ρ, kgm^{-3}) of argon in the range of temperatures 90-170°K and pressures 1-60 bar are presented in Fig. 3.

Table 1. Speed of Sound in Gaseous Argon

p	T = 90	95	100	105	110	115	120	125	130
0	177.0	182.5	187.0	191.3	195.7	199.8	204.3	208.6	212.5
1	174.3	179.9	184.9	189.6	194.1	198.5	203.1	207.5	211.5
5	—	—	—	—	186.7	192.3	197.6	202.5	207.2
10	—	—	—	—	—	—	189.9	195.9	201.7
15	—	—	—	—	—	—	—	186.6	194.6
20	—	—	—	—	—	—	—	—	185.7
	T = 135	140	145	150	155	160	165	170	
0	216.0	220.0	223.9	227.8	231.4	235.4	239.3	243.1	
1	215.2	219.4	223.5	227.4	231.0	235.0	238.9	242.7	
5	212.0	216.6	221.1	225.4	229.4	233.3	237.2	241.1	
10	207.1	212.3	217.4	222.1	226.7	230.9	235.1	239.1	
15	201.5	207.6	213.0	218.2	223.4	228.2	232.8	237.2	
20	194.0	201.8	208.5	214.4	220.3	225.4	230.5	235.3	
25	185.0	194.8	203.3	210.4	216.8	222.6	228.1	233.3	
30	—	186.0	197.0	205.6	213.1	219.5	225.5	231.2	
35	—	—	188.6	200.0	208.9	216.3	222.9	229.0	
40	—	—	—	193.2	204.3	213.1	220.6	226.9	
45	—	—	—	182.8	199.5	209.9	218.2	225.3	
50	—	—	—	—	193.0	206.6	216.0	223.9	
55	—	—	—	—	183.5	202,8	214.2	222.7	
60	—	—	—	—	220.7	200.6	212.3	221.7	

Table 2. Speed of Sound in Liquid Argon

p	T = 138	140	142	144	146	148	150
30	400.3	—	—	—	—	—	—
35	416.3	385.0	346.7	—	—	—	—
40	—	403.3	370.1	331.0	—	—	—
45	—	419.6	390.2	356.5	316.2	256.4	—
50	—	—	407.4	376.7	343.6	304.5	248.2
55	—	—	423.8	394.2	365.7	335.0	295.8
60	—	—	—	409.5	384.5	—	326.5

Table 3. Speed of Sound in Argon in the Critical Region

p	T = 150	150.2	150.4	150.63	150.8	151	151.5	152	153	155	157
45	182.8	183.9	184.9	185.9	186.8	187.7	189.6	191.1	194.2	199.5	203.9
46	177.1	178.9	180.8	182.2	183.5	184.7	187.0	189.1	192.5	198.4	203.0
47	165.1	170.3	173.9	176.5	178.5	180.1	183.7	186.5	190.8	197.0	202.1
48	203.4	171.3	159.3	167.3	171.0	173.7	179.5	183.2	188.8	195.9	201.1
48.5	220.7	203.7	181.2	152.3	164.2	169.1	176.6	181.2	187.7	195.2	200.5
49	231.6	—	205.7	182.2	141.6	159.5	173.2	178.9	186.1	194.6	200.0
49.5	—	—	—	206.1	188.9	155.4	168.0	176.1	184.5	193.8	199.5
50	—	—	—	—	208.0	191.0	158.8	172.9	182.8	193.0	199.0
50.5	—	—	—	—	—	209.3	164.3	169.0	180.8	192.2	198.4
51	—	—	—	—	—	221.4	186.0	159.3	178.6	191.2	197.9
52	—	—	—	—	—	239.2	217.3	186.7	173.5	189.2	196.9
53	—	—	—	—	—	253.4	—	212.1	169.7	187.1	195.8
54	—	—	—	—	—	—	—	231.8	186.0	185.2	194.7
55	—	—	—	—	—	—	—	244.3	208.5	183.5	193.6

Temperature everywhere is expressed in degrees Kelvin, absolute; pressure is in bars.

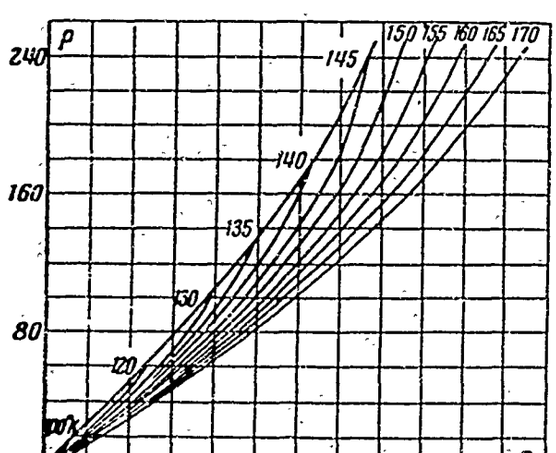

Fig. 3.

Possible error in measuring the speed of sound does not exceed 0.2% for most experiments; error of determination of density was 0.2-0.3%. Real scattering of experimental points, as a rule, is less than these magnitudes.

Submitted
16 October 1963

Literature

1. I. S. Radovskiy. Experimental research of the speed of sound in argon on the line of saturation. PMTF, 1963, No. 3.

2. I. S. Radovskiy. Installation for studying thermodynamic properties of gases at low temperatures by the ultra-acoustic method. Advanced scientific-technical and industrial experience, GOSINTI, 19[illegible]. Issue 9.

3. J. Hilsenrath et al. Tables of thermodynamic and transport properties of air, argon. Oxford, 1960.

4. A. Michels et al. Compressibility isotherms of argon of temperatures between -25° and -155°C, and at densities up to 640 amagat [sic]. Physica, 1958, 24, 8, 659.

TEMPERATURE STATE OF A SEMITRANSPARENT SPHERICAL SHELL

V. S. Zarubin

(Moscow)

There is considered a thin spherical shell with a diathermal medium in its cavity. In distinction from [1] it is considered that the shell is semitransparent and has different optical characterisitics in the region of shortwave (solar) and longwave (natural) radiations. In other respects formulation of the problem is analogous to work [1]. In particular, the temperature over the thickness of the shell is considered to be invariable, and transmission of heat by thermal conduction along the shell will be disregarded.

From without, the shell is struck by specific radiant heat flows $q_1(\$, \psi)$ and $q_2(\$, \psi)$ varying along the surface, where $\$$ and ψ — angular coordinates of the point of a sphere ($0 \leq \$ \leq \pi$, $0 \leq \psi \leq 2\pi$). Here and henceforth, parameters with index 1 pertain to shortwave, and with index 2, to longwave radiation. The degree of absorption, reflection and transmission by the shell of radiant fluxes $q_1(\$, \psi)$ and $q_2(\$, \psi)$ is characterized correspondingly by coefficients A_1', R_1', D_1', and A_2', R_2', D_2', which in general can change along the surface.

It is assumed that radiant fluxes $D_1'q_1(\$, \psi)$ and $D_2'q_2(\$, \psi)$, passing through the shell, are radiated from its internal surface

diffusely. Diffuse, also is reflection and natural radiation by the internal surface of the shell. The balance of radiant fluxes on this surface for a unit area with coordinates ϑ, ψ gives

$$q_1^*(\vartheta, \psi) = R_1 q_1^\circ + D_1' q_1(\vartheta, \psi) \tag{1}$$

$$q_2^*(\vartheta, \psi) = R_2 q_2^\circ + D_2' q_2(\vartheta, \psi) + \varepsilon q_0(\vartheta, \psi), \qquad q_0(\vartheta, \psi) = \sigma_0 T^4(\vartheta, \psi) \tag{2}$$

Here $q^*(\vartheta, \psi)$ and q° — effective and incident specific radiant fluxes; ε and R — degree of blackness and reflectance of the internal surface of the shell, generally depending on ϑ and ψ; σ_0 — radiation factor of an ideal black body; $T(\vartheta, \psi)$ — temperature of the shell.

For the above assumptions magnitude q° is constant for any point on the internal surface and is equal to [1]

$$q^\circ = \int_0^{\pi} \int_0^{2\pi} q^*(\alpha, \beta) \frac{\sin \alpha}{4\pi} d\alpha \, d\beta = \text{const} \tag{3}$$

where α and β — angles, reading of which is analogous to angles ϑ and ψ.

From expressions (1) and (3) it follows that

$$q_1^\circ = \frac{1}{1 - R_{1,m}} \int_0^{\pi} \int_0^{2\pi} D_1' q_1(\alpha, \beta) \frac{\sin \alpha}{4\pi} d\alpha \, d\beta \tag{4}$$

$$q_1^*(\vartheta, \psi) = D_1' q_1(\vartheta, \psi) + \frac{R_1}{1 - R_{1,m}} \int_0^{\pi} \int_0^{2\pi} D_1' q_1(\alpha, \beta) \frac{\sin \alpha}{4\pi} d\alpha \, d\beta \tag{5}$$

where $R_{1,m}$ — value of reflectance with respect to shortwave radiation averaged over the internal surface of the shell:

$$R_{1,m} = \int_0^{\pi} \int_0^{2\pi} R_1 \frac{\sin \alpha}{4\pi} d\alpha \, d\beta$$

For determination of magnitudes q_2° and $q_2^*(\vartheta, \psi)$ from expression (2) it is necessary to preliminarily eliminate radiant flux $q_0(\vartheta, \psi)$. This is possible by composing for a unit area of the sphere the equation of heat balance for a steady temperature state:

$$\begin{aligned} &q_1^*(\vartheta, \psi) - q_1^\circ + q_2^*(\vartheta, \psi) - q_2^\circ = \\ &= (1 - R_1') q_1(\vartheta, \psi) - D_1 q_1^\circ + (1 - R_2') q_2(\vartheta, \psi) - D_2 q_2' - \varepsilon' q_0(\vartheta, \psi) \end{aligned} \tag{6}$$

where ε' – degree of blackness of the external surface of the shell, where $\varepsilon' = A_2'$; D_1 and D_2 – transmitting ability of a shell with respect to radiant fluxes q_1° and q_2° falling on its internal surface.

After eliminating $q_0(\vartheta, \psi)$ from relationships (2) and (6), we obtain equation

$$(\varepsilon + \varepsilon')\, q_2^*(\vartheta, \psi) = [\varepsilon(1 - R_2') + \varepsilon' D_2']\, q_2(\vartheta, \psi) + \\ + [\varepsilon(1 - D_2) + \varepsilon' R_2]\, q_2^\circ + \varepsilon A_1' q_1(\vartheta, \psi) + \varepsilon A_1 q_1^\circ \qquad (7)$$

whose solution, taking into account relationships (3)-(5), gives

$$\{(\varepsilon + \varepsilon') - [\varepsilon(1 - D_2) + \varepsilon' R_2]_m\}\, q_2^\circ = \int_0^\pi \int_0^{2\pi} [\varepsilon(1 - R_2') + \varepsilon' D_2']\, q_2(\alpha, \beta) \frac{\sin\alpha}{4\pi}\, d\alpha\, d\beta + \\ + [\varepsilon A_1]_m\, q_1^\circ + \int_0^\pi \int_0^{2\pi} \varepsilon A_1' q_1(\alpha, \beta)\, \frac{\sin\alpha}{4\pi}\, d\alpha\, d\beta \qquad (8)$$

where index m signifies averaging over the surface of the spnere:

$$F_m = \int_0^\pi \int_0^{2\pi} F(\alpha, \beta) \frac{\sin\alpha}{4\pi}\, d\alpha\, d\beta$$

Later substituting relationships (4), (5), (7), and (8) in formula (6), we obtain

$$(\varepsilon + \varepsilon')\, q_0(\vartheta, \psi) = A_1' q_1(\vartheta, \psi) + A_2' q_2(\vartheta, \psi) + \frac{A_1}{1 - R_{1,m}} \int_0^\pi \int_0^{2\pi} D_1' q_1(\alpha, \beta) \frac{\sin\alpha}{4\pi}\, d\alpha\, d\beta + \\ + \frac{A_2}{\varepsilon + \varepsilon' - [\varepsilon(1 - D_2) + \varepsilon' R_2]_m} \left\{ \int_0^\pi \int_0^{2\pi} \varepsilon A_1' q_1(\alpha, \beta)\, \frac{\sin\alpha}{4\pi}\, d\alpha\, d\beta + \right. \\ + \frac{[\varepsilon A_1]_m}{1 - R_{1,m}} \int_0^\pi \int_0^{2\pi} D_1' q_1(\alpha, \beta) \frac{\sin\alpha}{4\pi}\, d\alpha\, d\beta + \\ \left. + \int_0^\pi \int_0^{2\pi} [\varepsilon(1 - R_2') + \varepsilon' D_2']\, q_2(\alpha, \beta) \frac{\sin\alpha}{4\pi}\, d\alpha\, d\beta \right\} \qquad (9)$$

From this there is found the distribution of temperature on the surface of the shell:

$$T(\vartheta, \psi) = \left[\frac{q_0(\vartheta, \psi)}{\sigma_0}\right]^{\cdot}$$

If optical characteristics of the shell do not vary on the surface, expression (9) is somewhat simplified:

$$(\varepsilon + \varepsilon')\, q_0(\theta, \psi) = A_1' q_1(\theta, \psi) + A_2' q_2(\theta, \psi) +$$
$$+ \frac{1}{\varepsilon' A_2 + (\varepsilon' + \varepsilon) D_2} \left(A_1 D_1' \frac{1 - R_2}{1 - R_1} (\varepsilon + \varepsilon') + A_1' \varepsilon A_2 \right) \times$$
$$\times \int_0^{\pi} \int_0^{2\pi} q_1(\alpha, \beta) \frac{\sin \alpha}{4\pi} d\alpha\, d\beta + A_2 \frac{\varepsilon A_2' + (\varepsilon + \varepsilon') D_2'}{\varepsilon' A_2 + (\varepsilon + \varepsilon') D_2} \int_0^{\pi} \int_0^{2\pi} q_2(\alpha, \beta) \frac{\sin \alpha}{4\pi} d\alpha\, d\beta \qquad (10)$$

In the particular case for an opaque shell ($D_1 = D_1' = D_2 = D_2' = 0$) formula (10) leads to results obtained earlier [1].

Submitted
15 February 1964

Literature

1. V. S. Zarubin. Temperature state of a thin spherical shell. PMTF, 1963, No. 6.

ONE PARAMETER OF HARDENING

N. S. Vilesova and V. S. Namestnikov

(Novosibirsk)

Recently Yu. N. Rabotnov [1, 2] advanced the hypothesis that rate of creep $p^{\cdot}$ is determined by the current value of stress σ and a certain number of parameters q^s

$$p^{\cdot} = \Phi(\sigma, q^s) \tag{1}$$

where he considered that

$$dq^s = a^s dp + b^s d\sigma + c^s dt + d^s dT$$

where a^s, b^s, c^s, and d^s — functions of stress σ, creep p, time t, and temperature T.

If in relationship (1) there is only one parameter, dq = dp, it is reduced to the normal hypothesis of hardening.

The case when in relationship (1) there are parameters $dq^1 = dp$, $dq^2 = pd\sigma$ was studied in [3]. Here we managed to account for observed systematic deviations of the hypothesis of hardening from experimental data [4].

Below are results of study on the basis of another very simple assumption that

$$p^{\cdot} = \Phi(\sigma, q) \qquad \left(q = \int \sigma dp\right) \tag{2}$$

We know [4, 5] that a good approximation of the hypothesis of hardening is given by relationship

$$\dot{p}p^{\alpha} = k\sigma^{n} \tag{3}$$

Consequently, (2) may be taken in the form

$$\dot{p}q^{\alpha} = k\sigma^{n+\alpha} \tag{4}$$

When σ = const, $q = \sigma p$; (3) follows directly from (4). Thus, the constants in equations (3) and (4) are the same.

Let us consider the following experiment. A sample creeps under constant stress σ_1 during time t_*, and there is accumulated deformation p_*. At moment t_* stress suddenly is increased to σ_2, and the test continues (Fig. 1). In order to obtain the curve of the subsequent behavior by the hypothesis of hardening, it is necessary to shift section $A''B$ of curve σ_2 forward in such a manner that point A'' coincides with point A' (we obtain section $A'B'$); by hypothesis (2), as it is easy to show [4], it is necessary to shift section AB forward to coincidence of points A and A' (we obtain section $A'B''$). Point A is found from condition $p_0 = p_*\sigma_1/\sigma_2$. Consequently, the curve corresponding to hypothesis (2) is located higher than the curve constructed by the hypothesis of hardening, and, obviously, should correspond better to experiment.

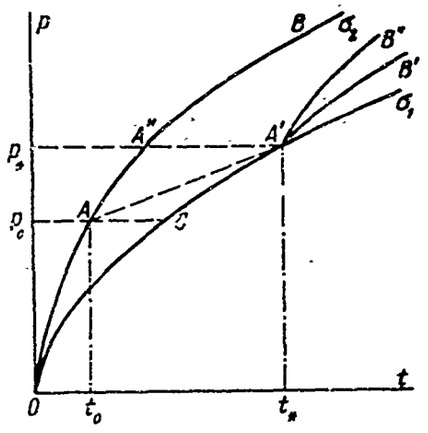

Fig. 1.

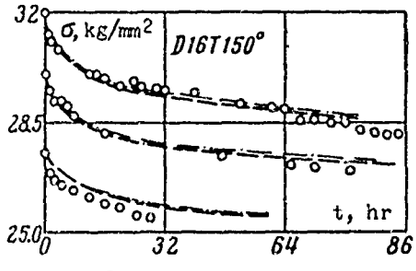

Fig. 2.

If stress is lowered instantly from magnitude σ_2 to σ_1, it is easy to prove that the curve after unloading, by relationship (2), is located lower than the curve corresponding to

the hypothesis of hardening. We compare hypothesis (2) with available experimental data [4, 5]; subsequently, we shall apply it in the form (4).

With a stress varying in steps on the i-th step, integrating (4) for conditions

$$\sigma = \sigma_i = \text{const when } t \geq t_{i0},\ p = p_{i0} \text{ when } t = t_{i0}$$

we obtain

$$p_i = p_{i0} - p_{i0}' + \left\{(p_{i0})^{1/m} + \frac{k(t - t_{i0})}{m}\sigma_i^n\right\}^m \tag{5}$$

$$p_{i0}' = \frac{1}{\sigma_i}\sum_{j=2}^{i}\sigma_{j-1}(p_{j0} - p_{j-10}), \qquad m(\alpha + 1) = 1 \tag{6}$$

With stress, varying according to the law

$$\sigma = \sigma_0 \pm \sigma^{\cdot}(t - t_0) \tag{7}$$

and initial conditions

$$p = p_0,\ \sigma = \sigma_0,\ q = q_0, \text{ when } t = t_0 \tag{8}$$

by integrating (4) we obtain

$$p = p_0 + k\int_{t_0}^{t}\{\sigma_0 \pm \sigma^{\cdot}(\tau - t_0)\}^{n+\alpha} q^{-\alpha}\,d\tau \tag{9}$$

$$q = \left\{q_0^{1/m} + \frac{k\sigma_0^{n+\alpha+2}}{m(n+\alpha+2)}\left[\mp 1 \pm \left\{1 \pm \frac{\sigma^{\cdot}}{\sigma_0}(t - t_0)\right\}^{n+\alpha+2}\right]\right\}^m$$

At $p_0 = \sigma_0 = q_0 = t_0 = 0$ equality (9) is completely integrable; in this case

$$p = p_4\left\{1 + \frac{1}{m(n+1)}\right\}^{1-m} \tag{10}$$

where p_4 — deformation, calculated by hypothesis of hardening in usual form (3).

In other cases the integral in equality (9) must be calculated numerically.

The curve of relaxation of stresses by hypothesis (4) has the form

$$t = \frac{\ldots}{k(2E)^{\alpha-1}} \int_{\sigma}^{\sigma_0} \sigma^{-n-\alpha} (\sigma_0^2 - \sigma^2)^{\alpha} \, d\sigma \qquad (11)$$

where E — elastic modulus, and σ_0 — initial stress. For whole number values of α, the integral in the right part is easily taken. It is not difficult to show that the curve of relaxation (11) lies above the curve calculated by (3), which, of course, is obvious if one refers to Fig. 1 and considers relaxation the limiting case of creep for an intermittently decreasing load.

In Fig. 4 are curves of creep under a load varying in steps, reproduced from [5]. In this and subsequent [sic] figures the broken lines correspond to the hypothesis of hardening (3), and the dot-dash lines correspond to hypothesis (4). As can be seen, with increased load hypothesis (4) better corresponds to experiment than (3) (see curves 333-2 and 56-8). If at a certain time part of the load is removed, and then is restored, hypotheses (3) and (4) give the same curve (curve a-1).

In Fig. 3 are curves of creep during monotonically varying load [5]. It is clear that with an increasing load hypothesis (4) better corresponds to experiment than (3), and for a decreasing load it is somewhat worse.

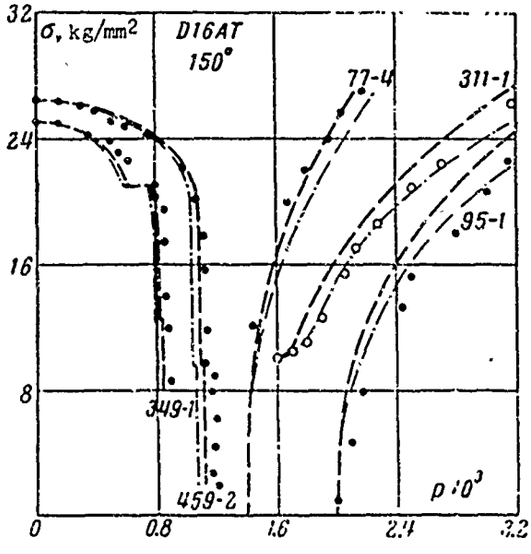

Fig. 3.

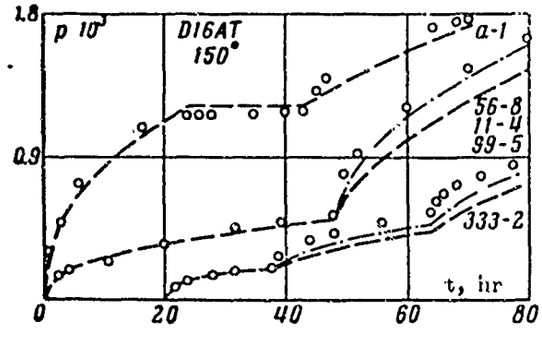

Fig. 4.

Curves of relaxation [4], built by (11), differ little from curves corresponding to hypothesis (3) (Fig. 2).

Here we have not considered for an increasing load the curves of creep during stresses exceeding the elastic limit, since in these cases hypothesis (3) gives increased curves of creep [5]; conformity (4) with experiment here will be still worse.

Leaving aside the last case, it is possible to summarize that the new parameter of hardening without introduction of additional constants allowed us for nondecreasing loads to obtain better conformity with experiment as compared to the usual theory of hardening. For a diminishing load conformity of the new theory with experiment is somewhat worse; however, it is possible to free oneself from this divergence if, as in [3], one considers that when $\sigma \cdot \sigma < 0$ hypothesis (3) is in effect.

Submitted
5 November 1963

Literature

1. Y. N. Rabotnov. On the Equation of State for Creep. Progr. Appl. Mech., the Prager Anniversary Volume, the Macmillan Co., N.Y., 1963.

2. Y. N. Rabotnov. On the Equation of State of Creep. Proc. of the Joint International Confer. on Creep, 1963.

3. V. S. Namestnikov and Yu. N. Rabotnov. Hypothesis of equation of state during creep. PMTF, 1961, No. 3.

4. V. S. Namestnikov and A. A. Khvostunkov. Creep of duralumin under variable loads. PMTF, 1960, No. 4.

5. V. S. Namestnikov. Creep cf aluminum alloy under variable loads. PMTF, 1964, No. 2.

ROLLING A VISCO-ELASTIC CYLINDER ON A BASE OF THE SAME MATERIAL

R. Ya. Ivanova

(Novosibirsk)

We consider the contact problem of linear visco-elasticity. Many problems of this class are solved with application of the Laplace transform; solution of the given problem is based on principles of the theory of heredity. In the problem there is considered only one form of nucleus — the exponential, although there may be applied any degenerate nucleus. The problem about rolling of a cylindrical body on a visco-elastic support in two-dimensional form was solved by G. A. Boychenko [1], but with significant simplifications. In recent years analogous problems have evoked interest in the United States. Witness to this are many works, and, in particular, the work of Hunter [?] [2].

Below, this problem is solved by another method. The roller and base are considered prepared from one and the same material. Such material may even be steel, since there are grounds to assume that for small stresses, steel behaves as a linearly viscous material.*

*V. S. Postnikov. Internal friction of pure metals and alloys at high temperatures. Dissertation for scientific degree of doctor of physical-mathematical sciences, Kemerovo, 1959.

In the solution of the problem there are used the following assumptions.

1. Motion of the roller starts at moment of time $t = -\infty$ and continues with constant speed c.

2. The problem is considered two-dimensional.

3. Material of the roller and base obeys the Boltzmann-Vol'terra law:

$$\sigma_{ij} = \lambda^{\circ}\theta + 2\mu^{\circ}\varepsilon_{ij},$$

where λ°, μ° — integral operators of form

$$\lambda^{\circ} = \lambda(1 - \lambda^{*}), \qquad \mu^{\circ} = \mu(1 - \mu^{*})$$

and

$$\lambda^{*}\varphi(t) = \int_{-\infty}^{t} \Lambda(t-\tau)\varphi(\tau)\,d\tau, \qquad \mu^{*}\varphi(t) = \int_{-\infty}^{t} M(t-\tau)\varphi(\tau)\,d\tau$$

4. There is no volume aftereffect, i.e., $\lambda^{\circ} + \mu^{\circ} = \lambda + \mu$.

Here λ, μ — elastic constants; $\Lambda(t - \tau)$, $M(t - \tau)$ — functions, determined experimentally. There exist materials, for which these functions are close to exponential.

For the considered medium, in which the roller moves, the problem will be formulated as the first basic problem of the theory of elasticity, but in the solution elastic constants will be replaced correspondingly by operators, which will give us the possibility to account for changed elastic properties of the material in time. This proposition was called by Yu. N. Rabotnov [3] Vol'terra's principle.

Following Boychenko [1], we shall use the Muskhelishvili relationships [4]. If the elastic body occupies the lower half-plane and the value of stresses on the boundary are $Y_y = -p(x)$, $X_y = t(x)$ (Fig. 1), derivative of boundary values of displacements on coordinate x should satisfy Muskhelishvili relationship

$$\Phi^{+}(x) + \varkappa\Phi^{-}(x) = 2\mu(U'_{1x} + iV'_{1x})$$

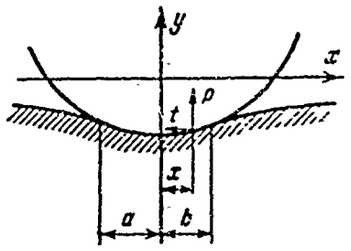

Fig. 1.

Replacing elastic constants λ and μ by operators λ°, μ°, we obtain for points of the base

$$\Phi_1^+(x) + \varkappa^\circ \Phi_1^-(x) = 2\mu^\circ (U_{1x}' + iV_{1x}') \qquad (1)$$

for points of the roller

$$\Phi_2^-(x) + \varkappa^\circ \Phi_2^+(x) = 2\mu^\circ (U_{2x}' + iV_{2x}') \qquad (2)$$

where

$$\Phi_1 = -\Phi_2$$

Applying the Sokhotskiy-Plemel' formula for limiting values of functions Φ_1 and Φ_2, we subtract equation (2) from equation (1). We obtain a singular integral equation, containing p(x) and t(x)

$$-\int_{-a}^{b} \frac{p(s) + it(s)}{s - x}\, ds = A^\circ [-i(U_{1x}' - U_{2x}') + (V_{1x}' - V_{2x}')] \qquad \left(A^\circ = \frac{2\pi\mu^\circ}{1 + \varkappa}\right)$$

Here limits of integration are taken from $-a$ to b, since outside the contact section $p(x) = t(x) = 0$.

Dividing the imaginary and real part, we write two singular equations

$$-\int_{a}^{b} \frac{p(s)}{s - x}\, ds = A^\circ (V_{1x}' - V_{2x}'), \qquad \int_{-a}^{b} \frac{t(s)}{s - x}\, ds = A^\circ (U_{1x}' - U_{2x}') \qquad (3)$$

We solve the first of these equations, since tangential stresses are determined in [1].

Based on the absence of volume aftereffect (Assumption 4), we present operator A° in the following form

$$A^\circ = \pi(\lambda + \mu)\left[1 - \frac{\lambda + \mu}{\lambda + 2\mu} \frac{1}{1 - \mu^* \mu'/(\lambda + 2\mu)}\right]$$

Let us assume that $\Gamma(t - \tau)$ will be the resolvent of nucleus $M(t - \tau)$. Then

$$A^\circ = a_1 + b_1 \Gamma^* \qquad (4)$$

Here

$$a_1 = \pi(\lambda + \mu) - \frac{\pi(\lambda + \mu)^2}{\lambda + 2\mu} \qquad b_1 = -\frac{\pi\mu(\lambda + \mu)^2}{(\lambda + 2\mu)^2}, \qquad \Gamma^*\varphi(t) = \int_{-\infty}^{t} \Gamma(t - \tau)\varphi(\tau)\, d\tau$$

With even motion of the roller, motion of medium can be assumed steady with respect to a system of coordinates, travelling forward together with the center of the roller. Then displacement and stress will not depend explicitly on time but will be functions only of coordinates.

We introduce a motionless system of coordinates so that

$$y_1 = y, \qquad x_1 = x + ct.$$

We substitute for the variable in formula (4):

$$x_1 = x + ct, \quad x_1 = \xi + c\tau, \quad t - \tau = \frac{\xi - x}{c}$$

$$\Lambda\varphi(x) = a_1\varphi(x) + \frac{b_1}{c}\int_x^\infty \Gamma\left(\frac{\xi - x}{c}\right)\varphi(\xi)\,d\xi = a_1\varphi(x) + \frac{b_1}{c}\Gamma_1^*\varphi(x)$$

Replacing the arc of circumference of the roller by an arc of a parabola, one may assume that on the line of contact $V_{1x}' - V_{2x}' \approx x/R$.

Thus

$$V_{1x}' - V_{2x}' = g(x) = x/R \quad \text{for} \quad -a \leqslant x \leqslant b \tag{5}$$

$$V_{1x}' - V_{2x}' = g(x) = V_{1x}' \quad \text{for} \quad x > b \tag{6}$$

Here V_{1x}' is a certain, still unknown, function.

Equation (3) in new variables has the form

$$-\int_{-a}^{b} \frac{p(s)}{s - x}\,ds = \Lambda g(x) = f(x)$$

Solution of this equation according to the Carleman method will be

$$p(x) = \frac{1}{\pi^2}\left(\frac{b - x}{a + x}\right)^{1/2}\int_{-a}^{b}\left(\frac{a + s}{b - s}\right)^{1/2}\frac{f(s)}{s - x}\,ds + \frac{C'}{\sqrt{(a + x)(b - x)}} \tag{7}$$

From the requirement of boundedness of p(x) for x = b, it follows that $C' = 0$.

We take resolvent Γ of definite form. For instance,

$$\Gamma\left(\frac{\xi - x}{c}, \lambda_i\right) = \sum_{i=1}^{k} A_i \exp\left[-\lambda_i\left(\frac{\xi - x}{c}\right)\right]$$

In this case operator

$$A\varphi(x) = a_1\varphi(x) + \frac{b_1}{c}\sum_{i=1}^{k}\lambda_i\int_x^{\infty} A_i \exp\left[-\lambda_i\left(\frac{\xi - x}{c}\right)\right]\varphi(\xi)\,d\xi$$

$$p(x) = \frac{1}{\pi^2}\left(\frac{b-x}{a+x}\right)^{1/2}\int_{-a}^{b}\left(\frac{a+s}{b-s}\right)^{1/2}\frac{f(s)}{s-x}\,ds = \frac{1}{\pi^2}\left(\frac{b-x}{a+x}\right)^{1/2}$$

$$\int_{-a}^{b}\left(\frac{a+s}{b-s}\right)^{1/2}\frac{1}{s-x}\left[a_1 g(s) + \frac{b_1}{c}\sum_{i=1}^{k}\lambda_i\int_s^{\infty} A_i \exp\left[-\lambda_i\left(\frac{\xi - s}{c}\right)\right] g(\xi)\,d\xi\right] ds$$

$$= \frac{1}{\pi^2}\left(\frac{b-x}{a+x}\right)^{1/2}\int_{-a}^{b}\left(\frac{a+s}{b-s}\right)^{1/2}\frac{1}{s-x}\left[a_1 g(s) + \frac{b_1}{c}\sum_{i=1}^{k}\lambda_i\int_s^{b} A_i \cdot \right.$$

$$\left. \cdot \exp\left[\lambda_i\left(\frac{s-\xi}{c}\right)\right] g(\xi) + \frac{b_1}{c}\sum_{i=1}^{k}\int_b^{\infty} A_i \exp\left[\lambda_i\left(\frac{s-\xi}{c}\right)\right] g(\xi)\,d\xi\right] ds \qquad (8)$$

We simplify the right side of equation (8), considering condition (5):

$$\int_{-a}^{b}\left(\frac{a+s}{b-s}\right)^{1/2}\frac{1}{s-x}\,a_1 g(s)\,ds + \frac{a_1}{R}\int_{-a}^{b}\left(\frac{a+s}{b-s}\right)^{1/2}\frac{s}{s-x}\,ds$$

We designate

$$\int_b^{\infty} A_i \exp\left[-\lambda_i\frac{s}{c}\right] v_{1\xi}'(\xi)\,d\xi = C_i \qquad (9)$$

where $V_{1x}' = g(x)$ when $x > b$.

After transformation, equation (8) takes form

$$p(x) = \frac{1}{\pi^2}\left(\frac{b-x}{a+x}\right)^{1/2}\int_{-a}^{b}\left(\frac{a+s}{b-s}\right)^{1/2}\left\{\frac{a_1}{R}s + \right.$$

$$\left. + \frac{b_1}{c}\sum_{i=1}^{k}\lambda_i\int_s^{b} A_i \exp\left[-\lambda_i\left(\frac{\xi - s}{c}\right)\right]\frac{\xi}{R}\,d\xi + \frac{b_1}{c}\sum_{i=1}^{k}\lambda_i C_i \exp\left(\lambda_i\frac{\xi}{c}\right)\right\}\frac{ds}{s-x} =$$

$$= -\frac{1}{\pi^2}\left(\frac{b-x}{a+x}\right)^{1/2}\int_{-a}^{b}\left(\frac{a+s}{b-s}\right)^{1/2}\frac{1}{s-x}\left[s\left(\frac{a_1}{R} + \frac{b_1}{R}\sum_{i=1}^{k}A_i\right) + \sum_{i=1}^{k}\exp\left(\frac{\lambda_i s}{c}\right)\frac{b_1}{c}\lambda_i C_i - \right.$$

$$\left. - \sum_{i=1}^{k}\left(b + \frac{c}{\lambda_i}\right)\frac{b_1}{R}\exp\left(-\lambda_i\frac{b}{c}\right)\exp\left(\lambda_i\frac{s}{c}\right) + \frac{b_1 c}{R}\sum_{i=1}^{k}\frac{A_i}{\lambda_i}\right]\frac{ds}{s-x} =$$

$$= \frac{1}{\pi^2}\left(\frac{b-x}{a+x}\right)^{1/2}\int_{-a}^{b}\left(\frac{a+s}{b-s}\right)^{1/2}\left[m_1' s + \sum_{i=1}^{k} m_{2i}\exp\left(\lambda_i\frac{s}{c}\right) + m_3\right]\frac{ds}{s-x} \qquad (10)$$

Here

$$m_1' = \frac{a_1}{R} + \frac{b_1}{R}\sum_{i=1}^{k}A_i, \qquad m_3 = \frac{b_1 c}{R}\sum_{i=1}^{k}\frac{A_i}{\lambda_i}$$

$$m_{2i} = \frac{b_1}{c}\lambda_i C_i - \frac{b_1}{R}\left(b + \frac{c}{\lambda_i}\right)\exp\left(-\frac{\lambda_i}{c}b\right)$$

We cannot calculate

$$\int_{-a}^{b} \left(\frac{a+s}{b-s}\right)^{1/2} \exp\frac{\lambda_i s}{c}\, ds$$

in closed form. Therefore, below there are used two terms of the series expansion of function $\exp(\lambda_i s/c)$:

$$\exp\frac{\lambda_i s}{c} = 1 + \frac{\lambda_i s}{c}$$

This is justified for materials with sufficiently large relaxation time τ, i.e., when $s \ll c\tau$.

Subsequently, calculation of $p(x)$ is conducted by approximate formula

$$p(x) = \left(\frac{b-x}{a+x}\right)^{1/2} \int_{-a}^{b} \left(\frac{a+s}{b-s}\right)^{1/2} \frac{m_1' s + m_2'}{s-x}\, ds \qquad (11)$$

$$m_1' = m_1 + \sum_{i=1}^{k} m_{2i}\frac{\lambda_i}{c}, \qquad m_2' = m_3 + \sum_{i=1}^{k} m_{2i}$$

We calculate the integral in the right part of (10):

$$\int_{-a}^{b} \left(\frac{a+s}{b-s}\right)^{1/2} \frac{m_1' s + m_2'}{s-x}\, ds = J(x)$$

For that we consider another known integral [5]

$$\Omega(z) = \frac{1}{2\pi i}\int_{\Lambda^*} \left[\left(\frac{a+\xi}{b-\xi}\right)^{1/2} m_1'\xi + m_2'\right]\frac{d\xi}{\xi - z} =$$

$$= \left(\frac{a+z}{b-z}\right)^{1/2}(m_1' z + m_2') - a_q z^q - a_{q-1} z^{q-1} - \ldots - a_0$$

where ξ belongs to the region bounded by contour Λ^*; a_q, a_{q-1}, ..., a_0 – coefficients of series expansion for sufficiently large ξ of function

$$\left(\frac{a+\xi}{b-\xi}\right)^{1/2}(m_1'\xi + m_2') = -i\left[1 + \frac{1}{\xi}\left(\frac{a+b}{2}\right) + \frac{1}{\xi^2}\left(\frac{ab}{4} - \frac{a^2}{8} + \frac{3b^2}{8}\right) + \cdots\right] \times$$

$$\times (m_1'\xi + m_2') \approx -i(m_1'\xi + m_2''), \qquad \left(m_2'' = \frac{a+b}{2} b m_1' + m_2'\right)$$

Thus

$$\Omega(z) = (m_1' z + m_2')\left(\frac{a+z}{b-z}\right)^{1/2} + i(m_1' z + m_2'')$$

We introduce for consideration one more integral:

$$J(z) = \int_L \sqrt{\frac{a+s}{b-s}} \frac{m_1's + m_2'}{s-z} ds$$

where s belongs to L. Subtending contours to arcs, we obtain

$$J(z) = \pi i \Omega(z) = \pi i \left[\left(\frac{a+z}{b-z} \right)^{1/2} (m_1'z + m_2') + i (m_1'z + m_2'') \right] \tag{12}$$

Considering that

$$F(z) = \frac{1}{2\pi i} J(z) \to F^+(x) = \frac{1}{2\pi i} J^+(x) \quad \text{when } z \to x$$

by the Sokhotskiy-Plemel' formulas we obtain

$$F^+(z) = \frac{1}{2} \psi(x) + \frac{i}{2\pi i} \int_L \frac{\psi(s)\, ds}{s-x} \quad \left(\psi(x) = \left(\frac{a+x}{b-x} \right)^{1/2} (m_1'x + m_2') \right)$$

Thus

$$\frac{1}{2\pi i} J^+(x) = \frac{1}{2} \left(\frac{a+x}{b-x} \right)^{1/2} (m_1'x + m_2') + \frac{1}{2\pi i} \int_{-a}^{b} \left(\frac{a+s}{b-s} \right)^{1/2} \frac{m_1's + m_2'}{s-x} ds \tag{13}$$

On the other hand, from (12) it follows that

$$J^+(x) = \pi i \left[\left(\frac{a+x}{b-x} \right)^{1/2} (m_1'x + m_2') + i (m_1'x + m_2'') \right] \tag{14}$$

Comparing (13) and (14), we find

$$\int_{-a}^{b} \left(\frac{a+s}{b-s} \right)^{1/2} \frac{m_1's + m_2'}{s-x} ds = -\pi (m_1'x + m_2'')$$

Finally, we obtain the formula for stresses:

$$p(x) = -\frac{1}{\pi} \left(\frac{b-x}{a+x} \right)^{1/2} (m_1'x + m_2') \tag{15}$$

For determination of final points a and b of the contact section, we have two conditions.

1. Requirement of boundedness of p(x) when x = -a:

$$m_1' x + m_2'' = 0 \text{ when } x = -a.$$

2. Condition of equilibrium

$$\int_{-a}^{b} p(s)\, ds = P$$

From the first condition it follows that

$$a = m_2'' / m_1' \tag{16}$$

From the second condition

$$\frac{1}{\pi}\int_{-a}^{b}\left(\frac{b-s}{a+s}\right)^{1/2}(m_1's+m_2'')\,ds = m_1'(a-b)\left(b+\frac{3a}{16}\right)-\frac{m_2''(a+b)}{2}=P$$

Or, considering (16),

$$P=-\frac{5}{16}\frac{m_2''^2}{m_1'}+\frac{11}{16}m_2''b+m_1'b^2 \tag{17}$$

Equation (17) gives the possibility of determining b only in the case when we know $C_i(b)$, on which m_1' and m_2'' in turn depend. For determination of b we use the condition of unloadedness of section $x > b$. We solve the second basic problem of the theory of elasticity, considering p(x) known, and replace the elastic constant by operators

$$2\mu^\circ(U_{1x}'-iV_{1x}')=(\varkappa^\circ+1)\,\Phi(x) \tag{18}$$

but

$$\Phi(x)=\frac{1}{2\pi i}\int_{-a}^{b}\frac{p(s)+it(s)}{s-x}\,ds \tag{19}$$

Substituting (19) in (18) and separating the imaginary and real part, we have

$$V_{1x}'=-\frac{1+\varkappa^\circ}{4\pi\mu^\circ}\int_{-a}^{b}\frac{p(s)}{s-x}\,ds=-A_1^\circ\int_{-a}^{b}\frac{p(s)}{s-x}\,ds\quad(x>b) \tag{20}$$

$$A_1^\circ=\frac{1}{2\pi(\lambda+\mu)}+\frac{1}{2\pi\mu}+\frac{1}{2\pi\mu c}\Gamma_1^*=a'+b'\Gamma_1^*$$

Here Γ_1^* is determined by formula (5).

The integral in the right part of (20) no longer has peculiarities and is easily calculated

$$\int_{-a}^{b}\frac{p(s)}{s-x}\,ds=-\frac{a+b}{2}m_1'+(m_2''+m_1'x)\left[1-\left(\frac{x-b}{x+a}\right)^{1/2}\right]=f_1(x)$$

Now

$$V_{x1}'=-A_1^\circ f_1(x)=-a'f_1(x)-b'\Gamma_1^*f_1(x)=-a'f_1(x)-$$

$$-b'\int_x^\infty\sum_{i=1}^{k}\lambda_iA_i\exp\left[-\lambda_i\left(\frac{\xi-x}{c}\right)\right]\left\{\frac{a+b}{2}m_1'-(m_2''+m_1'\xi)\left[1-\left(\frac{\xi-b}{\xi+a}\right)^{1/2}\right]\right\}d\xi$$

If one were to expand function $\sqrt{(\xi - b)/(\xi + a)}$ in a series of powers of ξ^{-1}, limiting oneself to two terms of the expansion (only for convenience of recording), it is possible to approximately calculate integral

$$\int_x^\infty \exp\frac{-\lambda_i s}{c}\left(\frac{\xi - b}{\xi + a}\right)^{1/2} d\xi.$$

As a result we obtain

$$V_{1x}' = b' \sum_{i=1}^{k} \lambda_i A_i \Phi_{0i}\left[-E_i\left(-\frac{\lambda_i x}{c}\right)\right]\exp\left(\frac{\lambda_j x}{c}\right) + \frac{\Phi_1}{x} \qquad (21)$$

Here

$$\Phi_{0i} = d_1 - d_2\frac{\lambda_i}{c}, \qquad \Phi_1 = a'd_1 - b'\sum_{i=1}^{k}\lambda_i A_i d_2$$

$$d_1 = \frac{m_1'}{4\cdot 2!}(3a^2 + 2ab - b^2) - \frac{a+b}{2}m_2''$$

$$d_2' = \frac{m_2'}{4\cdot 2!}(3a^2 + 2ab - b^2) - \frac{m_1'}{8\cdot 3!}(3b^2 + 3ab^2 - 9a^2b - 15a^3).$$

Thus, determining by the formula (21) function V_{1x}', it is possible by the formula (9) to calculate C_i.

Submitted
19 December 1963

Literature

1. G. A. Boychenko. Rolling resistance of hereditary-elastic bodies. News of AS of USSR, OTN, 1955, No. 9.

2. Hunter [?]. Contact problem of rolling of hard cylinder in a visco-elastic half-space. Applied mechanics, Transactions of American society of engineers, 1961, 4.

3. Yu. N. Rabotnov. Equilibrium of an elastic medium with aftereffect. PMM, 1948, Vol. 12, No. 1.

4. N. I. Muskhelishvili. Certain basic problems of the mathematical theory of elasticity. Press of Academy of Sciences of USSR, 1954.